

UNIVERSITY OF SALERNO

---



DEPARTMENT OF CHEMISTRY AND BIOLOGY

Ph.D. Course in "Chemistry" - XXXIII Cycle

Ph. D. Thesis in Chemistry

**NEW APPLICATIONS OF ESTER/AMIDE  
SURROGATES IN ORGANIC SYNTHESIS**

**Tutor:**

Prof. Alessandra Lattanzi

**Co-tutor:**

Prof. Amedeo Capobianco

**Ph.D. Coordinator:**

Prof. Claudio Pellecchia

**Ph.D. Student:**

Chiara Volpe

Matr. 8800100036

---

2020 - 2021



to Nicola, the best part of my life



## ACKNOWLEDGEMENTS

*I would like to thank my Tutor, Prof. Alessandra Lattanzi, for her careful supervision. The last three years have been very challenging, but she taught me so much.*

*Thanks to Sara for her valuable advice.*

*I want to express my gratitude to my colleagues Stefania, Antonio e Francesca for their continued support. I hope we will be able to repeat soon our evenings together.*

*Thanks to Assunta for her constant presence in the beautiful moments and in the most difficult ones.*

*Thanks to Luisa e Maria Cristina for the moments we have shared in the last nine years and that I hope will continue for a long time.*

*Thanks to Chiara and Chiara for their presence, even at a distance.*

*My greatest gratitude goes to my amazing family and most of all to Nicola.*





# Index

ABSTRACT .....	iv
LIST OF ABBREVIATIONS .....	vii
1. ORGANOCATALYSIS: AN OVERVIEW.....	9
1.1 Origins and benefits .....	9
1.2 Mechanistic aspects .....	12
1.2.1 Brønsted base catalysis.....	14
1.2.2 Hydrogen bond catalyzed reactions.....	22
1.3 Bifunctional organocatalysis.....	30
2. ONE-POT TRANSFORMATIONS IN ORGANIC SYNTHESIS.....	36
2.1 One-pot strategy .....	36
2.1.1 Tandem reactions.....	38
2.1.2 One-pot synthesis: applications and limitations .....	41
2.2 One-pot synthesis of (-)-oseltamivir .....	45
3. MASKED ESTERS/AMIDES .....	49
3.1 Ester/amide surrogates: general features.....	49
3.2 <i>N</i> -Acyl pyrazoles in organic synthesis .....	52
3.2.1 Masked esters/amides as electrophiles .....	52
3.2.2 Masked esters/amides as nucleophiles .....	66
RESEARCH OBJECTIVES.....	76
4. CATALYTIC ENANTIOSELECTIVE ONE-POT APPROACH TO <i>CIS</i> - AND <i>TRANS</i> -2,3-DIARYL SUBSTITUTED 1,5-BENZOTHAZEPINES.....	77
4.1 Background.....	77
4.2 Results and discussion.....	86
CONCLUSIONS.....	106
5. 1,5,7-TRIAZABICYCLO[4.4.0]DEC-5-ENE (TBD) TRIGGERED DIASTEREOSELECTIVE [3+2]	

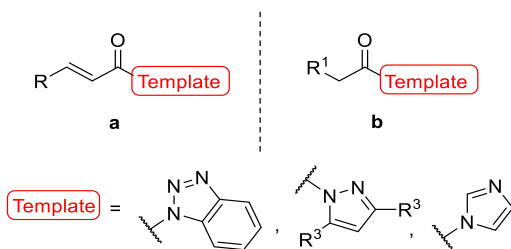


<b>CYCLOADDITION OF AZOMETHINE IMINES AND PYRAZOLEAMIDES .....</b>	<b>107</b>
<b>5.1 Background .....</b>	<b>107</b>
<b>5.2 Results and discussion .....</b>	<b>114</b>
<b>CONCLUSIONS .....</b>	<b>131</b>
<b>6. DIRECT <math>\alpha</math>-IMINATION OF <i>N</i>-ACYL PYRAZOLES WITH NITROSOARENES .....</b>	<b>132</b>
<b>6.1 Background .....</b>	<b>132</b>
<b>6.1.1 Nitrosobenzene in organic synthesis .....</b>	<b>138</b>
<b>6.1.2 Ehrlich-Sachs reaction .....</b>	<b>144</b>
<b>6.2 Results and discussion .....</b>	<b>148</b>
<b>CONCLUSIONS .....</b>	<b>163</b>
<b>7. NITRONE/IMINE SELECTIVITY SWITCH IN BASE-CATALYSED REACTION OF ARYL ACETIC ACID ESTERS WITH NITROSOARENES: JOINT EXPERIMENTAL AND COMPUTATIONAL STUDY .....</b>	<b>164</b>
<b>7.1 Background .....</b>	<b>164</b>
<b>7.2 Results and discussion .....</b>	<b>168</b>
7.2.1 Mechanistic investigations .....	180
7.2.3 Theoretical studies .....	186
7.2.3.1 Oxidative pathway to nitrone 215.....	190
7.2.3.2 Pathway to imine 172 .....	192
7.2.3.3 E1cB .....	195
7.2.3.4 Thermodynamic approach.....	197
<b>CONCLUSIONS .....</b>	<b>201</b>
<b>8. EXPERIMENTAL SECTION.....</b>	<b>202</b>
<b>8.1 General experimental conditions.....</b>	<b>202</b>
<b>8.2 Catalytic enantioselective one-pot approach to cis- and trans-2,3-diaryl substituted 1,5-benzothiazepines .....</b>	<b>203</b>
<b>8.3 1,5,7-Triazabicyclo[4.4.0]-dec-5-ene (TBD) Triggered</b>	

<b>diastereoselective [3+2] cycloaddition of azomethine imines and pyrazoleamides (TBD).....</b>	<b>230</b>
<b>8.4 Direct <math>\alpha</math>-imination of <i>N</i>-acylpyrazoles with nitrosoarenes</b>	<b>252</b>
<b>8.5 Nitron/imine selectivity switch in the base catalyzed reaction of arylacetic esters with nitrosoarenes.....</b>	<b>289</b>

## ABSTRACT

Masked esters/amides are scaffolds endowed with a great potential in the field of organic synthesis. This PhD project has been conceived, in the context of non-covalent organocatalysis, with the aim to exploit unsaturated (**a**) and saturated (**b**) masked esters/amides (Figure A) as starting materials to accomplish the synthesis of different classes of organic compounds in a one-pot fashion.



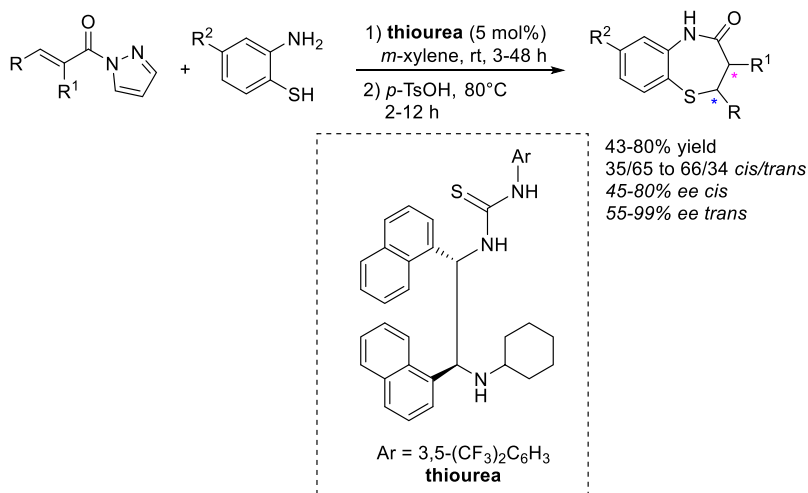
**Figure A.** General structure of an  $\alpha,\beta$ -unsaturated (**a**) and a saturated (**b**) masked ester/amide.

Masked esters/amides (Figure A) exhibit some important features which make them valid substrates for organocatalytic one-pot sequences. Firstly, the presence of a nitrogen-based heterocycle renders them more reactive if compared with esters or amides: the heterocycle “steals” electron density from the molecule, resulting in an enhanced electrophilicity at the  $\beta$  position of reagent **a** or an enhanced acidity of  $\alpha$ -proton in type **b** substrates. Secondly, nitrogen atoms of the heterocycle offer to these substrates more possibilities of interaction with an organocatalyst through further H-bonds formation. This provides a major rigidity in the transition state and a subsequent increase in the stereochemical outcome of the reaction. Finally, another important property of these compounds, due to the

ability of the aza-heterocycle as leaving group, is the possibility to obtain ester or amide functionality through simple treatment with alcohols or amines via typical addition/elimination mechanism (hence the name “ester/amide surrogates”).

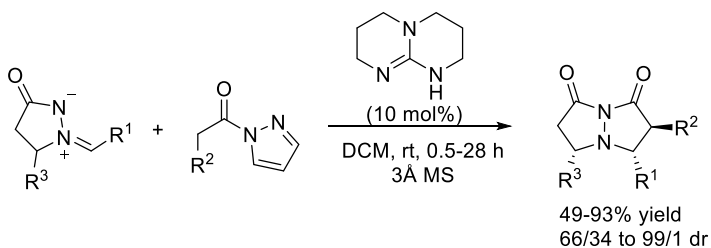
We tried to achieve the stereocontrolled formation of carbon-carbon and carbon-heteroatom bonds to obtain cyclic compounds of different nature and size (such as benzothiazepines and bicyclic pyrazolidinones) and non-cyclic compounds, such as imines,  $\beta$ -aminoalcohols and nitrones.

In this doctoral thesis, the first stereoselective cascade sulfa-Michael/lactamization sequence for the synthesis of *cis*- and *trans*-2,3-diaryl substituted 1,5-benzothiazepines has been developed, starting from  $\alpha,\beta$ -unsaturated *N*-acylpyrazoles and 2-aminothiophenols. The two steps are promoted by catalytic amounts of a readily available bifunctional thiourea and *p*-toluenesulfonic acid, respectively. Our work provides access to both *N*-unprotected diastereoisomers of the product with satisfactory results (Scheme A). Moreover, we demonstrated that these products can be easily elaborated to prepare libraries of compounds for biological tests.



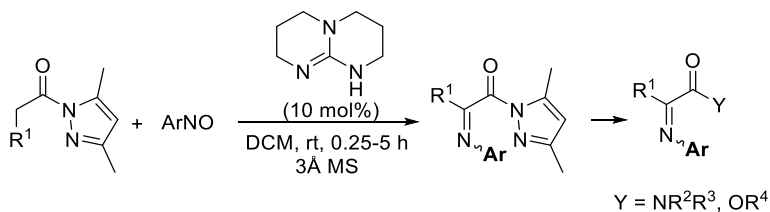
**Scheme A.** Our approach for the synthesis of *cis*- and *trans*-2,3-diaryl substituted 1,5-benzothiazepines from  $\alpha,\beta$ -unsaturated *N*-acylpyrazoles.

Regarding the use of reagent **b**, the greatest acidity of alpha protons easily allows the formation of an enolate which can react with an opportune electrophile, thus creating a first addition product. The presence of a nucleophilic site on this product, results in an intramolecular cyclization with the formation of an heterocyclic compound. In this case, we developed a diastereoselective one-pot [3+2] cycloaddition of *N,N'*-cyclic azomethine imines and *N*-acylpyrazoles to access bicyclic pyrazolidinones (Scheme B). Despite literature precedents, our protocol contemplates the use of readily available starting materials and a catalytic amount of a commercial base under mild reaction conditions.



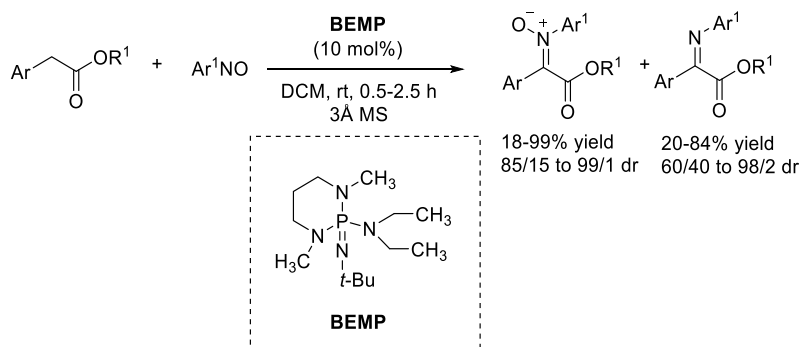
**Scheme B.** Stereoselective synthesis of tetrahydropyrazolo[1,2-a]-pyrazole-1,7-diones.

If the first adduct cannot give following reactions, the presence of heterocyclic ring enables a subsequent simple elaboration with synthesis of esters and amides for example. About this, we worked out a facile synthesis of  $\alpha$ -iminoesters derivatives by reacting nitrosobenzenes with acylpyrazoleamides: the nucleophilic addition of the enolate to nitrosoarene, followed by dehydration, leads to the formation of these compounds. Moreover, the  $\alpha$ -imino *N*-acyl pyrazoles, a new class of compounds never reported before, represent new versatile intermediates to easily access a range of synthetically useful derivatives in convenient one-pot transformations (Scheme C).



**Scheme C.** Direct  $\alpha$ -Imination of *N*-acylpyrazoles with nitrosoarenes and one-pot functionalization.

Finally we discovered that the use of esters, instead of acylpyrazoles, for reaction with nitrosoarenes leads to interesting results: depending on the substituents in the aromatic ring of the esters, and therefore on the acidity of the  $\alpha$ -proton, our catalytic system afforded nitrones and imines with good selectivity in most cases (Scheme D). Our protocol enables a facile access to nitrones and imines working under mild reaction conditions and with readily available reagents. Nitrones are useful starting materials in cycloaddition reactions for the formation of nitrogen-based heterocycles.



**Scheme D.** Synthesis of nitrones and imines through the reaction of arylacetic esters and nitrosoarenes.

## LIST OF ABBREVIATIONS

aq.	aqueous
Ar	aryl
BEMP	2- <i>tert</i> -Butylimino-2-diethylamino-1,3-dimethylperhydro-1,3,2-diazaphosphorine
BTMG	2- <i>t</i> -butyl-1,1,3,3-tetramethyl guanidine
Bu	butyl
cat.	catalyst/s
CPME	cyclopentyl methyl ether
DCC	<i>N,N'</i> -dicyclohexylcarbodiimide
DCM	dichloromethane
DDQ	2,3-Dichloro-5,6-dicyano-1,4-benzoquinone
DIC	<i>N,N'</i> -Diisopropylcarbodiimide
DMAP	4-Dimethylaminopyridine
DMP	Dimethylpyrazole
<i>ee</i>	enantiomeric excess
eq.	equivalent/s
h	hour(s)
MTBD	7-Methyl-1,5,7-triazabicyclo[4.4.0]dec-5-ene
NBA	Nitrobenzoic acid
Nu	nucleophile
<i>p</i>	<i>para</i>
PMB	<i>p</i> -Methoxybenzyl

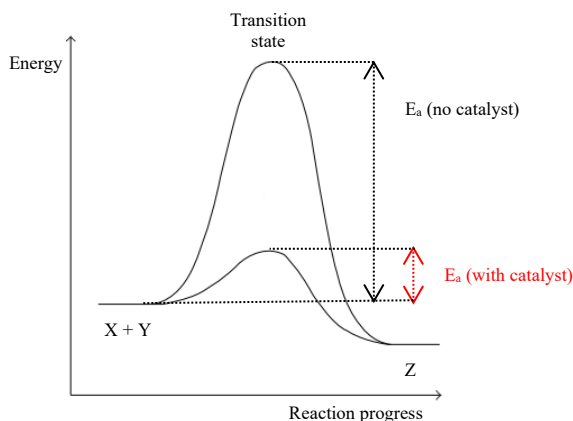


<i>p</i> -TsOH	<i>p</i> -toluenesulfonic acid
rt	room temperature
<i>t</i>	<i>tert</i>
<i>t</i> -Bu	<i>t</i> -butyl
TEBAC	triethylbenzylammonium chloride
TBD	1,5,7-triazabicyclo[4.4.0]dec-5-ene
TBO	1,4,6-triazabicyclo [3.3.0]oct-4-ene
TMG	1,1,3,3-Tetramethylguanidine

# 1. ORGANOCATALYSIS: AN OVERVIEW

## 1.1 Origins and benefits

The term “catalysis” dates back to 1836, when Berzelius wanted to explain the ability of some chemical substances to influence various decompositions and chemical transformations. Some decades later, Ostwald suggested the following definition: “*a catalyst accelerates a chemical reaction without affecting the position of the equilibrium*”.<sup>1</sup> In particular chemical bonds are established between the catalyst and reactants, thus forming an highly reactive complex. This interaction affects the rate of achievement of equilibrium of the reaction, but not influences the position of the equilibrium. (Figure 1.1).

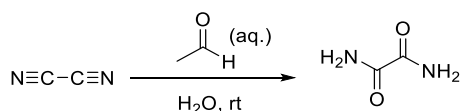


**Figure 1.1** Schematic illustration of the effect of a catalyst on the transformation of X and Y into Z.

<sup>1</sup> W. Ostwald, “Die Überwindung des wissenschaftlichen Materialismus,” in *Verhandlungen der Gesellschaft Deutscher Naturforscher und Ärzte*, **1895**, 155.

In addition to metal complexes and enzymes, some organic molecules can also facilitate chemical transformations. The term “organocatalyst” precisely refers to the use of a low molecular weight organic compound which, in catalytic ratio, is able to promote a chemical reaction.

The first organocatalytic reaction was accidentally discovered in 1859 by Justus von Liebig, who observed the formation of oxamide from dicyan in the presence of an aqueous solution of acetaldehyde (Scheme 1.1). He identified acetaldehyde as the catalyst of the reaction, detecting some analogies with the enzyme activity. Later, this reaction laid the basis for the industrial Degussa synthesis of oxamide.



**Scheme 1.1** von Liebig's synthesis of oxamide.

Natural products, such as cinchona alkaloids and amino acids, were the first molecules used as organic catalysts.<sup>2</sup> Over the years, thanks to the pioneering work of List, Barbas, MacMillan and others,<sup>3</sup> organocatalysis underwent a significant growth. A huge number of new organocatalysts, progressively more sophisticated and endowed

---

<sup>2</sup> (a) G. Bredig, W. S. Fiske, *Biochem. Z.* **1912**, 7; (b) H. Pracejus, Justus Liebig's, *Ann. Chem.* **1960**, 634, 9; (c) H. Pracejus, H. Mätje, *J. Prakt. Chem.* **1964**, 24, 195; (d) U. Eder, G. Sauer, R. Wiechert, *Angew. Chem. Int. Ed.* **1971**, 10, 496; (e) Z. G. Hajos, D. R. Parrish, *J. Org. Chem.* **1974**, 39, 1615.

<sup>3</sup> (a) B. List, R. A. Lerner, C. F. Barbas III, *J. Am. Chem. Soc.* **2000**, 122, 2395; (b) B. List, *Tetrahedron* **2002**, 58, 5573; (c) K. A. Ahrendt, C. J. Borths, D. W. C. MacMillan, *J. Am. Chem. Soc.* **2000**, 122, 4243.

with higher efficiency, have been developed and applied to a wide range of chemical transformations with excellent results.<sup>4</sup>

Organocatalysts are chiral or achiral molecules composed by C, H, N, S, and P, but N- and P-based compounds are the most important and studied. Among these, amine catalysts are more readily accessible than phosphorus ones, given their natural abundance. In fact no phosphorous-containing chiral substrates can be found in nature, and therefore these catalysts require to be synthesized.<sup>5</sup>

As mentioned above, a first important benefit deriving from the use of a catalyst, is the reduction of the activation energy of a process, resulting in an increased reaction rate. Moreover, the opportunity to make the reaction in presence of substoichiometric amounts of the catalyst is cheaper and safer, in opposition to asymmetric syntheses that involve for example the use of a stoichiometric amount of precious and expensive chiral reagents (as in the case of chiral auxiliaries). For these reasons, catalysis (including heterogeneous catalysis, biocatalysis, and especially organocatalysis) represents a very significant topic in the branch of green chemistry, which works in order to reduce the environmental impact of chemical processes.

Organocatalysis have proved to be greener than conventional catalysis because:

- It works under mild reaction conditions, thus avoiding energy waste;
- Air-stable reagents are usually employed and anhydrous

---

<sup>4</sup> P. I. Dalko, *Enantioselective Organocatalysis*, Wiley-VCH: Weinheim, 2007.

<sup>5</sup> For a review on phosphines, see: J.L. Methot, W.R. Roush, *Adv. Synth. Catal.* **2004**, 346, 1035.

conditions are not strictly required. In this way the cost of the synthesis is lower;<sup>6</sup>

- A wide range of functional groups, that could be sensitive in other conditions, is well tolerated. This results in a reduced need for protecting groups and a subsequent lowering in the total steps of the reaction;
- It operates with low toxic substances;
- It avoids the formation of metallic waste and the presence of traces of metals in the products, which is of critical importance for applications in medicinal chemistry.

## 1.2 Mechanistic aspects

Organocatalytic reactions are commonly divided into two main categories, depending on the interaction between catalyst and substrate/s in the transition state. In particular we talk about covalent catalysis if covalent bonds are formed between the catalyst and reagent/s (with energies higher than 15 kcal mol<sup>-1</sup>). The latter branch is called non-covalent catalysis, since the interactions involved are non-covalent bonds, such as ion pairing, neutral host-guest interactions, acid-base associations, H-bonding (with energies usually lower than 4 kcal mol<sup>-1</sup>).<sup>7</sup>

Another distinction concerns the chemical nature of the organocatalyst. In this case we can identify four typologies, which include most of the organocatalysts: Lewis base, Lewis acid, Brønsted base or Brønsted acid.<sup>8</sup>

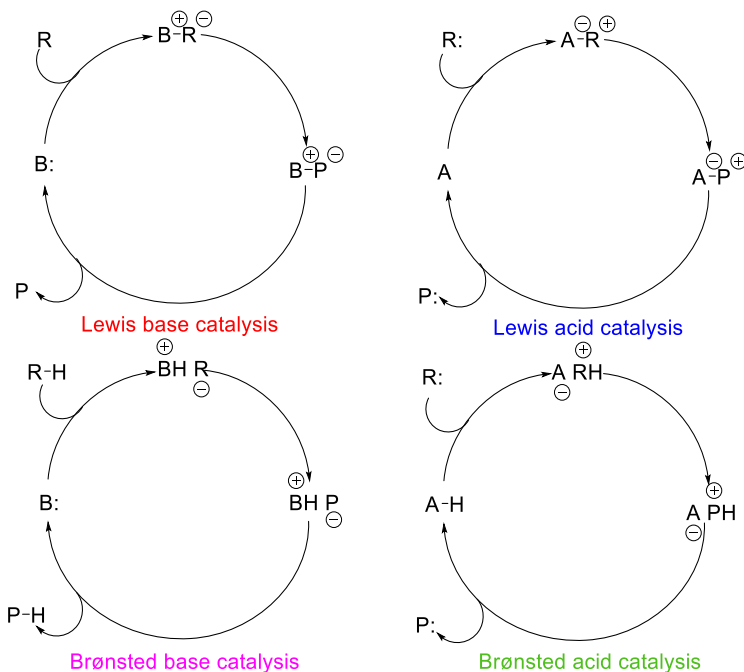
---

<sup>6</sup> D.W.C. MacMillan, *Nature* **2008**, 455, 304.

<sup>7</sup> A. Berkessel, H. Gröger, *Asymmetric Organocatalysis*, Wiley-VCH: Weinheim, **2005**.

<sup>8</sup> J. Seayad, B. List, *Org. Biomol. Chem.* **2005**, 3, 719.

A schematic illustration of the four corresponding catalytic cycles is depicted in Scheme 1.2. In the case of Lewis base catalysis we have, first of all, the nucleophilic addition of the catalyst (represented as B:) to the reagent (R). The so formed complex undergoes a reaction and then the product (P) and the catalyst are released. A Lewis acid catalyst (A) activates a nucleophilic substrate (R:) in a similar way, namely accepting its electron pair. Brønsted base and acid catalytic cycles start with a (partial) deprotonation or protonation, respectively. In the next two sections more detailed information about Brønsted base and hydrogen bond catalysis (which may be considered as the lower limit of the Brønsted acid catalysis) are illustrated.



**Scheme 1.2** Organocatalytic cycles according to the chemical nature of the catalyst.

### 1.2.1 Brønsted base catalysis

IUPAC defines a Brønsted base (BB) as “*a molecular entity capable of accepting a hydron (proton) from an acid (i.e. a 'hydron acceptor') or the corresponding chemical species.*”<sup>9</sup>

In organic transformations, proton transfer is the key step which activates one of the reaction components before a new bond is formed and the coupling of the reactants happens: Brønsted base catalysts help the reaction making reactants more nucleophilic.

In contrast with covalent interactions found in amine catalysis and hydrogen bonding interactions observed in BA catalysis (as illustrated in the next section), ion pairing are the most important interactions that are established between a substrate and a BB catalyst, thus falling in the field of non-covalent organocatalysis.

Dates back to 1912, thanks to the significant work of Bredig and Fiske, the discovery that simple cinchona alkaloids can act as chiral Brønsted base catalysts in promoting enantioselective reactions. By using quinine and quinidine in the reaction of HCN with benzaldehyde they obtained chiral cyanohydrins of opposite chirality, albeit with low *ee* ( $\leq 10\%$ ).<sup>10</sup> Other contributions arise from Wynberg, whose studies validated cinchona alkaloids as powerful chiral Brønsted bases.<sup>11</sup> Over the years the cinchona alkaloid scaffolds underwent numerous modifications and improvements,

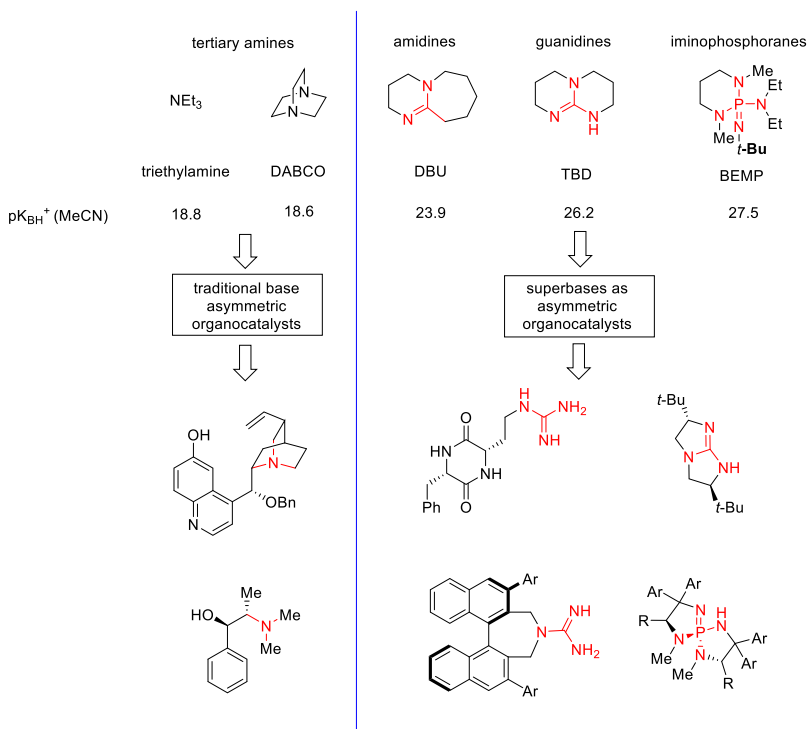
---

<sup>9</sup> IUPAC. Compendium of Chemical Terminology, 2nd ed. (the "Gold Book"). Compiled by A. D. McNaught and A. Wilkinson. Blackwell Scientific Publications, Oxford (1997). Online version (2019-) created by S. J. Chalk. ISBN 0-9678550-9-8. doi: 10.1351/goldbook.

<sup>10</sup> G. Bredig, W. S. Fiske, *Biochem. Z.* **1912**, 7.

<sup>11</sup> For examples, see: a) H. Wynberg, R. Helder, *Tetrahedron Lett.* **1975**, 16, 4057; b) K. Hermann, H. Wynberg, *J. Org. Chem.* **1979**, 44, 2238; c) H. Hiemstra, H. Wynberg, *J. Am. Chem. Soc.* **1981**, 103, 417.

thus rendering them efficiently suitable in a wide range of synthetic transformations and placing them among the privileged chiral motifs in asymmetric synthesis.<sup>12</sup> Recently a novel group of basic catalysts began to emerge, with the aim to satisfy the growing need for stronger basic functionalities in organic synthesis. Thus, in addition to tertiary amines, “organosuperbases” such as guanidines, amidines and iminophosphoranes, are among the most common structures found in Brønsted base catalysis. (Figure 1.2).

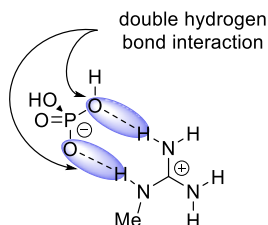


**Figure 1.2** Traditional Brønsted base and organosuperbases in organocatalysis.

<sup>12</sup> C. E. Song, *Cinchona Alkaloids in Synthesis and Catalysis: Ligands, Immobilization and Organocatalysis*, Wiley-VCH, Weinheim, 2009.

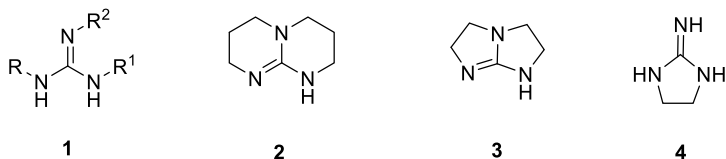


Guanidine motif is widely diffuse in nature. It is located for example in peptides, as part of the side chain of arginine, where is present in the protonated form and acts in the recognition of anionic substrates, such as carboxylate, nitronate and phosphate<sup>13</sup> stabilizing them through the formation of two parallel hydrogen bonds (Figure 1.3).



**Figure 1.3** Structure of methylguanidinium dihydrogenorthophosphate.

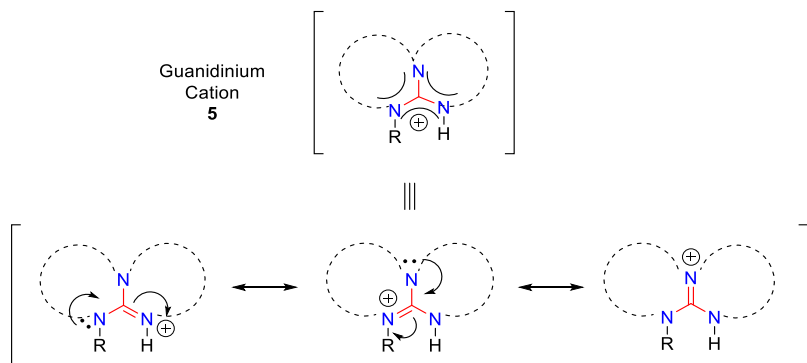
From a structural point of view, there is a distinction between three structure types: open-chain, monocyclic and bicyclic guanidines. Open-chain guanidines **1** present a more flexible structure if compared with others. Bicyclic structures are based on the 1,5,7-triazabicyclo[4.4.0]dec-5-ene (TBD, **2**) and 1,4,6-triazabicyclo[3.3.0]oct-4-ene (TBO, **3**) scaffolds, while monocyclic catalysts are based on imidazolidin-2-imine motif **4** (Figure 1.4).



**Figure 1.4** Structures of open-chain, bicyclic and monocyclic guanidine scaffolds.

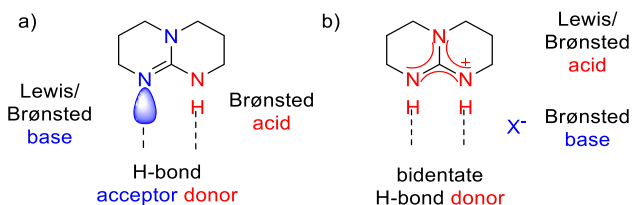
<sup>13</sup> (a) C. L. Hannon, E. V. Anslyn, *Bioorganic Chemistry Frontiers*; Springer-Verlag: Berlin, **1993**; Vol. 3. (b) F. P. Schmidtchen, M. Berger, *Chem. Rev.* **1997**, *97*, 1609.

Guanidine motif has character of a very strong organic base, a property connected to the resonance stability of its conjugate acid, the guanidinium cation **5** (Figure 1.5).<sup>14</sup>



**Figure 1.5** Localized and delocalized forms of the guanidinium cation.

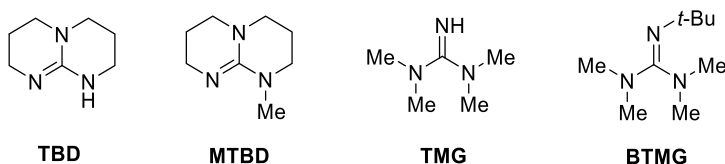
Guanidines and their corresponding guanidinium salts are endowed with a wide range of useful chemical functionalities: in addition to Brønsted basicity, free guanidines can be efficient Lewis bases as well as hydrogen-bond donors and acceptors (Figure 1.6, a). Moreover, guanidinium salts exhibit weak Brønsted acidity and are bidentate cationic hydrogen-bond donors (Figure 1.6, b).



**Figure 1.6** Potentially useful functionalities in free guanidine bases (a) and guanidinium salts (b) exemplified for TBD.

<sup>14</sup> Y. Yamamoto, S. Kojimai, S. *In The Chemistry of Amidines and Imidates*; S. Patai, Z. Rappoport, Eds.; John—Wiley & Sons: New York, **1991**; Vol. 2.

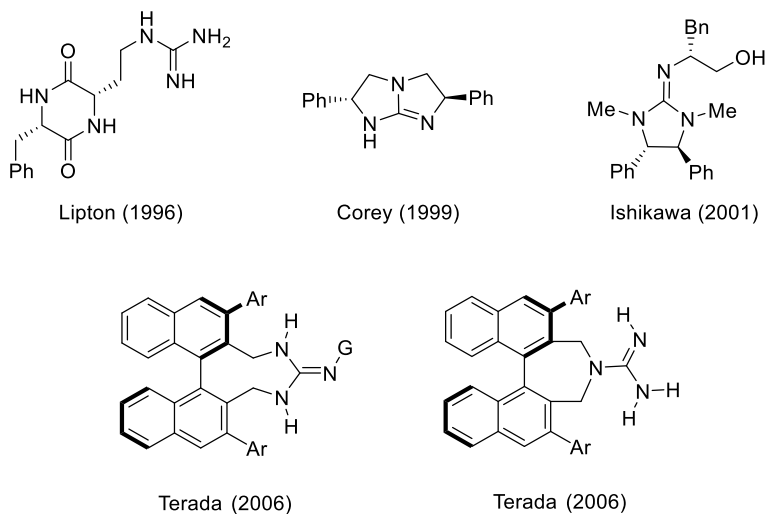
However, given their significant character of Brønsted basicity, guanidines are mainly used as Brønsted basic catalysts. Simple structures such as TBD, MTBD, (*N*-methyl-TBD), TMG (1,1,3,3-tetramethylguanidine), BTMG (2-*t*-butyl-1,1,3,3-tetramethylguanidine) are presumably the most used achiral guanidine catalysts, thus they are commercially available and are showed in Figure 1.7.



**Figure 1.7** Commercially available achiral guanidine bases.

Regarding instead asymmetric organocatalysis, since the initial studies of Lipton in 1996, a small but impressive collection of chiral guanidine-based catalysts continued to appear up to the present and they were successfully employed in a wide range of asymmetric transformations (Figure 1.8).<sup>15</sup>

<sup>15</sup> (a) M. S. Iyer, K. M. Gigstad, N. D. Namdev, M. Lipton, *J. Am. Chem. Soc.* **1996**, *118*, 4910. (b) E. J. Corey, M. J. Grogan, *Org. Lett.* **1999**, *1*, 157. (c) T. Ishikawa, Y. Araki, T. Kumamoto, H. Seki, K. Fukuda, T. Isobe, *Chem. Commun.* **2001**, 245; (d) M. Terada, H. Ube, Y. Yaguchi, *J. Am. Chem. Soc.* **2006**, *128*, 1454; (e) H. Ube, N. Shimada, M. Terada, *Angew. Chem. Int. Ed.* **2010**, *49*, 1858; (f) M. Terada, M. Nakano, H. Ube, *J. Am. Chem. Soc.* **2006**, *128*, 16044; (g) M. Terada, D. Tsushima, M. Nakano, *Adv. Synth. Catal.* **2009**, *351*, 2817; (h) M. Nakano, M. Terada, *Synlett* **2009**, 1670.



**Figure 1.8** Chiral guanidine catalysts.

Phosphazenes are another important class of superbases in organic synthesis acting as Brønsted-base catalysts, as mentioned above. The exceptional basicity of phosphazenes was reported for the first time in 1987 by Schwesinger.<sup>16</sup> The  $pK_a$  values are available for a large number of phosphazene-based structures and are the result of the pioneering work of Kaljurand's group.<sup>17</sup> They found that phosphazenes surpass in basicity the derivatives of guanidines, being their  $pK_a$  values within the range 26–47  $pK_a$  units. As for guanidines, the extraordinary basicity of these compounds was attributed to the great resonance stabilization of the corresponding acids. BEMP (see Figure 1.2) represents an example of achiral iminophosphorane base and it is commercially available. Over the years a variety of chiral iminophosphoranes, that can serve as organosuperbase catalysts for

<sup>16</sup> R. Schwesinger, H. Schlemper, *Angew. Chem. Int. Ed. Engl.* **1987**, 26, 1167.

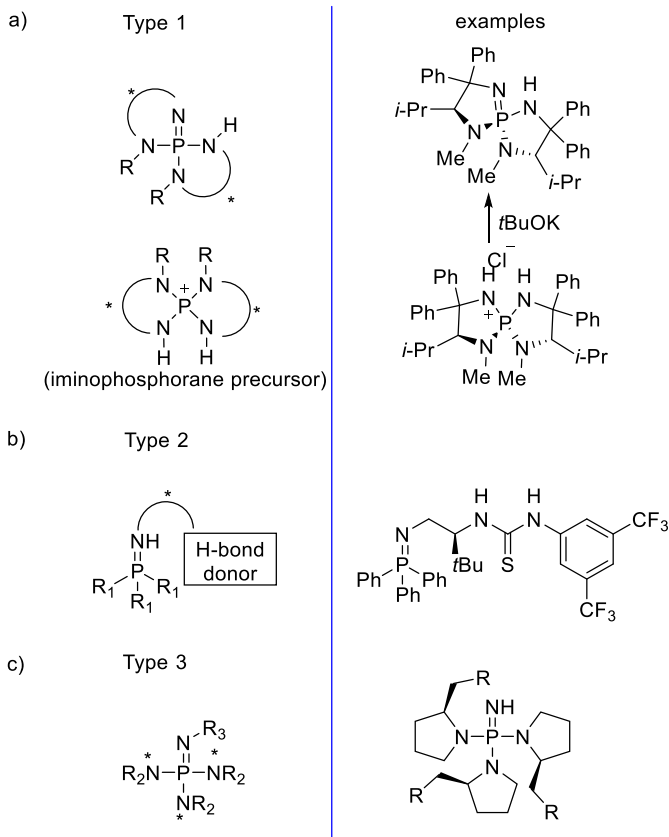
<sup>17</sup> I. Kaljurand, I. A. Koppel, A. Kütt, *Journal of Physical Chemistry A* **2007**, 111, 1245.

asymmetric synthesis, were successfully synthesized and applied in organic synthesis. They are classified into three main groups based on their structure.<sup>18</sup> When phosphorus is the central atom of a spirocyclic system, we talk about Type 1 iminophosphoranes. These are generally formed in situ, from the corresponding salts, by using an inorganic base which allows the N-H deprotonation (Figure 1.9, a). Type 2 iminophosphoranes possess an additional functional group capable of H-bond interactions, thus they are bifunctional systems (Figure 1.9, b) and they will be explored in paragraph 1.3. In Type 3 iminophosphoranes, the chiral group is present not on the imine moiety but on nitrogen atoms single-bonded to the phosphorous (Figure 1.9, c).

---

<sup>18</sup> H. Krawczyk, M. Dziegielewski, D. Deredas, A. Albrecht, Ł. Albrecht, *Chem. Eur. J.* **2015**, *21*, 10268.

## chiral iminophosphoranes



**Figure 1.9** Classification of chiral iminophosphoranes.

All structures illustrated in this section are useful Brønsted base catalysts in organic transformations. Classic examples of Brønsted base catalyzed reactions are the addition reaction of HCN to aldehydes for the synthesis of chiral cyanohydrins,<sup>19</sup> the Strecker reaction (see paragraph 1.3),<sup>20</sup> the Michael reaction of glycine

<sup>19</sup> (a) J. Oku, S. Inoue, *J. Chem. Soc., Chem. Commun.* **1981**, 229; (b) J.-I. Oku, N. Ito, S. Inoue, *Macromol. Chem.* **1982**, 183, 579; (c) K. Tanaka, A. Mori, S. Inoue, *J. Org. Chem.* **1990**, 55, 181.

<sup>20</sup> E. J. Corey, M. J. Grogan, *Org. Lett.* **1999**, 1, 157.

derivatives in the presence of a guanidine-based catalyst<sup>15c</sup> and the desymmetrization of cyclic *meso*-anhydrides.<sup>21</sup>

### 1.2.2 Hydrogen bond catalyzed reactions

As mentioned before, non-covalent organocatalysis is built just on non-covalent interactions, namely hydrogen bonds or ion pairs formation. Hydrogen bond interactions are able to activate electrophilic substrates (carbonyl compounds, imines,...) toward attack from a nucleophilic reagent. Thus hydrogen bonding represents, together with iminium ion formation in covalent catalysis and substrate coordination to a metallic Lewis acid center, an activation strategy to increase electrophilicity of the substrates (Scheme 1.3).<sup>22</sup>

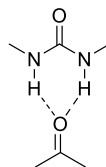
Electrophilic activation by ...



... iminium ion formation



... coordination to metal Lewis-acid



... hydrogen bonding

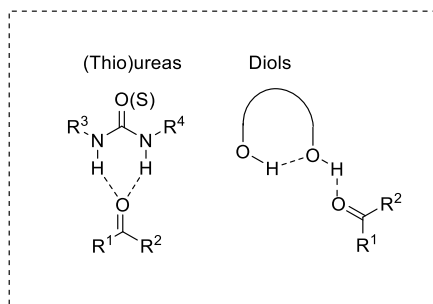
**Scheme 1.3** Electrophilic activation of the carbonyl group by iminium ion formation, coordination to metal Lewis-acid and hydrogen bonding.

All these three cases result in a lowering of LUMO energy of the electrophilic reagent, thus facilitating the reaction. Among various interaction-types, hydrogen-bond represents a powerful tool which is

<sup>21</sup> (a) Y. Chen, S.-K. Tian, L. Deng, *J. Am. Chem. Soc.*, **2000**, *122*, 9542; (b) S.-K. Tian, Y. Chen, J. Hang, L. Tang, P. Mcdaid, L. Deng, *Acc. Chem. Res.*, **2004**, *37*, 621.

<sup>22</sup> (a) P. M. Pihko, *Hydrogen Bonding in Organic Synthesis*, Wiley-VCH: Weinheim **2009**; (b) M. S. Taylor, E. N. Jacobsen, *Angew. Chem. Int. Ed.* **2006**, *45*, 1520; (c) X. You, W. Wang, *Chem. Asian. J.* **2008**, *3*, 516.

able to activate Lewis basic substrates through general acid catalysis. In general compounds such as ureas, thioureas and diols are classified as hydrogen-bonding catalysts (Figure 1.10).



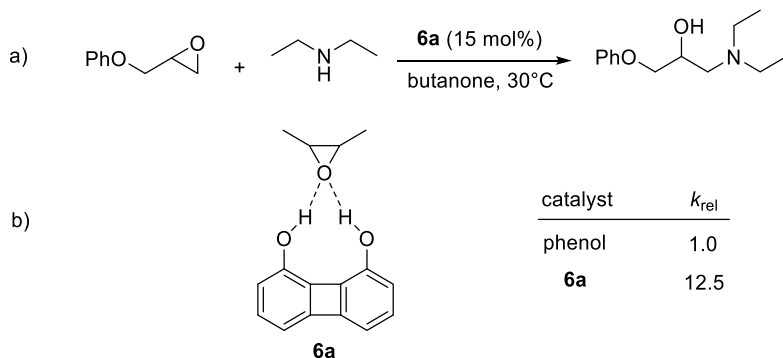
**Figure 1.10** Hydrogen-bonding catalysts.

The ability of hydrogen-bond donors to promote organic reactions was established in 1942, when Wassermann observed beneficial effect on Diels–Alder reactions in the presence of phenols or carboxylic acids.<sup>23</sup> Pioneering studies by Hine’s group identified 1,8-biphenylene diol **6a** as an efficient catalyst for epoxides activation toward nucleophilic attack by diethylamine (Scheme 1.4, a).<sup>24</sup> The reaction catalyzed by this diol was found to be about 13 times faster than the same reaction catalyzed by phenol: authors proposed that the enhanced activity of biphenylenediol in solution compared to phenol derived from the possibility, in the case of **6a**, to act as a double H-bond donor toward the electrophile (Scheme 1.4, b). This hypothesis was also supported with a solid-state 1:1 structure of the catalyst and the substrate.

<sup>23</sup> A. Wassermann, *J. Chem. Soc.* **1942**, 618.

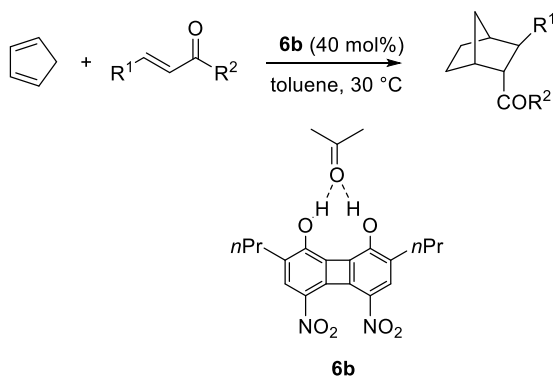
<sup>24</sup> (a) J. Hine, S. -M. Linden, V. M. Kanagasabapathy, *J. Am. Chem. Soc.* **1985**, *107*, 1082; (b) J. Hine, S. Hahn, D. E. Miles, K. Ahn, *J. Org. Chem.* **1985**, *50*, 5092; (c) J. Hine, S. -M. Linden, V. M. Kanagasabapathy, *J. Org. Chem.* **1985**, *50*, 5096; (d) J. Hine, S. Hahn, D. E. Miles, *J. Org. Chem.* **1986**, *51*, 577.





**Scheme 1.4** Biphenylenediol-promoted epoxide-opening reaction.

In 1990 Kelly extended these notions to carbonyl compounds, thus discovering that the related biphenylenediol **6b** was able to promote Diels-Alder reactions between cyclopentadiene and  $\alpha,\beta$ -unsaturated carbonyl dienophiles thanks to the coordination, through H-bonds formation, of the electrophilic reagent, thus increasing its reactivity (Scheme 1.5).<sup>25</sup>



**Scheme 1.5** Diol-catalyzed Diels-Alder reaction.

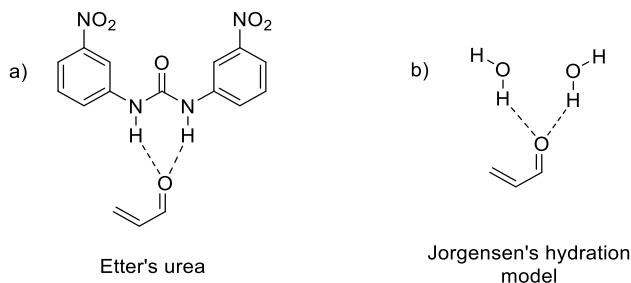
<sup>25</sup> T. R. Kelly, P. Meghani, V. S. Ekkundi, *Tetrahedron Lett.* **1990**, *31*, 3381.

A great number of studies was carried out over the years, thus leading to the development of new Brønsted acid catalysts and in particular to the discovery of several types of hydrogen-bond donors, such as ureas and thioureas. Particular attention has been paid to these derivatives thanks to their ability in molecular recognition by establishing H-bond interactions. They are able to recognize nitrates, carboxylic and sulfonic acids and other anions through multi-hydrogen bonds. Several years ago, different groups reported that urea and thiourea not only recognize organic compounds but could also activate them, thus acting as acid catalysts: the discovery is due to Etter and co-workers, who observed that diaryl urea possessing electron-withdrawing substituents is able to form cocrystals with a variety of proton acceptors such as nitroaromatic compounds, ethers, carbonyl compounds and sulfoxides (Figure 1.11, a).<sup>26</sup> Concomitantly, Jorgensen proved that for Diels–Alder and other pericyclic reactions the coordination of two water molecules to the carbonyl function results in an enhancement of the reaction rate (Figure 1.11, b).<sup>27</sup> X-ray structural studies also confirmed this hypothesis.<sup>26b</sup>

---

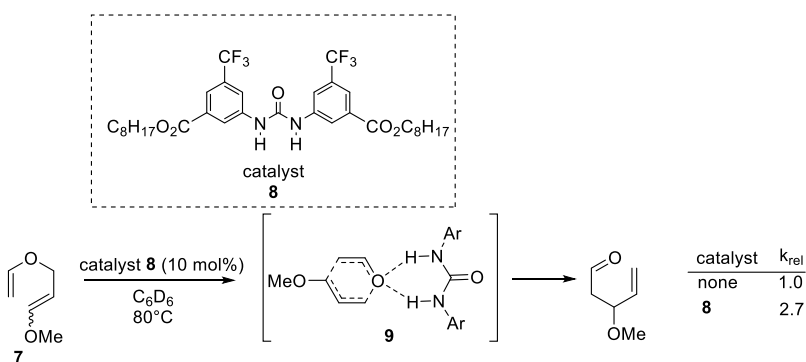
<sup>26</sup> (a) M. C. Etter, Z. Urbańczyk-Lipkowska, M. Zia-Ebrahimi, T. W. Panunto, *J. Am. Chem. Soc.* **1990**, *112*, 8415; (b) M. C. Etter, *Acc. Chem. Res.* **1990**, *23*, 120; (c) M. C. Etter, *J. Phys. Chem.* **1991**, *95*, 4601.

<sup>27</sup> (a) J. F. Blake, W. L. Jorgensen, *J. Am. Chem. Soc.*, **1991**, *113*, 7430; (b) J. F. Blake, D. Lim, W. L. Jorgensen, *J. Org. Chem.*, **1994**, *59*, 803.



**Figure 1.1** Bis hydrogen-bond interactions.

Curran and Kuo were the first, in 1994, to use urea derivatives with the aim to promote an organic reaction: they demonstrated, by combining the ideas of Kelly, Etter and Jorgensen, that urea **8** is a competent organic catalyst in the allylation of cyclic sulfinyl radicals with allyltributylstannane<sup>28</sup> and for the Claisen rearrangement of allyl vinyl ethers.<sup>29</sup> In the latter case, the bis hydrogen-bonded transition state model **9** was introduced in order to explain the accelerating effect of the urea **8** in the Claisen rearrangements of the ether **7** (Scheme 1.6).

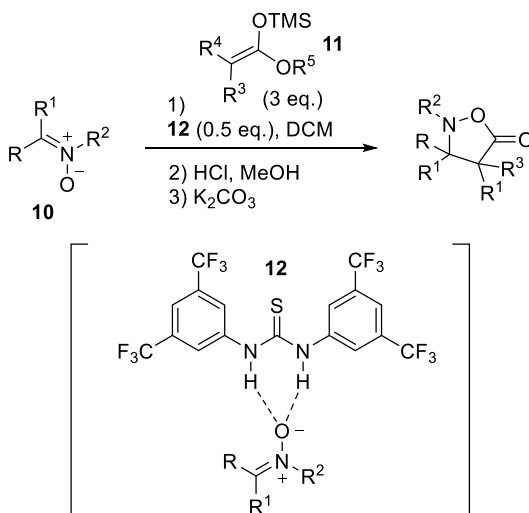


**Scheme 1.6** Claisen rearrangement catalyzed by achiral urea **8**.

<sup>28</sup> D. P. Curran, L. H. Kuo, *J. Org. Chem.*, **1994**, *59*, 3259.

<sup>29</sup> D. P. Curran, L. H. Kuo, *Tetrahedron Lett.*, **1995**, *36*, 6647.

Based on Curran's studies, Schreiner and colleagues developed the electron-deficient thiourea **12** that has become a powerful tool in organocatalytic field, promoting Diels-Alder and dipolar cycloaddition reactions for example.<sup>30</sup> In Scheme 1.7 is represented the nucleophilic addition of ketene silyl acetals **11** to nitrones **10** thanks to the activation of the electrophilic reagent by double hydrogen-bond interaction with **12**.<sup>31</sup>



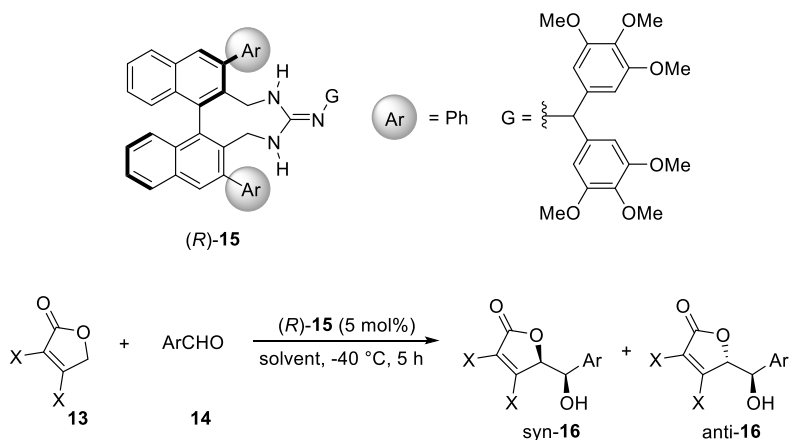
**Scheme 1.7** Nucleophilic addition of ketene silyl acetals to nitrones.

As concerns asymmetric transformations catalyzed by chiral organic molecules, the formation of H-bonded complexes results in a very well-organized three-dimensional environment and a subsequent improvement in the stereochemical outcome of the reaction. Wynberg reported, in 1981, that the cinchona alkaloids quinine, quinidine, cinchonine and cinchonidine, each of which bearing free

<sup>30</sup> (a) A. Wittkopp, P. R. Schreiner, *Chem. –Eur. J.*, **2003**, *9*, 407; P. R. Schreiner, *Chem. Soc. Rev.*, **2003**, *32*, 289; (c) P. R. Schreiner, A. Wittkopp, *Org. Lett.*, **2002**, *4*, 217.

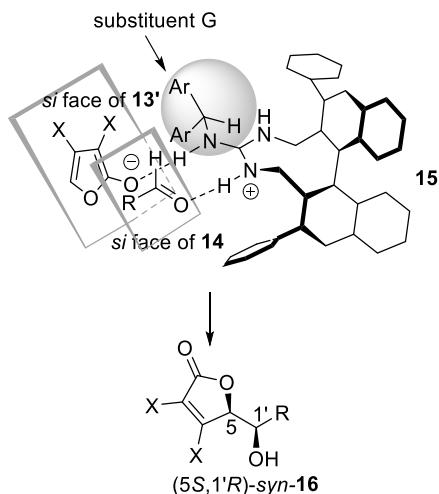
<sup>31</sup> T. Okino, Y. Hoashi, Y. Takemoto, *Tetrahedron Lett.*, **2003**, *44*, 2817.

OH groups in proximity to the basic quinuclidine nitrogen, catalyze enantioselective conjugate addition reactions to carbonyl compounds. Also guanidinium ions can successfully act as dual hydrogen-bond donor scaffolds (see Figure 1.3). The bidentate nature of the binding interaction is particularly attractive because it removes some conformational degrees of freedom, so they constitute an appealing type of suitable organocatalysts. One challenge in the design of chiral guanidinium catalysts is that stereochemical elements can often be introduced at sites remote from the planar active site. To overcome this obstacle, Terada prepared guanidines which contain an axially chiral binaphthyl backbone that positions the 3 and 3' aryl substituents in proximity to the active site (see Figure 1.8). These molecules functioned as an efficient catalyst for the vinylogous aldol reaction of dibromofuranone **13** with a range of aromatic aldehydes **14**.<sup>15c</sup> The corresponding products **16** were obtained in high yields, with good diastereocontrol and excellent enantioselectivities for the *syn*-isomer (Scheme 1.8).



**Scheme 1.8** Vinylogous aldol reaction of dihalofuran-2(5H)-ones with aromatic aldehydes catalyzed by **15**.

Authors proposed the following transition state model in order to explain the *syn*-selectivity: a guanidinium ion, generated by the deprotonation of the furanone derivative, would interact not only with this anion **13'** but also with the aldehyde **14**, thus creating a double hydrogen-bond interaction (Figure 1.12). Furthermore, the anionic derivative **13'** is close to substituent G of the catalyst **15** in the transition state. The observed stereoselectivity can be explained with this transition state model, in which the aldehyde **14** would approach **13'** from the far side of substituent G, while keeping away from the phenyl substituent at the 3,3'-positions of the binaphthyl backbone. Moreover, the aldehyde would avoid the steric repulsion between its R substituent and the X substituent at the C4 position of the furan ring. In this way, the *si*-face of aldehyde can be attacked by the nucleophile, thus giving the *syn*-product **16**.



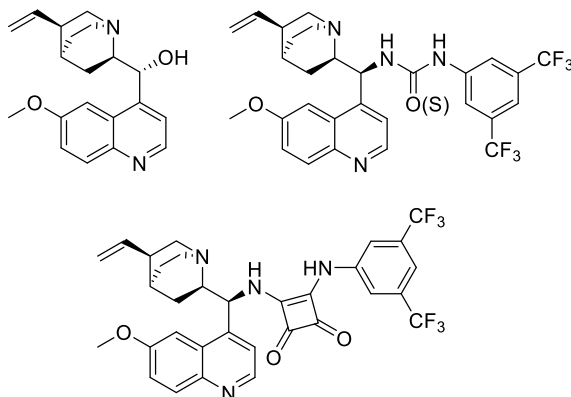
**Figure 1.12** Plausible transition state of *syn*-selective vinylogous aldol reaction.

### 1.3 Bifunctional organocatalysis

A large number of the known organocatalysts are endowed with more than one active center, thus falling in the field of bifunctional organocatalysis. These catalysts usually have a Brønsted acid and a Brønsted/Lewis basic centre. This design allows the activation of both pronucleophile, via deprotonation, and electrophile, via H-bonding interactions. Furthermore it positions the two reactants in a close proximity, allowing a faster and more selective conversion toward products. In this way, in fact, an acceleration of the reaction is generally observed, since substrates are closer each other and is more restricted the space in which the reaction occurs. Moreover, an improvement in the stereochemical outcome of the reaction arises, given the transition state geometrically well-organized and rigid. Hydrogen-bond interactions are the forces that most frequently stabilize the intermediates and the transition state by forming definite geometries and increasing the reaction rate.

The most simple example of bifunctional organocatalysts are represented by cinchona alkaloids. In fact quinine, quinidine, cinchonine and cinchonidine have in their structures a tertiary quinuclidine nitrogen, that represents the basic center, and an hydroxyl group, namely an H-bond donor group, that constitutes the Brønsted-acid center. One particular class of catalysts, that has received considerable attention, is that of the bifunctional Brønsted base/H-bond donor organocatalysts. These catalysts typically possess both a tertiary amine group, such as cinchona alkaloid-derived amines, and an efficient hydrogen-bond donor group, such

as urea, thiourea, (thio)squaramide or sulphonamide, appropriately positioned on a chiral scaffold (Figure 1.13).



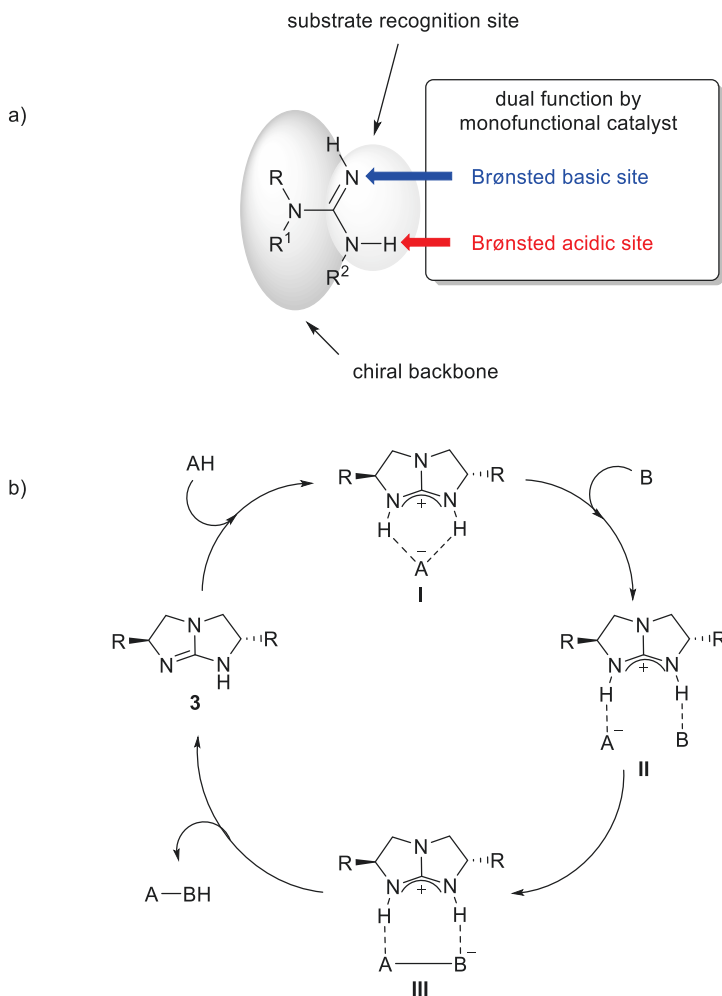
**Figure 1.13** Examples of some classes of bifunctional organocatalysts.

Although this class continues to demonstrate synthetic utility, it is not without limitations: reaction times could be often long, even with the most reactive reagent combinations, and the range of pronucleophiles and electrophiles employable could be sometimes limited. These problems arise from the relatively weak Brønsted basicity of the tertiary amine moiety, thus providing an insufficient activation of the pronucleophile.

In these cases the use of more active catalysts is desirable. An important class of powerful bifunctional organocatalysts is represented by the guanidine-based catalysts, as mentioned above. These compounds are monofunctional catalysts but endowed with an acid/base dual function: after deprotonation of the pronucleophile, they capture nucleophilic reagents through hydrogen-bond interactions. Moreover, the NH proton acts as a Brønsted acid, namely it is able to activate an electrophilic reagent (Scheme 1.9, a). Mechanistically, most of guanidine Brønsted base catalyst, thanks to



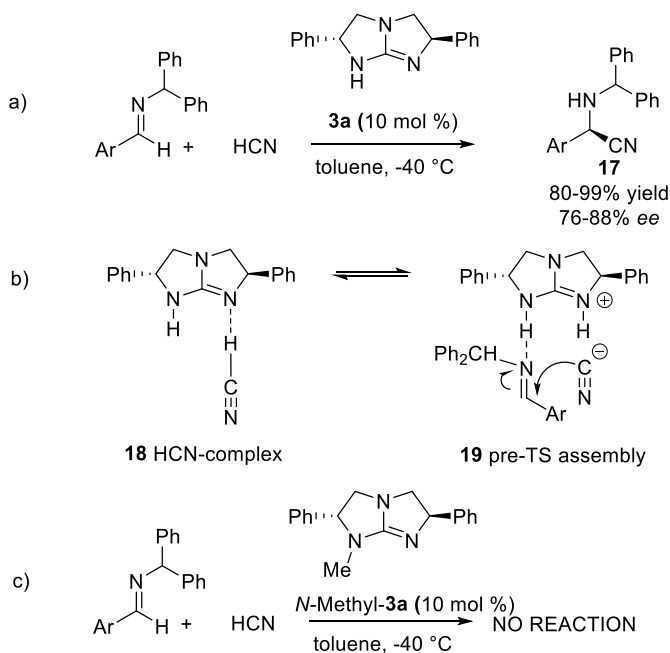
the aforementioned features, operate through the following mechanism: firstly the free guanidine base **3** deprotonates the substrate AH forming the hydrogen-bonded ion pair **I**. The pre-coordination of the second substrate B to the guanidinium cation, through a second hydrogen-bond interaction, leads to the pre-transition state complex **II**. After the reaction between the two reagents, an hydrogen-bonded product complex **III** is formed. The following re-protonation releases the product and reintroduces the base in the catalytic cycle (Scheme 1.9, b). In this way, guanidine Brønsted bases generally catalyze addition reactions.



**Scheme 1.9** (a) Catalytic design of chiral guanidine bases. (b) General mechanism of guanidine Brønsted base organocatalysis.

The Strecker reaction is a classic example of Brønsted base catalyzed reaction. The first organocatalyzed enantioselective Strecker reaction arises from the studies of Corey and Grogan in 1999.<sup>15a</sup> They reported the C<sub>2</sub>-symmetric guanidine compound **3a** as an efficient catalyst of the process (Scheme 1.10, a). They suggested that in the

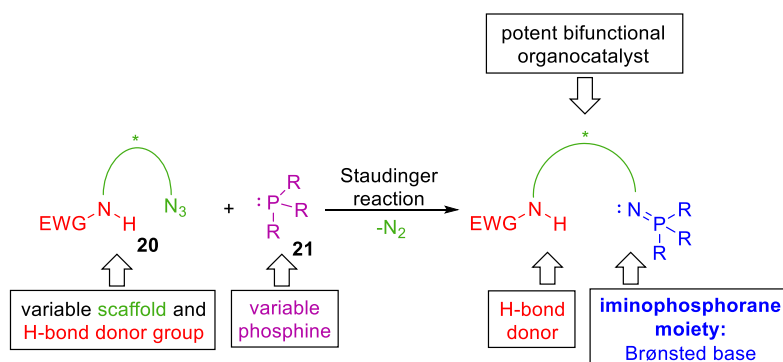
first step of the catalytic cycle an hydrogen bond interaction is established between HCN and the catalyst, resulting in the guanidinium cyanide complex **18**. A subsequent increase in acidity of the NH proton of the catalyst allows donation of a hydrogen bond to the aldimine to form the pre-transition-state termolecular assembly **19**. The subsequent attack of the cyanide ion to the hydrogen-bond activated aldimine affords the Strecker addition product (*R*)-**17** (Scheme 1.10, b). Authors demonstrated the importance of hydrogen-bond formation by using the corresponding *N*-methyl-**3a** catalyst, which has proved to be an entirely inactive catalyst in the reaction (Scheme 1.10, c).



**Scheme 1.10** (a) Enantioselective Strecker reaction catalyzed by guanidine **3a**; (b) Catalytic action of **3a**; (c) No reaction occurs when *N*-Methyl-**3a** catalyst is used.

Recently Dixon's group developed a new class of bifunctional organocatalysts that possess an even stronger Brønsted basic group (see Figure 1.2 for  $pK_a$  values of iminophosphoranes).<sup>32</sup>

He combined the synergistic effects of a stronger Brønsted base and an H-bond donor, thus synthesizing an elegant class of new catalysts with high reactivity and selectivity. They exploited the Staudinger reaction of a triarylphosphine **21** and an enantiopure organoazide **20**, possessing an H-bond donor group, in order to create a strongly Brønsted basic iminophosphorane moiety through the favorable loss of dinitrogen gas (Scheme 1.11).



**Scheme 1.11** Concept and design of a new class of bifunctional iminophosphorane-based organocatalysts.

A wide range of bifunctional (thio)ureas were synthesized and successfully applied to the nitro-Mannich reaction of nitromethane with *N*-Diphenylphosphinoyl ketimines.<sup>32</sup>

<sup>32</sup> M. G. Núñez, A. J. M. Farley, D. J. Dixon, *J. Am. Chem. Soc.* **2013**, *135*, 16348.

## 2. ONE-POT TRANSFORMATIONS IN ORGANIC SYNTHESIS

### 2.1 One-pot strategy<sup>33</sup>

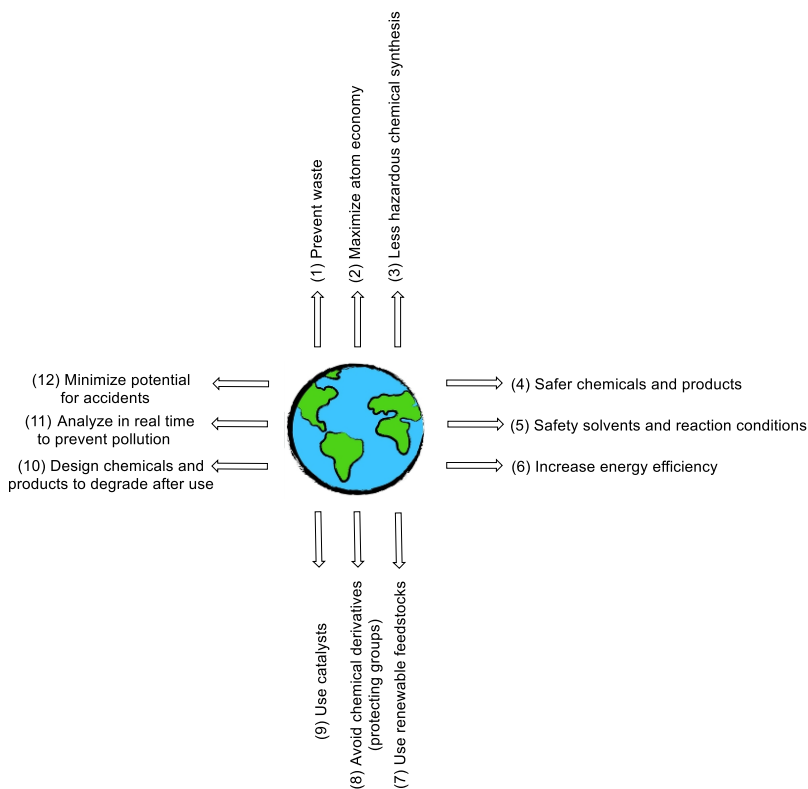
Pollution and waste disposal problems require a chemical synthesis to be efficient and environmentally sustainable. The synthesis of structurally complex target molecules is often based on a “stop and go” sequence of individual reactions, which involves tedious isolation processes, thus wasting time, energies, solvents and other resources. However, inspired by nature, considering in particular the ability of biological systems to carry out the synthesis of elaborate molecules through successive transformations but in a continuous process (enzymatic transformations are a significant example),<sup>34</sup> chemists have focused interest in developing new strategies that allow access to structurally complex scaffolds in a convenient way. A powerful approach to achieve this goal is the development of catalytic methodologies which enable a consecutive multiple-bond formation. When possible, an effective approach is to perform several chemical reactions in a single reaction vessel, namely operate a one-pot transformation. It is effective because, carrying out several synthetic transformations and bond-forming steps in a single pot, it allows to avoid separation processes and purification of reaction intermediates, thus minimizing chemical waste, saving time and

---

<sup>33</sup> Y. Hayashi, *Chem. Sci.*, **2016**, *7*, 866.

<sup>34</sup> For reviews on this topic, see: (a) J. Staunton, K. Weissman, *J. Nat. Prod. Rep.* **2001**, *18*, 380. (b) C. Khosla, R. S. Gokhale, J. R. Jacobsen, D. E. Cane, *Annu. Rev. Biochem.* **1999**, *68*, 219. (c) C. Khosla, *Chem. Rev.* **1997**, *97*, 2577.

simplifying practical aspects. One-pot reactions embody some of the principles of green chemistry, so they are a powerful tool that can be used in order to conduct a synthesis in a greener fashion (Figure 2.1).<sup>35</sup>

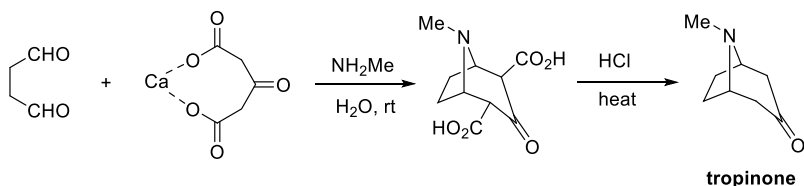


**Figure 2.1** 12 principles of green chemistry.

A milestone in organic chemistry is the one-pot synthesis of tropinone, developed by Robinson over 100 years ago exploiting a double Mannich reaction (Scheme 2.1).<sup>36</sup>

<sup>35</sup> P. T. Anastas, J. C. Warner, *Green Chemistry—Theory and Practice*, Oxford University Press, Oxford, **1998**.

<sup>36</sup> R. Robinson, *J. Chem. Soc., Trans.*, **1917**, 762.



**Scheme 2.1** Robinson's one-pot synthesis of tropinone.

From this first case, many other examples involving one-pot reactions have been elegantly utilized over the year for the synthesis of biological products, such as progesterone,<sup>37</sup> endiandric acid<sup>38</sup> and proto-daphniphylline.<sup>39</sup>

### 2.1.1 Tandem reactions

Different terms can be used to describe multi-step reactions taking place in one-pot way. *Domino*, *cascade* and *tandem reaction* are synonyms and are the terms commonly used to indicate this strategy approach.

Tietze defined a *domino reaction* as a “*process involving two or more bond-forming transformations (usually C-C bonds) which take place under the same reaction conditions without adding additional reagents and catalysts, and in which the subsequent reactions result as a consequence of the functionality formed in the previous step*”.<sup>40</sup>

In the strictest definition of the term, the reaction conditions remain unchanged between the successive steps and no other reagents and catalysts are added after the initial step (Figure 2.2, a). On the

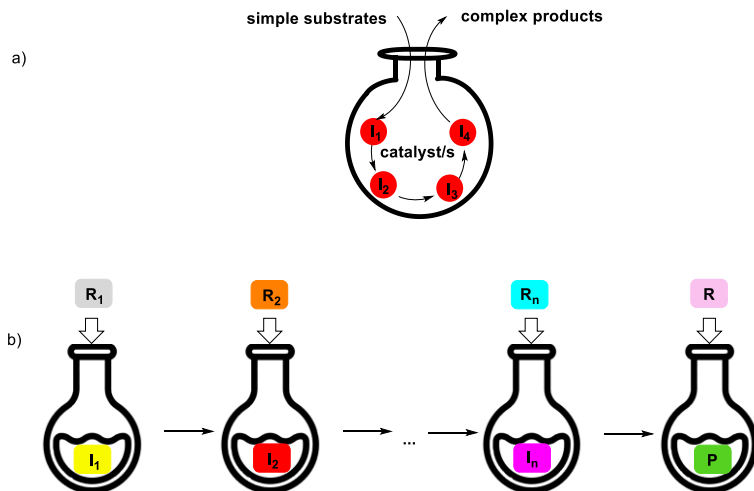
<sup>37</sup> W. S. Johnson, M. B. Gravestock, B. E. McCarry, *J. Am. Chem. Soc.*, **1971**, 93, 4332.

<sup>38</sup> K. C. Nicolaou, N. A. Petasis, R. E. Zipkin, J. Uenishi, *J. Am. Chem. Soc.*, **1982**, 104, 5555.

<sup>39</sup> S. Piettre, C. H. Heathcock, *Science*, **1990**, 248, 1532.

<sup>40</sup> L. F. Tietze, *Chem. Rev.* **1996**, 96, 115.

contrary, one-pot procedures similarly allow two or more reactions to be carried out consecutively, avoiding isolation and purification of intermediates, but the addition of new reagents or the change of conditions after the first reaction are permitted (Figure 2.2, b). Thus, any cascade reaction is also a one-pot procedure, while the opposite is not always valid.



**Figure 2.2** (a) General scheme for a tandem process; (b) Scheme for a general one-pot transformation.

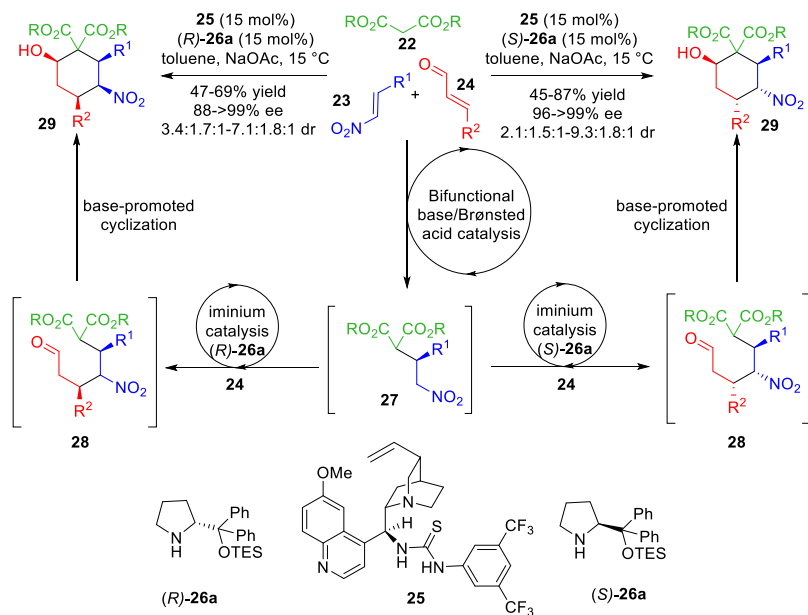
Although often intramolecular transformations are involved, cascade reactions can also occur intermolecularly, thus falling in the field of multicomponent reactions.

By mixing for example the fields of covalent aminocatalysis and bifunctional base/Brønsted acid catalysis, a cascade sequence for the synthesis of highly functionalized cyclohexanes has been successfully developed by Dixon (Scheme 2.2).<sup>41</sup> In the

<sup>41</sup> Y. Wang, R.-G. Han, Y.-L. Zhao, S. Yang, P.-F. Xu, D. J. Dixon, *Angew. Chem. Int. Ed.* **2009**, *48*, 9834.



methodology, firstly, malonate ester **22** and nitroalkene **23** were preferentially activated by bifunctional thiourea catalyst **25**, with the consequent stereoselective formation of the Michael adduct **27**. Then the cyclic secondary amine catalyst (*S*)-**26a** activates, via iminium ion formation, the  $\alpha,\beta$ -unsaturated aldehyde **24** toward nucleophilic attack from adduct **27**, resulting in the regioselective formation of the second Michael adduct **28**. This intermediate **28** then undergoes a base-promoted aldol cyclization to afford the desired functionalized cyclohexane **29** in good yield, with moderate diastereoselectivity and high enantiomeric excesses. Moreover, the use of enantiomer *R* of the chiral secondary amine catalyst **26a**, leads to the preferential formation of the product **29** with all substituents in a *cis* relationship.



**Scheme 2.2** Triple domino Michael/Michael/cyclization multicomponent reaction for the synthesis of polysubstituted cyclohexanes.

This is an elegant example of a multicomponent cascade reaction, promoted by two catalysts. As shown in the scheme, there are no interferences coming from the outside, but all catalysts and reagents are present from the beginning and each reaction is just a consequence of the previous step. A lot of other examples regarding the synthesis of complex molecular scaffolds through cascade reactions can be found to date in the literature.<sup>42</sup>

### 2.1.2 One-pot synthesis: applications and limitations

Several considerations must be taken into account in the design of a multistep synthesis. Firstly, for the realization of a multistep process, the retrosynthesis of the target molecule allows the choice of the appropriate reagents and of the optimal reaction conditions in order to minimize waste of resources, according to the principles of green chemistry (see Figure 2.1). The reaction sequence is accurately designed according to the principles of step and redox economy, namely trying to minimize the number of reaction steps to a target molecule, as proposed by Wender,<sup>43</sup> and unnecessary changes in the oxidation states of intermediates, as suggested by Baran and Hoffman.<sup>44</sup> Then the reaction conditions are opportunely selected in accordance with atom economy, that is producing the smallest amount of byproducts.<sup>45</sup> Finally, when feasible, carry out all reaction

---

<sup>42</sup> (a) Y. Wang, H. Lu, P. -F. Xu, *Acc. Chem. Res.* **2015**, *48*, 1832; (b) P. Chauhan, S. Mahajan, D. Enders, *Acc. Chem. Res.* **2017**, *50*, 2809.

<sup>43</sup> (a) P. A. Wender, M. P. Croatt, B. Witulski, *Tetrahedron* **2006**, *62*, 7505; (b) P. A. Wender, V. A. Verma, T. J. Paxton, T. H. Pillow, *Acc. Chem. Res.* **2008**, *41*, 40; (c) P. A. Wender, *Nat. Prod. Rep.* **2014**, *31*, 433.

<sup>44</sup> N. Z. Burns, P. S. Baran, R. W. Hoffmann, *Angew. Chem. Int. Ed.* **2009**, *48*, 2854.

<sup>45</sup> (a) B. M. Trost, *Science* **1991**, *254*, 1471; (b) B. M. Trost, *Angew. Chem. Int. Ed.*, **1995**, *34*, 259.

steps in a single pot is highly desirable, since without isolation or purification of the intermediates, the amounts of solvents, waste, time, labour and cost is significantly reduced. The one-pot synthesis of (-)-oseltamivir is a wonderful example of the great potential of a one-pot synthesis (see Section 2.2).

Several reaction-types could give better results if conducted in a one-pot fashion. These cases are listed below.

- The intermediate compound is unstable:



**Scheme 2.2**

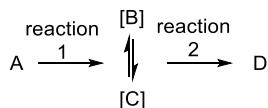
When the reaction of A to provide the product C proceeds via B, that is an unstable compound, the isolation of B results in a lower yield. Thus, carrying out both successive reactions in the same pot, will lead to a better yield (Scheme 2.2). An example of this case can be found in the Hayashi one-pot synthesis of (-)-oseltamivir.<sup>46</sup> In fact the Michael adduct **32**, obtained with excellent diastereo- and enantioselectivity, undergoes isomerization with subsequent reduced syn/anti selectivity in response to a purification procedure (see Scheme 2.7). Thus, a one-pot reaction sequence was essential for an optimal result concerning product **32**.

- The intermediate is a smelly, hazardous or toxic substance: the possibility to carry out experiments without the need to isolate intermediates with bad smells or with high risks represents a great

<sup>46</sup> T. Mukaiyama, H. Ishikawa, H. Koshino, Y. Hayashi, *Chem. Eur. J.* **2013**, *19*, 17789.

advantage in terms of security and health.

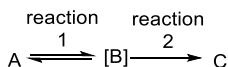
- An equilibrium exists between intermediate compounds:



**Scheme 2.3**

For reactions going from A to D in which interchangeable intermediates B and C, both able to produce the desired product D, are observed, there is no need to isolate these intermediates. In fact from them, the same product will be obtained (Scheme 2.3).

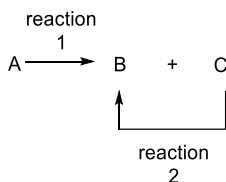
- The starting material and the intermediate compound are in equilibrium:



**Scheme 2.4**

When the intermediate B exists in equilibrium with the starting material A, conducting the reaction in a one-pot fashion will result in a better results in terms of yield and selectivity if compared with the same reaction conducted in a two-pot isolated sequence (Scheme 2.4). For example in a multicatalyst sequence, in which reaction 1 and reaction 2 are promoted by different catalytic species, after the formation of the intermediate B, this will be subtracted from the reaction medium to give the product C thanks to the action of the second catalyst. This will prevent the equilibration between A and B with following improved results at the end of the reaction, for example in terms of enantioselectivity of the product C.

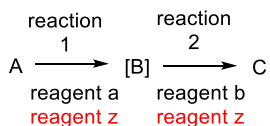
- A conversion between side-products of the reaction with intermediate compound or final product is possible:



Scheme 2.5

When a reaction leads to product B and side product C, and C is also convertible to B through a second reaction, both reactions 1 and 2 can be carried out successively in the same reactor, thus avoiding the separation of the two compounds B and C (Scheme 2.5). In the one-pot synthesis of (-)-oseltamivir by Hayashi group, both side-products **35** and **36** can be conveniently transformed into the desired product **34** by treating with  $\text{Cs}_2\text{CO}_3$  in EtOH in the same reaction vessel (see Scheme 2.7)<sup>46</sup>.

- The same reagents are employed in subsequent reactions:



Scheme 2.6

If the same reagent (**reagent z** in Scheme 2.6) is involved in successive reactions, it is advantageous to perform these reactions in the same pot (Scheme 2.6). An example can be found again in the synthesis of (-)-oseltamivir, in which cesium carbonate was utilized as base in five different transformations (see Scheme 2.7).<sup>46</sup>

The one-pot approach is convenient, but it has to be designed very carefully: the generation of by- and side-products has to be minimized, since their accumulation could affect following reactions and could also reduce yields. The solvent choice is crucial since, if a change of solvent is required during the synthesis, that employed in the previous step must have a low boiling point, in order to allow the easy removal from the reaction mixture. Finally, the use of reagents with a low boiling point and in stoichiometric amounts with respect to the reactant is highly desirable. In alternative, the remaining reagents can be deactivated before employing the next reaction conditions. In summary, reactions with few by- and side-products are conveniently suitable for one-pot synthetic sequences, in particular those that proceed with stoichiometric amount of the different reagents and that involve the use of low boiling solvents. If some undesired products or reagents remain in the reaction mixture, the reactivity of these compounds can be controlled by adding opportune additives which allow the next reaction or reactions to work successfully. Thus, a one-pot sequence is not a simple combination of separately optimized reaction conditions, it cannot be improvised, but requires intelligence and a deep knowledge of chemistry.

## 2.2 One-pot synthesis of (-)-oseltamivir

A lot of drugs can be conveniently synthesized exploiting one-pot approaches.<sup>46,47</sup> An elegant example is represented by the one-pot synthesis of (-)-oseltamivir, an highly functionalized cyclohexene,

---

<sup>47</sup> For selected examples, see: (a) H. Ishikawa, M. Honma, Y. Hayashi, *Angew. Chem. Int. Ed.* **2011**, *50*, 282; (b) Y. Hayashi, D. Sakamoto, D. Okamura, *Org. Lett.* **2016**, *18*, 4.

developed by Hayashi's group. They firstly reported a two-pot synthesis of the target molecule<sup>48</sup> and subsequently improved their synthesis by developing a one-pot strategy, consisting of nine reactions steps, with 36% overall yield (Scheme 2.7).<sup>46</sup> All steps occur in just one reactor, with reaction conditions changed only six times over nine reaction steps.

The diphenylprolinol silyl ether catalyst **26** promotes the asymmetric formation of Michael adduct **32** starting from  $\alpha$ -alkoxyaldehyde **30** and (*Z*)-*N*-2-nitroethenylacetamide **31**. The adduct **32** shows some instability, due to the facile isomerization, thus conducting the reaction without the need to purify this product has a positive effect on diastereo- and enantioselectivity of the reaction (see Scheme 2.2). The successive step is a domino Michael (between the anion of nitroalkane **32** and the ethyl acrylate derivative **33**)/Horner-Wadsworth-Emmons/retro-aldol reaction, that provides the three compounds **34**, **35** and **36**. The side-products **35** and **36** are conveniently transformed into the desired ethyl cyclohexenyl carboxylate **34**, through an Horner-Wadsworth-Emmons elimination and a retro-Michael reaction respectively, by adding EtOH in the reaction mixture (see Scheme 2.5). A base-catalyzed isomerization and a thio-Michael reaction are the successive steps, which lead to the formation of adduct **37**. Then the nitro-group of **37** is reduced to amino-group with the formation of **38**. The final retro-Michael reaction of the thiol group leads to the formation of the desired product **39**. After the reduction of the nitro moiety with Zn, NH<sub>3</sub>

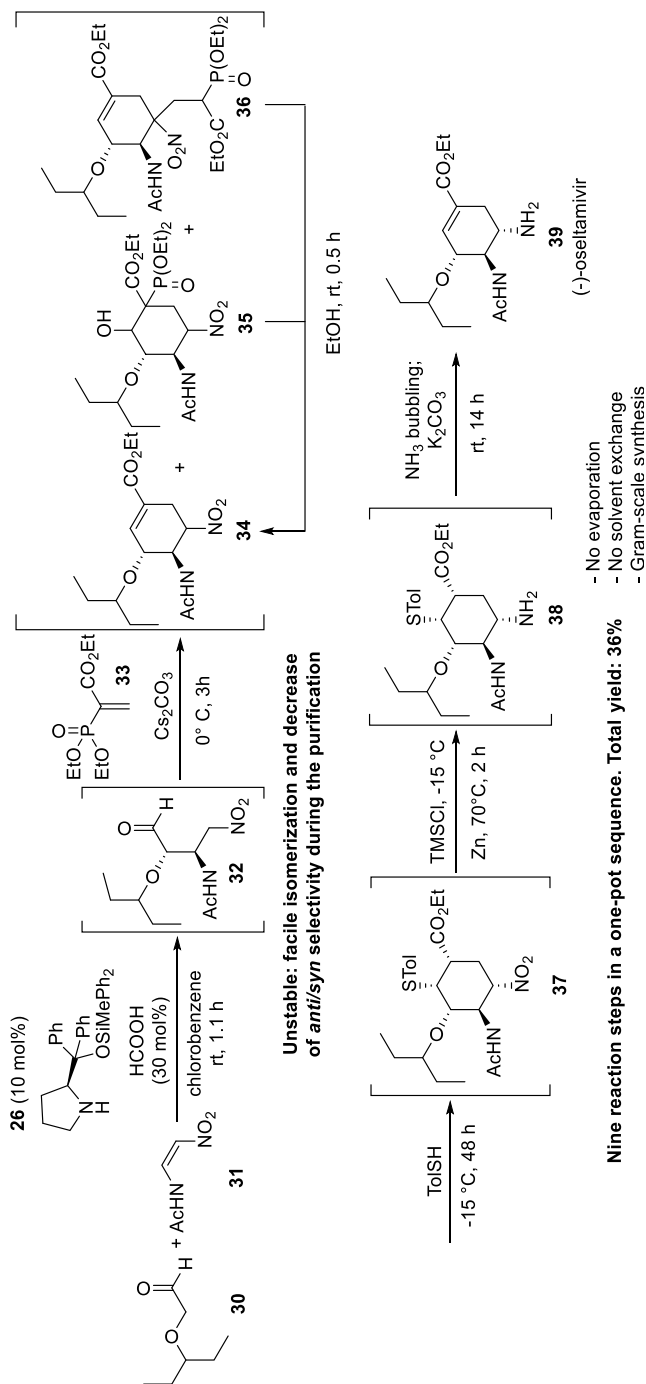
---

<sup>48</sup> (a) H. Ishikawa, T. Suzuki, H. Orita, T. Uchimaru, Y. Hayashi, *Chem. Eur. J.* **2010**, *16*, 12616; (b) H. Ishikawa, T. Suzuki, Y. Hayashi, *Angew. Chem. Int. Ed.* **2009**, *48*, 1304.

bubbling is required to cleave zinc. This kind of “in situ work-up” is necessary to successfully carry out the successive transformation. It should be noted that the same reagent, namely cesium carbonate, was used in five different transformations (see Scheme 2.6): (1) it is the base of the Michael reaction between nitroalkane **32** and vinylphosphonate **33**; (2) it takes part in the intramolecular Horner-Wadsworth-Emmons reaction; (3) it is used, in addition to EtOH, for the retro-aldol/Horner-Wadsworth-Emmons reactions from **35** to **34** and the retro-Michael reaction from **36** to **34**; (4) it promotes the C5 isomerization of **34** for (5) the Michael reaction between the thiol and **34**, reaction conducted at a lower temperature (-15 °C) to avoid the elimination of HNO<sub>2</sub> from **34**.

The present synthesis represents the first example of a stereochemically complex drug synthesized in a single pot with a significant yield and moreover, this one-pot synthesis does not involve evaporation or change of solvent processes. Thus, this constitutes the perfect example of the power of a carefully developed one-pot reaction sequence.





Scheme 2.7 One-pot synthesis of (-)-oseltamivir.

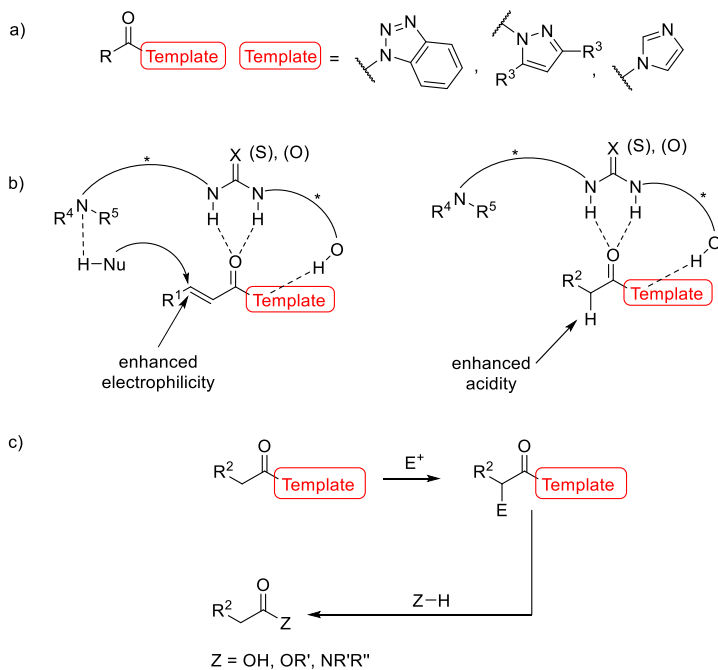
## 3. MASKED ESTERS/AMIDES

### 3.1 Ester/amide surrogates: general features<sup>49</sup>

Masked esters/amides represent a new useful class of organic compounds. Certain features render them particularly suitable reagents in organocatalytic one-pot sequences. They are characterized by the presence, in their structure, of a nitrogen-based heterocycle in acyclic position (Scheme 3.1, a). Nitrogen atoms of the heterocycle allow these substrates a better interaction with the organocatalyst through formation of additional H-bonding networks. These interactions result in a positive outcome on both reactivity and stereoselectivity. The rigidity of the structure in the transition state enables high levels of selectivity, moreover the coordination of the catalyst decreases the LUMO of the substrate facilitating the reaction, in particular an enhanced electrophilicity at the  $\beta$  position of  $\alpha,\beta$ -unsaturated reagents and an easier formation of the enolate in methylene compounds are observed, respectively (Scheme 3.1, b). The last crucial property of *N*-acyl aza-heterocycles concerns the ability of the heterocycle as leaving group, so giving the possibility to obtain esters or amides through an addition-elimination step using alcohols or amines as nucleophiles (Scheme 3.1, c).

---

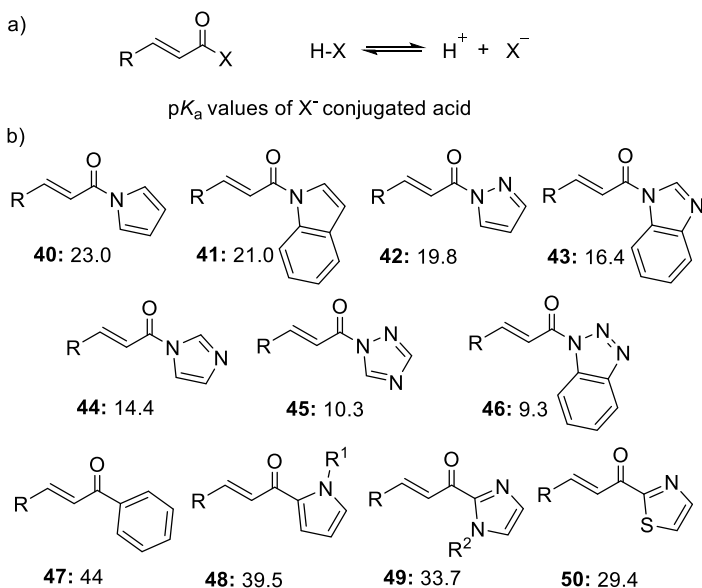
<sup>49</sup> For reviews on ester surrogates, see: (a) D. Monge, H. Jiang, Y. Alvarez-Casao, *Chem. Eur. J.* **2015**, *21*, 4494; (b) G. Desimoni, G. Faita, P. Quadrelli, *Chem. Rev.* **2015**, *115*, 9922; (c) N. Kumagai, M. Shibasaki, *Chem. Eur. J.* **2016**, *22*, 15192.



**Scheme 3.1.** Masked esters/amides

As mentioned above, after the reaction, the amide-type bond cleavage gives the chance to obtain a variety of functionalized building blocks. The C(O)-N bond cleavage releases the heterocyclic anion  $X^-$  (Schema 3.2, a). A greater stability of the anion derives from a lower value of  $pK_a$  of the conjugate acid (Schema 3.2, b).<sup>50</sup>

<sup>50</sup> (a) F. G. Bordwell, *Acc. Chem. Res.* **1988**, *21*, 456; (b) P. S. Baran, J. M. Richter, *Essentials of Heterocyclic Chemistry-I*; retrieved from: <http://www.scripps.edu/baran/heterocycles/Essentials1-2009.pdf>.



**Scheme 3.2.** (a) General scheme for the C(O)-X bond cleavage; (b)  $pK_a$  values of the conjugated acid of several nitrogen-based heterocycles.

For compounds **48-50**, the cleavage concerns a carbon-carbonyl bond, so the  $pK_a$  values of the corresponding conjugated acids, are those in which a carbon-hydrogen bond has to be dissociate. A reference compound for this class is represented by chalcone **47** (R = Ph), and the assumed  $pK_a$  value for the cleavage of the phenyl-carbonyl bond is reported. On the basis of the  $pK_a$  values, two main clusters of compounds can be identified. Reagents **40-46** belong to the first cluster and they are suitable compounds for modifications of their products through substitution of the heterocycle fragment with more useful functional groups. Among them, compounds **45** and **46** should have the most easily cleavable carbon-nitrogen bonds (due to the lowest  $pK_a$  of the conjugate acid of the heterocycle). While reagents of the second cluster (**48-50**) are expected to generate stable

products in which the substitution of the heterocycle with other groups will be more difficult with respect to the compounds belonging to the first cluster. In this section we will focus on amides **40-46** listed in Scheme 3.2 and in particular on structures **42**, bearing a pyrazole moiety with different substitutions.

### 3.2 *N*-Acyl pyrazoles in organic synthesis

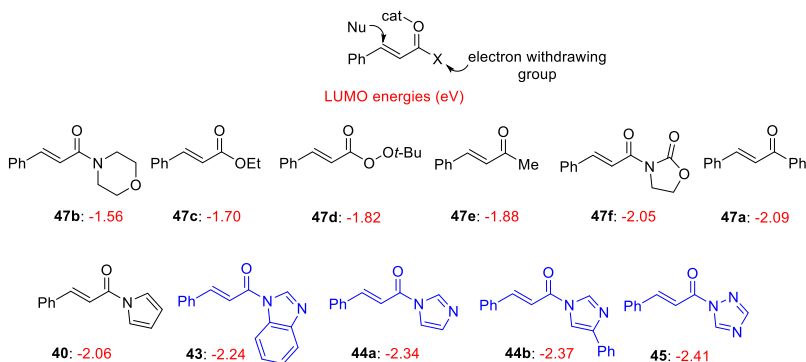
As mentioned above, *N*-Acylpyrazoles recently began to attract organic chemists, thanks to their higher reactivity if compared with the corresponding esters and amides, both as Michael acceptors and enolate equivalents. Moreover they can be successfully employed as alternative starting materials using milder reaction conditions and, after the reaction, the corresponding product can be easily elaborated to afford common carbonyl compounds or other derivatives.

In the literature there are several examples about the use of pyrazoleamides, both  $\alpha,\beta$ -unsaturated and methylene compounds, exploiting metal- and organocatalyzed methodologies and in the next two sections some representative examples are shown.

#### 3.2.1 Masked esters/amides as electrophiles

$\alpha,\beta$ -unsaturated carbonyl derivatives have proved to be suitable starting materials in catalytic enantioselective reactions that, in general, are aimed at functionalizing either the activated double bond, or the entire C=C-C=O fragment or the carbonyl group only. The reaction of a nucleophile to the  $\beta$ -position of an  $\alpha,\beta$ -unsaturated carbonyl compound depends on the electron-withdrawing character of the substituents in the electrophile: an higher electron withdrawing

character of the acyl group results in a lower LUMO value of the corresponding enone (Scheme 3.3).<sup>51</sup> As shown below, enones bearing aromatic aza-heterocycles (compounds **43-45** in Scheme 3.3) are characterized by the lowest LUMO energy and are, subsequently, the most reactive species.



**Scheme 3.3.** LUMO energies (eV) of enones with different substituents.

Among ester surrogates,  $\alpha,\beta$ -unsaturated-*N*-Acyl pyrazoles have been mostly used as Michael acceptors by exploiting Lewis acids-based catalysts. Nitroalkanes in particular are useful nucleophilic reagents, since the conjugate addition of nitroalkanes to  $\alpha,\beta$ -unsaturated carbonyl compounds provides  $\gamma$ -nitrocarbonyl products, which represent very useful intermediates in organic synthesis.<sup>52</sup>

In 2002, Kanemasa reported a Michael addition of nitromethane to  $\alpha,\beta$ -unsaturated pyrazolamides. This methodology relies on the use

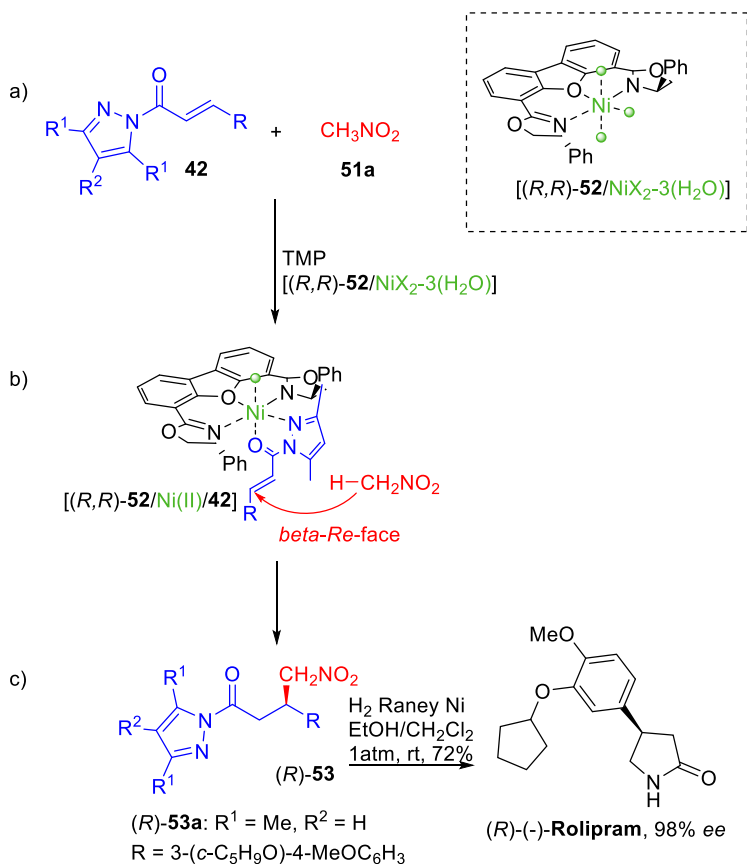
<sup>51</sup> (a) T. Ohshima, T. Nemoto, S. Tosaki, H. Kakei, V. Gnanadesikan, M. Shibasaki, *Tetrahedron* **2003**, *59*, 10485; (b) S. Matsunaga, T. Kinoshita, S. Okada, S. Harada, M. Shibasaki, *J. Am. Chem. Soc.* **2004**, *126*, 7559.

<sup>52</sup> For some examples on conjugate addition of nitroalkanes to  $\alpha,\beta$ -unsaturated carbonyl compounds, see: (a) Kwiatkowski, P.; Cholewiak, A.; Kasztelan, A. *Org. Lett.* **2014**, *16*, 5930. (b) Rodrigo, E.; Ruano, J. L. G.; Cid, M. B. *J. Org. Chem.* **2013**, *78*, 10737. (c) Quintavalla, A.; Lanza, F.; Montroni, E.; Lombardo, M.; Trombini, C. *J. Org. Chem.* **2013**, *78*, 12049. (d) Jia, Z. X.; Luo, Y. C.; Cheng, X. N.; Xu, P. F.; Gu, Y. C. *J. Org. Chem.* **2013**, *78*, 6488.

of catalytic amounts of a chiral Lewis acid and a secondary amine (TMP) as catalysts in order to activate the electrophile and nitromethane **51a** respectively.<sup>53</sup> The NiX<sub>2</sub> complex of DBFOX/Ph **52** proved to be a brilliant catalyst for the reaction (Scheme 3.4, a). The enantiomeric excess of the products is excellent (up to >99% ee) and the catalyst tolerates a wide class of R substituents on **42**. The octahedral structure of the complex was determined by X-ray diffraction analysis and this studies have allowed to propose for the reacting complex the structure [(*R,R*)-**52**/Ni(II)/**42**] illustrated in Scheme 3.4, b. The approach of nitromethane takes place on the *re*-face of the coordinate carbonyl reagent, thus affording adducts **53** with the (*R*) absolute configuration. Finally, by exploiting the ability of pyrazole as leaving group, authors carried out, through one only additional step, the synthesis of the antidepressant and phosphodiesterase inhibitor (*R*)-Rolipram (Scheme 3.4, c).

---

<sup>53</sup> K. Itoh, S. Kanemasa, *J. Am. Chem. Soc.* **2002**, *124*, 13394.



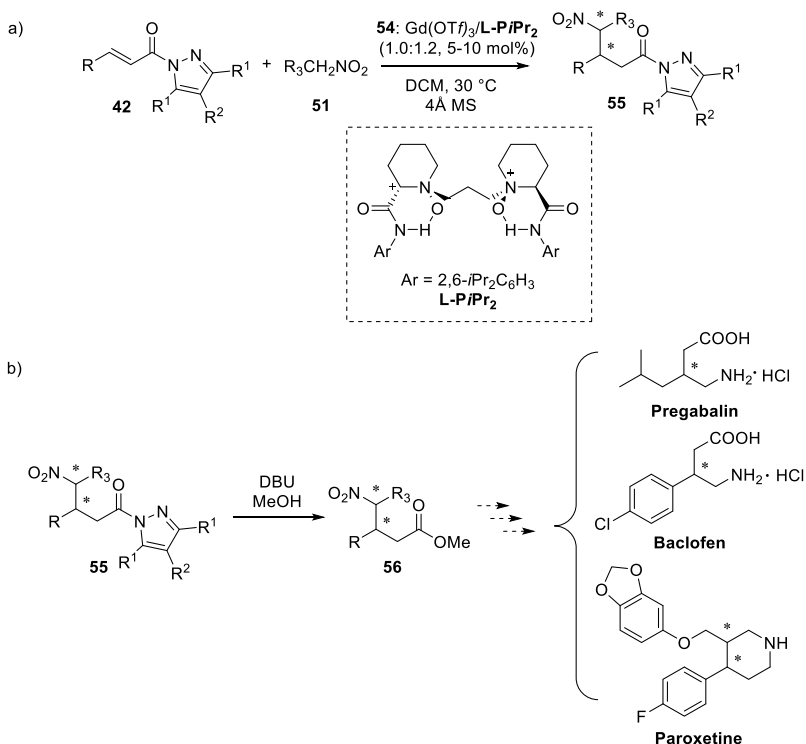
**Scheme 3.4.** (a) Enantioselective Michael addition of nitromethane to enones; (b) Structure of the reacting complex; (c) Synthesis of (*R*)-(-)-Rolipram.

Starting from these results, in 2015, Feng developed a metal-catalyzed methodology to accomplish the asymmetric synthesis of  $\gamma$ -nitroesters **56**.<sup>54</sup> He used an *N,N'*-dioxide/Gd(III) complex **54**, developed by his group, to promote the asymmetric conjugate addition of nitroalkanes **51** to  $\alpha,\beta$ -unsaturated *N*-acylpyrazoles **42**

<sup>54</sup> Q. Yao, Z. Wang, Y. H. Zhang, X. H. Liu, L. L. Lin, X. M. Feng, *J. Org. Chem.* **2015**, *80*, 5704.



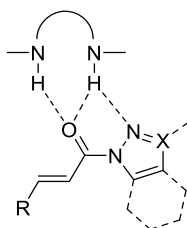
(Scheme 3.5, a). The resulting  $\gamma$ -nitropyrazolamides **55**, after displacement of the pyrazole moiety with a methoxy group, were transformed in  $\gamma$ -nitroesters **56**, which are useful starting materials for the synthesis of some pharmacological and biological derivatives such as Pregabalin, Baclofen and Paroxetine (Scheme 3.5, b).



**Scheme 3.5.** (a) Synthetic route to  $\gamma$ -nitropyrazolamides; (b) Transformation of  $\gamma$ -nitropyrazolamides to  $\gamma$ -nitroesters and then to their pharmacological and biological derivatives.

A certain number of other metal-catalyzed methodologies are reported in literature regarding the use of  $\alpha,\beta$ -unsaturated masked esters in epoxidation,<sup>55</sup> cyclopropanation,<sup>56</sup> Michael,<sup>57</sup> radical,<sup>58</sup> Diels-Alder<sup>59</sup> and dipolar cycloaddition<sup>60</sup> reactions.

Less numerous are the examples concerning the use of  $\alpha,\beta$ -unsaturated *N*-acyl pyrazoles in organocatalyzed methodologies. As mentioned above, the presence of nitrogen-based heterocycles as templates offers further possibilities of H-bond interactions with the organocatalyst (Figure 3.1).



**Figure 3.1.** Interaction of  $\alpha,\beta$ -unsaturated *N*-acyl pyrazoles and (benzo)triazoles with an H-bond donor catalyst.

<sup>55</sup> (a) T. Nemoto, T. Ohshima, M. Shibasaki, *J. Am. Chem. Soc.* **2001**, *123*, 9474; (b) S. Matsunaga, T. Kinoshita, S. Okada, S. Harada, M. Shibasaki, *J. Am. Chem. Soc.* **2004**, *126*, 7559; (c) T. Kinoshita, S. Okada, S.-R. Park, S. Matsunaga, M. Shibasaki, *Angew. Chem., Int. Ed.* **2003**, *42*, 4680.

<sup>56</sup> H. Kakei, T. Sone, Y. Sohtome, S. Matsunaga, M. Shibasaki, *J. Am. Chem. Soc.* **2007**, *129*, 13410.

<sup>57</sup> (a) S.-Y. Park, H. Morimoto, S. Matsunaga, M. Shibasaki, *Tetrahedron Lett.* **2007**, *48*, 2815; (b) T. Mita, K. Sasaki, M. Kanai, M. Shibasaki, *J. Am. Chem. Soc.* **2005**, *127*, 514; (c) I. Fujimori, T. Mita, K. Maki, M. Shiro, A. Sato, S. Furusho, M. Kanai, M. Shibasaki, *Tetrahedron* **2007**, *63*, 5820; (d) J. Zhang, X. Liu, R. Wang, *Chem. Eur. J.* **2014**, *20*, 4911; (e) B. A. Provencher, K. J. Bartleson, Y. Liu, B. M. Foxman, L. Deng, *Angew. Chem., Int. Ed.* **2011**, *50*, 10565; (f) M. Agostinho, S. Kobayashi, *J. Am. Chem. Soc.* **2008**, *130*, 2430.

<sup>58</sup> (a) M. P. Sibi, G. Petrovic, *Tetrahedron: Asymmetry* **2003**, *14*, 2879; (b) C. Kashima, H. Yokoyama, S. Shibata, K. Fujisawa, T. Nishio, *J. Heterocycl. Chem.* **2003**, *40*, 717.

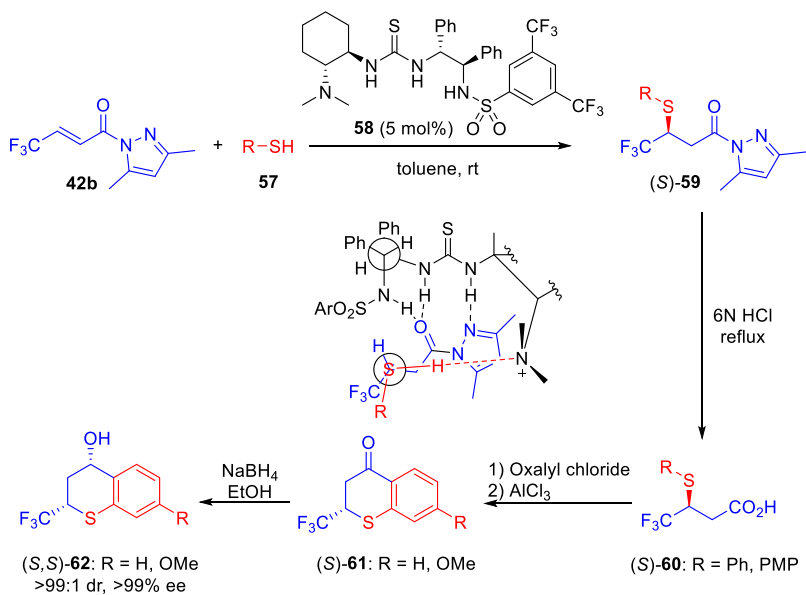
<sup>59</sup> (a) C. Kashima, Y. Miwa, S. Shibata, H. Nakazono, *J. Heterocycl. Chem.* **2003**, *40*, 681; (b) M. P. Sibi, J. Chen, L. Stanley, *Synlett* **2007**, *2007*, 298; (c) K. Ishihara, M. Fushimi, *J. Am. Chem. Soc.* **2008**, *130*, 7532.

<sup>60</sup> (a) M. Hori, A. Sakakura, K. Ishihara, *J. Am. Chem. Soc.* **2014**, *136*, 13198; (b) A. Sakakura, M. Hori, M. Fushimi, K. Ishihara, *J. Am. Chem. Soc.* **2010**, *132*, 15550; (c) M. P. Sibi, K. Itoh, C. P. Jasperse, *J. Am. Chem. Soc.* **2004**, *126*, 5366.

Most of these examples involve the use of bifunctional organocatalysts with a (thio)urea moiety as double H-bond donor, able to establish additional hydrogen-bond interactions with nitrogen atoms of the heterocycle.

Usually, Michael reactions form a new C–C bond, as shown in the aforementioned examples, but this reaction is also suitable for the formation of new C–X bonds, where X represents a nitrogen, oxygen, sulfur or phosphor atom. With the enantioselective sulfa-Michael reaction the construction of chiral scaffolds bearing a sulfur atom at the stereogenic center is possible. To date, only few recent examples exploiting *N*-acyl-pyrazoles as Michael acceptors are reported in the literature, but all with excellent results. In 2012 Wang and colleagues reacted (*E*)-4,4,4-Trifluoro-1-(3,5-dimethyl-1H-pyrazol-1-yl)but-2-en-1-one **42b** with different arylthiophenols **57** in the presence of catalytic amounts of the multifunctional organocatalyst **58** (Scheme 3.6).<sup>61</sup> The corresponding Michael adducts **59** were obtained with excellent results in terms of both yield and enantioselectivity. The absolute configuration of adducts was determined to be (*S*) by converting two selected products into acids **60** and then to the corresponding thiochromanonones **61**, which were subsequently reduced to (*S,S*)-**62** of known configuration. The stereochemical outcome of the reaction can be rationalized figuring the nucleophilic attack of the thiol to the  $\beta$ -*si*-face of the acylpyrazole **42**, meanwhile engaged by H-bonding with the catalyst, as shown in Scheme 3.6.

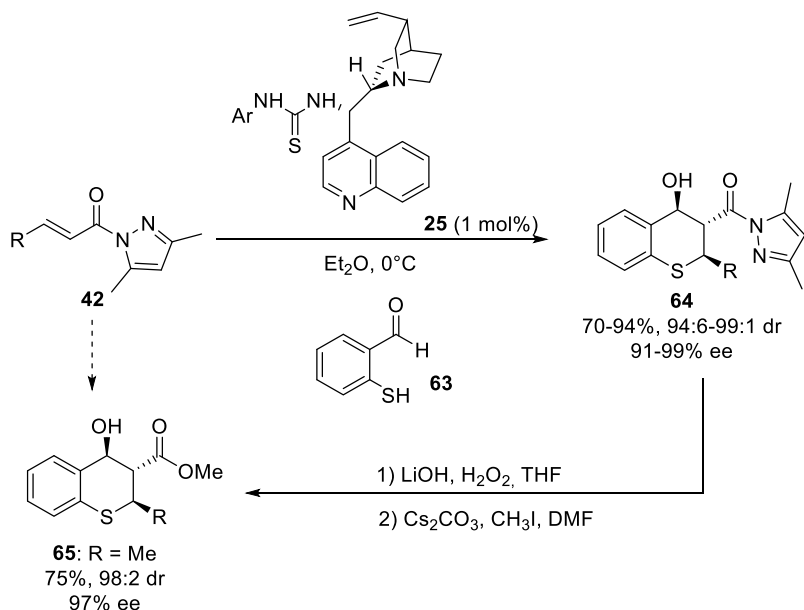
<sup>61</sup> X.-Q. Dong, X. Fang, H.-Y. Tao, X. Zhou, C.-J. Wang, *Adv. Synth. Catal.* **2012**, 354, 1141.



**Scheme 3.6** Organocatalyzed sulfa-Michael addition to enones.

Starting from these results, Wang's group also developed a methodology for the construction of the thiochromane ring **64**.<sup>62</sup> By using 2-mercaptobenzaldehyde **63**, the  $\alpha,\beta$ -unsaturated compounds **42** give rise to a cascade reaction in which the first sulfa-Michael adduct undergoes an intramolecular aldol reaction with the formation of the thiochromane **64**. The reaction was carried out in the presence of a very low amount of the cinchona alkaloid-derived thiourea catalyst **25** (Scheme 3.7). Moreover heterocycles **64** can be readily transformed into  $\beta$ -hydroxy esters, such as **65**, by hydrolysis of the pyrazole moiety followed by a methylation reaction, without loss of diastereomeric and enantiomeric excess.

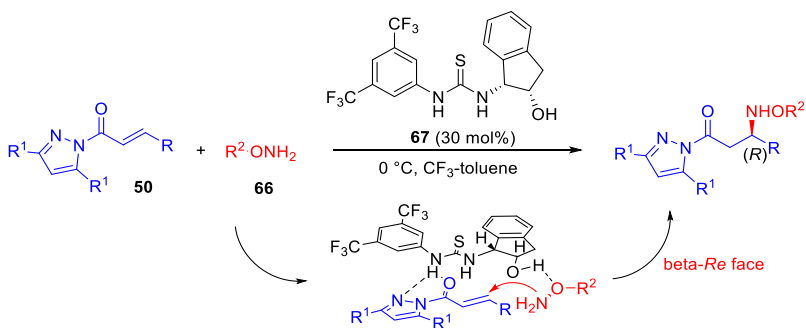
<sup>62</sup> X.-Q. Dong, X. Fang, H.-Y. Tao, X. Zhou, C.-J. Wang, *Chem. Commun.* **2012**, 48, 7238.



**Scheme 3.7** Asymmetric cascade sulfa Michael/aldol reaction of unsaturated-*N*-acylpyrazoles and 2-mercaptobenzaldehyde.

In addition to sulfa-Michael reaction, the aza-Michael reaction is also interesting, since it allows easy access to chiral  $\beta$ -amino acids. The aza-Michael reaction between alkenes **42** and *O*-alkylhydroxylamines **66** was performed with thiourea **67** as organocatalyst.<sup>63</sup> The reaction, shown below in Scheme 3.8, probably occurs through the schematized mechanism in which both electrophile and nucleophile are coordinated to the organocatalyst, with the subsequent addition of hydroxylamines to the  $\beta$ -face of the alkene **42**.

<sup>63</sup> M. P. Sibi, K. Itoh, *J. Am. Chem. Soc.* **2007**, *129*, 8064.

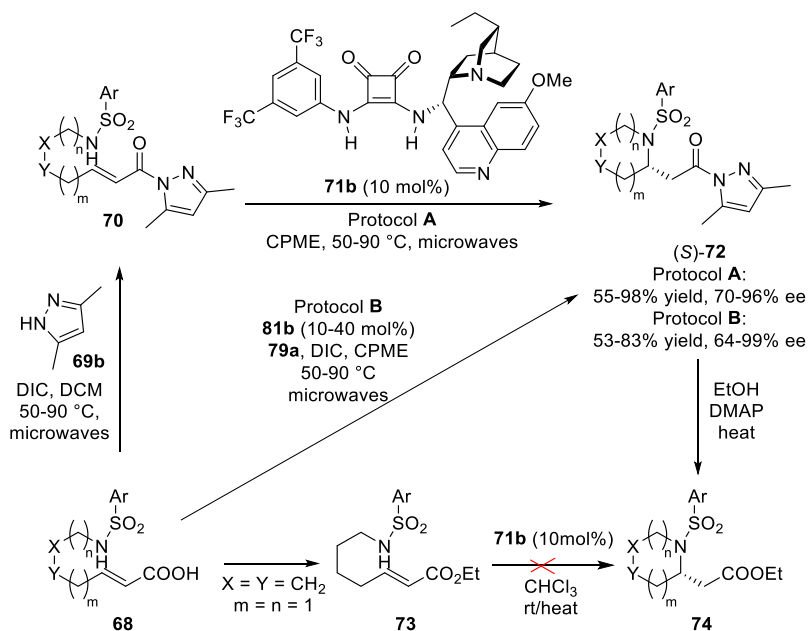


**Scheme 3.8** Proposed mechanism for thiourea-organocatalyzed aza-Michael addition to enones.

An interesting intramolecular variant of the aza-Michael reaction was reported in 2014 by a Spanish group. They reacted  $\alpha,\beta$ -unsaturated acylpyrazoles **70** endowed with a NH group bearing a tosyl substituent. This scaffold allows an intramolecular addition of nitrogen atom to the  $\beta$ -position of the unsaturated carbonyl compound in the presence of hydroquinine-derived squaramide **71b** as organocatalyst.<sup>64</sup> The reaction affords the variously substituted cyclic products **72**, with *S* absolute configuration of the stereocenter, in significant results (Scheme 3.9, Protocol A). The reaction can also be performed with a tandem sequence in which the acid **68** is reacted with the 3,5-dimethylpyrazole **69b** and diisopropyl carbodiimide (DIC) and then, the *in situ* formed coupling product **70**, in the presence of the organocatalyst **71b**, reacts intramolecularly to afford products (*S*)-**72** in moderate yields and with appreciable enantioselectivities (Scheme 3.9, Protocol B). This methodology allows access to five- and six-membered ring heterocycles **72**, such

<sup>64</sup> M. Sanchez-Rosello, C. Mulet, M. Guerola, C. del Pozo, S. Fustero, *Chem. Eur. J.* **2014**, *20*, 15697.

as piperidine, morpholine, piperazine, pyrrolidine, depending on X and Y atoms and on the length of *m* and *n* chains in reagents **68** and **70**. Moreover, the presence of the pyrazole moiety offers the possibility to transform derivatives **72** into the corresponding esters **74** by treating with alcohols in basic conditions. Finally, the acid **68** was transformed into the corresponding ethyl ester **73**, but any attempt to perform the intramolecular aza-Michael reaction on this substrate with the squaramide organocatalyst **71b** was unsuccessful. This is a striking example of the higher reactivity of masked esters compared with corresponding esters and in fact Michael adduct (*S*)-**72** can be obtained only through the “masked route” (Scheme 3.9).



**Scheme 3.9** Intramolecular squaramide-organocatalyzed aza-Michael reaction of enones.

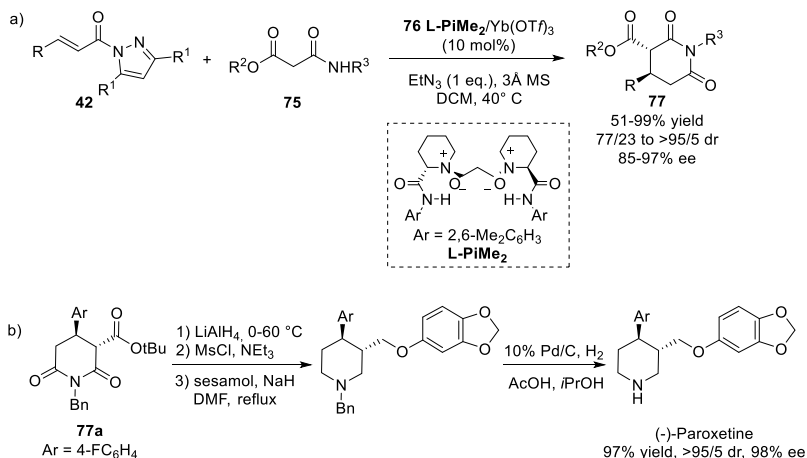
All examples above reported, exploit pyrazole moiety for functionalizations on previously obtained scaffolds. By using instead opportune binucleophilic reagents, thanks to the ability of the pyrazole as leaving group, the formation of interesting heterocyclic scaffolds can be achieved, as shown in the following examples.

The previously displayed Michael addition of nitroalkanes to  $\alpha,\beta$ -unsaturated *N*-acylpyrazoles leads to the formation of  $\gamma$ -nitroester derivatives.<sup>53,54</sup> These are useful starting materials for the enantioselective construction of the lactam structure, but a reductive amination cyclization step is previously required. In order to overcome this additional step, Feng and co-workers used amidomalonates **75** as alternative nucleophiles, thus developing a highly enantioselective tandem Michael/ring-closure reaction for the synthesis of variously substituted chiral glutarimides **77**.<sup>65</sup> They reacted  $\alpha,\beta$ -unsaturated pyrazoleamides **42** with amidomalonates **75** in the presence of a chiral *N,N'*-dioxide–Yb(OTf)<sub>3</sub> complex **76** thus obtaining the corresponding products **77** in high yields and with high diastereo- and enantioselectivities (Scheme 3.10, a). Moreover the piperidine-2,6-dione scaffold **77a** represents a key intermediate for the synthesis of pharmacological compounds, as demonstrated by authors with the synthesis (-)-Paroxetine, which was isolated in 66% overall yield and 98% ee after a further four-step transformation (Scheme 3.10, b).

---

<sup>65</sup> Y. Zhang, Y. Liao, X. Liu, Q. Yao, Y. Zhou, L. Lin, X. Feng, *Chem. Eur. J.* **2016**, *22*, 15119.

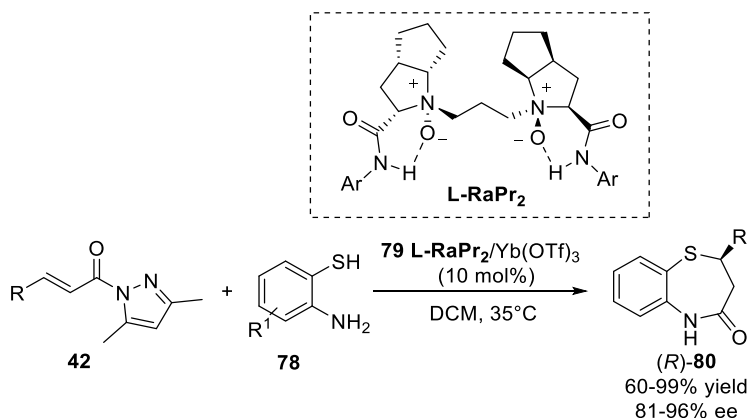




**Scheme 3.10** (a) Catalytic Michael/ring-closure reaction of  $\alpha,\beta$ -unsaturated *N*-acylpyrazoles with amidomalones and (b) Asymmetric synthesis of (-)-Paroxetine.

One year later, the same group developed a methodology for the enantioselective synthesis of 1,5-benzothiazepines by exploiting  $\alpha,\beta$ -unsaturated pyrazoleamides **42** and 2-aminothiophenols **78** in a cascade sulfa-Michael/cyclization reaction catalyzed by the chiral Ytterbium complex **79**. The reaction gives access to NH-free 1,5-benzothiazepines **80** in high yields and enantioselectivities (Scheme 3.11).<sup>66</sup>

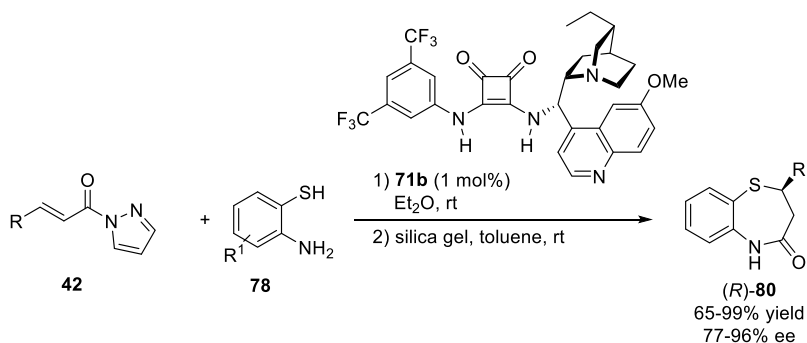
<sup>66</sup> G. J. Wang, Y. Tang, Y. Zhang, X. H. Liu, L. L. Lin, X. M. Feng, *Chem. Eur. J.* **2017**, *23*, 554.



**Scheme 3.11** Enantioselective synthesis of NH-free 1,5-benzothiazepines.

Simultaneously to the Feng work, our group developed an organocatalyzed methodology for the enantioselective one-pot synthesis of NH-free 1,5-benzothiazepines **80**.<sup>67</sup> By reacting  $\alpha,\beta$ -unsaturated *N*-acylpyrazoles **42** and 2-aminothiophenols **78** in the presence of a very low amount of the Cinchona alkaloid-derived squaramide **71b** we obtained the corresponding products **80** in high yields and with high enantiomeric excesses (Scheme 3.12). Both these methodology allow access to NH-unprotected products, which are then immediately suitable for *N*-alkylation or acylation, namely typical derivatizations to create libraries of compounds for biological screening. Both groups highlighted this significant characteristic by synthesizing (*R*)-Thiazesim with excellent results.

<sup>67</sup> S. Meninno, C. Volpe, A. Lattanzi, *Chem. Eur. J.* **2017**, *23*, 4547.

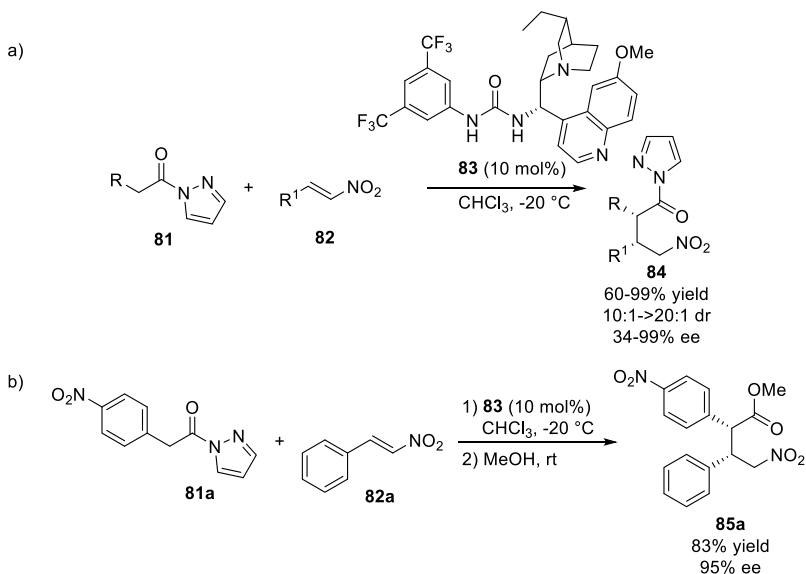


**Scheme 3.12** Our enantioselective organocatalyzed one-pot synthesis of NH-free 1,5-benzothiazepines.

### 3.2.2 Masked esters/amides as nucleophiles

In 2012, Barbas and co-workers firstly discovered that pyrazoleamides **81** can be useful carbon nucleophiles since they enolize, in the presence of an urea-tertiary amine **83**, thus giving an asymmetric Michael addition toward nitrostyrenes **82** (Scheme 3.13, a).<sup>68</sup> The presence of the pyrazole moiety acts as an activating and directing group but it is also a good leaving group, useful feature for versatile post-functionalizations of the adducts **84**, as proved in this case by the authors with the one-pot synthesis of ester derivatives **85** (Scheme 3.13, b).

<sup>68</sup> B. Tan, G. Hernández-Torres, C. F., III Barbas, *Angew. Chem. Int. Ed.* **2012**, *51*, 5381.

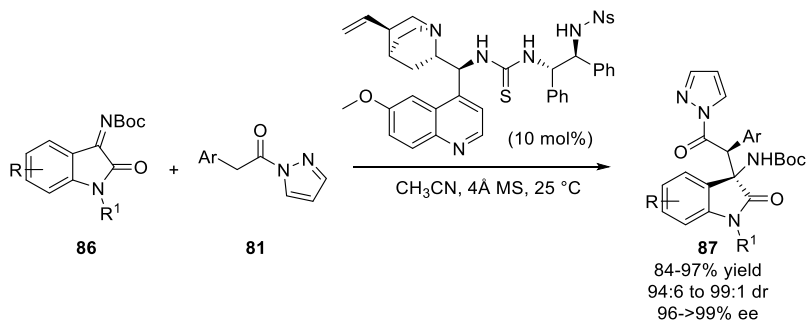


**Scheme 3.13** (a) Enantioselective Michael addition of pyrazoleamides to nitrostyrenes and (b) One-pot synthesis of ester derivative **85a**.

Starting from this first work, a variety of methodology involving the use of pyrazolamides as nucleophiles have been reported in the literature for the synthesis of different scaffolds. In this section some representative examples are reported.

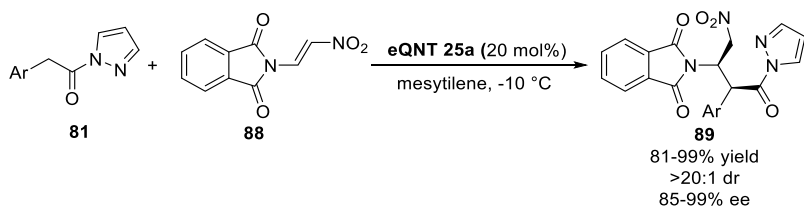
In 2014 Wu's group reacted pyrazoleamides **81** with isatin-derived *N*-Boc ketimines **86**, thus developing a Mannich-type reaction with the formation of  $\beta$ -amino carbonyl derivatives **87** with excellent results (Scheme 3.14).<sup>69</sup> The corresponding 3-substituted 3-amino-2-oxindoles **87** are suitable materials for further functionalization, esterification for example, as demonstrated by the authors.

<sup>69</sup> T.-Z. Li, X.-B. Wang, F. Sha, X.-Y. Wu, *J. Org. Chem.* **2014**, *79*, 4332.



**Scheme 3.14** Organocatalyzed enantioselective Mannich reaction of pyrazoleamides with isatin-derived ketimines.

In 2017, Chinese scientists proposed an original synthesis of  $\gamma$ -nitro  $\beta$ -aminoacid derivatives **89** bearing two consecutive trisubstituted stereogenic centers. They set up a Michael reaction of acylpyrazoles **81** toward  $\beta$ -phthalimidonitroethene **88** catalyzed by the bifunctional thiourea **25a** obtaining very good results (Scheme 3.15).<sup>70</sup> Also these products, due to the presence of the pyrazole moiety, are suitable for further functionalizations.

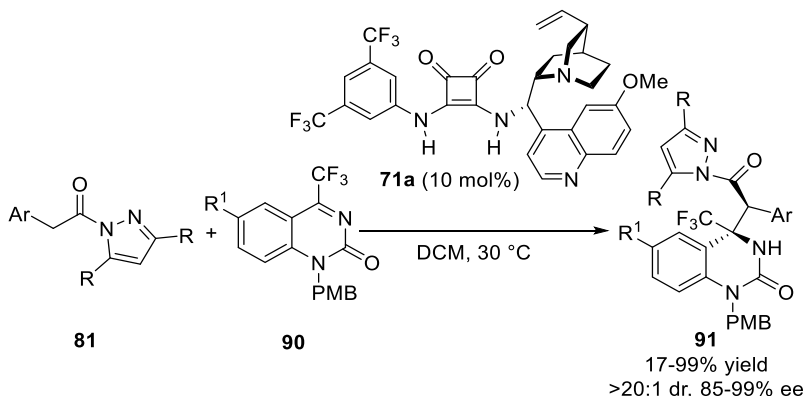


**Scheme 3.15** Organocatalyzed asymmetric Michael reaction of pyrazoleamides and  $\beta$ -phthalimidonitroethene.

One year later, the same group exploited cyclic trifluoromethyl ketimines **90** as electrophiles in a Mannich reaction with pyrazoleamides for the construction of dihydroquinazolinone scaffold

<sup>70</sup> Y. Luo, K.-X. Xie, D.-F. Yue, X.-M. Zhang, X.-Y. Xu, W.-C. Yuan, *Tetrahedron* **2017**, *73*, 6217.

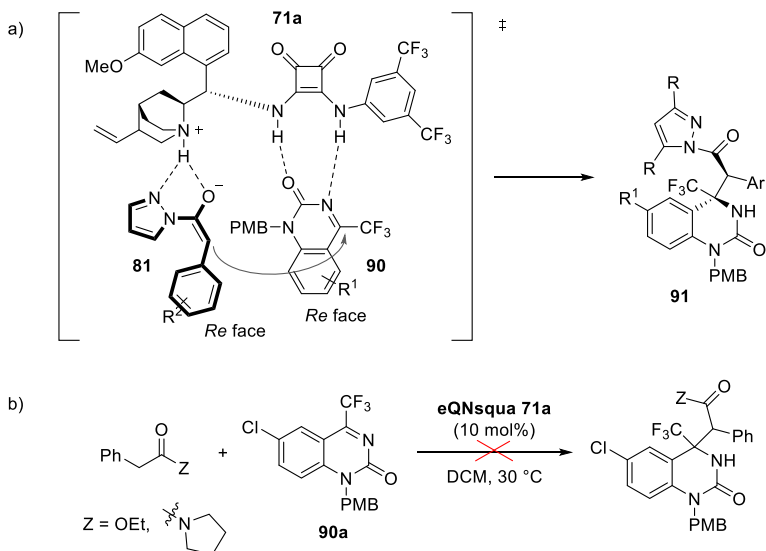
**91**.<sup>71</sup> A wide range of products bearing quaternary and tertiary stereogenic centers can be easily obtained in good to excellent yields and high diastereo- and enantiocontrol (Scheme 3.16).



**Scheme 3.16** Enantioselective synthesis of dihydroquinazolinones.

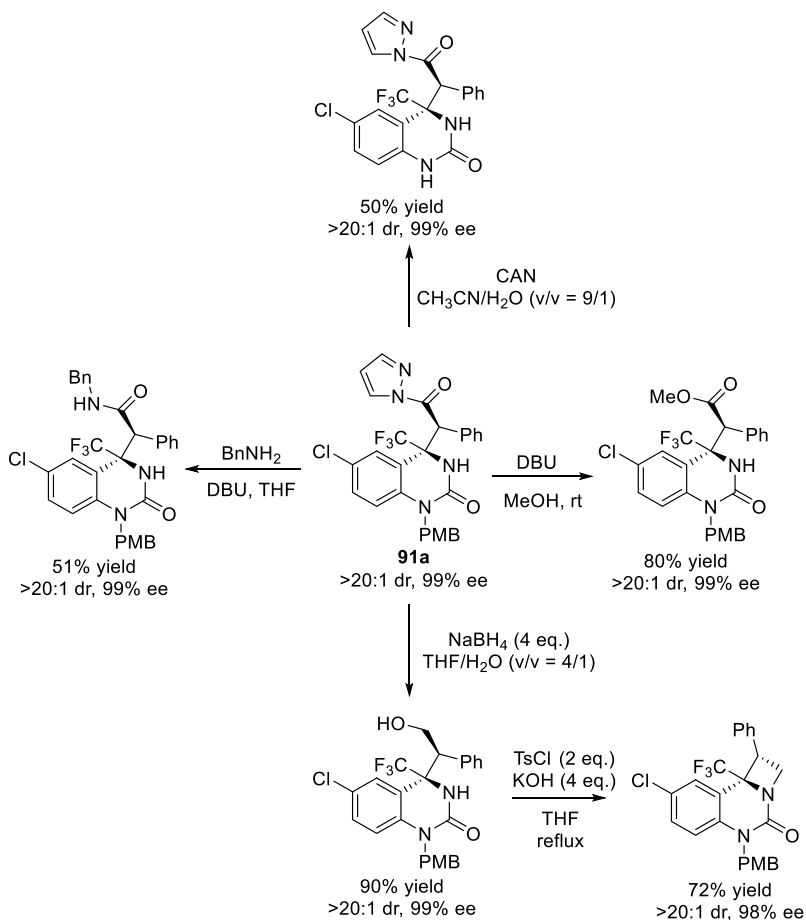
The pyrazole group acts both on reactivity and stereoselectivity of ester surrogates, as highlighted in the proposed mechanism of the reaction. Readily deprotonation of **81** by the tertiary amine moiety of catalyst generates the corresponding enolate which could interact, through H-bond networks, with the protonated amine. Simultaneously, ketimine **90** is engaged with the squaramide motif through hydrogen-bond interactions. Then the *re*-face of enolized pyrazoleamide attacks the *re*-face of ketimine thus giving the major stereoisomer of product **91** (Scheme 3.17, a). No reaction occurs starting from esters or amides thus demonstrating, once again, the higher reactivity of masked esters compared to their parent structures (Scheme 3.17, b).

<sup>71</sup> Y. Luo, K.-X. Xie, D.-F. Yue, X.-M. Zhang, X.-Y. Xu, W.-C. Yuan, *Org. Biomol. Chem.* **2018**, *16*, 3372.



**Scheme 3.17** (a) A plausible transition state model and (b) Reaction performed on esters and amides.

This work in particular represents an excellent example of the synthetic value of acylpyrazoles, since products **91** were efficiently transformed into amides, esters, alcohols and tricyclic compounds in good to excellent yields and without loss in enantioselectivities, as summarized in Scheme 3.18.



**Scheme 3.18** Possible transformations of Mannich products **91**.

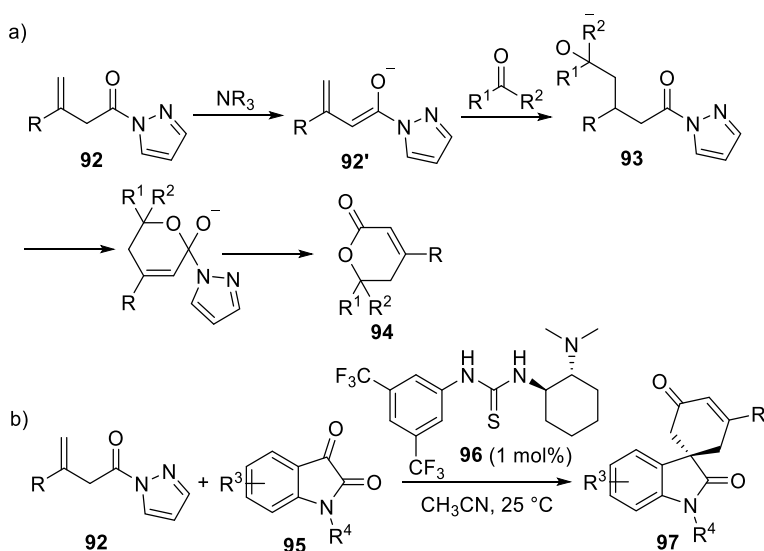
As mentioned above, pyrazoleamides can be used in cascade reactions for the synthesis of heterocyclic compounds.

In 2014 Wu and co-workers exploited allyl pyrazoleamides for the development of a vinylogous aldol/cyclization cascade reaction with isatins.<sup>72</sup> They speculated that vinylogous enolate **92'**, derived from

<sup>72</sup> T.-Z. Li, Y. Jiang, Y.-Q. Guan, F. Sha, X.-Y. Wu, *Chem. Commun.* **2014**, 50, 10790.



deprotonation of **92**, in the presence of a suitable catalyst would attack activated ketones to form intermediate **93** and the following intramolecular cyclization, with detachment of the pyrazole, would allow access to dihydropyranones **94** (Scheme 3.19, a). In particular they reacted  $\beta,\gamma$ -unsaturated pyrazoleamides **92** with isatins **95**, thus obtaining spirocyclic oxindole-dihydropyranones **97**. The reaction takes place in the presence of a very low amount of the commercially available Takemoto thiourea **96** and provide excellent results (Scheme 3.19, b).

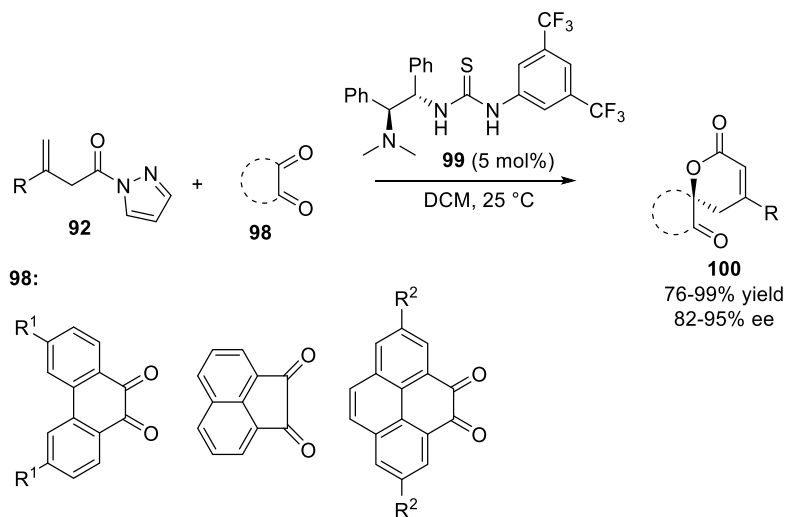


**Scheme 3.19** (a) Synthetic strategy towards chiral dihydropyranones and (b) Enantioselective vinylogous aldol/cyclization cascade reaction to spirocyclic oxindole-dihydropyranones.

One year later the same group exploited once again  $\beta,\gamma$ -unsaturated ester surrogates, using the benzotriazole as more efficient leaving group, in a vinylogous Michael/cyclization cascade reaction, catalyzed by dimeric Cinchona alkaloids, with isatyldiene

malononitriles for the synthesis of spirocyclic oxindoles.<sup>73</sup>

Other suitable electrophiles in the reaction with  $\beta,\gamma$ -unsaturated amides **92** are *o*-quinones. The Wu's group, developed a vinylogous aldol/cyclization cascade reaction between allyl pyrazoleamides **92** and *o*-quinones **98** for the synthesis of spirocyclic lactones **100** in the presence of thiourea **99** as organocatalyst, achieving good to high ee values for the spiro-products (Scheme 3.20).<sup>74</sup>



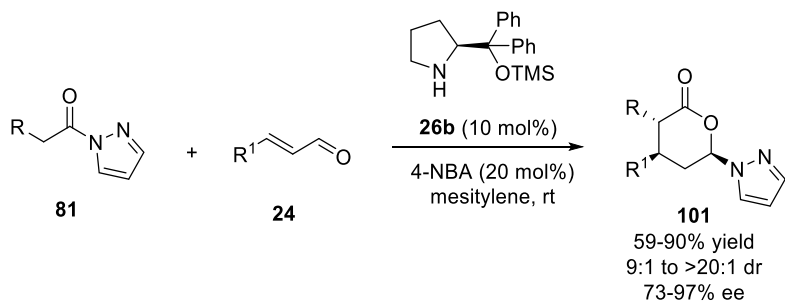
**Scheme 3.20** Enantioselective vinylogous aldol/cyclization cascade reaction of  $\beta,\gamma$ -unsaturated amides are *o*-quinones.

Last examples shown in this section concern the development of a one-pot organocatalyzed Michael/cyclization reaction between  $\alpha,\beta$ -unsaturated aldehydes **24** and pyrazoleamides **81** in the presence of a readily available prolinol catalyst **26b**, to access highly functionalized  $\delta$ -lactones **101** (Scheme 3.21).<sup>75</sup>

<sup>73</sup> T.-Z. Li, J. Xie, Y. Jiang, F. Sha, X.-Y. Wu, *Adv. Synth. Catal.* **2015**, 357, 3507.

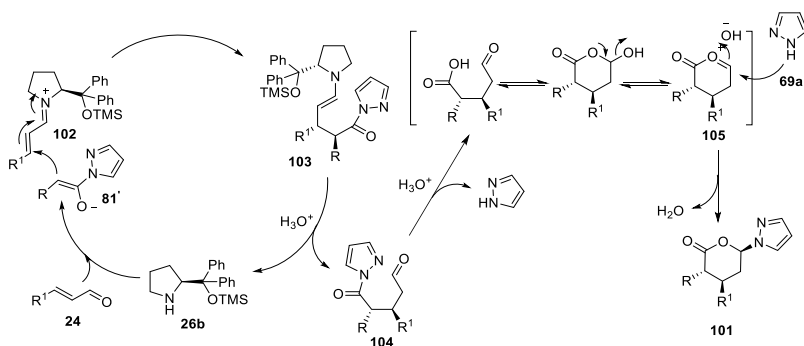
<sup>74</sup> Y. Jiang, J.-H. Fu, T.-Z. Li, F. Sha, X.-Y. Wu, *Org. Biomol. Chem.* **2016**, 14, 6435.

<sup>75</sup> S. Agrawal, N. Molleti, V. K. Singh, *Chem. Commun.* **2015**, 51, 9793.



**Scheme 3.21** Organocatalyzed enantio- and diastereo-selective synthesis of highly substituted  $\delta$ -lactones via Michael/cyclization cascade.

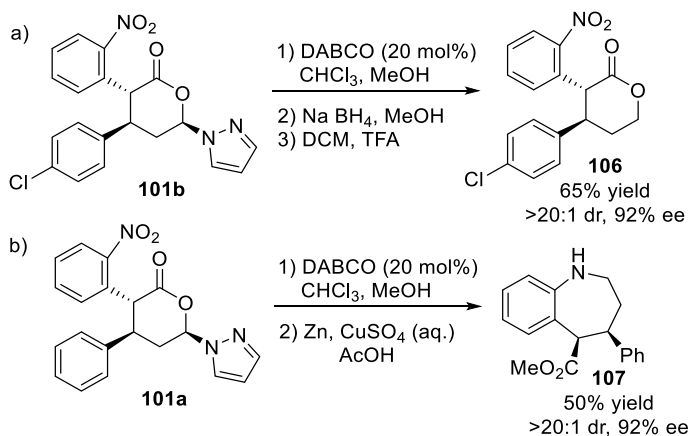
Singh and colleagues explained the interesting mechanism of the reaction and the rearrangement of the pyrazole moiety as shown below in Scheme 3.22. Firstly, the catalyst activates the aldehyde **24** through formation of the iminium ion **102**, then the Michael addition of enolate **81'** gives rise to intermediate **103** from which the released Michael adduct **104** forms lactone **105**. The subsequent nucleophilic attack of pyrazole **69a** provides the  $\delta$ -lactone product **101**.



**Scheme 3.22** Plausible reaction pathway.

Very useful post functionalizations from  $\delta$ -lactone, were demonstrated. Starting from product **101b**, pyrazole can be detached with the formation of  $\delta$ -lactone **106**, maintaining the

enantioselectivity (Scheme 3.22, a). Moreover, a ring expansion can be carried out from **101a** with the formation of the benzazepine scaffold **107**, key-intermediate in the synthesis of several pharmaceutically active compounds (Scheme 3.22, b).



**Scheme 3.22** (a) Cleavage of pyrazole from  $\delta$ -lactone **101b** and (b) Synthesis of benzazepine **107** from  $\delta$ -lactone **101a**.

## RESEARCH OBJECTIVES

Ester/amide surrogates are very useful starting materials for the construction of carbon-carbon or carbon-heteroatom bonds in a stereocontrolled fashion, by exploiting bifunctional organocatalysis. The main target of this present doctoral work is to exploit ester/amide surrogates, both as electrophiles and nucleophiles, in the development of organocatalyzed methodologies for the stereoselective construction of diverse heterocyclic scaffolds. Moreover,  $\alpha$ -functionalizations of masked esters can be easily carried out, thus allowing simple access to intermediates which represent useful building-blocks in cycloaddition and multicomponent reactions.

Another goal of the study is represented by the possibility of further derivatization of products, which can be conveniently carried out in a one-pot fashion, thanks to the inherent features of ester surrogates. Finally, efforts into clarification of some reaction pathways are carried out with the support of NMR spectroscopy or through computational methods.

## 4. CATALYTIC ENANTIOSELECTIVE ONE-POT APPROACH TO *CIS*- AND *TRANS*-2,3-DIARYL SUBSTITUTED 1,5-BENZOTHIAZEPINES

### 4.1 Background

The synthesis of molecules exhibiting a certain activity in living systems has always fascinated chemists. In particular, synthetic chemistry applied to medical field is essential for the discovery and synthesis of biologically active compounds, which could represent potential new drugs.<sup>76</sup> The development of privileged heterocyclic scaffolds represents, especially, an ever-growing area of research in medicinal chemistry. The term ‘privileged scaffold’ was first used by Evans et al. in 1988 in relation to the heterocycle 1,4-benzodiazepine-2-one, that was described as “*a single molecular framework able to provide ligands for diverse receptors*”.<sup>77</sup> In other words the molecular framework of a ‘privileged scaffold’ is endowed with versatile binding extensions which render it capable of interacting with high affinity to a range of different biological targets. Benzothiazepines are a class of heterocyclic scaffolds equipped with well-known biological activities, mainly acting in nervous and cardiovascular systems.<sup>78</sup> The use of benzothiazepines in the medical field dates back to the entry of the anti-depressant Thiazesim into the

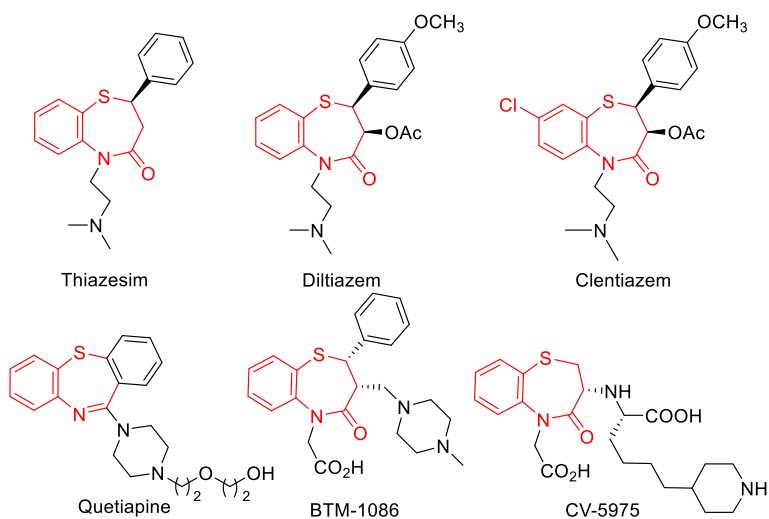
---

<sup>76</sup> K. D. Mjos, C. Orvig, *Chem. Rev.*, **2014**, *114*, 4540.

<sup>77</sup> B. E. Evans, K. E. Rittle, M. G. Bock, R. M. Di Pardo, R. M. Freidinger, W. L. Whitter, G. F. Lundell, D. F. Veber, P. S. Anderson, *J. Med. Chem.*, **1988**, *31*, 2235.

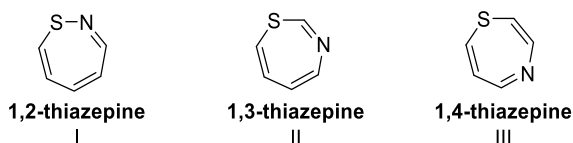
<sup>78</sup> For a review of 1,5-benzothiazepines as versatile pharmacophores see: J. B. Bariwal, K. D. Upadhyay, A. T. Manvar, J. C. Trivedi, J. S. Singh, K. S. Jain, A. K. Shah, *Eur. J. Med. Chem.* **2008**, *43*, 2279.

pharmaceutical market, followed by Diltiazem and Clentiazem. Further optimization of the substituents on the benzothiazepine nucleus resulted in the development of other drugs, such as quetiapine, BTM-1086 and CV-5975. These are the most famous benzothiazepines-based drugs and are represented in Figure 4.1.



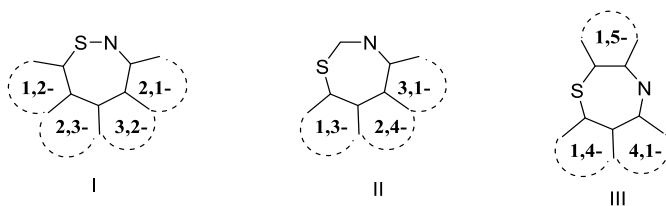
**Figure 4.1** Drugs with a thiazepine core.

Benzothiazepines present a benzene ring condensed with a thiazepine ring, namely a seven-membered heterocyclic compound containing a sulfur and a nitrogen atom ring. These heteroatoms can occupy different positions in the ring, thus giving rise to three possible structural isomers of thiazepines, namely 1,2-, 1,3- and 1,4-thiazepines (Figure 4.2).



**Figure 4.2** Classification of thiazepines.

Moreover, depending on the position of benzene ring, different isomers can be derived from each of the three thiazepines and in particular the ten possible isomers are shown below in Figure 4.3.



**Figure 4.3** Structural isomers of thiazepines.

To date, the most interesting compounds are derived from the type III scaffold, the 1,5-benzothiazepine structures in particular (Figure 4.3).

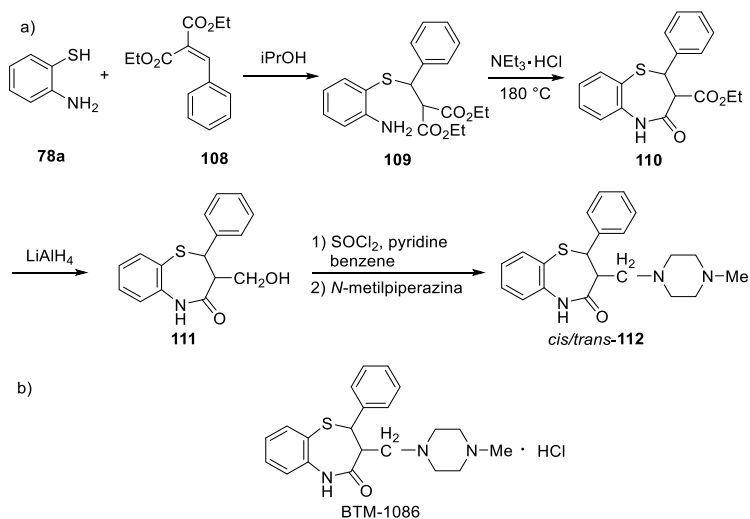
Despite their importance, only few methods have been developed for the stereoselective synthesis of benzothiazepines.<sup>79</sup> The most commonly used method to build the 1,5-benzothiazepine skeleton exploits the reaction of aminothiophenols with chalcones, under acid or basic reaction conditions. The first methodologies reported to prepare both enantioenriched forms, relied on optical resolution of the racemates. In particular, the first example of optically active disubstituted benzothiazepines dates back to 1983 and it is due to the experiments of Ohno and co-workers.<sup>80</sup> They reacted 2-aminothiophenol **78a** with diethyl benzylidenemalonate **108** thus obtaining the aminocarboxylic acid derivative **109**. The subsequent

<sup>79</sup> For reviews on the synthesis of 1,5-benzothiazepines, see: (a) K. Asano, S. Matsubara, *ACS Catal.* **2018**, *8*, 6273; (b) D. Saha, G. Jain, A. Sharma, *RSC Adv.* **2015**, *5*, 70619; (c) B. C. Sekhar, *Acta Chim. Slov.* **2014**, *61*, 651; (d) A. Levai, A. Kiss-Szikszai, *ARKIVOC* **2008**, *2008*, 65; (e) A. Levai, *J. Heterocycl. Chem.* **2000**, *37*, 199; (f) A. Chimirri, R. Gitto, S. Grasso, A. M. Monforte, M. Zappala, *Adv. Heterocycl. Chem.* **1995**, *63*, 61.

<sup>80</sup> S. Ohno, K. Izumi, K. Mizukoshi, K. Kato, M. Hori, *Chem. Pharm. Bull.* **1983**, *31*, 1780.



ring closure afforded the 3-alkyl-2-aryl benzothiazepine **110**. Compound **110** was then reduced with  $\text{LiAlH}_4$  to the 3-hydroxymethyl derivative **111**. The substitution of hydroxyl group with a chlorine atom and the following reaction with *N*-methylpiperazine afforded the racemic *cis/trans* products **112** (Scheme 4.1, a). The diastereomers were then separated and the *cis* product was optically resolved with tartaric acid in methanol to afford the optically pure (-)-*cis*-**112**. Its hydrochloride salt, BTM-1086 (Scheme 4.1, b), showed antiulcer and gastric secretory effects.



**Scheme 4.1** Ohno's synthesis of disubstituted 1,5 benzothiazepines.

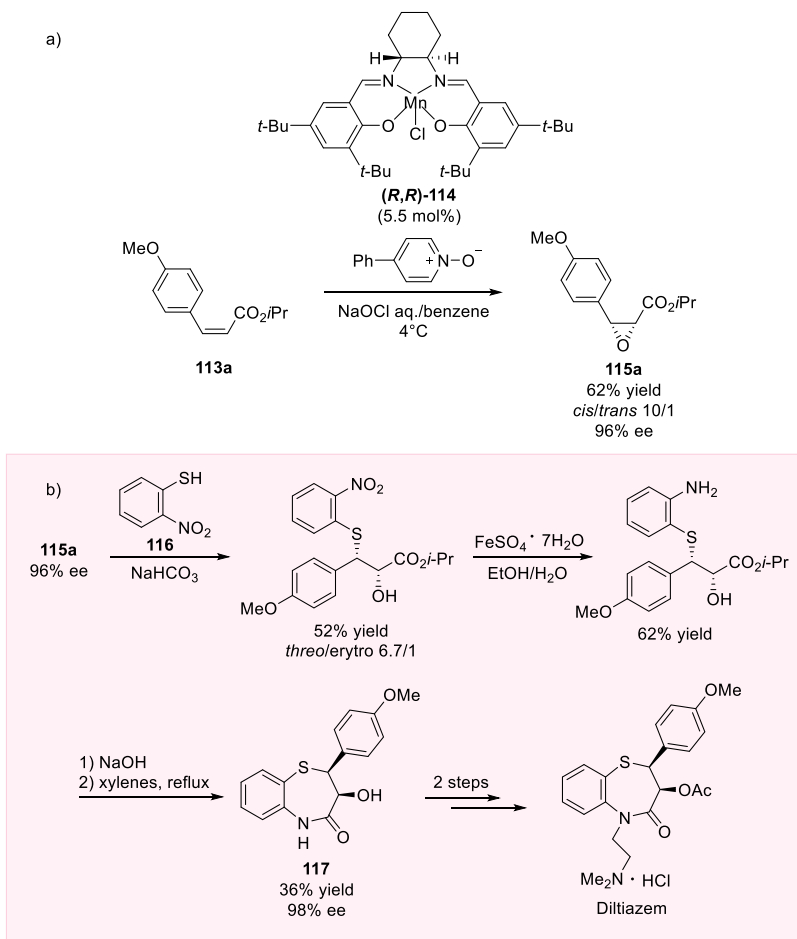
Other methodologies rely on elaboration of pre-formed enantiomerically enriched building blocks. Since the mid-1990s a certain number of methodological studies, then extended to the synthesis of enantiopure benzothiazepines, began to appear in the literature. For example, optically active glycidic esters, synthesized through an asymmetric epoxidation, proved to be key intermediates

in the synthesis of Diltiazem.<sup>81</sup> This method, developed thanks to the pioneering studies of Seiyaku is, to date, the most efficient industrial process for the synthesis of this pharmacophore. Various approaches allowing the synthesis of enantioenriched glycidic esters and employed in the synthesis of Diltiazem have been reported during the years. Among them, the following two examples are noteworthy. Jacobsen and colleagues carried out a study on the enantioselective epoxidation of cinnamate esters **113** using a chiral manganese complex (salen)Mn(III) **114** (Scheme 4.2, a).<sup>82</sup> In this reaction, *cis*-olefin substrates are essential to achieve epoxides with high enantiocontrol. Then the synthesis of diltiazem was carried out from epoxide **115a**. Ring opening of the epoxide by 2-nitrothiophenol **116** was carried out stereospecifically. The enantiomeric integrity of the epoxide remains untouched, as demonstrated with the isolation of product **117**, recovered with 98% of enantiomeric excess. Two additional steps on **117** skeleton provided the desired Diltiazem (Scheme 4.2, b).

---

<sup>81</sup> (a) T. Hashiyama, *Yuki Gosei Kagaku Kyokaishi* **1999**, 57, 394; (b) T. Furutani, *Yuki Gosei Kagaku Kyokaishi* **2001**, 59, 510; (c) M. Seki, *Yuki Gosei Kagaku Kyokaishi* **2003**, 61, 236.

<sup>82</sup> E. N. Jacobsen, L. Deng, Y. Furukawa, L. E. Martínez, *Tetrahedron*, **1994**, 50, 4323.

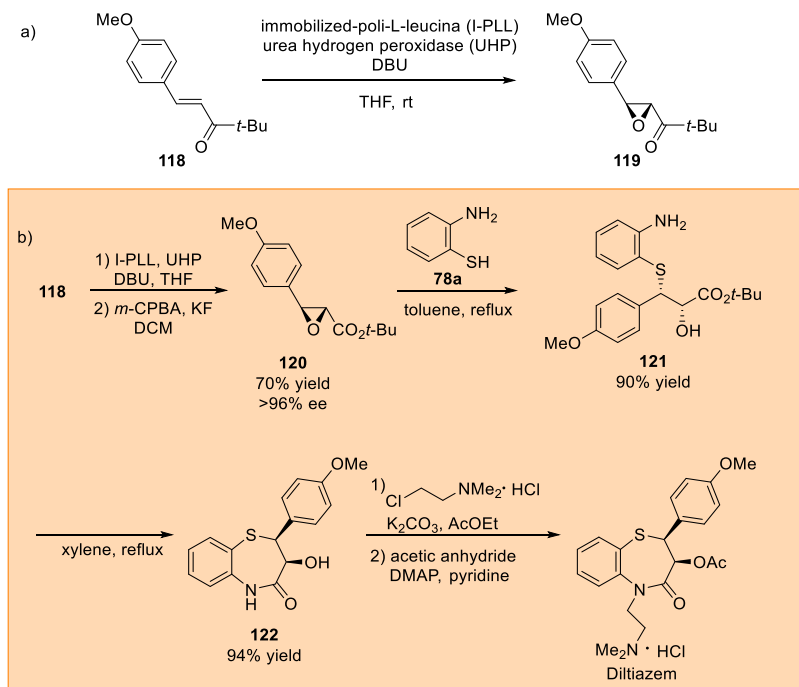


**Scheme 4.2** (a) (Salen)Mn(III)-catalyzed asymmetric epoxidation of cinnamate esters and (b) Synthesis of Diltiazem.

Some years later, in 1997, Roberts developed an improved procedure for the Juliá-Colonna asymmetric epoxidation of  $\alpha,\beta$ -unsaturated ketones and carried out the synthesis of Diltiazem from the corresponding enantioenriched epoxide.<sup>83</sup> The unsaturated ketone

<sup>83</sup> B. M. Adger, J. V. Barkley, S. Bergeron, M. W. Cappi, B. E. Flowerdew, M. P. Jackson, R. McCague, T. C. Nugent, S. M. Roberts, *J. Chem. Soc., Perkin Trans. 1*, **1997**, 3501.

**118** was efficiently treated with a readily available oxidant urea hydrogen peroxide (UHP) in the presence of DBU and an immobilised poly-L-leucine catalyst (Scheme 4.3, a). Then, the enantiomerically pure epoxy ketone **119** underwent a Baeyer–Villiger oxidation, giving the corresponding epoxy ester **120**. The use of *o*-aminothiophenol **78a** for the ring opening of epoxide afforded alcohol **121** with excellent yield. After dissolution of alcohol **121** in refluxing xylene, the diltiazem intermediate **122** was efficiently obtained. Finally, alkylation and acetylation steps allowed to obtain Diltiazem (Scheme 4.3, b).



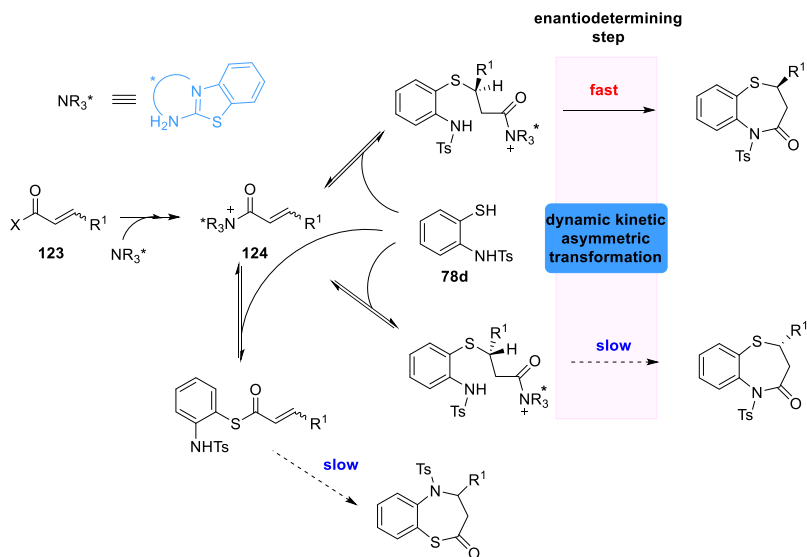
**Scheme 4.3** (a) Juliá-Colonna epoxidation with poly-L-leucine catalyst and (b) Synthesis of Diltiazem.

All methods reported in this section relied on optical resolution of the racemates or on elaboration of starting enantiopure building blocks. Thus, general methods have not been reported to prepare this class of benzothiazepines in a real catalytic fashion. In this context, only recently, Asano and Matsubara developed an efficient organocatalyzed protocol to obtain *trans*-2,3-disubstituted 1,5-benzothiazepines.<sup>84</sup> They carried out a chiral isothioureacatalyzed cycloaddition of activated  $\alpha,\beta$ -unsaturated anhydrides **123** and *N*-protected 2-aminothiophenols **78**. The  $\alpha,\beta$ -unsaturated acylammonium **124** are the intermediates involved in the process. Previous studies on regio- and enantioselective [4+3] cycloadditions involving acylammonium intermediates, revealed that the sulfa-Michael addition of 2-aminothiophenol to these intermediates is reversible, and the subsequent intramolecular lactamization is the stereo-determining step, namely a dynamic kinetic asymmetric transformation is involved (Scheme 4.4).<sup>85</sup>

---

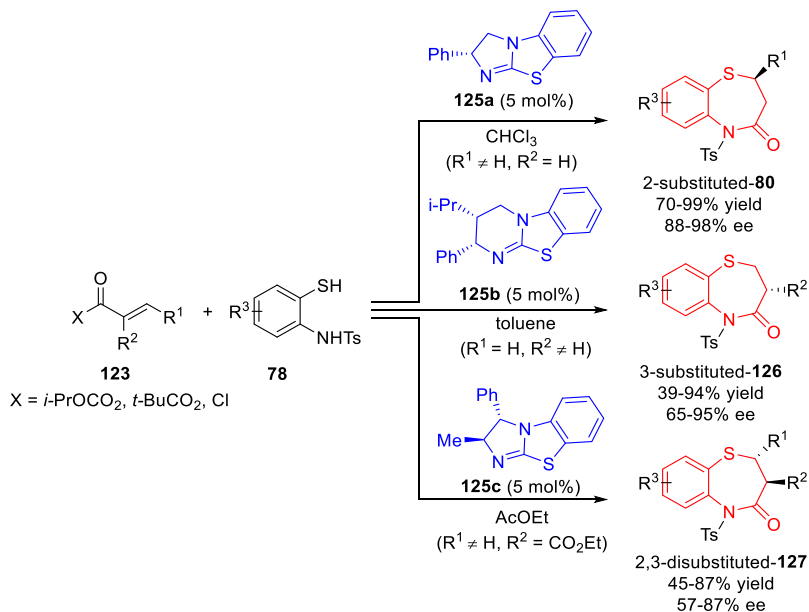
<sup>84</sup> Y. Fukata, K. Yao, R. Miyaji, K. Asano, S. Matsubara, *J. Org. Chem.*, **2017**, *82*, 12655.

<sup>85</sup> Y. Fukata, K. Asano, S. Matsubara, *J. Am. Chem. Soc.*, **2015**, *137*, 5320.



**Scheme 4.4** Isothioureacatalyzed net [4+3] cycloaddition toward optically active 2-substituted 1,5-benzothiazepines.

This mechanistic feature is responsible for the generally high enantioselectivity observed. A formal [4 + 3] cycloaddition reaction was devised under chiral isothioureacatalysis. This strategy allowed to carry out the synthesis of enantioenriched 1,5-benzothiazepines bearing various substitution patterns, i.e. the 2-substituted-**80**, the 3-substituted-**126** and 2,3-disubstituted-**127** scaffolds. In the case of 2,3-disubstituted 1,5-benzothiazepines the process proved to be highly diastereoselective, leading to *trans*-isomers, bearing a 3-carboxyethyl group, in good yield and good to high ee values (Scheme 4.5). The limit of the methodology is that only disubstituted *trans*-benzothiazepines, bearing an ester moiety at C3 position are obtainable. Moreover, these products show *N*-protected atoms, thus rendering necessary additional deprotection steps before further functionalization.

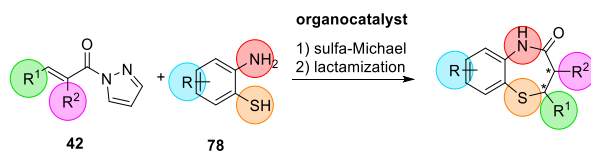


**Scheme 4.5** Synthetic approach to mono- and di-substituted 1,5-benzothiazepines.

## 4.2 Results and discussion

In 2017, we described an efficient method to obtain *N*-unprotected 2-substituted 1,5-benzothiazepines through a one-pot sulfa-Michael/lactamization sequence, promoted by a readily available bifunctional squaramide and silica gel respectively, by reacting *trans*-3-substituted  $\alpha,\beta$ -unsaturated *N*-acylpyrazoles and 2-aminothiophenols. Good to excellent results in terms of both yields and enantioselectivities were obtained (see Scheme 3.12).<sup>67</sup> Starting from these encouraging results and considering the paucity of catalytic methods for the synthesis of 2,3-disubstituted-1,5-benzothiazepines from readily available reagents, we decided to investigate this challenging goal. With our pleasure we were able to

develop a one-pot approach for the first enantioselective catalytic synthesis of *N*-unprotected *cis*- and *trans*-2,3-diaryl-1,5-benzothiazepines, starting from  $\alpha,\beta$ -unsaturated pyrazoleamides and 2-aminothiophenols. The two steps sequence is based on a bifunctional organocatalyzed sulfa-Michael reaction, followed by *p*-toluenesulfonic acid catalysed lactamization. Moreover, since the *N*-deprotection step is not required, the enantioenriched 1,5-benzothiazepines are immediately available for further functionalization, namely *N*-alkylation or acylation, which allow the creation of libraries of compounds for biological screening (Scheme 4.6).<sup>86</sup>



**Scheme 4.6** General scheme for the one-pot synthesis of optically active *cis*- and *trans*-disubstituted-1,5-benzothiazepines.

The activated olefins **42** have been easily synthesized through a two-step sequence, namely a condensation reaction between aromatic aldehydes **14** and arylacetic acids **128** followed by a DCC-mediated coupling reaction of the previously formed *trans*-cinnamic acid **129** and pyrazole **69a**, as reported in the literature.<sup>87</sup> The 2-aminothiophenols were obtained by hydrolysis of the corresponding

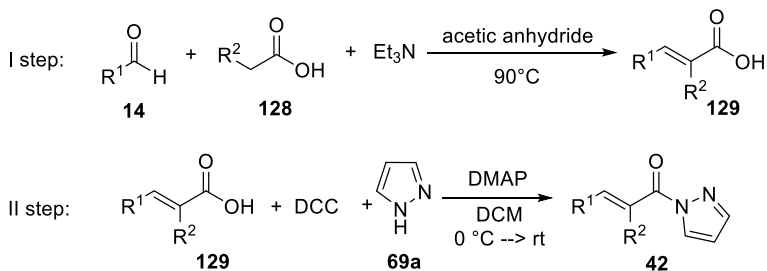
<sup>86</sup> S. Meninno, I. Quaratesi, C. Volpe, A. Mazzanti, A. Lattanzi, *Org. Biomol. Chem.* **2018**, *16*, 6923.

<sup>87</sup> (a) M. Pieroni, G. Annunziato, E. Azzali, P. Dessanti, C. Mercurio, G. Meroni, P. Trifiro, P. Vianello, M. Villa, C. Beato, M. Varasi, G. Costantino, *Eur. J. Med. Chem.*, **2015**, *92*, 377; (b) J. Zhang, X. Liu, R. Wang, *Chem. Eur. J.* **2014**, *20*, 4911.

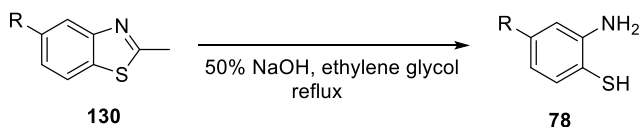


benzothiazoles **130** under basic reaction conditions (Scheme 4.7).<sup>88</sup>

alkenes synthesis:



2-aminothiophenols synthesis:



**Scheme 4.7** General scheme for the synthesis of reagents **42** and **78**.

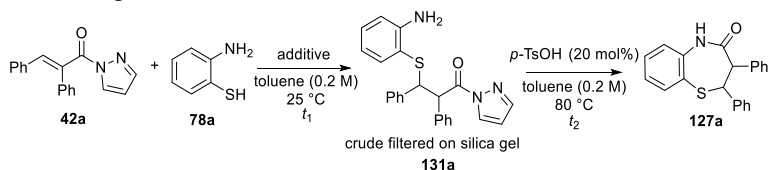
Our investigation began with  $\alpha,\beta$ -unsaturated *N*-acylpyrazoles **42** as starting Michael acceptors and 2-aminothiophenols **78** to check both the issue of diastereo- and enantioselectivity.

At the outset of the study, in the development of a diastereoselective version of the reaction, model alkene **42a** and 2-aminothiophenol **78a** were treated with various additives. By using silica gel, under our previously reported conditions,<sup>67</sup> almost no product was observed. In fact, after 21 hours, Michael adduct **131a** was formed in 21% yield, albeit with complete *anti*-diastereoselectivity (Table 4.1, es. 1). Triethylamine afforded comparable results in terms of yield, but with lower diastereoselectivity (es. 2). Neutral and basic alumina

<sup>88</sup> (a) G. Manfroni, F. Meschini, M. L. Barreca, P. Leyssen, A. Samuele, N. Iraci, S. Sabatini, S. Massari, G. Maga, J. Neyts, V. Cecchetti, *Bioorg. Med. Chem.* **2012**, *20*, 866; (b) Y. Fukata, K. Asano, S. Matsubara, *J. Am. Chem. Soc.* **2015**, *137*, 5320.

allowed to achieve good yields and diastereoselectivities of adduct **131a**, after a short reaction time (es. 3 and 4). By adding 2-aminothiophenol **78a** in two portions, an enhanced yield of **131a** was observed (es. 5). Finally, the lactamization step on isolated adduct **131a**, was conducted in the presence of a catalytic amount of *p*-TsOH and by heating the reaction mixture at 80 °C. In these conditions, the desired cyclic product *cis*-**127a** was quantitatively formed (es. 4).

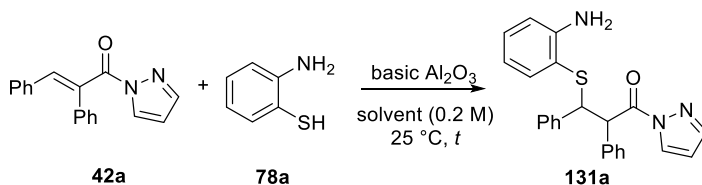
**Table 4.1** Additive screening in the racemic synthesis of 1,5-benzothiazepine **127a**.<sup>[a]</sup>



Es.	Additive (mg or eq.)	$t_1$ [h]	<i>anti/syn</i> <b>131a</b> <sup>[b]</sup>	Yield <b>131a</b> [%] <sup>[c]</sup>	$t_2$ [h]	Yield <i>cis</i> - <b>127a</b> [%] <sup>[d]</sup>
1	silica gel (113 mg)	21	100/0	21	-	-
2	NEt <sub>3</sub> (0.5 eq.)	48	75/25	28	-	-
3	neutral Al <sub>2</sub> O <sub>3</sub> (10 eq.)	5	85/15	72	-	-
4	basic Al <sub>2</sub> O <sub>3</sub> (10 eq.)	4	84/16	79	18	98
5 <sup>[e]</sup>	basic Al <sub>2</sub> O <sub>3</sub> (10 eq.)	6	83/17	89	-	-

<sup>[a]</sup> Unless otherwise noted reactions were conducted with **42a** (0.1 mmol), **78a** (0.11 mmol) and additive in dry toluene (0.2 M). <sup>[b]</sup> Determined by <sup>1</sup>H-NMR analysis of crude reaction mixture. <sup>[c]</sup> Determined by <sup>1</sup>H-NMR spectroscopy using 1,3,5-(MeO)<sub>3</sub>C<sub>6</sub>H<sub>3</sub> as an internal standard. <sup>[d]</sup> Yield of product **127a** purified by flash chromatography. <sup>[e]</sup> **78a** added in two portions.

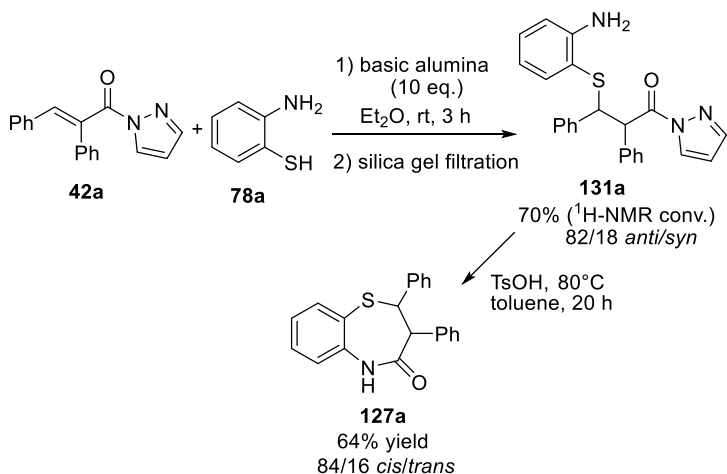
Subsequently, a solvent screening on the first reaction step was conducted and diethyl ether was found to be the most effective solvent (Table 4.2, es. 5).

**Table 4.2** Solvent screening in the racemic synthesis of **131a**.<sup>[a]</sup>

Es.	Solvent	<i>t</i> [h]	<i>anti/syn</i> <b>131a</b> <sup>[b]</sup>	Yield <b>131a</b> [%] <sup>[c]</sup>
1	toluene	5	83/17	70
2	CHCl <sub>3</sub>	24	85/15	27
3	acetonitrile	5	89/11	60
4	EtOAc	4	85/15	40
5	Et <sub>2</sub> O	2	82/18	73

<sup>[a]</sup> Unless otherwise noted reactions were conducted with **42a** (0.1 mmol), **78a** (0.11 mmol) added in two portions and additive in dry solvent (0.2 M). <sup>[b]</sup> Determined by <sup>1</sup>H-NMR analysis of crude reaction mixture. <sup>[c]</sup> Determined by <sup>1</sup>H-NMR spectroscopy using 1,3,5-(MeO)<sub>3</sub>C<sub>6</sub>H<sub>3</sub> as an internal standard.

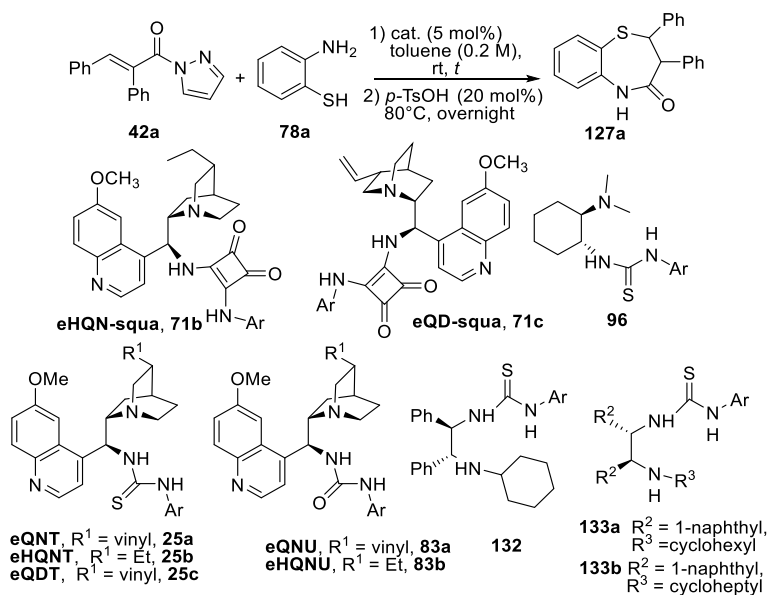
In conclusion, readily available basic alumina promoted the Michael step of the reaction and the corresponding adduct **131a** was obtained in good yield and *anti/syn* ratio, while working at room temperature. After silica gel filtration, the crude reaction mixture was heated in toluene at 80 °C in the presence of 20 mol% loading of *p*-toluenesulfonic acid to give the benzothiazepine **127a** in 64% overall isolated yield and comparable diastereoselective ratio (Scheme 4.8).



**Scheme 4.8** Optimized reaction sequence to racemic *cis/trans* **127a**.

After these results, our efforts focused on the development of an asymmetric version of the reaction, by using a variety of bifunctional organocatalysts.

A first screening of the organocatalysts has been carried out in toluene at room temperature on the model substrate **42a** with **78a** (Table 4.3). Hydroquinine-derived squaramide **71b**, utilized in our previous study, was checked in the one-pot sulfa-Michael/lactamization sequence (es. 1). Product **127a** was obtained in moderate conversion, 83/17 *cis/trans* ratio and with satisfactory enantioselectivity. Carrying out the first step in diethyl ether did not improve the outcome of the reaction (es. 2). Quinidine-derived squaramide **71c** was found to be only slightly less effective than *pseudo*-enantiomer **71b** (es. 3). Takemoto thiourea **96** and a variety of *Cinchona*-derived thioureas **25a-c** proved to be not quite active, as well as the quinine-derived urea **83a** (es. 4-8).

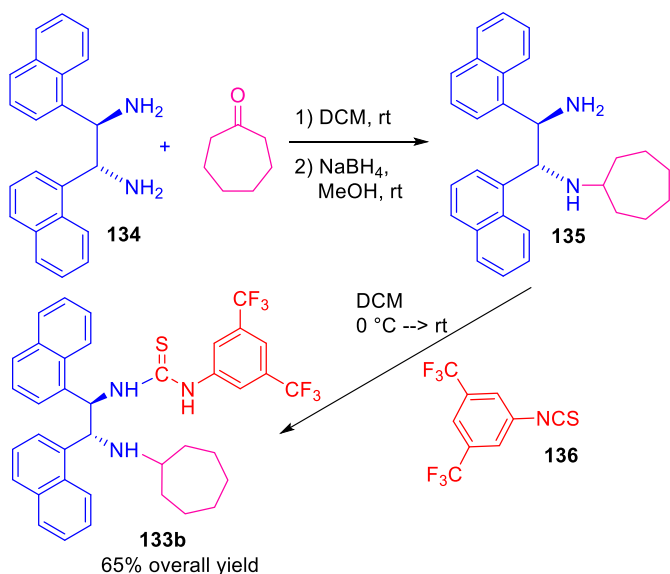
Table 4.3 Catalyst screening.<sup>[a]</sup>

Es.	cat.	<i>t</i> [h]	Yield <b>127a</b> [%] <sup>[b]</sup>	<i>cis/trans</i> <b>127a</b> <sup>[c]</sup>	<i>ee</i> <b>127a</b> [%] <sup>[d]</sup>
1	<b>71b</b>	5	56	83/17	75 (70)
2 <sup>[e]</sup>	<b>71b</b>	7	50	72/28	76 (65)
3	<b>71c</b>	5	43	80/20	-73 (-59)
4	<b>96</b>	6	25	72/28	-53 (-42)
5	<b>25a</b>	4	35	73/27	66 (53)
6	<b>25b</b>	4	24	83/17	74 (68)
7	<b>25c</b>	4	32	64/36	-57 (-50)
8	<b>83a</b>	7	33	70/30	73 (78)
9	<b>83b</b>	8	68	82/18	81 (62)
10	<b>132</b>	6	83	65/35	-79 (-94)
11	<b>133a</b>	6	70	54/46	80 (93)
12	<b>133b</b>	7	55	56/44	74 (95)

<sup>[a]</sup> Reaction conditions: **42a** (0.1 mmol), **78a** (0.11 mmol, added in two portions), cat. (0.005 mmol) in toluene (500  $\mu$ L) under N<sub>2</sub> atmosphere. After completion, *p*-toluenesulfonic acid monohydrate (0.02 mmol) was added. <sup>[b]</sup> Determined by <sup>1</sup>H-NMR analysis using 1,3,5-(MeO)<sub>3</sub>C<sub>6</sub>H<sub>3</sub> as an internal standard. <sup>[c]</sup> Determined by <sup>1</sup>H-NMR analysis of the crude reaction mixture. <sup>[d]</sup> Determined by chiral HPLC analysis on *cis*-**127a** and *trans*-**127a** (in parenthesis). <sup>[e]</sup> Reaction performed in Et<sub>2</sub>O.

On the contrary, urea catalyst **83b** was a good promoter of the reaction, affording product **127a** in good conversion, and good diastereo- and enantioselectivity towards the *cis*-isomer (es. 9).

Amine-thioureas **132**<sup>89</sup> and **133a**,<sup>90</sup> derived from 1,2-diaryl substituted diamines, proved to be effective catalysts of the process (es. 10 and 11). In these cases, the *cis*- and *trans*-diastereoisomers of **127a** were obtained in similar ratio, satisfactory combined yield and with an improved level of enantioselectivity (up to 94% ee for the *trans*-isomer). Given their ability to catalyze the reaction we synthesized catalyst **133b**, through a simple two-step protocol, in order to evaluate the effect of a bulkier group on the amine moiety (Scheme 4.9).



Scheme 4.9 Synthesis of catalyst **133b**.

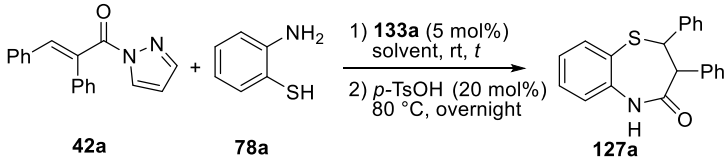
<sup>89</sup> S. Meninno, G. Croce, A. Lattanzi, *Org. Lett.* **2013**, *15*, 3436.

<sup>90</sup> S. Meninno, J. Overgaard, A. Lattanzi, *Synthesis* **2017**, *49*, 1509.

Starting from diamine **134**, a reductive amination with cycloheptanone was carried out. Diamine **135** was then reacted with isothiocyanate **136** to afford the final organocatalyst **133b** in good overall yield. Unfortunately, we did not achieve better results when using catalyst **133b** (Table 4.3, entry 12).

Due to the lack of protocols giving access to enantiomerically enriched *cis*- and *trans*-2,3-substituted-1,5-benzothiazepines, we considered highly desirable the development of a simple sequence that would enable their preparation under mild reaction conditions.

Amino thiourea **133a**, able to furnish both diastereoisomers of **127a**, was thus selected as catalyst to optimize other reaction parameters, with the aim to improve the enantioselectivity (Table 4.4). By working in toluene at 0°C a lower level of enantioselectivity for *cis*-**127a** was observed (es. 1). Dilution or concentration of the reaction mixture, when working at room temperature, had a negative effect on both conversion and enantioselectivity of the product (es. 2 and 3). It is known that in non-covalent catalysis, nonpolar solvents are generally the most suitable media, since they do not disturb the hydrogen bonding interactions established between the reactants and the organocatalyst. Among the aromatic solvents tested, *m*-xylene was found to be the most effective, affording both *cis*- and *trans*-**127a** with the highest yields and ee values. (Table 4.4, es. 9).

**Table 4.4** Optimization of the reaction conditions.<sup>[a]</sup>


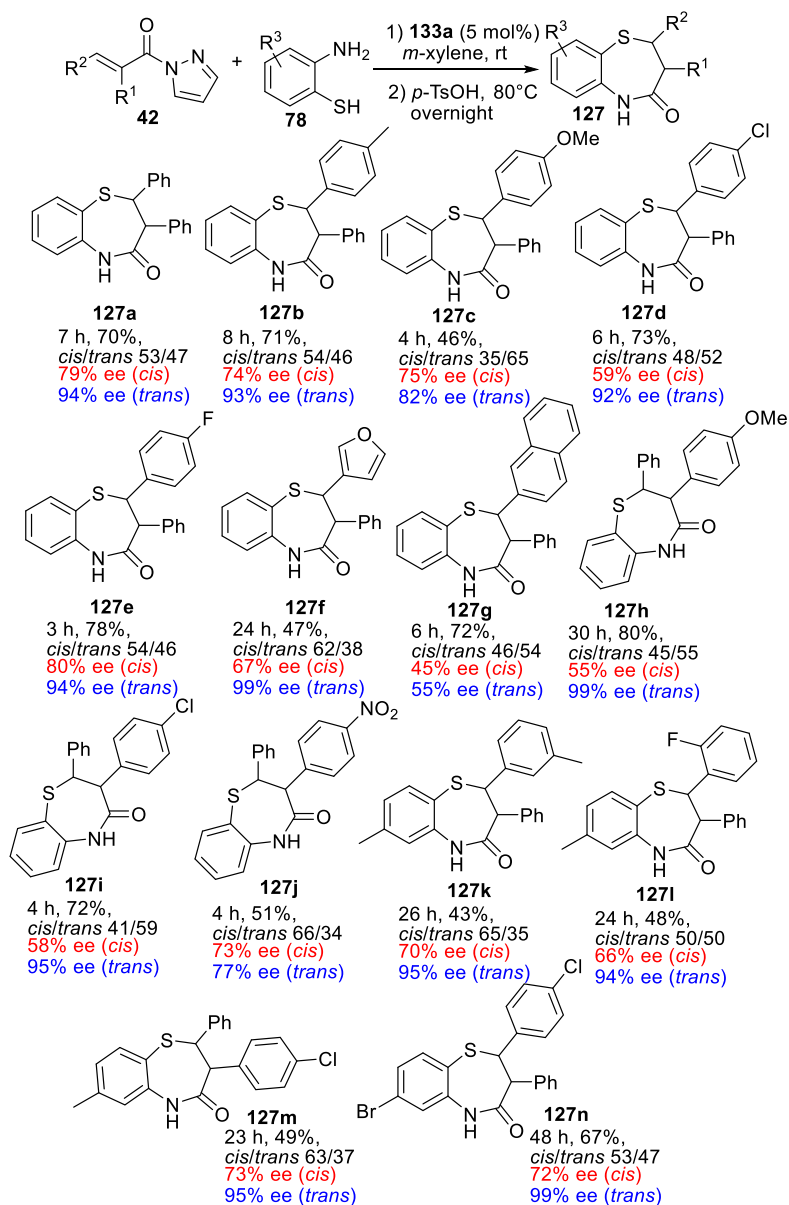
Es.	solvent	<i>t</i> [h]	Yield <b>127a</b> [%] <sup>[b]</sup>	<i>cis/trans</i> <b>127a</b> [%] <sup>[c]</sup>	<i>ee</i> <b>127a</b> [%] <sup>[d]</sup>
1 <sup>[e]</sup>	toluene	7	72	55/45	70 (94)
2 <sup>[f]</sup>	toluene	70	37	55/45	76 (92)
3 <sup>[g]</sup>	toluene	5	52	65/35	54 (86)
4 <sup>[h]</sup>	Et <sub>2</sub> O	5	54	48/52	60 (95)
5 <sup>[h]</sup>	CH <sub>2</sub> Cl <sub>2</sub>	26	25	64/36	54 (88)
6	C <sub>6</sub> H <sub>5</sub> Cl	7	58	57/43	66 (90)
7	mesitylene	7	61	51/49	80 (95)
8	xylenes	5	47	51/49	75 (94)
9	<i>m</i> -xylene	7	75	51/49	79 (95)
10	benzene	7	60	65/35	75 (90)

<sup>[a]</sup> Reaction conditions: **42a** (0.1 mmol), **78a** (0.11 mmol, added in two portions), **133a** (0.005 mmol) in solvent (500  $\mu$ L) under inert atmosphere. After completion, *p*-toluenesulfonic acid monohydrate (0.02 mmol) was added. <sup>[b]</sup> Determined by <sup>1</sup>H-NMR analysis with 1,3,5-(MeO)<sub>3</sub>C<sub>6</sub>H<sub>3</sub> as an internal standard. <sup>[c]</sup> Determined by <sup>1</sup>H-NMR analysis of the crude reaction mixture. <sup>[d]</sup> Determined by chiral HPLC analysis on analysis on *cis*-**127a** and *trans*-**127a** (in parenthesis). <sup>[e]</sup> Reaction performed at 0 °C. <sup>[f]</sup> Reaction performed at C = 0.05 M. <sup>[g]</sup> Reaction performed at C = 0.5 M. <sup>[h]</sup> Second step performed in toluene.

Under the optimized conditions (Table 4.4, es. 9), several *trans*-3-substituted  $\alpha,\beta$ -unsaturated *N*-acylpyrazoles **42** and 2-aminothiophenols **78** were investigated to explore the scope of the process (Table 4.5). 2-Aminothiophenol **78a** was first used as the nucleophile. 1,5-Benzothiazepines, bearing electron-rich substituents in the phenyl at position 2 (C2) (**127b-c**) were obtained with similar diastereoselectivity, although a lower level of



enantioselectivity was observed for *cis*-isomer of **127d**. Instead, alkenes **42** bearing electron-poor aromatic substituents or heteroaromatic residues at 2-position afforded both *cis*- and *trans*-diastereoisomers of benzothiazepines in good to acceptable yield and good to complete enantiocontrol (**127d-f**). The enantioselectivity of the reaction drastically dropped, for both isomers, when a more sterically demanding 2-naphthyl moiety was installed at the  $\beta$ -position of alkene **42g**.

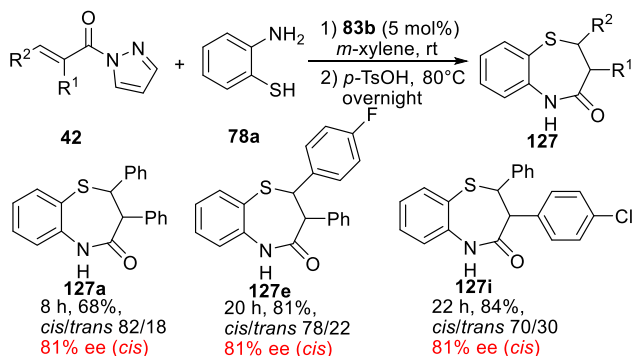
Table 4.5 Substrate scope.<sup>[a]</sup>

<sup>[a]</sup> Reaction conditions: **42** (0.2 mmol), **78** (0.22 mmol, added in two portions), **133a** (0.010 mmol) in toluene (1 mL) under inert atmosphere. After completion, *p*-toluenesulfonic acid monohydrate (0.04 mmol) was added. Yields of isolated products are given.

Alkenes **42** bearing phenyl at 3-position were also converted to the corresponding products with high enantioselectivities for the *trans*-isomer and moderate for the *cis*-isomers (**127h-i**), while products **127j** were obtained with 73% and 77% ee. Unluckily, our methodology was incompatible with  $\alpha,\beta$ -unsaturated acylpyrazoles bearing alkyl substituents, which provided low conversion to the corresponding products after prolonged reaction time. Substituted 2-aminothiophenols **78** were then reacted with different alkenes and both *cis*- and *trans*-2,3-disubstituted 1,5-benzothiazepines **127k-n** were isolated in comparable ratio, moderate to satisfactory yield and high to excellent enantioselectivity for the *trans*-isomer, also when the  $\beta$ -aromatic ring is endowed with an *ortho*-substitution (**127l**). As shown in Table 4.3, *cis*-2,3-substituted 1,5-benzothiazepines were predominantly formed, with improved enantioselectivities, when the hydroquinine-derived urea **83b** was used (es. 9).

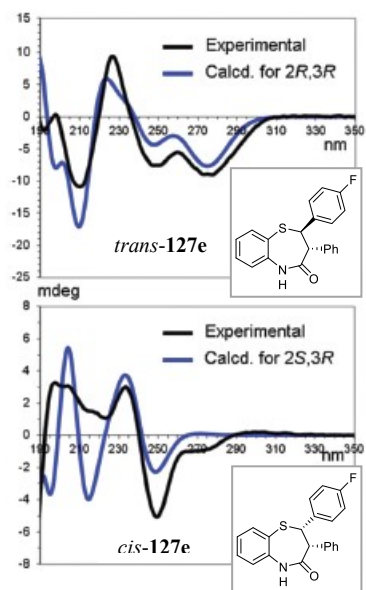
Then we briefly investigated the reaction with catalyst **83b**, working in *m*-xylene at room temperature (Table 4.6).

**Table 4.6** One-pot sequence mediated by catalyst **83b**.<sup>[a]</sup>



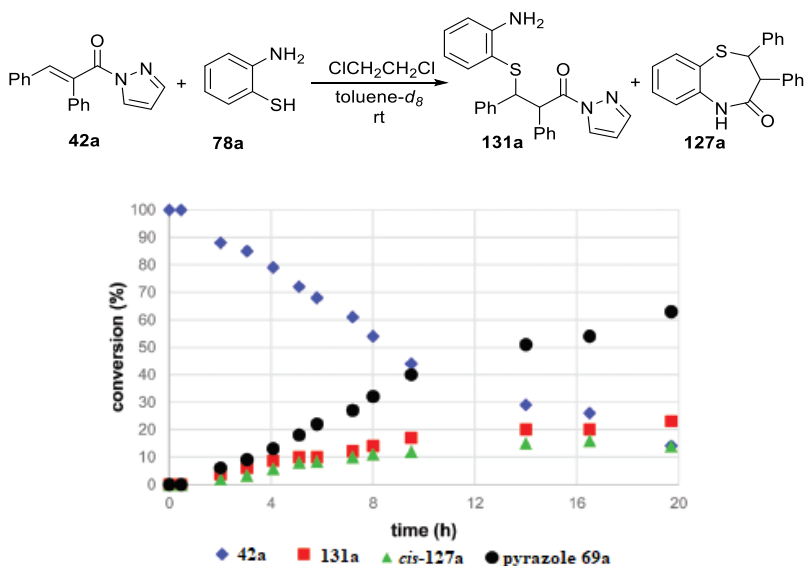
<sup>[a]</sup> Reaction conditions: **42** (0.2 mmol), **78** (0.22 mmol, added in two portions), **83b** (0.010 mmol) in toluene (1 mL) under inert atmosphere. After completion, *p*-toluenesulfonic acid monohydrate (0.04 mmol) was added. Yields of isolated products are given.

Since it was not possible to obtain good crystals for any compound, a theoretical approach was required, in order to establish the absolute configuration of products. This part was carried out in collaboration with Professor Mazzanti, from University of Bologna, who employed a hybrid approach based on NMR spectroscopy and Electronic Circular Dichroism (ECD), supported by DFT conformational analysis and TD-DFT calculation of ECD spectra to assign the relative and absolute configuration of compounds *trans*-**127e** and *cis*-**127e**. The relative configuration was assigned thanks to the analysis of coupling constants between the two CH protons at position 2 and 3 of 1,5-benzothiazepine, and the ECD spectra were successfully simulated considering the *2R,3R* absolute configuration for *trans*-**127e**, and the *2R,3R* absolute configuration of *cis*-**127e** (Figure 4.4).



**Figure 4.4** TD-DFT simulations of the ECD spectra of *trans*-**127e** and *cis*-**127e**.

The absolute configuration of the other compounds **127** was assigned by analogy. At this point, mechanistic investigations were carried out with the aim to elucidate the regio- and stereochemical outcome of the reaction with model compound. The uncatalyzed reaction of **42a** with **78a** was performed in toluene- $d_8$  and monitored via  $^1\text{H}$  NMR over time (Figure 4.5). Interestingly, in the absence of any catalyst, low amounts (<10%) of adduct **131a** and product *cis*-**127a** were detected in the reaction mixture after 5 hours. Moreover, the amount of free pyrazole is always higher than the amount of *cis*-**127a**, which was the only detected diastereoisomer together with Michael adduct **131a**. Specifically, after 7 hours 12% of adduct **131a** with 87/13 diastereomeric ratio, 10% of *cis*-**127a**, 62% of **42a** and 27% of free pyrazole could be identified in the reaction mixture. This uncatalyzed parallel reaction would explain the lower enantioselectivity observed for *cis*-diastereoisomer. Moreover, this experiment showed that a competitive 1,2-addition/elimination reaction occurred on the starting alkene **42a**, thus giving the corresponding  $\alpha,\beta$ -unsaturated thioester **134a**.

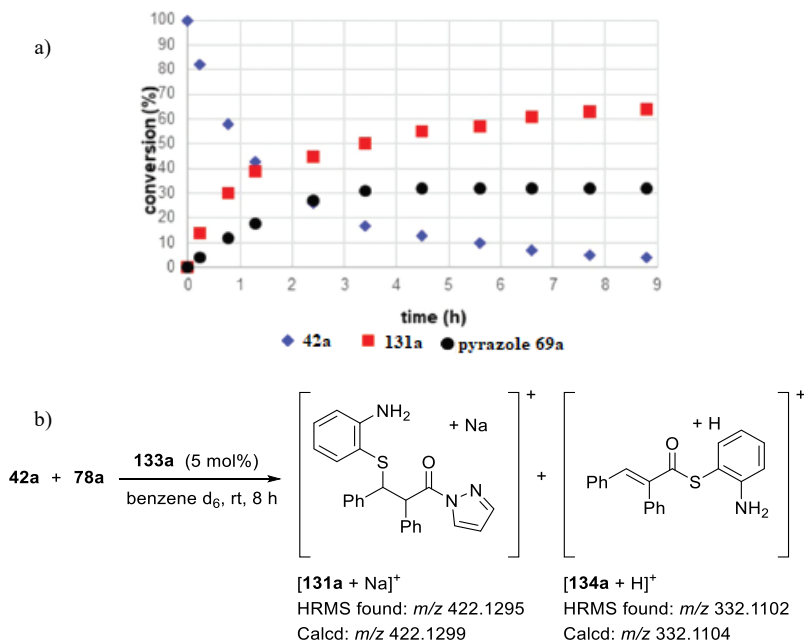


**Figure 4.5** Reaction progress profile over time in the presence of 1,2-dichloroethane as internal standard without catalyst in toluene  $\text{d}_8$  at rt.

Another experiment was performed in benzene- $\text{d}_6$ <sup>91</sup> in the presence of 5 mol% of catalyst **133a** (Figure 4.6). As shown in the plot, the progressive formation of adduct **131a** with a constant level of diastereoselectivity, of about 65/35, was detected over time. Cyclic compound **127a** was not observed in the reaction mixture, thus proving that the uncatalyzed reaction does not affect the process, when a faster conversion of alkene **42a** to **131a** is promoted by the organocatalyst. The estimated conversion to the adduct is consistent with the final isolated yield of **127a** reported in Tables 4.4 and 4.5. Secondly, the organocatalyst promoted the competitive 1,2-addition/

<sup>91</sup> The selection of benzene- $\text{d}_6$  as the solvent, instead of toluene- $\text{d}_8$ , arises from the necessity to have an aromatic solvent showing the 6-9 ppm region of spectrum as free as possible of solvent signals, in order to facilitate the analysis.

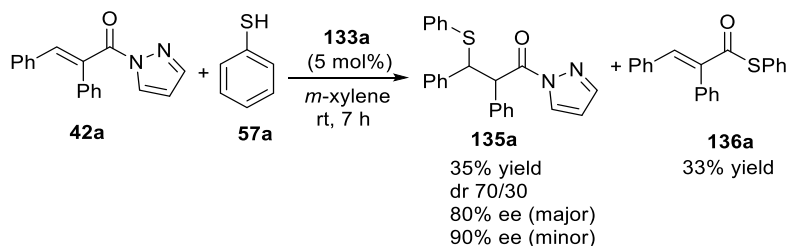
elimination reaction, as demonstrated by detection of 30% of free pyrazole at the end of reaction (Figure 4.6, a). An evidence attesting the presence of both adduct **131a** and unsaturated thioester **134a** derived from high resolution mass spectrometry analysis (HRMS) of the crude reaction mixture (Figure 4.6, b).



**Figure 4.6** (a) Reaction progress profile over time in the presence of 1,2-dichloroethane as internal standard with 5 mol% of **133a** in benzene- $d_6$  at room temperature and (b) HRMS analysis of the crude reaction mixture.

Moreover, the diastereoisomeric mixture of adduct **131a** was found to be unstable on silica gel, which promotes the cyclization of *syn*-**131a** to the corresponding *trans*-**127a**, thus impacting on the original diastereoisomeric ratio of **131a** determined on the crude mixture by  $^1\text{H-NMR}$  analysis.

Since the isolation of thioester **134a** was not possible using silica gel chromatography, we decided to investigate the reaction of model alkene **42a** with thiophenol **57a** in the presence of catalyst **133a** under the optimized reaction conditions (Scheme 4.10).

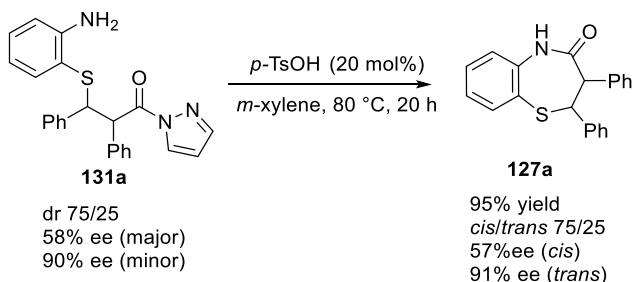


**Scheme 4.10** Asymmetric sulfa-Michael reaction of **42a** with thiophenol.

The Michael adduct **135a** was recovered in 35% yield, 70/30 diastereomeric ratio and good ee values, both for major and minor diastereoisomers. Moreover, the 1,2-addition product **136a** was obtained in 33% yield. This experiment confirmed that the competitive 1,2-addition/elimination reaction is partially promoted by our organocatalyst, by lowering the overall yield of the benzothiazepines **127**.

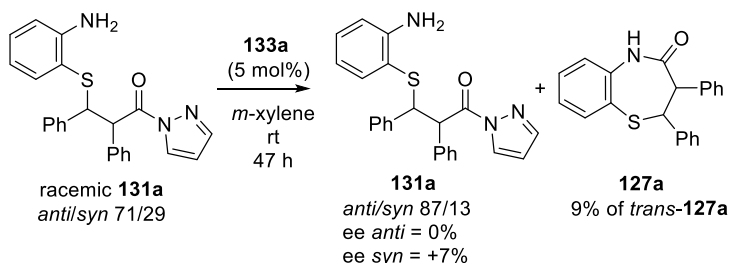
Finally, we decided to investigate the lactamization step. In this regard, the diastereo- and enantiomerically enriched **131a** was heated at 80 °C in *m*-xylene, in the presence of 20 mol% of *p*-TsOH, in order to control the stereochemical integrity over the cyclization step (Scheme 4.11).





**Scheme 4.11** Cyclization of diastereo- and enantioenriched mixture of adduct **131a**.

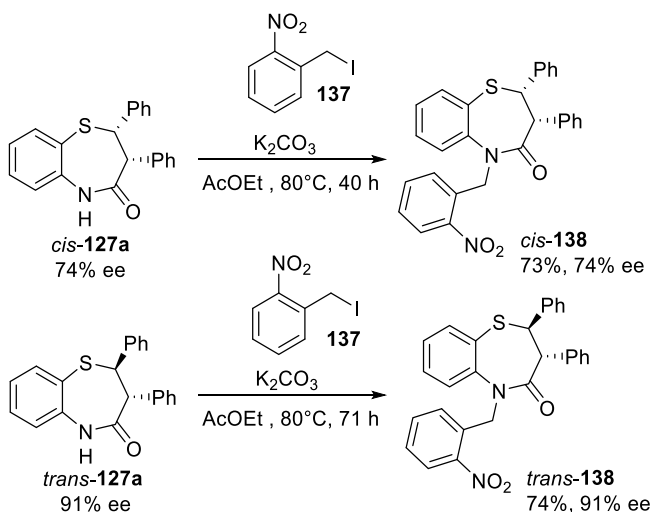
The same level of diastereo- and enantioselectivity of the starting adduct **131a** was observed on *cis/trans*-**127a**, ruling out the possibility of a retro-sulfa Michael/sulfa-Michael process that would lead to epimerization/racemization. In addition, we treated a racemic mixture of the adduct **131a**, in 71/29 diastereomeric ratio, with catalyst **133a** for two days, under usual conditions at room temperature (Scheme 4.12). A poor amount (<10%) of *trans*-**127a** was detected after 47 hours, thus demonstrating that the organocatalyzed lactamization process is negligible within the reaction times reported in Table 4.5.



**Scheme 4.12** Treatment of racemic adduct **131a** with organocatalyst at rt.

In summary, all performed mechanistic investigations confirmed the sulfa-Michael reaction being the prevalent process with respect to 1,2-addition/elimination pathway, when using the amine thiourea catalyst **133a** (Figure 4.6). The uncatalyzed Michael and lactamization reactions (Figure 4.5), as well as catalyst promoted lactamization (Scheme 4.12), could alter the overall outcome in terms of diastereo- and enantioselectivity, but they proved to be poorly effective processes during the reaction times shown in Table 4.5.

In order to demonstrate the synthetic utility of our methodology, we carried out *N*-alkylation of both enantioenriched *cis*- and *trans*-**127a**. The reaction was performed in ethyl acetate at 80 °C with *o*-nitrobenzyl iodide **137**, by working under basic conditions (Scheme 4.13) and the corresponding *N*-alkylated derivatives were obtained in good yield as pure *cis*-**138** or *trans*-**138**, maintaining the level of enantioselectivity.



**Scheme 4.13** *N*-alkylation of enantioenriched *cis*-**127a** and *trans*-**127a**.

## CONCLUSIONS

The first one-pot organocatalytic sulfa-Michael/lactamization sequence to both *cis*- and *trans*-2,3-disubstituted 1,5-benzothiazepines in optically enriched form has been developed, starting from readily available *trans*-2,3-disubstituted  $\alpha,\beta$ -unsaturated *N*-acylpyrazoles and 2-aminothiophenols. This methodology, which proceeds under mild reaction conditions, is promoted by a readily available chiral amine-thiourea or urea and cheap *p*-toluenesulfonic acid. The NH-free 2,3-substituted 1,5-benzothiazepines are obtained in moderate to good yield and diastereoselectivity, while good to complete enantiocontrol is observed. Mechanistic studies allowed to establish that the sulfa-Michael reaction is the stereodetermining step and the stereoselectivity is maintained during the cyclization step. The process provides access to both diastereomers with useful level of enantioselectivities, but it is particularly advantageous in view of the crucial elaboration of the seven-membered ring scaffold. The *N*-deprotection step is not required, thus making the enantioenriched products immediately suitable for *N*-alkylation or *N*-acylation, which are typical derivatizations to create libraries of compounds for biological screening.

## 5. 1,5,7-TRIAZABICYCLO[4.4.0]DEC-5-ENE (TBD) TRIGGERED DIASTEREOSELECTIVE [3+2] CYCLOADDITION OF AZOMETHINE IMINES AND PYRAZOLEAMIDES

### 5.1 Background

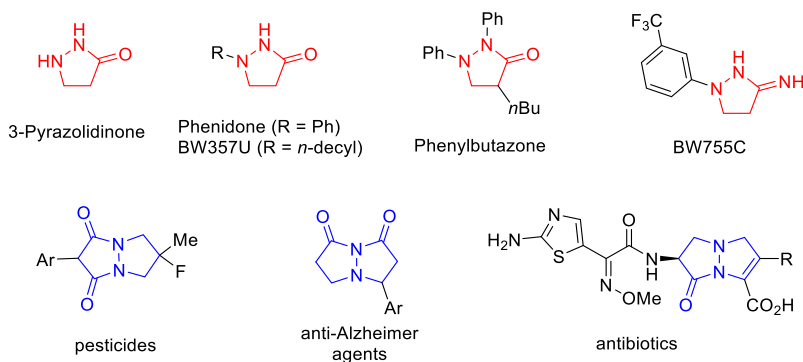
Nitrogen-based heterocyclic scaffolds can be considered the most important structural components of pharmaceuticals.<sup>92</sup> Analysis of U.S FDA databases reveals that 59% of small-molecule drugs contains a nitrogen heterocycle, with the five-membered ring representing a recurrent motif.<sup>93</sup>

3-Pyrazolidinone and its derivatives are a class of organic compounds characterized by a five-membered ring including a nitrogen-nitrogen covalent bond, with at least an acyl group in their skeleton (Figure 5.1). Pyrazolidinone derivatives are endowed with a wide range of biological and pharmaceutical activities, ranging from anti-inflammatory (phenylbutazone) and anorectic (BW357U) activities to inhibition capacity of cyclooxygenase and lipoxygenase (BW755C and phenidone respectively). Bicyclic pyrazolidinones are common drugs acting as pesticides, anti-Alzheimer agents, antibiotics and others. The aforementioned structures are depicted in Figure 5.1.

---

<sup>92</sup> For reviews on nitrogen heterocycles, see: (a) E. Vitaku, D. T. Smith, J. T. Njardarson, *J. Med. Chem.* **2014**, *57*, 10257; (b) C. T. Walsh, *Tetrahedron Lett.* **2015**, *56*, 3075.

<sup>93</sup> <http://cbc.arizona.edu/njardarson/group/content/disease-focused-pharmaceutical-posters>.



**Figure 5.1** Representative examples of bioactive 3-pyrazolidinone derivatives.

Given their wide applicability and biological activity, pyrazolidin-3-one derivatives, bicyclic skeletons in particular, constitute very attractive synthetic targets. Their enantio- and/or diastereoselective synthesis represents an attractive challenge for synthetic organic chemists.

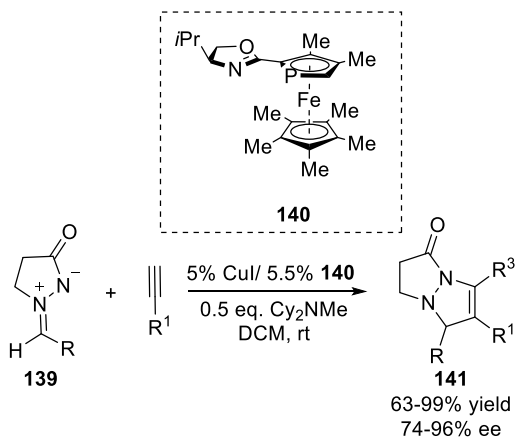
1,3-Dipolar cycloaddition reactions provide easy access to five-membered heterocycles, affording the corresponding products with high stereo- and regioselectivity in a single step.<sup>94</sup> In particular, azomethine imines are useful dipoles in cycloaddition reactions, thanks to their facile synthesis and benchtop stability.<sup>95</sup> They react with a wide range of dipolarophiles, such as olefins, alkynes, enones, isocyanides and allenes, thus providing dinitrogen heterocyclic products.<sup>96</sup> Pioneering studies of Fu and coauthors, illustrated a

<sup>94</sup> For selected reviews, see: (a) A. Padwa, W. H. Pearson, *Synthetic Applications of 1,3-Dipolar Cycloaddition Chemistry Toward Heterocycles and Natural Products*, Wiley: Hoboken, NJ, **2002**. (b) K. V. Gothelf, K. A. Jørgensen, *Chem. Rev.* **1998**, *98*, 863.

<sup>95</sup> H. Dom, A. Otto, *Angew. Chem., Int. Ed. Engl.* **1968**, *7*, 214.

<sup>96</sup> For a review on 1,3-dipolar cycloadditions of azomethine imines, see: C. Najera, J. M. Sansano, M. Yus, *Org. Biomol. Chem.* **2015**, *13*, 8596.

Cu(I)/phosphaferrocene-oxazoline (**140**) catalyzed asymmetric cycloaddition of azomethine imines **139** to terminal alkynes (Scheme 5.1).<sup>97</sup> This reaction led to the corresponding products **141** with excellent results.

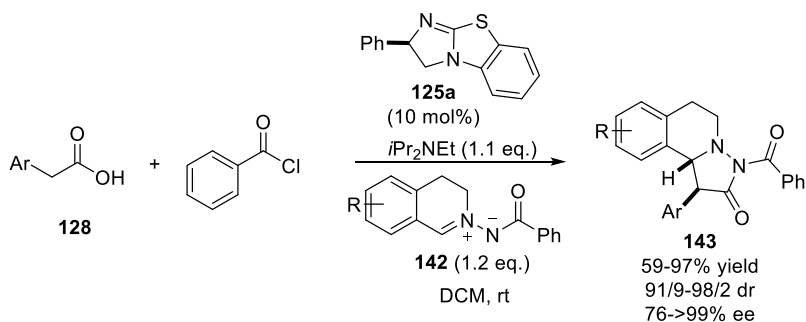


**Scheme 5.1** 1,3-dipolar cycloaddition of azomethine imines to alkynes.

Additionally, Studer and colleagues demonstrated that the *N*-iminoisoquinolinium ylides **142** are also promising 1,3-dipoles in asymmetric 1,3-dipolar cycloadditions.<sup>98</sup> They reacted azomethine imines **142** with active esters in the presence of the Lewis basic catalyst **125a**. The active esters are readily *in situ* generated from the corresponding arylacetic acids **128**. Bicyclic products **143** were obtained with excellent diastereocontrol and high enantioselectivity (Scheme 5.2).

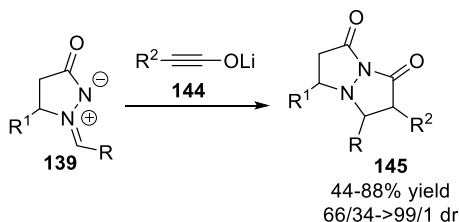
<sup>97</sup> R. Shintani, G. C. Fu, *J. Am. Chem. Soc.* **2003**, *125*, 10778.

<sup>98</sup> L. Hesping, A. Biswas, C. G. Daniliuc, C. Muck-Lichtenfeld, A. Studer, *Chem. Sci.* **2015**, *6*, 1252



**Scheme 5.2** Stereoselective Lewis base catalyzed formal 1,3-dipolar cycloaddition of azomethine imines with active esters.

Starting from these results, Winterton and Ready recently reported a synthetic route to pyrazolidinones involving a [3+2]-cycloaddition reaction of azomethine imines with lithium ynolates (Scheme 5.3).<sup>99</sup> Compared to previous cycloaddition examples, this transformation provides access to bicyclic pyrazolidinones **145**, which are at higher oxidation state than products **141**. Moreover, this reaction sets two contiguous stereocenters with good to high diastereoselectivity.

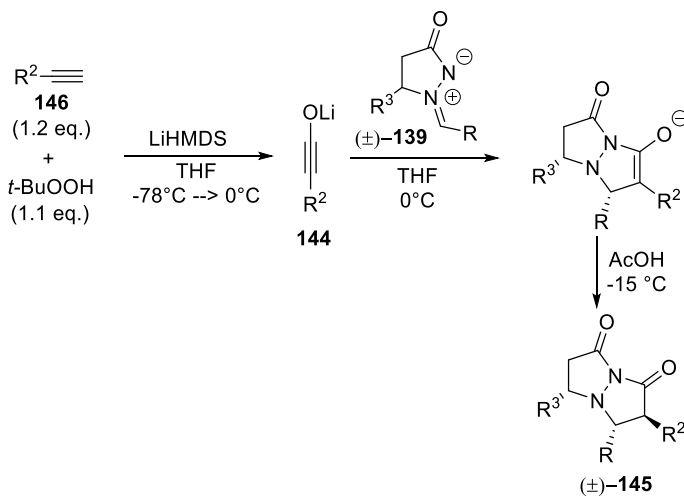


**Scheme 5.3** [3+2]-cycloadditions of azomethine imines and ynolates.

This synthesis was developed in a convenient one-pot route, albeit strictly controlled reaction conditions are required (Scheme 5.4). The opportune alkyne **146** and *t*-BuOOH were combined and treated with

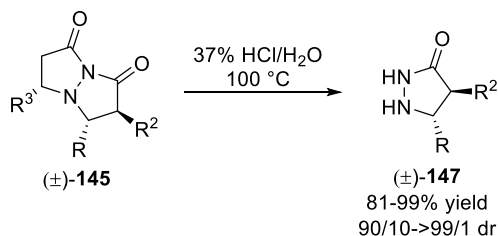
<sup>99</sup> S. E. Winterton, J. M. Ready, *Org. Lett.* **2016**, *18*, 2608.

an overstoichiometric amount of LiHMDS at low temperature to form the corresponding lithium ynolate **144**. Subsequent introduction of the azomethine imine **139** afforded cycloadduct **145**, after quenching under mildly acidic conditions at  $-15^{\circ}\text{C}$ .



**Scheme 5.4** One-pot synthesis of pyrazolidinones **145**.

Moreover, authors showed that the imide bond could be readily hydrolyzed and, after protonation of nitrogen atom, C(R<sub>3</sub>)-N bond could be cleaved. In this regard, by heating bicyclic products **145** to  $100^{\circ}\text{C}$  in aqueous HCl, the monocyclic derivatives **147** were obtained in excellent yields (Scheme 5.5).

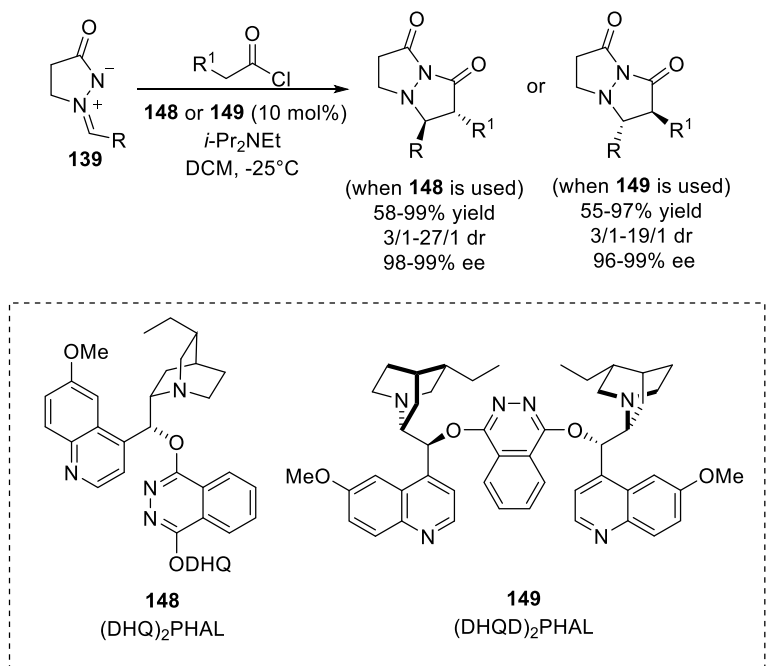


**Scheme 5.5** C-N bond cleavage of bicyclic pyrazolidinones.

In the same year, the Kerrigan's group assembled the pyrazolidinone



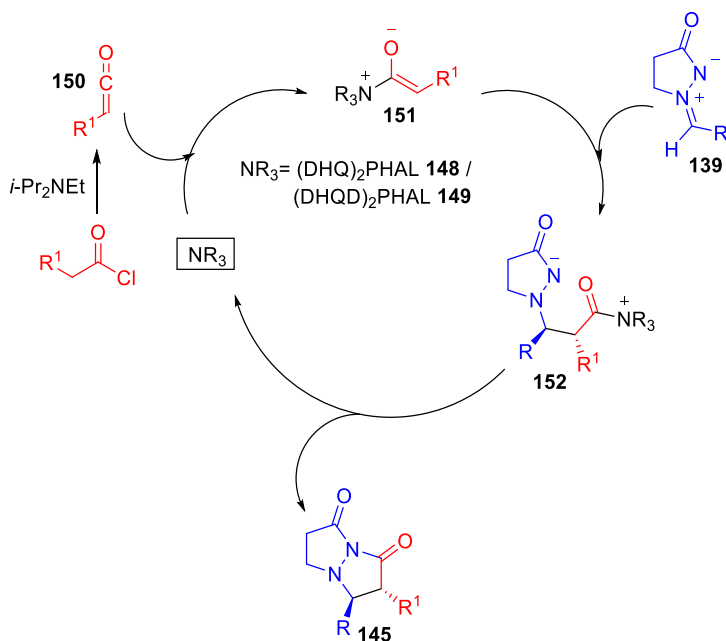
motif **145** through an alkaloid-catalyzed asymmetric formal [3+2] cycloaddition of azomethine imines **139** with *in situ* generated ketenes (Scheme 5.6).<sup>100</sup> This diastereo- and enantioselective process was promoted by commercially available *Cinchona*-alkaloid dimers and the corresponding products were isolated in good to excellent yields and with good to excellent diastereo- and enantioselectivity. Moreover, both enantiomers of **145** can be accessed in high optical purity by employing the pseudoenantiomeric catalysts **148** and **149**.



**Scheme 5.6** Alkaloid-catalyzed asymmetric [3+2] cycloaddition of ketenes with azomethine imines.

<sup>100</sup> M. Mondal, K. A. Wheeler, N. J. Kerrigan, *Org. Lett.* **2016**, *18*, 4108.

The proposed mechanism for the formation of compounds **145** starts from the *in situ* generation of ketene **150**, by treating acyl chlorides with DIPEA. Subsequent addition of chiral catalyst **148** or **149** in the reaction mixture, results in the formation of the ammonium enolate **151**. The attack of the ammonium enolate to the azomethine imine **139** provides access to zwitterionic species **152**, which subsequently undergoes cyclization to afford product **145** with the simultaneous regeneration of the alkaloid catalyst (Scheme 5.7).



**Scheme 5.7** Proposed mechanism for catalytic asymmetric synthesis of bicyclic pyrazolidinones.

## 5.2 Results and discussion

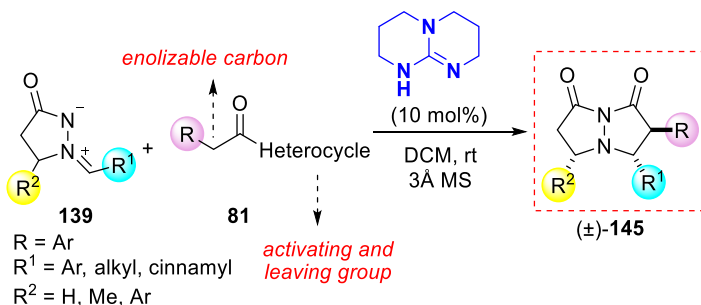
Previously reported examples are based on the *in situ* generation of the reactive species, under controlled reaction conditions. The development of more practical and mild routes, which pay also attention to step- and pot-economies is then highly desirable.

In 2012, Barbas showed that pyrazoleamides can be rather easily deprotonated at  $\alpha$ -position and the corresponding enolates are useful carbon nucleophiles. Moreover, the pyrazole moiety serves as both activating and directing group, but it is also a good leaving group.<sup>68</sup>

With these informations in hand, we designed an efficient method to obtain bicyclic pyrazolidinones **145** through a cascade one-pot Mannich reaction followed by intramolecular amidation. This sequence, promoted by catalytic amounts of the commercial base TBD, reacts *N*-acylpyrazoles **81** and *N,N'*-cyclic azomethine imines **139**. When working under mild reaction conditions, a variety of tetrahydropyrazolo[1,2-*a*]-pyrazole-1,7-diones **145** with up to three stereocentres were synthesized and good to excellent results in terms of both yields and diastereoselectivities were recorded (Scheme 5.8).<sup>101</sup>

---

<sup>101</sup> C. Volpe, S. Meninno, A. Capobianco, G. Vigliotta, A. Lattanzi, *Adv. Synth. Catal.* **2019**, *361*, 1018.

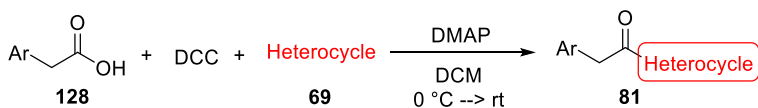


**Scheme 5.8** Our strategy for the stereoselective synthesis of tetrahydropyrazolo[1,2-a]-pyrazole-1,7-diones **145**.

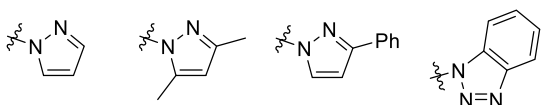
The activated pro-nucleophiles **81** have been easily synthesized via a DCC-mediated coupling reaction of arylacetic acids **128** with the opportune heterocycle **69**, as reported in the literature (Scheme 5.9, a).<sup>87b</sup> The azomethine imines **139** were obtained through a two-step sequence, namely a cyclization of an appropriate  $\alpha,\beta$ -unsaturated ester **153** with hydrazine, followed by condensation reaction of the 3-pyrazolidinone **154** with aldehydes **14** (Scheme 5.9, b).<sup>102</sup>

<sup>102</sup> (a) S. T. Perri, S. C. Slater, S. G. Toske, J. D. White, *J. Org. Chem.* **1990**, *55*, 6037; (b) E. Gould, T. Lebl, A. M. Z. Slawin, M. Reid, A. D. Smith, *Tetrahedron* **2010**, *66*, 8992; (c) R. Shintani, G. C. Fu, *J. Am. Chem. Soc.* **2003**, *125*, 10778.

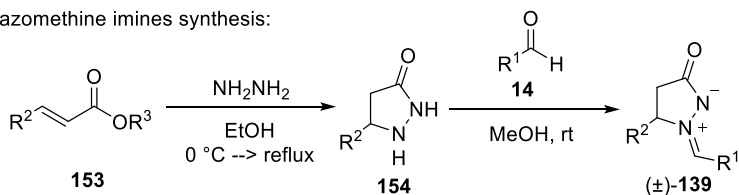
masked esters synthesis:



Heterocycle:

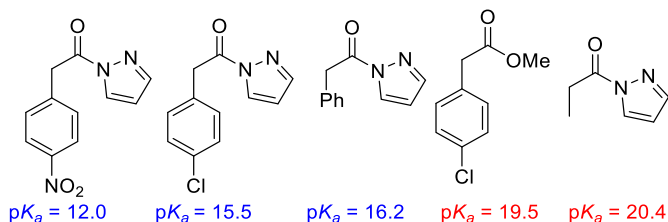


azomethine imines synthesis:



**Scheme 5.9** Synthesis of the reagents.

At the outset of the study, in collaboration with professor Amedeo Capobianco, the theoretical determination of  $pK_a$  in water was carried out for selected aryl- and alkyl-acetic derived pyrazoleamides and for *p*-chloro phenylacetic methyl ester at density functional level of theory, following a procedure reported by the group of Muñoz (Figure 5.2).<sup>103</sup>

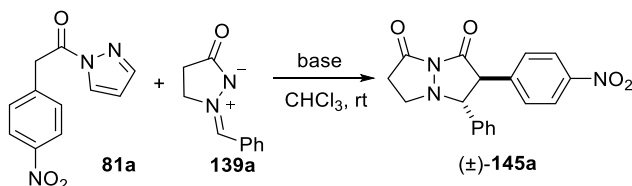


**Figure 5.2** Predicted  $pK_a$  of pyrazoleamides and ester in water.

<sup>103</sup> (a) R. Casanovas, M. Adrover, J. Ortega-Castro, J. Frau, J. Donoso, F. Muñoz, *J. Phys. Chem. B* **2012**, *116*, 10665; (b) R. Casanovas, J. Ortega-Castro, J. Frau, J. Donoso, F. Muñoz, *Int. J. Quantum Chem.* **2014**, *114*, 1350.

These results confirmed the role played by the heterocycle in enhancing the acidity at the  $\alpha$ -carbon, thus allowing the use of tertiary amine catalysts and justifying the observed inactivity of esters and aliphatic pyrazoleamides.<sup>68</sup>

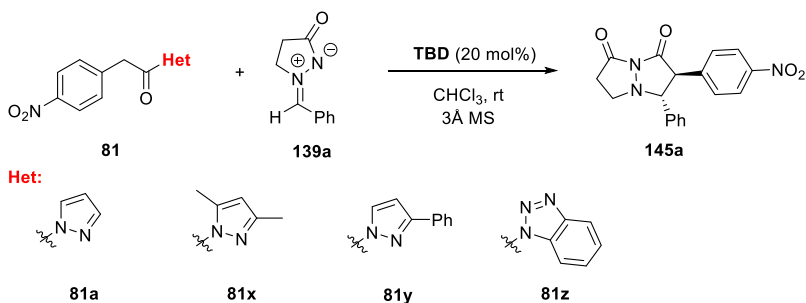
Firstly, model pyrazoleamide **81a** was reacted with azomethine imine **139a** in the presence of a stoichiometric amount of different bases, by working in chloroform at room temperature (Table 5.1). With our pleasure, common organic bases such as DABCO, triethylamine and DIPEA proved to be good catalysts, affording product **145a** in moderate yields while high *trans*-diastereoselectivity was observed (es. 1-3). Stronger organic and inorganic bases, *t*-BuOK and cesium carbonate respectively, furnished better yields, while maintaining high diastereoselectivities (es. 4 and 6). DBU yielded 50% of the product after a short reaction time (es. 7). More basic TBD proved to be more useful, furnishing product **145a** with the highest yield and in 96/4 *trans/cis* ratio, after a shorter time (es. 8). The use of the strongest base BEMP, after a comparable reaction time, did not enhance the final yield (es. 9). Interestingly, the conversion to **145a** and the diastereoselectivity were unchanged when only 20 mol% TBD was employed (es. 10). Finally, a control experiment attested that the reaction did not proceed in absence of the base (es. 11).

**Table 5.1** Base catalyzed formal [3+2] cycloaddition.<sup>[a]</sup>

Es.	Base	<i>t</i> [h]	Yield <b>145a</b> [%] <sup>[b]</sup>	<i>trans/cis</i> <b>145a</b> <sup>[c]</sup>
1	DABCO	18	51	96/4
2	NEt <sub>3</sub>	20	52	94/6
3	DIPEA	19	50	96/4
4	<i>t</i> -BuOK	20	66	96/4
5	K <sub>2</sub> CO <sub>3</sub>	29	28	95/5
6	CS <sub>2</sub> CO <sub>3</sub>	20	60	97/3
7	DBU	1	50	96/4
8	TBD	0.5	73	96/4
9	BEMP	0.5	60	96/4
10 <sup>[d]</sup>	TBD	1	65	96/4
11	-	1	nr	-

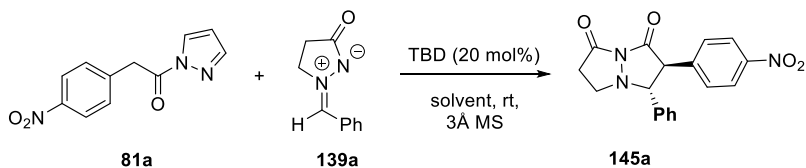
<sup>[a]</sup> Unless otherwise noted reactions were performed with **81a** (0.1 mmol), **139a** (0.1 mmol) and base (0.1 mmol) in CHCl<sub>3</sub> (0.5 mL). <sup>[b]</sup> Yield of both isolated diastereoisomers. <sup>[c]</sup> Determined by <sup>1</sup>H-NMR analysis. <sup>[d]</sup> 20 mol % of catalyst was used.

Additional optimization studies on the model reaction were then carried out by using the best catalyst TBD. In particular, changes in the heterocyclic moiety of pyrazolemides **81** confirmed the unsubstituted pyrazole as the best group, which afforded bicyclic pyrazolidinone **145a** with the highest yield (Table 5.2, es. 1). Subsequently, a solvent screening was conducted and dichlorometane was found to be the most effective (Table 5.3, es. 3).

**Table 5.2** Substrate screening.<sup>[a]</sup>

Es.	Het	<i>t</i> [h]	yield <b>145a</b> [%]	<i>trans/cis</i> <b>145a</b> <sup>[b]</sup>
1	<b>81a</b>	1.25	65	96/4
2	<b>81x</b>	1.25	60	95/5
3	<b>81y</b>	1.25	31	95/5
4	<b>81z</b>	1.25	62	96/4

<sup>[a]</sup> Unless otherwise noted reactions were conducted with **81** (0.1 mmol), **139a** (0.1 mmol), **TBD** (0.02 mmol), 3Å MS (~100 mg) in dry chloroform (0.5 mL) under nitrogen. <sup>[b]</sup> Determined by <sup>1</sup>H-NMR spectroscopy.

**Table 5.3** Solvent screening.<sup>[a]</sup>

Es.	solvent	<i>t</i> [h]	yield <b>145a</b> [%]	<i>trans/cis</i> <b>145a</b> <sup>[b]</sup>
1	$\text{CHCl}_3$	1.25	65	96/4
2	$\text{CH}_3\text{CN}$	4	54	96/4
3	$\text{CH}_2\text{Cl}_2$	0.5	79	96/4
4	THF	18	65	96/4
5	$\text{ClCH}_2\text{CH}_2\text{Cl}$	0.5	67	96/4
6	$\text{ClC}_6\text{H}_5$	8	64	96/4

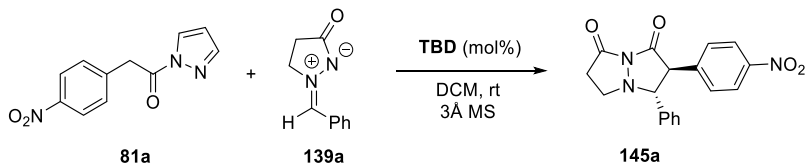
<sup>[a]</sup> Unless otherwise noted reactions were conducted with **81a** (0.08 mmol), **139a** (0.08 mmol), **TBD** (0.016 mmol), 3Å MS (~100 mg) in 0.4 mL of solvent under nitrogen. <sup>[b]</sup> Determined by <sup>1</sup>H-NMR spectroscopy.

Further reduction of catalyst to 10 mol% loading, by working in dichloromethane with a slight excess of dipole **139a** assured a rapid formation of the product in excellent yield and with high *trans/cis*



ratio (Table 5.4, es. 3).

**Table 5.4** Optimization of reaction parameters.<sup>[a]</sup>



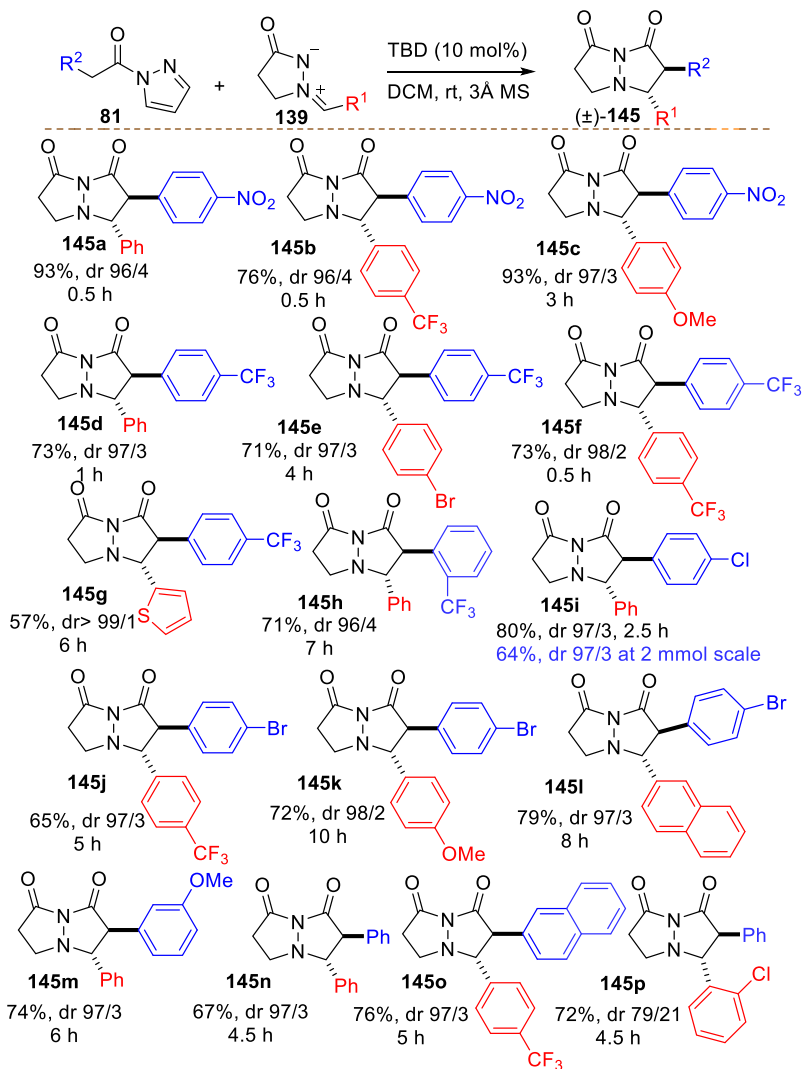
Es.	TBD [mol%]	<b>81a</b> [eq.]	<b>139a</b> [eq.]	<i>t</i> [h]	yield <b>145a</b> [%]	<i>trans/cis</i> <b>145a</b> <sup>[b]</sup>
1	20	1 eq.	1 eq.	1.75	79	96/4
2	10	1 eq.	1 eq.	2 h	75	96/4
3 <sup>[c]</sup>	10	1 eq.	1.2 eq.	0.5	93	96/4
4	5	1 eq.	1.3 eq.	2.5	73	96/4

<sup>[a]</sup> Unless otherwise noted reactions were conducted with **81a** (0.1 mmol), **139a** (0.1–0.13 mmol), **TBD** (5–20 mol%), 3Å MS (~100 mg) in dichloromethane (0.5 mL) under nitrogen. <sup>[b]</sup> Determined by <sup>1</sup>H-NMR spectroscopy. <sup>[c]</sup> Reaction conducted on 0.15 mmol of **81a**.

Under the optimized conditions (Table 5.4, es. 3), several pyrazoleamides **81** and azomethine imines **139** were investigated to explore the scope of the methodology (Table 5.5). Our TBD-catalyzed sequence was successfully applied to a variety of azomethine imines and pyrazoleamides, leading to the corresponding *trans*-bicyclic pirazolidinones **145**, bearing two contiguous stereocenters, with good to excellent yields after reasonable reaction times. *N*-acylpyrazoles **81** bearing electron-poor and electron-rich aromatic rings, as well as aromatic and heteroaromatic *N,N'*-cyclic azomethine imines **139** were well-tolerated and high levels of *trans*-diastereoselectivity were observed (**145a–o**). The stereoselectivity of the reaction dropped when an *ortho*-substituted azomethine imine was used and the corresponding product **145p** was recovered in good yield albeit with 79/21 *trans/cis* ratio. The reaction, performed at 2 mmol scale of pyrazoleamide **81i**, afforded the corresponding

product **145i** with slightly reduced yield, while maintaining the diastereoselectivity.

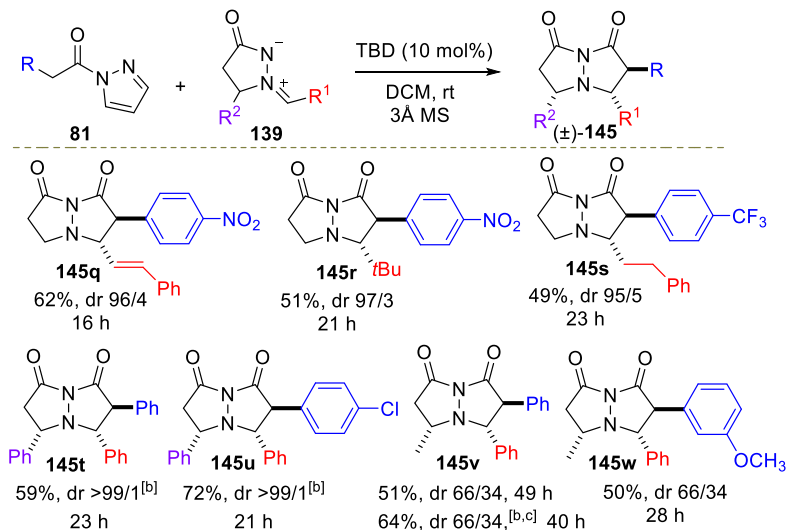
**Table 5.5** Substrate scope.<sup>[a-c]</sup>



<sup>[a]</sup> Reaction conditions were performed at 0.15 mmol scale **81**, **139** (0.18 mmol), TBD (0.015 mmol), 3Å MS (~150 mg) at  $C = 0.2$  M. <sup>[b]</sup> Isolated yield of both diastereoisomers. <sup>[c]</sup> *Trans/cis* ratio determined by <sup>1</sup>H-NMR analysis.

In order to increase the synthetic value of our methodology, further investigations concerning the nature of compounds **139** were carried out. In this regard, azomethine imines of type **139** were previously reported to be unreactive when bearing an alkenyl or alkyl groups at R<sup>1</sup> position (Table 5.6). Hence, we decided to check our system with these compounds. With our delight, the corresponding cycloaddition products **145q-s** were obtained in moderate to good yields, while excellent diastereoselectivities were recorded. Moreover, by reacting a more sterically demanding 5-phenyl substituted azomethine imine with pyrazoleamides, in the presence of 20 mol% of catalyst, a single *trans,cis*-isomer out of four possible diastereoisomers for heterocycles **145t-u** was observed.

**Table 5.6** [3+2] Cycloaddition of less reactive and racemic **139**.<sup>[a-c]</sup>

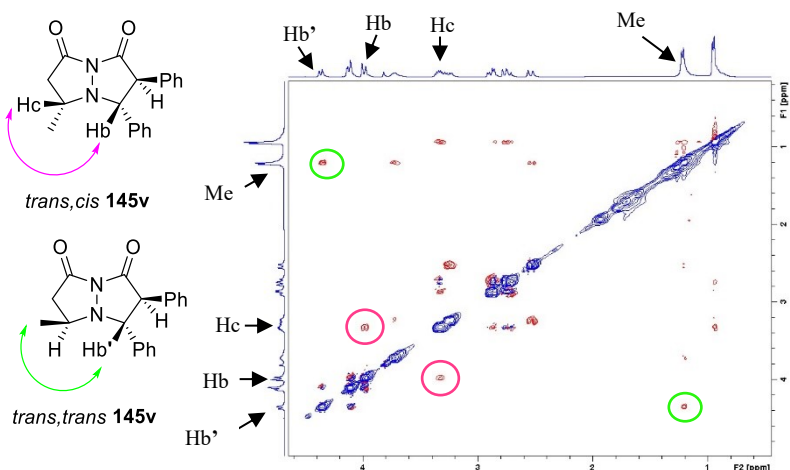


<sup>[a]</sup> Reaction conditions: **81** (0.15 mmol), **139** (0.18 mmol), TBD (0.015 mmol), 3 Å MS (~150 mg) at C = 0.2 M. Isolated yields. The major diastereoisomer is depicted.

<sup>[b]</sup> 20 mol% of TBD was used. <sup>[c]</sup> The reaction was carried out in 1,2-dichloroethane at 40 °C.

This result would suggest that the enolate approach occurs on the less-hindered face of the azomethine imine. In fact, when a less hindered azomethine imine, bearing the 5-methyl group was used, the corresponding **145v-w** products were obtained as a mixture of *trans,cis* and *trans,trans* diastereoisomers, in moderate yield and diastereomeric ratio, attesting the importance of the steric hindrance at position 5 for the diastereocontrol. Moreover, the yield can be improved by performing the reaction with 20 mol% of TBD in 1,2-dichloroethane at 40 °C (**145v**).

The relative configuration of both diastereoisomers for **145v** was confirmed by comparison with previously reported literature data,<sup>100</sup> by NOESY experiments (Figure 5.3) and computed <sup>1</sup>H-NMR spectra (Table 5.7). As shown in Figure 5.3, for the major diastereoisomer cross-peaks for protons H<sub>b</sub> and H<sub>c</sub> (magenta circles) were observed, thus attesting their spatial proximity (namely *cis*-relationship) and the relative configuration *trans/cis* of other substituents. On the contrary, cross-peaks for H<sub>b</sub>' and the methyl group (green circles) in the minor diastereoisomer results in a *trans/trans* relationship of the substituents on pyrazolidinone ring.



**Figure 5.3** Relative configuration of *trans/cis* and *trans/trans* **145v** by NOESY (400 MHz, CDCl<sub>3</sub>). A section of <sup>1</sup>H-NMR spectrum containing the non-aromatic protons of the diastereomeric mixture of **145v** (dr 66/34) is shown.

NMR computations, performed by professor Capobianco of University of Salerno, were carried out by following the literature procedure.<sup>104</sup> The calculated signals of the spectrum were in agreement with the experimental spectrum, thus proving to be useful for the assignment and subsequent interpretation of the bidimensional spectra.

**Table 5.7** Predicted <sup>1</sup>H-NMR.<sup>[a]</sup>

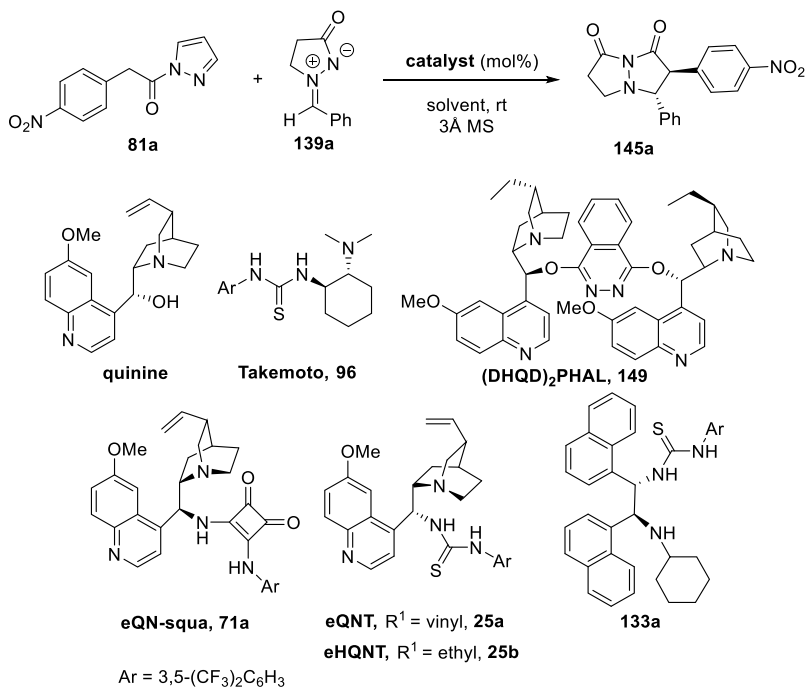
set of protons for <b>145v</b>	<i>trans,trans</i> - <b>145v</b>	<i>trans,cis</i> - <b>145v</b>
Ha	3.89	3.95
Hb	4.15	3.71
Hc	3.65	3.15
CH <sub>3</sub>	1.10	0.86

[a] Chemical shift (ppm, vs TMS).

<sup>104</sup> P. H. Willoughby, M. J. Jansma, T. R. Hoye. *Nat. Protoc.* **2014**, *9*, 643.

Additional efforts have been spent to develop an enantioselective version of the reaction. In this regard, a variety of bifunctional organocatalysts were employed in the reaction between model compounds **81a** and **139a**, working in dichloromethane at room temperature, with modest success (Table 5.8, es 1-6). Encouraging results were achieved by using hydroquinine-derived thiourea **25b** (es. 7). A short optimization of reaction parameters allowed, by working at 20 mol% loading of **25b** in mesitylene at room temperature, the isolation of optically active **145a** in good yield, with high diastereoselectivity and 70% ee. (es. 9).

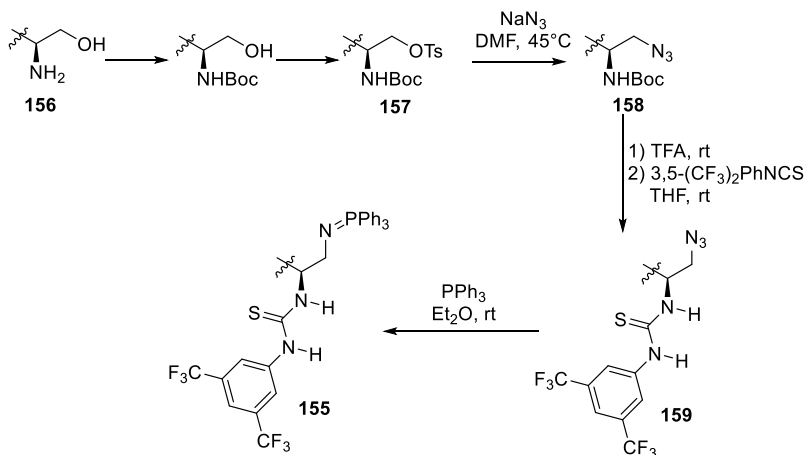
As shown in Table 5.8, the asymmetric pathway requires very long reaction time. Hence, we thought that the use of stronger basic catalyst could overcome the problem of conversion. With this aim, bifunctional catalysts **155a-b**, endowed with an iminophosphorane moiety (see Section 1.3), were synthesized according to procedures reported in the literature by the Dixon's group (Scheme 5.10).<sup>32</sup> The six-step procedure starts from optically active  $\beta$ -aminoalcohols **156**. Subsequent protection steps afforded derivative **157**, which was readily transformed into the corresponding azide **158**.

**Table 5.8** Catalyst screening in the enantioselective synthesis of **145a**.<sup>[a]</sup>

Es.	catalyst (mol%)	solvent	<i>t</i> [h]	yield <b>145a</b> [%]	<i>trans/cis</i> <b>145a</b> <sup>[b]</sup>	ee <b>145a</b> [%] <sup>[c]</sup>
1	<b>quinine</b> (20)	DCM	16	70	97/3	3
2	<b>96</b> (10)	DCM	21.5	64	94/6	6
3	<b>149</b> (15)	DCM	68	75	96/4	28
4	<b>71a</b> (10)	DCM	49	23	95/5	7
5	<b>25a</b> (10)	DCM	53	47	96/4	-9
6	<b>133a</b> (20)	DCM	47	37	97/3	16
7	<b>25b</b> (15)	DCM	52	76	96/4	30
8	<b>25b</b> (15)	toluene	38	57	96/4	50
9	<b>25b</b> (20)	mesytilene	159	60	96/4	70

<sup>[a]</sup> Unless otherwise noted reactions were conducted with **81a** (0.08 mmol), **139a** (0.096 mmol), **catalyst** (10–20 mol%), 3 Å MS (~100 mg) in 0.4 mL of solvent under nitrogen. <sup>[b]</sup> Determined by <sup>1</sup>H-NMR spectroscopy. <sup>[c]</sup> Determined by HPLC on a chiral stationary phase.

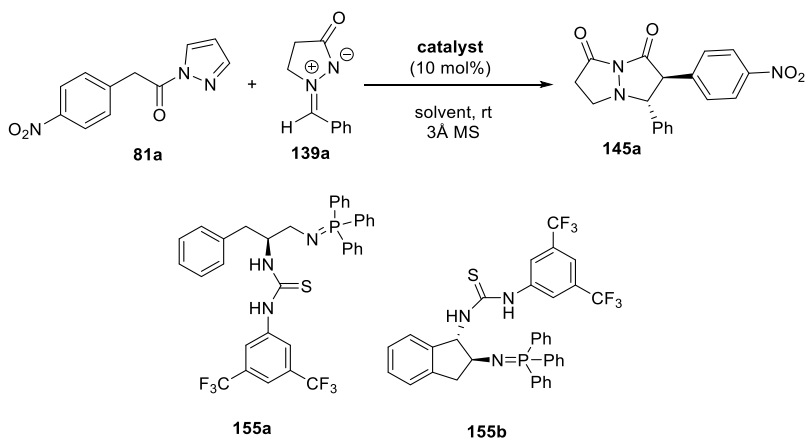
Further deprotection of the amine moiety and reaction with an isothiocyanate furnished the thiourea derivative **159**. The last step features the Staudinger reaction of triarylphosphine and the enantiopure organoazide **159**. The corresponding iminophosphorane moiety was achieved through loss of dinitrogen gas and the formation of bifunctional catalyst **155** was observed.



**Scheme 5.10** General scheme for the synthesis of bifunctional iminophosphorane **155**.

Organocatalysts **155a-b**, synthesized through the general procedure reported in Scheme 5.10, were employed in the model reaction between **81a** and **139a**, working in dichloromethane at room temperature (Table 5.9). Both catalysts proved to be more active than those reported in Table 5.8, affording the corresponding products in good yields and with high diastereoselectivity after reasonable reaction times, but scarce levels of enantioselectivity were observed (es. 1-2).

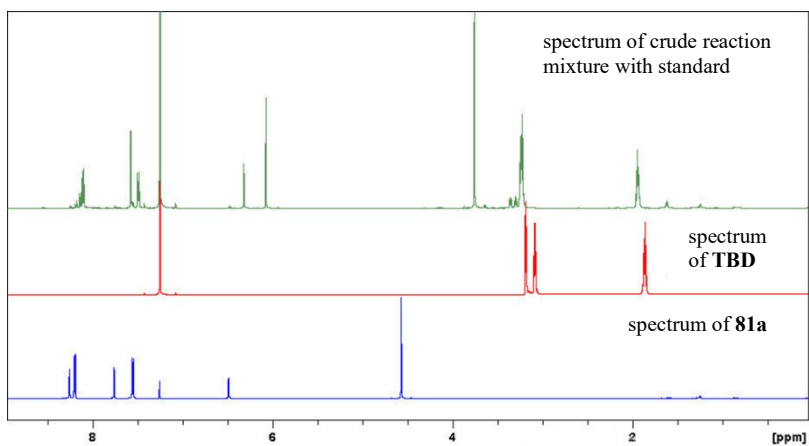
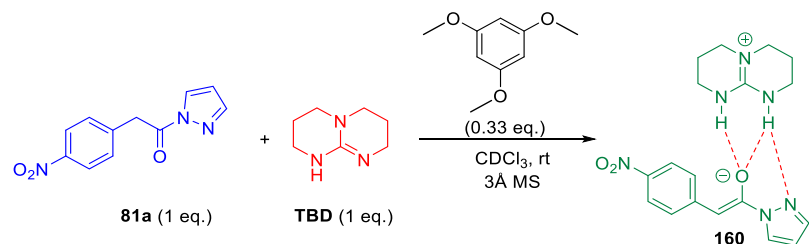


**Table 5.9** Enantioselective synthesis of **145a** catalyzed by bifunctional iminophosphoranes **155**.<sup>[a]</sup>

Es.	catalyst	solvent	<i>t</i> [h]	yield <b>145a</b> [%]	<i>trans/cis</i> <b>145a</b> <sup>[b]</sup>	ee <b>145a</b> [%] <sup>[c]</sup>
1	<b>155a</b>	DCM	4	77	97/3	11
2	<b>155b</b>	DCM	23	59	96/4	21

<sup>[a]</sup> Reactions were conducted with **81a** (0.08 mmol), **139a** (0.096 mmol), **catalyst** (10 mol%), 3Å MS (~100 mg) in 0.4 mL of dichloromethane under nitrogen. <sup>[b]</sup> Determined by <sup>1</sup>H-NMR spectroscopy. <sup>[c]</sup> Determined by HPLC on a chiral stationary phase.

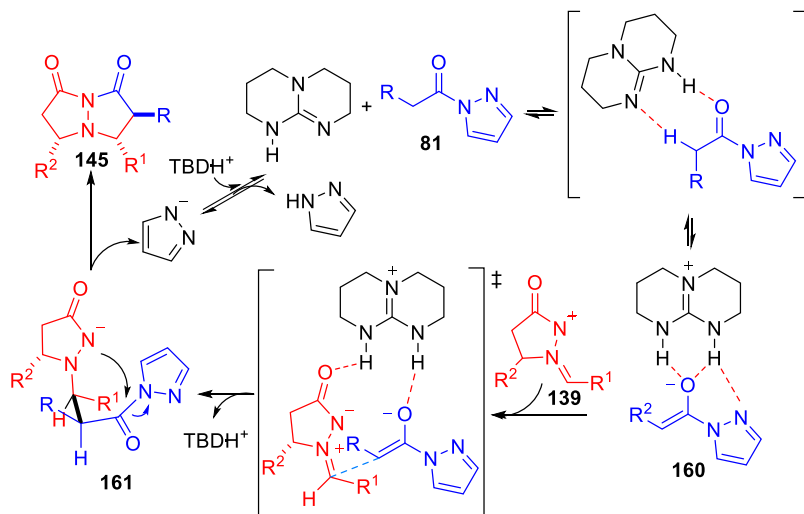
Finally, mechanistic studies were carried out to elucidate the formation of species in the reaction mixture. In this regard a 1:1 mixture of pyrazoleamide **81a** and TBD was analysed through <sup>1</sup>H-NMR in CDCl<sub>3</sub>. As shown in Figure 5.4, the signal of the two methylene protons at 4.58 ppm disappeared, whereas one proton singlet emerged at 7.58 ppm, attesting the formation of a guanidinium-enolate complex **160** (Figure 5.5).



**Figure 5.5**  $^1\text{H-NMR}$  in  $\text{CDCl}_3$  (600 MHz) of crude reaction mixture with standard (1,3,5-trimethoxybenzene), **TBD** and **81a**.

On the basis of all data, a reaction mechanism was hypothesized as follow. The azomethine imine **139** would interact through H-bonding networks established within the complex **160**. The approach with the enolate **81'**, would occur in a Mannich type addition, via a less sterically hindered transition state, to give intermediate **161**.

The following intramolecular amidation would furnish product **145** while releasing the pyrazole anion, which would enter in the catalytic cycle to assist acid-base equilibria (Scheme 5.11).



**Scheme 5.11** Hypothetical catalytic cycle promoted by TBD.

Finally, some selected bicyclic pyrazolidinones **145** were subjected to a preliminary screening against Gram-negative *E. coli* and Gram-positive *S. aureus* bacteria. It was observed that compound **145n**, with unsubstituted phenyl rings, did not inhibit the growth when used up to 100 mg/mL. On the other hand phenyl-substituted compounds showed antimicrobial effects against *S. aureus*, with products **145e** and **145j** showing the highest percentage of growth inhibition, that is 85% and 63% respectively.

## CONCLUSIONS

In conclusion we developed a convenient one-pot [3+2] cycloaddition to access bioactive bicyclic pyrazolidinones by reacting readily available *N,N'*-cyclic azomethine imines and pyrazoleamides. Different features make this protocols suitable for a practical synthesis of this class of heterocycles, with respect to previously reported methodologies:

- Ready availability of reagents;
- Catalytic loadings of commercial and low-cost base;
- Mild reaction conditions are involved, being the reaction carried out at room temperature;
- Less reactive azomethine imines, derived from aliphatic aldehydes, can be successfully employed;
- Good results in terms of both yields and diastereoselectivities were achieved;
- Scalability of the reaction.

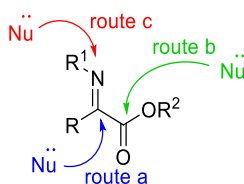
However, more effective organocatalysts have to be designed to achieve better activity and satisfactory levels of enantioselectivity.

## 6. DIRECT $\alpha$ -IMINATION OF *N*-ACYL PYRAZOLES WITH NITROSOARENES

### 6.1 Background

The discovery of the synthetic utility of  $\alpha$ -imino ester derivatives arises from the pioneering studies of Weinreb and Tschaen back to 1982.<sup>105</sup> These compounds proved to be useful in imino ene reactions for the synthesis of  $\alpha$ -amino acid derivatives.<sup>106</sup>

$\alpha$ -Imino esters are endowed with three distinct electrophilic positions on their scaffold, as depicted in Figure 6.1. Hence, three different nucleophilic addition to  $\alpha$ -imino esters may occur. Addition to carbon of imine moiety is highly represented in the literature (route a). Nucleophilic attack toward ester moiety is also possible, but less common (route b). Finally, nitrogen of imine may also undergoes nucleophilic attack (route c). The last reaction-type results in an inversion of the pole (umpolung) and it is extremely rare.



**Figure 6.1** Reactive positions of  $\alpha$ -imino esters.

Given their high versatility,  $\alpha$ -amino acid derivatives represented suitable starting materials in a variety of chemical transformations.<sup>107</sup>

<sup>105</sup> Tschaen, D. M.; Weinreb, S. M. *Tetrahedron Lett.* **1982**, 23, 3015.

<sup>106</sup> For reviews of imino ene reactions, see: (a) R. M. Borzilleri, S. M. Weinreb, *Synthesis* **1995**, 347; (b) S. M. Weinreb, *Top. Curr. Chem.* **1997**, 190, 131.

<sup>107</sup> For reviews, see: (a) B. Eftekhari-Sis, M. Zirak, *Chem. Rev.* **2017**, 117, 8326; (b) A. E. Taggi, A. M. Hafez, T. Lectka, *Acc. Chem. Res.* **2003**, 36, 10.

Thanks to the presence of an electron withdrawing ester moiety,  $\alpha$ -imino esters are more reactive when compared with other types of imines. They are widely exploited as precursors of natural and unnatural  $\alpha$ -amino acid derivatives,<sup>108</sup> in Mannich,<sup>109</sup> Friedel-Crafts<sup>110</sup> and cycloaddition<sup>111</sup> reactions, as well as organometallic<sup>112</sup> and Michael<sup>113</sup> additions.

The most commonly used methodologies to access  $\alpha$ -imino acid derivatives rely on the condensation of  $\alpha$ -keto acid derivatives **162** with an amine. The reaction takes place in the presence of an acid catalyst, with azeotropic removal of water or using a dehydrating agent, such as molecular sieves (Scheme 6.1).<sup>114</sup> This imination sequence generally requires high temperatures, long reaction times

---

<sup>108</sup> For selected examples, see: (a) G. Shang, Q. Yang, X. Zhang, *Angew. Chem. Int. Ed.* **2006**, *45*, 6360; (b) G. Li, Y. Liang, J. C. Antilla, *J. Am. Chem. Soc.* **2007**, *129*, 5830; (c) Q. Kang, Z.-A. Zhao, S.-L. You, *Org. Lett.* **2008**, *10*, 2031; (d) C. Zhu, T. Akiyama, *Adv. Synth. Catal.* **2010**, *352*, 1846; (e) D. Enders, A. Rembiak, B. A. Stöckel, *Adv. Synth. Catal.* **2013**, *355*, 1937.

<sup>109</sup> For selected examples, see: (a) M. Shimizu, Y. Takao, H. Katsurayama, I. Mizota, *Asian J. Org. Chem.* **2013**, *2*, 130; (b) M. Shimizu, D. Kurita, I. Mizota, *Asian J. Org. Chem.* **2013**, *2*, 208.

<sup>110</sup> For selected examples, see: (a) O. V. Larionov, A. de Meijere, *Adv. Synth. Catal.* **2006**, *348*, 1071; (b) L. C. Wieland, E. M. Vieira, M. L. Snapper, A. H. Hoveyda, *J. Am. Chem. Soc.* **2009**, *131*, 570; (c) Y. Qian, C. Jing, C. Zhai, W. H. Hu, *Adv. Synth. Catal.* **2012**, *354*, 301.

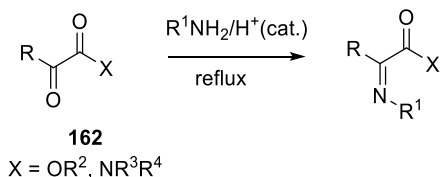
<sup>111</sup> For selected examples, see: (a) T. Hashimoto, H. Nakatsu, K. Yamamoto, K. Maruoka, *J. Am. Chem. Soc.* **2011**, *133*, 9730; (b) I. Gorokhovik, L. Neuville, J. Zhu, *Org. Lett.* **2011**, *13*, 5536; (c) P. Tolstoy, S. X. Y. Lee, C. Sparr, S. V. Ley, *Org. Lett.* **2012**, *14*, 4810; (d) M. A. Marsini, J. T. Reeves, J.-N. Desrosiers, M. A. Herbage, J. Savoie, Z. Li, K. R. Fandrick, C. A. Sader, B. McKibben, D.A. Gao, *et al. Org. Lett.* **2015**, *17*, 5614.

<sup>112</sup> For selected reviews and examples, see: (a) I. Mizota, M. Shimizu, *Chem. Rec.* **2016**, *16*, 688; (b) J. S. Dickstein, M. C. Kozlowski, *Chem. Soc. Rev.* **2008**, *37*, 1166; (c) P. Fu, M. L. Snapper, A. H. Hoveyda, *J. Am. Chem. Soc.* **2008**, *130*, 5530; (d) G. Huang, Z. Yin, X. Zhang, *Chem. Eur. J.* **2013**, *19*, 11992; (e) S. Fustero, P. Bello, J. Miro, M. Sánchez-Roselló, M. A. Maestro, J. González, C. del Pozo, *Chem. Commun.* **2013**, *49*, 1336.

<sup>113</sup> M. Espinosa, A. García-Ortiz, G. Blay, L. Cardona, M. C. Muñoz, J. R. Pedro, *RSC Adv.* **2016**, *6*, 15655.

<sup>114</sup> (a) P. W. Hickmott, *Tetrahedron* **1982**, *38*, 1975; (b) M. Boeykens, N. De Kimpe, K. Abbaspour Tehrani, *J. Org. Chem.* **1994**, *59*, 6973; (c) K. Taguchi, F. H. Westheimer, *J. Org. Chem.* **1971**, *36*, 1570.

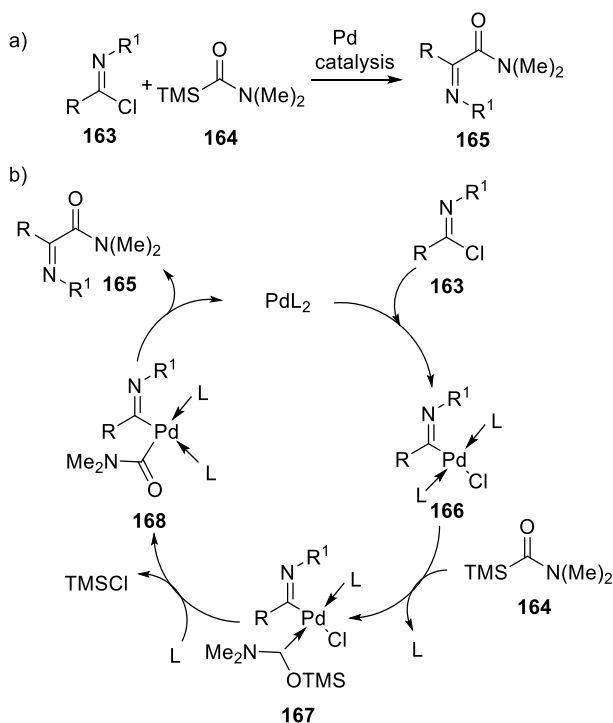
and the absence of acid-labile groups in the starting materials. Moreover  $\alpha$ -keto acid reagents are not readily available compounds.



**Scheme 6.1** Imination of  $\alpha$ -keto ester derivatives.

Metal-catalyzed procedures were successfully developed over the years. By reacting imidoyl chlorides **163** with a carbamoylsilane **164** in the presence of 4 mol% of a palladium-based catalyst, the corresponding  $\alpha$ -iminoamides **165** are obtained (Scheme 6.2,a).<sup>115</sup> The overall reaction can be illustrated through the following mechanism. Imidoyl chloride **163** and palladium catalyst gives rise to the imidoylpalladium specie **166**, that may be considered as an initial intermediate. The C=O rearrangement of **164** results in the formation of a nucleophilic carbene that is able to replace one of the ligands in complex **166**, affording specie **167**. Loss of TMSCl from **167** then provides the palladium-complex **168**. The following migration of carbamoyl moiety results in the expulsion of catalyst and product **165** (Scheme 6.2, b).

<sup>115</sup> R. F. Cunico, R. K. Pandey, *J. Org. Chem.* **2005**, *70*, 5344.



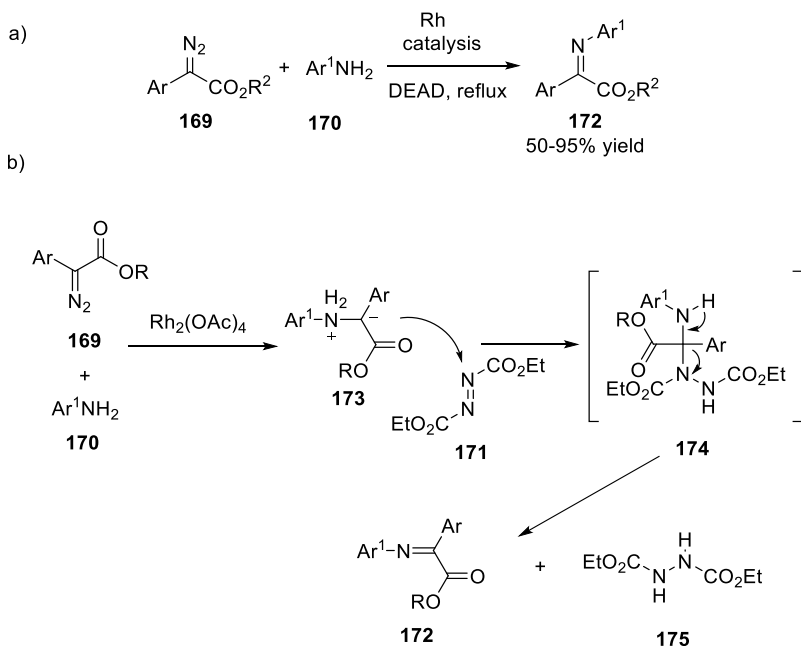
**Scheme 6.2** (a) Palladium-catalyzed synthesis of  $\alpha$ -iminoamides and (b) Mechanism of the reaction.

An efficient synthetic route to  $\alpha$ -imino esters was developed by Hu and colleagues. They reacted  $\alpha$ -diazoacetates **169** with arylamines **170** in the presence of 1 mol% of dirhodium(II) acetate and a stoichiometric amount of DEAD **171**. The resulting  $\alpha$ -imino esters **172** were isolated in 50–95% yields (Scheme 6.3, a).<sup>116</sup> The presence of DEAD is crucial, as highlighted through the reaction mechanism (Scheme 6.3, b). The ammonium ylide **173** is initially formed from the  $\alpha$ -diazo carbonyl compound **169** and aniline **170**, catalyzed by  $\text{Rh}_2(\text{OAc})_4$ . Then ylide **173**, trapped by **171**, gives rise to the

<sup>116</sup> H. Huang, Y. Wang, Z. Chen, W. H. Hu, *Synlett* **2005**, 16, 2498.



corresponding amination **174**. The bulky substituents on both diazo compounds and anilines promote the fragmentation of **174**, thus affording the desired  $\alpha$ -imino ester **172** while the simultaneous reduction of DEAD to **175** is observed.

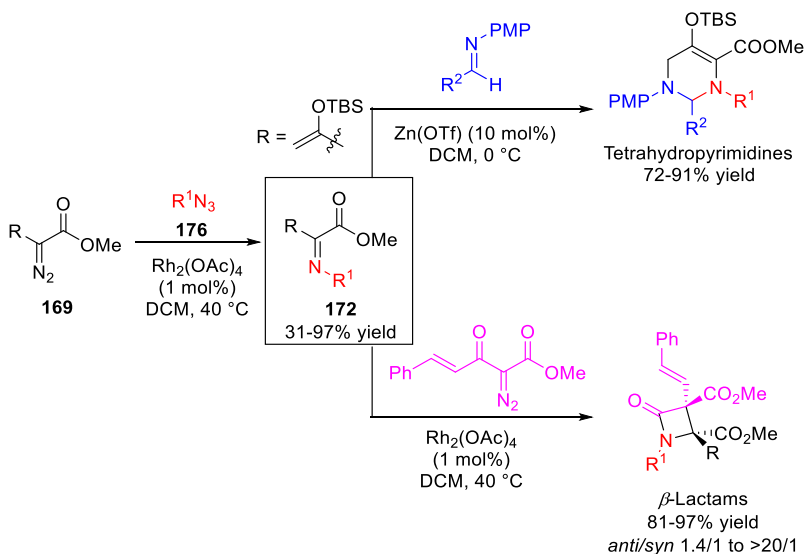


**Scheme 6.3** (a) Reaction of aryl diazoacetates with anilines and DEAD, promoted by a rhodium catalyst and (b) The proposed mechanism for the  $\alpha$ -imino esters formation.

Rhodium(II) acetate was found to be effective also for the reaction of the aforementioned  $\alpha$ -diazoesters **169** with organic azides **176**. By working at 40 °C, with 1 mol% loading of the catalyst, the  $\alpha$ -imino esters **172** were formed in 31–97% yield.<sup>117</sup> The isolated  $\alpha$ -imino esters were successfully employed in the synthesis of

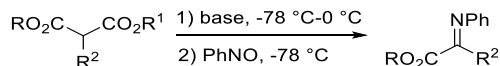
<sup>117</sup> M. D. Mandler, P. M. Truong, P. Y. Zavalij, M. P. Doyle, *Org. Lett.* **2014**, *16*, 740.

tetrahydropyrimidines and  $\beta$ -Lactams (Scheme 6.4).



**Scheme 6.4** Conversion of diazocarbonyl compounds to  $\alpha$ -imino esters and application to the synthesis of tetrahydropyrimidines and  $\beta$ -Lactams.

In 2008, Payette and Yamamoto reported an oxidative C-C bond cleavage for the synthesis of  $\alpha$ -imino esters, utilizing nitrosobenzene as oxidant.<sup>118</sup> The reaction occurs at low temperature, under strongly basic conditions and proved to be applicable to a variety of esters and dicarbonyl compounds (Scheme 6.5).



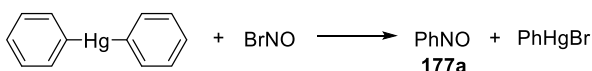
**Scheme 6.5** Nitrosobenzene-mediated oxidative decarboxylation of esters and dicarbonyl substrates.

<sup>118</sup> J. N. Payette, H. Yamamoto, *J. Am. Chem. Soc.* **2008**, *130*, 12276.

All previously illustrated protocols allow access to  $\alpha$ -imino ester derivatives in good to excellent results, but carefully controlled or harsh reaction conditions are required, as well as particular reagents or expensive metal-based catalysts have to be employed. Hence, more feasible synthetic routes to  $\alpha$ -imino acid derivatives would be highly desirable.

### 6.1.1 Nitrosobenzene in organic synthesis

At the end of nineteenth century, Adolf von Bayer first synthesized nitrosobenzene **177a**, by reacting diphenylmercury and nitrosyl bromide (Scheme 6.6).<sup>119</sup>



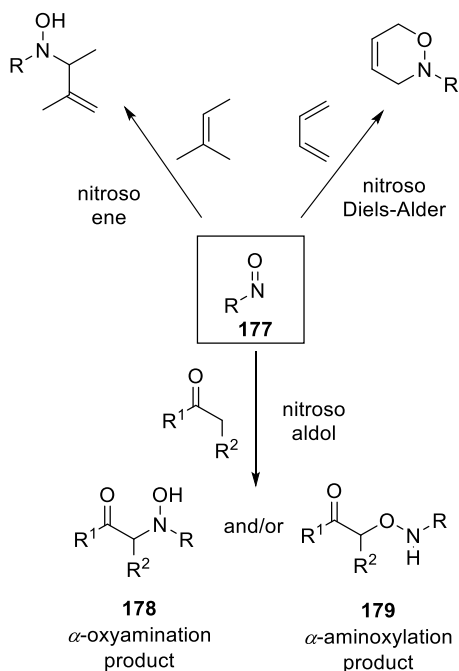
**Scheme 6.6** Baeyer's first preparation of nitrosobenzene.

The introduction of nitrogen and oxygen atoms in an organic compound has great synthetic utility. Molecules bearing amino and/or hydroxy moieties in their skeleton can be frequently found in natural products as well as in synthetic pharmaceutical compounds. Moreover, they represent very useful synthetic intermediates. Derivatives in which the heteroatom is located in proximity of another reactive functional group, such as a carbonyl portion, are particularly attractive, since they could undergo further chemical elaborations.

In this regard, nitroso compounds **177** proved to be a useful source for the synthesis of nitrogen- and oxygen-containing molecules,

<sup>119</sup> A. Baeyer, *Chem. Ber.* **1874**, 7, 1638.

thanks to the particular reactivity of the nitroso group.<sup>120</sup> In fact, the electrophilic character of both N and O atoms, allows the formation of two regioisomeric products in a nitroso aldol reaction, namely the  $\alpha$ -oxyamination **178** and the  $\alpha$ -aminoxylation **179** products.<sup>121</sup> Moreover it is a suitable enophile in nitroso ene<sup>122</sup> and nitroso Diels-Alder<sup>123</sup> reactions (Scheme 6.7).



**Scheme 6.7** Main reactivity of nitroso compounds.

<sup>120</sup> For reviews on the synthetic application of nitroso, see: (a) P. Merino, T. Tejero, I. Delso R. Matute, *Synthesis*, **2016**, 653; (b) J. Lee, L. Chen, A. H. West, G. B. Richter-Addo, *Chem. Rev.* **2002**, *102*, 1019; (c) P. Zuman, B. Shah, *Chem. Rev.* **1994**, *94*, 1621.

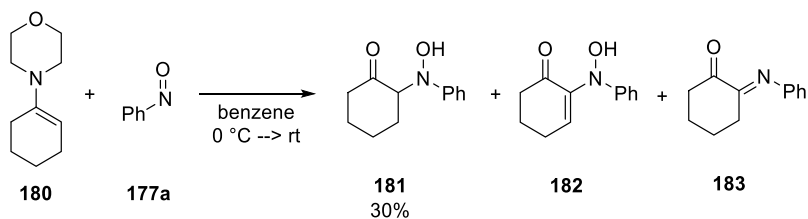
<sup>121</sup> H. Yamamoto, M. Kawasaki, *Bull. Chem. Soc. Jpn.* **2007**, *80*, 595.

<sup>122</sup> (a) W. Adam, O. Krebs, *Chem. Rev.* **2003**, *103*, 4131; (b) M. Baidya, H. Yamamoto, *Synthesis* **2013**, *45*, 1931; (7) A. V. Malkov, *Chem. Heterocycl. Compd.* **2012**, *48*, 39.

<sup>123</sup> (a) Y. Yamamoto, H. Yamamoto, *Eur. J. Org. Chem.* **2006**, 2031; (b) B. S. Bodnar, M. J. Miller, *Angew. Chem. Int. Ed.* **2011**, *50*, 5629; (c) A. G. Leach, K. N. Houk, *Chem. Commun.* **2002**, 1243; (e) J. Streith, A. Defoin, *Synthesis* **1994**, 1107.

The major problem about nitroso aldol reaction concerns its regioselectivity. Addition to the nitrogen atom of nitroso group gives rise to the corresponding  $\alpha$ -amino carbonyl compound **178**. On the contrary, if the addition takes place on the oxygen atom of the nitroso moiety, the formation of  $\alpha$ -hydroxy carbonyl products **179** is observed. Both processes result from the reaction of an enolizable carbonyl compound with a nitroso group. In general, the regioselectivity of the reaction depends on both catalyst and reaction conditions.

The first example of *N*-selective nitroso aldol reaction was reported by Lewis and colleagues in 1972.<sup>124</sup> They reacted 1-morpholino-1-cyclohexene **180** with nitrosobenzene **177a** and the desired  $\alpha$ -hydroxyamino ketone **181** was isolated in 30% yield. The byproducts amino enone **182** and imine **183** were also detected, while no traces of  $\alpha$ -aminoxylation product were observed at the end of the reaction (Scheme 6.8). The same reaction of morpholine enamine **180** can be significantly improved in the presence of methanol, which is able to increase the yield of **181** up to 60%.<sup>125</sup>



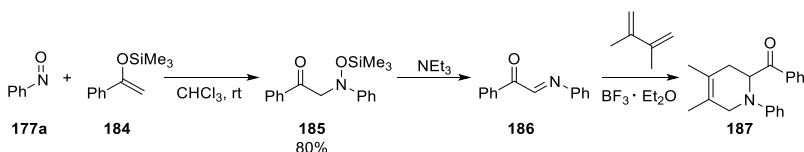
**Scheme 6.8** First example of regioselective *N*-nitroso aldol reaction.

Sasaki and Ohno applied this strategy to a variety of silyl enol ethers

<sup>124</sup> J. W. Lewis, P. L. Myers, J. A. Ormerod, *J. Chem. Soc., Perkin Trans. 1*, **1972**, 20, 2521.

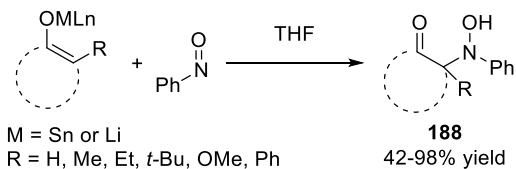
<sup>125</sup> N. Momiyama, H. Yamamoto, *J. Am. Chem. Soc.* **2005**, 127, 1080.

and the corresponding siloxyamino ketones were further transformed into heterocyclic derivatives.<sup>126</sup> For example, the reaction of nitrosobenzene with the silyl enol ether of acetophenone **184** afforded silyloxyamino ketone **185** in high yield. The subsequent treatment with triethylamine, followed by the [4+2] cycloaddition of derivative **186** with 2,3-dimethylbutadiene, in the presence of  $\text{BF}_3 \cdot \text{Et}_2\text{O}$ , provided the final cycloadduct **187** (Scheme 6.9).



**Scheme 6.9** *N*-nitroso aldol reaction of silyl enol ether with nitrosobenzene.

The reaction proved to be selective toward  $\alpha$ -oxyamination products when, *in situ*-generated or preformed, lithium and tin enolates are involved.<sup>127</sup> In absence of any promoter, cyclic and acyclic  $\alpha$ -hydroxyamino ketones **188** were successfully obtained (Scheme 6.10).



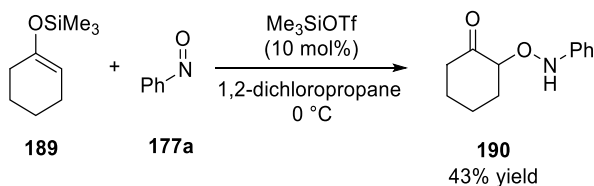
**Scheme 6.10** Reaction of nitrosobenzene with metal enolates.

As mentioned above, nitroso group could also behave as an oxy-electrophile, depending on the reaction conditions. For example *O*-

<sup>126</sup> (a) T. Sasaki, Y. Ishibashi, M. Ohno, *Chem. Lett.*, **1983**, 22, 863; (b) T. Sasaki, K. Mori, M. Ohno, *Synthesis*, **1985**, 3, 279.

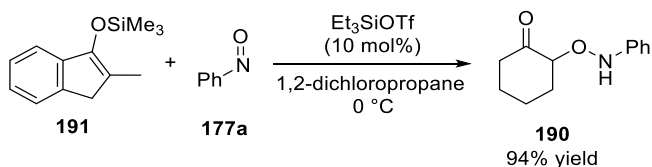
<sup>127</sup> N. Momiyama, H. Yamamoto, *Org. Lett.* **2002**, 4, 3579.

selective nucleophilic attack of silyl enol ethers **189** to nitrosobenzene **177a** takes place in the presence of a Lewis acid catalyst (Scheme 6.11).<sup>128</sup> In this case the  $\alpha$ -aminoxy ketone **190** was isolated as exclusive product.



**Scheme 6.11** Regioselective *O*-nitroso aldol reaction promoted by a Lewis acid.

A variety of Lewis acids proved to be effective in this *O*-selective nitroso aldol reaction. The reaction between nitrosobenzene and the silyl enol ether of 2-methyl-1-indanone **191** in the presence of 10 mol% loading of triethyl silyl triflate as Lewis acid catalyst, afforded the corresponding  $\alpha$ -aminoxy ketone **190** in excellent yield (Scheme 6.12).



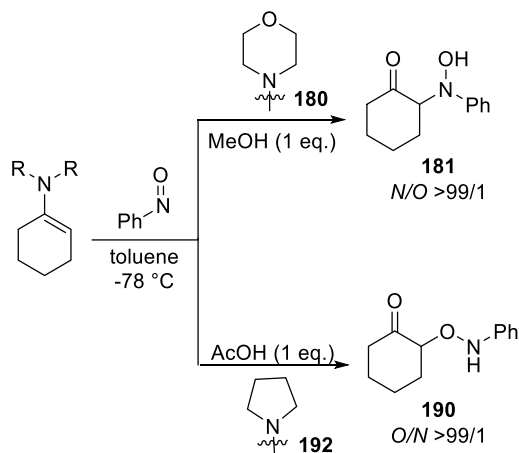
**Scheme 6.12** Lewis acid-induced *O*-selective nitroso aldol reaction.

Enamines represent also suitable nucleophiles in the synthesis of  $\alpha$ -aminoxy ketone.<sup>129</sup> Starting from 1-pyrrolidin-1-ylcyclohexene **192**

<sup>128</sup> (a) N. Momiyama, H. Yamamoto, *Angew. Chem. Int. Ed.* **2002**, *41*, 2986; (b) N. Momiyama, H. Yamamoto, *Angew. Chem. Int. Ed.*, **2002**, *41*, 3313.

<sup>129</sup> N. Momiyama, H. Torii, S. Saito, H. Yamamoto, *Proc. Natl. Acad. Sci. USA*, **2004**, *101*, 5374.

and nitrosobenzene, the aminoxy ketone **190** is selectively obtained when acetic acid is added to the reaction mixture. The same reaction, conducted on 1-morpholino-1-cyclohexene **180**, led the group of Lewis to detect the  $\alpha$ -aminoxylation product **181** (see Scheme 6.8). Initially the discrepancies with Lewis's experiment were only attributed to the structural difference of the enamine. In fact, when the morpholine enamine **180** was used, the formation of hydroxyamino ketone **181** was observed. On the contrary, the use of pyrrolidine enamine **192** led to the exclusive formation of aminoxy ketone **190**. Recently, the *O*-nitroso aldol reaction was found to be accelerated in the presence of Lewis or Brønsted acids (Scheme 6.13). The generation of the *N*-nitroso aldol product **181** was achieved in the presence of methanol at low temperature. On the other hand, the presence of acetic acid was able to promote the *O*-nitroso aldol pathway. Hence, both *N*- or *O*-nitroso aldol products can be regioselectively obtained, by simply switching the catalyst and the structure of the amine moiety in the enamine reagent.



Scheme 6.13 Regioselective *N*- and *O*-nitroso aldol reactions.



As highlighted in this section, different research groups gave their contribution in the fascinating area of nitroso chemistry, with particular attention toward the nitroso aldol reaction. In this regard, both metal and organic catalysts have been successfully employed in the development of regioselective nitroso aldol reactions. As shown above, complete regioselectivity can be achieved by appropriately varying reaction conditions. A great variety of substrates, including aldehydes, cyclic and acyclic ketones, as well as esters and amides, can be successfully employed.

### 6.1.2 Ehrlich-Sachs reaction

Dating back to 1899, the Ehrlich-Sachs reaction represents a powerful tool for the synthesis of imines and nitrones by employing aryl nitroso compounds.<sup>130</sup> A few bases have been reported to promote the reaction, mostly NaOH, alkoxides, carbonates,<sup>131</sup> using active methylene compounds as suitable starting materials. Arenemethyl cyanides, malonic esters,  $\beta$ -keto esters,  $\beta$ -diketones, fluorenes and cyclopentadienes exemplified the classes of reagents employed.<sup>132</sup>

When a 1:1 mixture of 4-substituted phenylacetonitriles **193** and nitrosobenzene were reacted in benzene, in the presence of a stoichiometric amount of aqueous sodium hydroxide and the phase transfer catalyst triethylbenzylammonium chloride (TEBAC),  $\alpha$ -

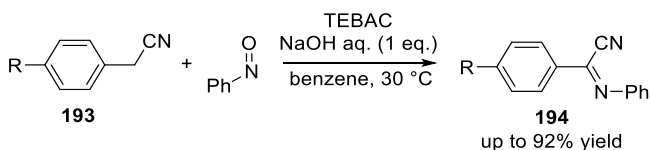
---

<sup>130</sup> P. Ehrlich, F. Sachs, *Chem. Ber.* **1899**, 32, 2341.

<sup>131</sup> (a) M. Colonna, *Gazz. Chim. Ital.* **1960**, 90, 117; (b) L. Horner, H. Hoffmann, H. G. Wippel, G. Klahre, *Chem. Ber.* **1959**, 92, 2499; (c) F. Kröhnke, G. Kröhnke, *Chem. Ber.* **1958**, 91, 1474.

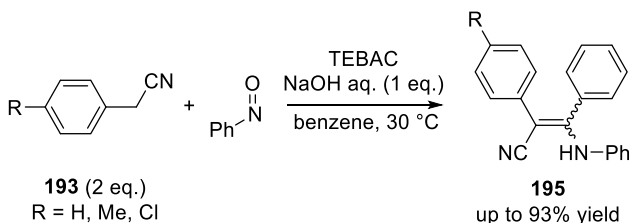
<sup>132</sup> (a) R. W. Layer, *Chem. Rev.* **1963**, 63, 489; (b) S. Dayagi, Y. Degani, *The Chemistry of the Carbon-Nitrogen Double Bond*; Patai, S., Ed.; New York, **1970**.

phenylimino-phenylacetonitriles **194** were obtained in high yield (Scheme 6.14).



**Scheme 6.14** Ehrlich-Sachs reaction of arenemethyl cyanides.

When 2 equivalents of **193** were treated with nitrosobenzene, under the same reaction conditions, the formation of 1-anilino-2-cyano-1,2-diphenylethene was observed. The enamines **195** were isolated in up to 93% yield (Scheme 6.15).<sup>133</sup>

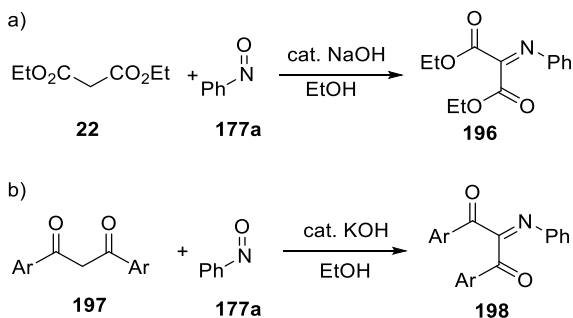


**Scheme 6.15** Synthesis of  $\alpha,\beta$ -disubstituted cinnamionitriles via Ehrlich-Sachs reaction.

In the early sixties, Mukaiyama et al. reported the nucleophilic attack of *in situ* generated enolates of diesters **22** at nitrogen atom of nitrosobenzene and the following dehydration, catalyzed by NaOH, to give the corresponding imines **196** (Scheme 6.16, a).<sup>134</sup> Subsequent studies by Moskal and colleagues described a similar condensation reaction of 1,3-diaronylmethanes **197** with nitrosobenzene for the synthesis of polyketone imines **198** (Scheme

<sup>133</sup> K. Takahashi, S. Kimura, Y. Ogawa, K. Yamada, H. Iida, *Synthesis* **1978**, 892.

<sup>134</sup> H. Nohira, K. Sato, T. Mukaiyama, *Bull. Chem. Soc. Jpn.* **1963**, 36, 870.

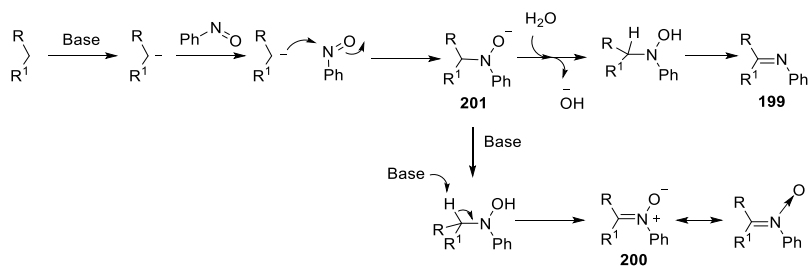
6.16, b).<sup>135</sup>

**Scheme 6.16** (a) Imination of diester and (b) diketone compounds.

Imines **199** and imine oxides **200** represent the two possible products of Ehrlich-Sachs reaction. The hypothesized mechanism of the reaction is depicted below (Scheme 6.17).

The starting methylene active compound is readily deprotonated by an opportune base and the corresponding enolate attacks the nitrogen atom of the nitroso group. This *N*-nitroso aldol reaction results in the formation of nitrosoaldolate **201**. At this point two competitive elimination pathways were proposed to occur: i) water elimination would give rise to imine **199**; ii) an unclear base-assisted deprotonation of nitrosoaldolate intermediate would result in the formation of nitrone **200**. Since then, studies to elucidate the reaction mechanism did not appear in the literature and prediction on the final product is not always straightforward. Reaction conditions and the acidity features of the pronucleophile play a crucial role in affecting the reaction outcome.

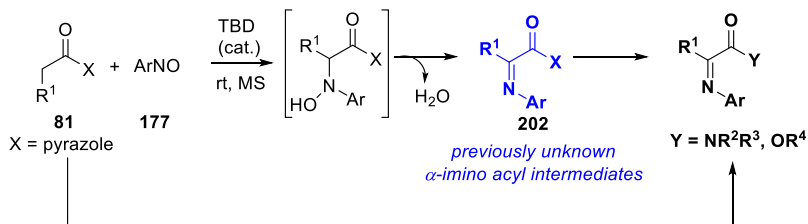
<sup>135</sup> (a) J. Moszew, A. Moskal, *Z. Nauk. UJ*, **1970**, *15*, 117; (b) A. J. Mirek, J. Moskal, A. Moskal, *Tetrahedron* **1975**, *31*, 2145.



**Scheme 6.17** Hypothesized mechanism of the Ehrlich-Sachs reaction.

## 6.2 Results and discussion

Previous examples shown for the synthesis of  $\alpha$ -imino ester derivatives require unusual reagents and catalysts, as well as strictly controlled or harsh reaction conditions. Our investigation on the reactivity of aryl acetic derived pyrazoleamides reported in chapter 5, indicated that the commercially available base, such as TBD was able to generate the enolate of these compounds under mild reaction conditions. These observations prompted us to investigate the reactivity of opportune acyl pyrazoles in the Ehrlich-Sachs reaction. The mild reaction conditions would have been useful to develop a new competitive methodology for a general direct  $\alpha$ -iminination of *N*-acyl pyrazoles (Scheme 6.18).<sup>136</sup>



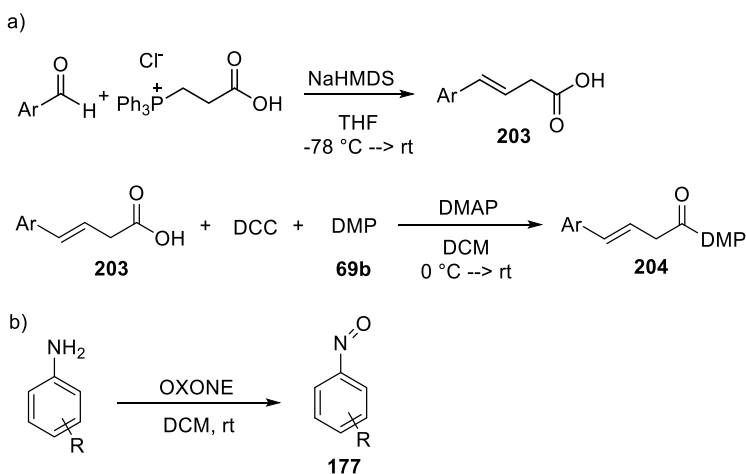
**Scheme 6.18** Outline of the direct  $\alpha$ -iminination of *N*-acyl pyrazoles with nitrosoarenes followed by one-pot functionalization.

According to the Ehrlich-Sachs mechanism, we envisaged that the firstly formed nitroso aldol intermediate would have undergone water elimination to provide previously unknown  $\alpha$ -imino acyl intermediates. The latter would have been exploited to set up one-pot approach to develop a formal  $\alpha$ -iminination sequence to a variety of

<sup>136</sup> C. Volpe, S. Meninno, G. Mirra, J. Overgaard, A. Capobianco, A. Lattanzi, *Org. Lett.* **2019**, *21*, 5305

carboxylic acid derivatives.

The pronucleophiles **81** have been easily synthesized via a DCC-mediated coupling reaction of arylacetic acids **128** with the opportune heterocycle **69** (see Scheme 5.9, a). The corresponding  $\beta,\gamma$ -unsaturated reagents **204** were prepared through a two-step procedure, namely a Wittig reaction<sup>137</sup> followed by coupling of the corresponding *trans*-styrylacetic acid **203** with the opportune heterocycle<sup>87b</sup>, as reported in the literature (Scheme 6.19, a). Nitrosoarenes **177** are known compounds, readily prepared according to the literature, through oxidation of variously substituted aromatic amines with OXONE (Scheme 6.19, b).<sup>138</sup>



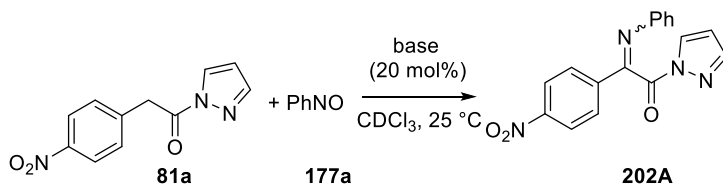
**Scheme 6.19** Synthesis of the reagents.

<sup>137</sup> R. Guo, J. Huang, X. Zhao, *ACS Catal.* **2018**, *8*, 926.

<sup>138</sup> W. Hu, Q. Zheng, S. Sun, J. Cheng, *Chem. Commun.* **2017**, *53*, 6263.

At the outset of the study, model compounds **81a** and **177a** were treated with 20 mol% loading of different bases in  $\text{CDCl}_3$  at room temperature (Table 6.1). With our pleasure common bases, such as DABCO and triethylamine, afforded the corresponding  $\alpha$ -imination product **202A** in good yield and with high diastereomeric ratio after a reasonable reaction time (es. 1 and 2). The reaction was completely regioselective, thus no traces of the  $\alpha$ -aminoxy *N*-acyl pyrazole were detected at the end of the reaction.<sup>127,128a</sup> Moreover, the presence of the nitron derivative was not observed. Inorganic or organic oxygen-containing bases proved to be less active and stereoselective (es. 3 and 4). Stronger bases, such as DBU, TBD, and BEMP provided product **202A** in high yield after a short reaction time (es. 5-7).

**Table 6.1** Base-catalyzed  $\alpha$ -imination of pyrazoleamide **81a** with nitrosobenzene.<sup>[a]</sup>



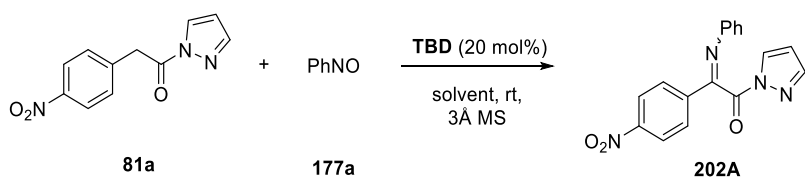
Es.	Base	<i>t</i> [h]	Conv. <b>202A</b> [%] <sup>[b]</sup>	<i>Z/E</i> <b>202A</b> <sup>[c]</sup>
<b>1</b>	DABCO	3	79	95/5
<b>2</b>	Et <sub>3</sub> N	1	78	95/5
<b>3</b>	CS <sub>2</sub> CO <sub>3</sub>	10	56	73/27
<b>4</b>	<i>t</i> -BuOK	14	7	85/15
<b>5</b>	DBU	0.5	89	80/20
<b>6</b>	TBD	0.5	90	95/5
<b>7</b>	BEMP	0.5	89	72/28

<sup>[a]</sup> Reaction conditions: **81a** (0.1 mmol), **177a** (0.12 mmol), base (0.02 mmol) in  $\text{CDCl}_3$  (0.5 mL) under nitrogen. <sup>[b]</sup> Yields of **202A** were determined by <sup>1</sup>H-NMR analysis using  $\text{CH}_2\text{Br}_2$  as an internal standard. <sup>[c]</sup> Dr ratio determined by <sup>1</sup>H-NMR analysis.

Among them, TBD proved to be superior, affording the product in excellent yield and with 95/5 diastereomeric ratio (es. 6).

A subsequent solvent screening, was conducted using 20 mol% loading of TBD and adding molecular sieves, in order to facilitate removal of water from the reaction mixture (Table 6.2). The best results, in terms of both yield and diastereoselectivity, were reached by using dichloromethane as the solvent. In this case, the desired product was obtained in quantitative yield and with high diastereomeric ratio after 2 hours (es. 2). The catalytic system proved to be effective also in toluene and diethyl ether, affording the  $\alpha$ -imino-*N*-acylpyrazole **202A** in excellent yield, but with a decreased *Z/E* ratio (es. 3 and 4). A more polar solvent, such as ethyl acetate, and a halogenated aromatic solvent, gave the worst results in terms of yield and diastereoselectivity of the final product (es. 5 and 6).

**Table 6.2** Solvent screening.<sup>[a]</sup>



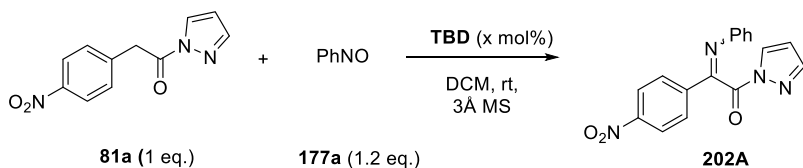
Es.	solvent	<i>t</i> [h]	Conv. <b>202A</b> [%] <sup>[b]</sup>	<i>Z/E</i> <b>202A</b> <sup>[c]</sup>
<b>1</b>	CHCl <sub>3</sub>	2	90	95/5
<b>2</b>	CH <sub>2</sub> Cl <sub>2</sub>	2	99	94/6
<b>3</b>	toluene	2	99	86/14
<b>4</b>	Et <sub>2</sub> O	2	93	91/9
<b>5</b>	EtOAc	2	72	86/14
<b>6</b>	chlorobenzene	2	68	87/13

<sup>[a]</sup> Unless otherwise noted reactions were conducted with **81a** (0.08 mmol), **177a** (0.096 mmol), TBD (0.016 mmol), 3Å MS (~20 mg) in 0.4 mL of anhydrous solvent under nitrogen atmosphere. <sup>[b]</sup> Determined by <sup>1</sup>H-NMR spectroscopy of crude reaction mixture using dibromomethane as an internal standard. <sup>[c]</sup> Determined by <sup>1</sup>H-NMR spectroscopy of crude reaction mixture.



Further reduction of the catalyst loading to 10 mol%, by working in dichloromethane, assured a rapid formation of the imination product **202A**, while maintaining excellent yield and high stereoselectivity (Table 6.3, es. 2). Reduction to 5 mol% loading proved to be not suitable, since the yield of product **202A** drastically dropped after a longer reaction time (es. 3).

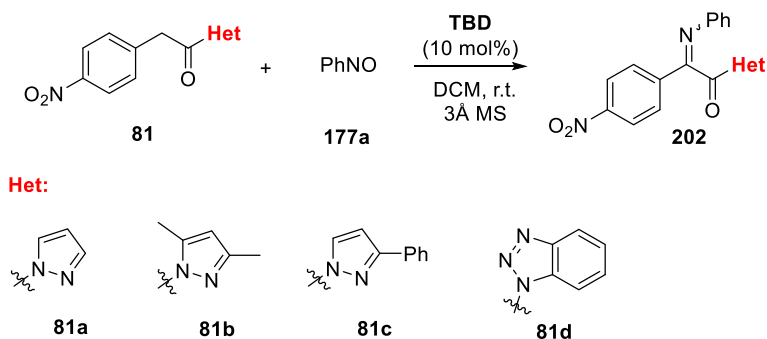
**Table 6.3** Optimization of the reaction parameters.<sup>[a]</sup>



Es.	TBD [mol%]	<i>t</i> [h]	conv. <b>202A</b> [%] <sup>[b]</sup>	<i>Z/E</i> <b>202A</b> <sup>[c]</sup>
1	20	0.4	99	94/6
2	10	0.4	99	93/7
3	5	1.5	65	93/7

<sup>[a]</sup> Unless otherwise noted reactions were conducted with **81a** (0.1 mmol), **177a** (0.09-0.12 mmol), TBD (5-20 mol%), 3Å MS (~40 mg) in anhydrous dichloromethane (0.5 mL) under nitrogen atmosphere. <sup>[b]</sup> Determined by <sup>1</sup>H-NMR spectroscopy of crude reaction mixture using dibromomethane as an internal standard. <sup>[c]</sup> Determined by <sup>1</sup>H-NMR spectroscopy of crude reaction mixture.

A final screening of differently substituted pyrazole moieties in pyrazoleimides **81** revealed the 3,5-dimethylpyrazole as the best group, affording  $\alpha$ -imino *N*-acylpyrazole **202a** with the highest yield (Table 6.4, es. 2). When acylbenzotriazole **81d** was used, the formation of a mixture of unidentified products was detected through <sup>1</sup>H-NMR analysis.

**Table 6.4** Substrate screening.<sup>[a]</sup>

Es.	Het	<i>t</i> [h]	yield <b>202</b> [%]	<i>Z/E</i> <b>202</b> <sup>[b]</sup>
1	<b>81a</b>	0.4	79 ( <b>202A</b> )	93/7
2	<b>81b</b>	0.4	87 ( <b>202a</b> )	98/2
3	<b>81c</b>	0.4	78 ( <b>202B</b> )	99/1
4	<b>81d</b>	0.4	- <sup>[c]</sup>	-

<sup>[a]</sup> Unless otherwise noted reactions were conducted with **81** (0.2 mmol), **177a** (0.24 mmol), TBD (0.02 mmol), 3Å MS (~45 mg) in anhydrous dichloromethane (1 mL) under nitrogen atmosphere. <sup>[b]</sup> Determined by <sup>1</sup>H-NMR spectroscopy of crude reaction mixture. <sup>[c]</sup> Reaction conducted with acylbenzotriazole **81d** led to the formation of a mixture of unidentified products.

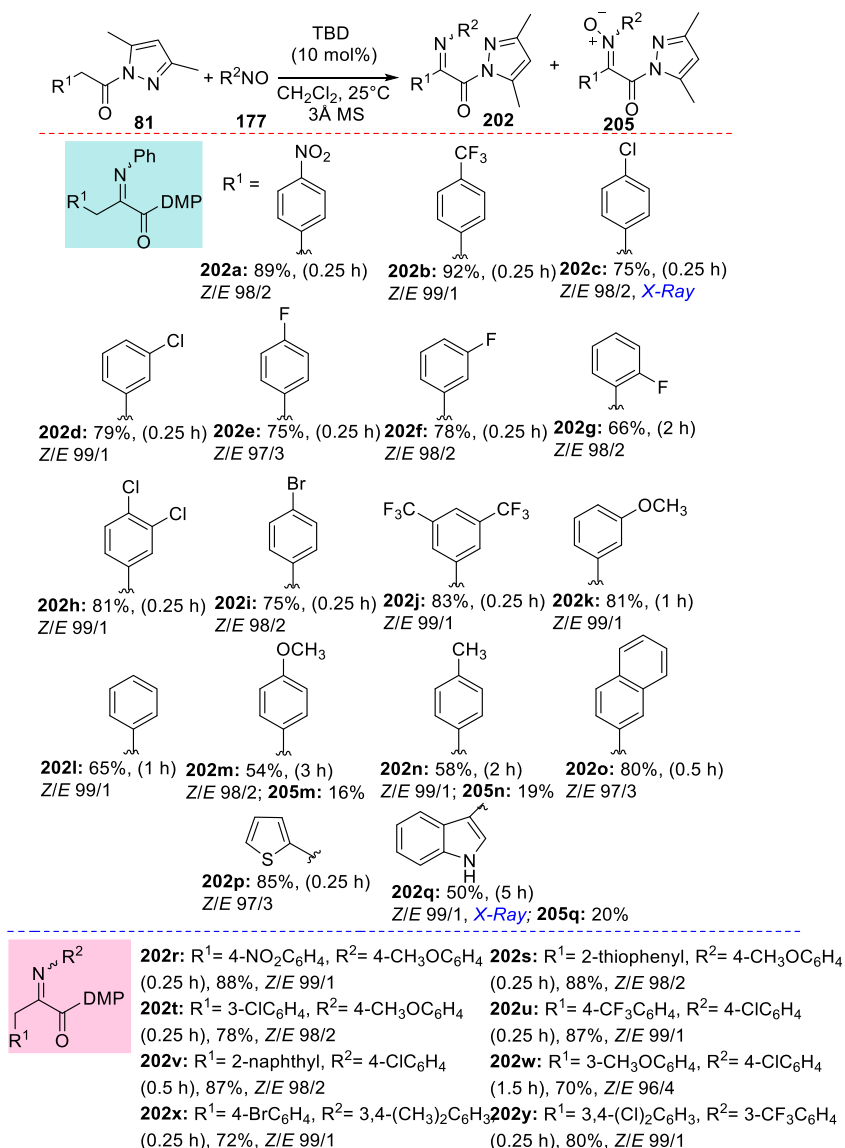
With the best reaction conditions in hand (Table 6.4, es. 2), the substrate scope using our system was explored. A variety of aromatic and heteroaromatic acetic acid-derived pyrazoles and nitrosobenzene proved to be suitable reagents (Table 6.5). The corresponding  $\alpha$ -imino products **202a-q** were isolated in good to high yields and with excellent *Z/E* ratios (up to 99/1). Only trace amounts ( $\leq 20\%$ ) of nitrones **205m** and **205n** were recovered at the end of the corresponding reactions. Unsubstituted *N*-acyl pyrazole and those bearing electron-withdrawing and halogen substituents at different positions of the benzene ring, rapidly afforded the corresponding imination products with excellent levels of diastereoselectivity. Compounds **81**, bearing electron-rich groups, provided moderate

yields of products **202m** and **202n** (54% and 58% respectively), while more pronounced amounts (albeit  $\leq 20\%$ ) of the corresponding nitrones **205m** and **205n** were observed. Interestingly, thiophenyl, *N*-unprotected 3-indolyl, and 2-naphthyl groups in the starting reagent **81** were also well-tolerated, with products **202** being recovered in good to high yields.

Single-crystal X-ray diffraction analyses, conducted on products **202c** and **202q**, in collaboration with Prof. Overgaard from Aarhus University, allowed to establish the formation of the *Z*-isomer. Moreover, for compound **202c**, DFT computations predicted for the *Z*-isomer an energy level of 3.4 kcal/mol lower compared to the energy level of the *E*-isomer.

A variety of nitrosoarenes, bearing electron-donating or withdrawing groups, were then reacted with *N*-acyl pyrazoles. To our delight, the expected products **202r-y** were obtained in good to high yields and with excellent *Z/E* ratios. Aliphatic pyrazoleamides, given the low acidity of the alpha protons (see Figure 5.2) were not tested in these reaction conditions.<sup>68</sup>

To evaluate the scalability of the process, a gram-scale reaction of compound **81b** (1.03 g) with nitrosobenzene was carried out. The product **202a** was recovered in 87% yield.

**Table 6.5** Substrate scope of *N*-acylpyrazoles **81** with nitrosoarenes.<sup>[a]</sup>

<sup>[a]</sup> Reaction conditions: **81** (0.2 mmol), **177** (0.24 mmol), TBD (0.02 mmol), 3Å MS (45 mg) in anhydrous dichloromethane (1 mL). Yields of isolated products after column chromatography. *Z/E* Ratio determined by <sup>1</sup>H-NMR analysis.

Then, we focused our attention on more challenging  $\beta,\gamma$ -unsaturated *N*-acyl pyrazoles **204**. Esters derivatives of products **206** are suitable starting materials in cycloaddition and multicomponent reactions for the synthesis of *aza*-heterocycles.<sup>139</sup> Unsaturated *N*-acyl pyrazoles **204** bearing aryl substituents at the  $\gamma$ -position were treated, under the previously optimized conditions, with different nitrosoarenes. The corresponding  $\alpha$ -imination products **206** were isolated in moderate to good yields and with moderate diastereomeric ratio, while excellent regioselectivity was observed (Table 6.6).

**Table 6.6** Substrate scope of *N*-acylpyrazoles **204** with nitrosoarenes.<sup>[a]</sup>



**206a:**  $R^1 = R^2 = Ph$ ,  $R^3 = H$   
76%, dr 72/28, (2 h)

**206b:**  $R^1 = Ph$ ,  $R^2 = 4-ClC_6H_4$ ,  $R^3 = H$   
70%, dr 72/28, (0.5 h)

**206c:**  $R^1 = R^2 = Ph$ ,  $R^3 = CH_3$   
62%, dr 65/35, (3 h)

**206d:**  $R^1 = 4-CF_3C_6H_4$ ,  $R^2 = 4-ClC_6H_4$ ,  $R^3 = H$   
66%, dr 77/23, (0.5 h)

**206e:**  $R^1 = 3-CH_3OC_6H_4$ ,  $R^2 = 3,4-(CH_3)_2C_6H_3$ ,  
 $R^3 = H$ , 65%, dr 70/30, (1.5 h)

**206f:**  $R^1 = 3,4-(Cl)_2C_6H_3$ ,  $R^2 = 4-CH_3OC_6H_4$ ,  
 $R^3 = H$ , 55%, dr 75/25, (0.5 h)

**206g:**  $R^1 = 4-CH_3C_6H_4$ ,  $R^2 = 4-CH_3OC_6H_4$ ,  
 $R^3 = H$ , 60%, dr 73/27, (3 h)

**206h:**  $R^1 = (CH_2)_2Ph$ ,  $R^2 = Ph$ ,  $R^3 = H$   
26%, dr 65/35, (3 h)

<sup>[a]</sup> Reaction conditions according to Table 6.5. Yields of isolated products after column chromatography.

Compounds **206** were found to be unstable on silica gel and mass spectrum of the polar mixture recovered after chromatography, allowed us to detect the presence of the nitrones of type **205** (Figure 6.2).

<sup>139</sup> For reviews, see: (a) B. Groenendaal, E. Ruijter, R. V. A. Orru, *Chem. Commun.* **2008**, 5474; (b) D. L. Boger, O. Huter, K. Mbiya, M. S. Zhang, *J. Am. Chem. Soc.* **1995**, *117*, 11839; (c) S. Jayakumar, M. P. S. Ishar, M. P. Mahajan, *Tetrahedron* **2002**, *58*, 379; (d) L. He, G. Laurent, P. Retailleau, B. Folleas, J.-L. Brayer, G. Masson, *Angew. Chem. Int. Ed.* **2013**, *52*, 11088; (e) H. Tanaka, I. Mizota, M. Shimizu, *Org. Lett.* **2014**, *16*, 2276.

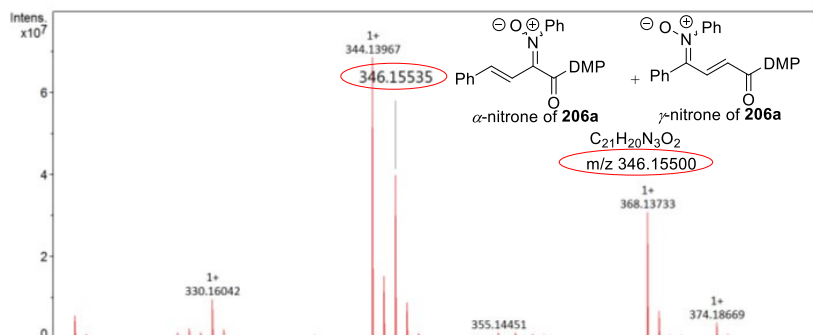
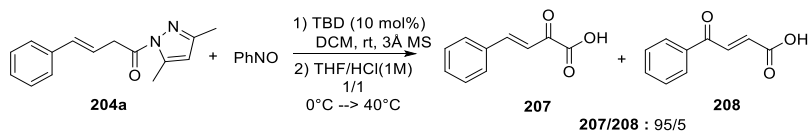


Figure 6.2 HRMS identification of unsaturated nitrones.

In order to evaluate the  $\alpha/\gamma$  regioselectivity of the catalytic system, the crude reaction mixture of model compound **206a** was hydrolyzed under acidic conditions (Scheme 6.20). The crude mixture was subsequently analysed by  $^1\text{H-NMR}$ , showing both  $\alpha$ - and  $\gamma$ -keto acids **207** and **208** in 95/5 ratio respectively, thus attesting the high regioselectivity of the reaction.



Scheme 6.20 One-pot imination and hydrolysis of  $\beta,\gamma$ -unsaturated *N*-acylpyrazoles.

The  $\alpha$ -imino ester derivatives **202** and **206** served for further one-pot functionalization for the synthesis of useful intermediates, taking advantage of the leaving group ability of the pyrazole group and proper nucleophiles. One-pot sequential procedures enabled the access to  $\alpha$ -imino amides, dipeptide precursors, and esters (Table 6.7). Primary and secondary amines and anilines proved to be suitable nucleophiles in the addition-elimination step, thus affording secondary and tertiary  $\alpha$ -imino amides **209a-e** in good to excellent

yields. However, for the less reactive anilines and bulky secondary amines, addition of DMAP as a co-catalyst in the second step was required, as well as the use of toluene as solvent in order to reach higher temperatures (**209b-c** and **e**). Moreover, the use of  $\alpha$ -amino acid ester salts, in combination with triethylamine, led to the formation of dipeptide precursors **210**. These products were isolated in good yield, without observing any racemization in the case of optically active **210b**.<sup>140</sup> A one-pot sequence was developed when using alcohols as the nucleophiles, with the corresponding diverse  $\alpha$ -imino esters **172** recovered in moderate to good yields. Particularly useful is the access to compound of type **172c**, frequently used in cycloaddition reaction to prepare heterocyclic products.<sup>141</sup> Finally, a one-pot imination-reduction sequence for the synthesis of  $\beta$ -amino alcohols was carried out. In this regard, crude intermediates **202** and **206** were treated with  $\text{NaBH}_4$  or  $\text{LiBH}_4$  in THF as the solvent (Scheme 6.21). This class of compounds are useful ligands in catalysis as well as suitable building blocks in total synthesis.<sup>142</sup> A typical synthetic strategy to access  $\beta$ -amino alcohols of type **211** involves the ring opening of styrene epoxides by anilines. Control of the regioselectivity is the crucial issue and a mixture of regioisomeric  $\beta$ -amino alcohols was usually observed.<sup>143</sup>

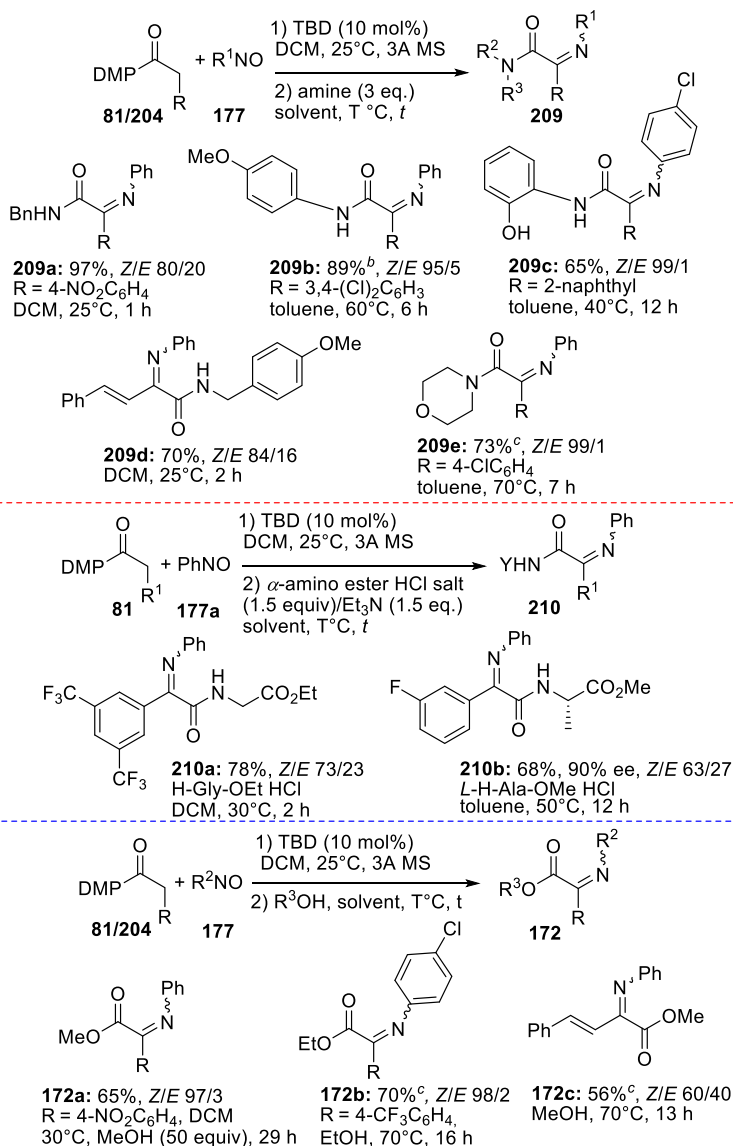
---

<sup>140</sup> The reaction was performed with *L*-Ala ester salt of 92% optical purity.

<sup>141</sup> For reviews, see: (a) B. Groenendaal, E. Ruijter, R. V. A. Orru, *Chem. Commun.* **2008**, 5474. (b) H. Tanaka, I. Mizota, M. Shimizu, *Org. Lett.* **2014**, *16*, 2276.

<sup>142</sup> For reviews, see: (a) I. Gallou, C. H. Senanayake, *Chem. Rev.* **2006**, *106*, 2843; (b) O. K. Karjalainen, A. M. P. Koskinen, *Org. Biomol. Chem.* **2012**, *10*, 4311.

<sup>143</sup> For reviews and examples, see: (a) A. K. Chakraborti, A. Kondaskar, S. Rudrawar, *Tetrahedron* **2004**, *60*, 9085; (c) T. Li, L. Jin, W. Zhang, H. N. Miras, Y.-F. Song, *ChemCatChem* **2018**, *10*, 4699.

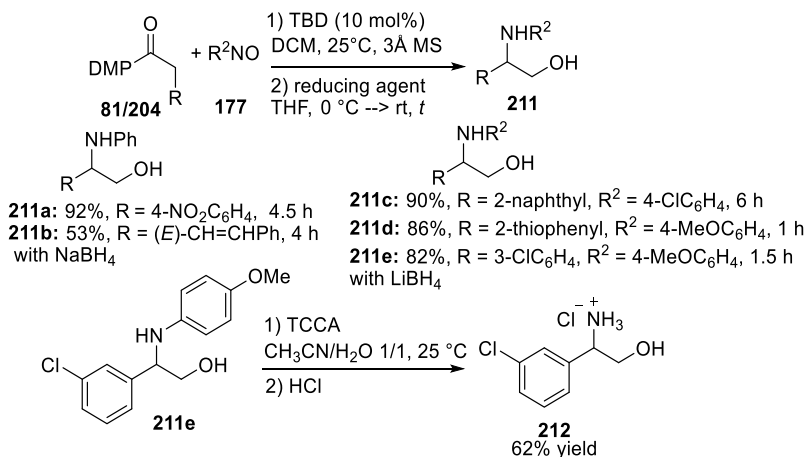
**Table 6.7** One-pot synthesis of  $\alpha$ -imino amides, dipeptide presursors and esters.<sup>[a]</sup>

<sup>[a]</sup> Reaction conditions for the first step according to Tables 6.5 and 6.6. <sup>[b]</sup> Toluene used as solvent for the first step. <sup>[c]</sup> 20 mol% of DMAP was added in the second step.



On the contrary, the one-pot route depicted in Scheme 6.21 represents a straightforward access to  $\beta$ -amino alcohols **211**.

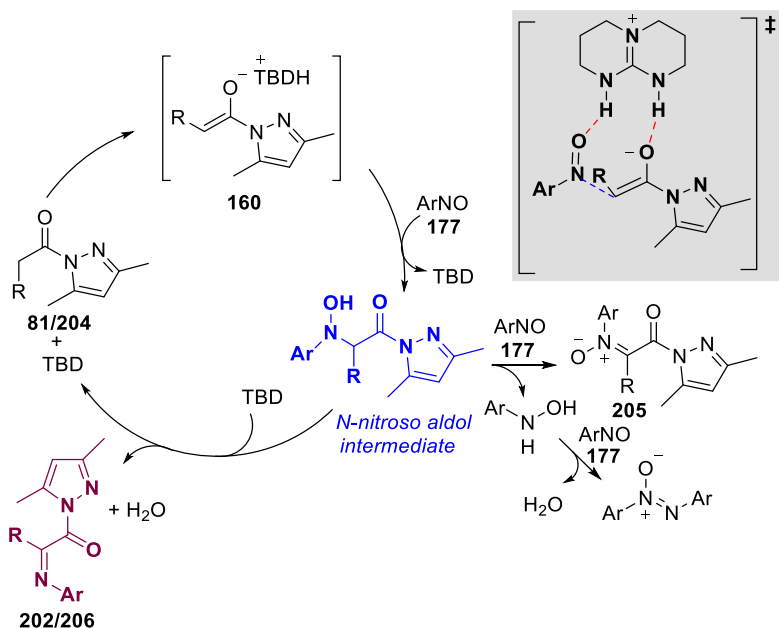
It has to be noted that a limited number of synthetic procedures, often characterized by several steps, can be found in the literature for the preparation of 2-aryl glycinols, useful building blocks for the synthesis of biologically active compounds.<sup>144</sup> We disclosed an alternative strategy to access 2-aryl glycinols deprotecting the PMP-derived  $\alpha$ -imino *N*-acylpyrazoles. The one-pot imination/reduction sequence, followed by deprotection with trichloroisocyanuric acid (TCCA) afforded the 2-arylglycinol salt **212** in 62% yield.



**Scheme 6.21** One-pot synthesis of  $\beta$ -amino alcohols.

<sup>144</sup> For selected examples, see: (a) M. Bandini, P. G. Cozzi, M. Gazzano, A. Umami-Ronchi, *Eur. J. Org. Chem.* **2001**, 2001, 1937; (b) H.-Y. Ku, J. Jung, S.-H. Kim, H. Y. Kim, K. H. Ahn, S.-G. Kim, *Tetrahedron: Asymmetry* **2006**, 17, 1111.

To rationalize the outcome of the reaction, we propose the catalytic cycle as shown in Scheme 6.22.



**Scheme 6.22** Hypothesized catalytic cycle.

The bifunctional catalyst TBD readily deprotonates pyrazoleamides **81** or **204**, leading to the formation of a guanidinium enolate complex **160**. Then the nitrosoarene **177**, engaged by H-bond interactions with the previous complex **160**, would undergo the attack of the enolate. The regioselective formation of the  $\alpha$ -hydroxyamino product, with the contemporary regeneration of the base, are observed. The *N*-nitroso aldol intermediate would rapidly undergo a base-catalyzed elimination of water to give the desired  $\alpha$ -imino *N*-acyl pyrazole. On the other hand, the formation of nitrones **205** might result from a minor competitive pathway. More specifically the *N*-nitroso aldol intermediate would undergo a nitrosoarene-mediated

dehydrogenation with the formation of an aryl hydroxyl amine. This byproduct then is able to react with nitrosoarene to form an azoxyarene, which was always isolated in similar amounts to nitrone **205**.

## CONCLUSIONS

In conclusion, we have developed a practical methodology to accomplish the direct  $\alpha$ -imination of readily available *N*-acyl pyrazoles with nitrosoarenes using catalytic amounts of a commercial base. Rapid and effective formation of  $\alpha$ -imino *N*-acyl pyrazoles was observed at room temperature. The protocol proved to be completely regioselective, while moderate to excellent levels of diastereoselectivity were achieved. The competitive formation of the nitronne derivatives was observed only when using particular substrates, pointing to the necessity of an in depth investigation on the mechanism of this reaction. Finally, this method showed great synthetic utility, as demonstrated with a variety of convenient one-pot transformations of  $\alpha$ -imino *N*-acyl pyrazoles.  $\alpha$ -Imino amides, esters, dipeptide precursors and  $\beta$ -amino alcohols were obtained with good to excellent results.

However, further investigations on the application of this system to other classes of carbonyl compounds were carried out and results are summarized in Chapter 7.

## 7. NITRONE/IMINE SELECTIVITY SWITCH IN BASE-CATALYSED REACTION OF ARYL ACETIC ACID ESTERS WITH NITROSOARENES: JOINT EXPERIMENTAL AND COMPUTATIONAL STUDY

### 7.1 Background

Nitrones exhibit the general structure, which is depicted in Figure 7.1. Hence, the main feature lies in the presence of an anionic oxygen and an electrophilic carbon atoms separated by a cationic nitrogen. These molecules are generally endowed with high stability, ease of handling and are also isolable through column chromatography.

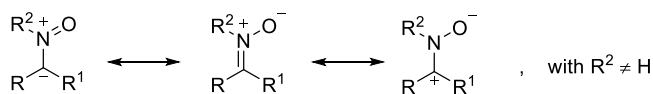


Figure 7.1 Resonance structures of a nitrone.

Nitrones constitute an important class of synthetic building blocks for the construction of complex scaffolds. In fact, they represent one of the most widely studied 1,3-dipoles, allowing access to a variety of heterocyclic compounds.<sup>145</sup> A great number of methodologies employ nitrones in cycloaddition reactions for the synthesis of isoxazolines and isoxazolidines,<sup>146</sup> heterocyclic motifs found in a

<sup>145</sup> (a) K. V. Gothelf, K. A. Jørgensen, *Chem. Rev.* **1998**, *98*, 863; (18) L. M. Stanley, M. P. Sibi, *Chem. Rev.* **2008**, *108*, 2887; (c) T. Hashimoto, K. Maruoka, *Chem. Rev.* **2015**, *115*, 5366.

<sup>146</sup> (a) P. Jiao, D. Nakashima, H. Yamamoto, *Angew. Chem. Int. Ed.* **2008**, *47*, 2411; (b) M. A. Voinov, T. G. Shevelev, T. V. Rybalova, Y. V. Gatilov, N. V. Pervukhina, A. B. Burdukov, I. A. Grigor'ev, *Organometallics* **2007**, *26*, 1607; (c) D. Nakashima, H. Yamamoto, *J. Am. Chem. Soc.* **2006**, *128*, 9626; (d) C. Palomo, M. Oiarbide, E. Arceo, J. M. García, R. López, A. González, A. Linden, *Angew. Chem. Int. Ed.* **2005**, *44*, 6187; (e) M. P. Sibi, Z. Ma, C. P. Jasperse, *J. Am. Chem. Soc.*, **2004**, *126*, 718; (f) W. S. Jen, J. J. M. Wiener, D. W. C. MacMillan, *J. Am. Chem. Soc.* **2000**, *122*, 9874.

variety of biologically active natural products.<sup>147</sup>

Several procedures for the synthesis of nitrones can be found in the literature (Scheme 7.2). They are readily obtained through the condensation of alkyl or aryl *N*-monosubstituted hydroxyl amines with aldehydes and ketones<sup>148</sup> (route a) and reaction of oximes with electrophiles<sup>149</sup> (route b). Oxidations of specific substrates enable the access to this scaffold. *N,N*-disubstituted hydroxylamines<sup>150</sup> (route c), secondary amines<sup>151</sup> (route d), *N*-alkyl- $\alpha$ -amino acids<sup>152</sup> (route e) and imines<sup>153</sup> (route f) proved to be suitable starting materials in the synthesis of nitrones with a variety of oxidizing reagents.

---

<sup>147</sup> (a) K. Kaur, V. Kumar, A. K. Sharma, G. K. Gupta, *Eur. J. Med. Chem.* **2014**, *77*, 121; (b) K. Koyama, Y. Hirasawa, A. E. Nugroho, T. Hosoya, T. C. Hoe, K.-L. Chan, H. Morita, *Org. Lett.*, **2010**, *12*, 4188.

<sup>148</sup> (a) J. Y. Pfeiffer, A. M. Beauchemin, *J. Org. Chem.* **2009**, *74*, 8381; (b) H.-S. Cheng, A.-H. Seow, T.-P. Loh, *Org. Lett.* **2008**, *10*, 2805; (c) R. E. Michael, K. M. Chando, T. Sammakia, *J. Org. Chem.* **2015**, *80*, 6930.

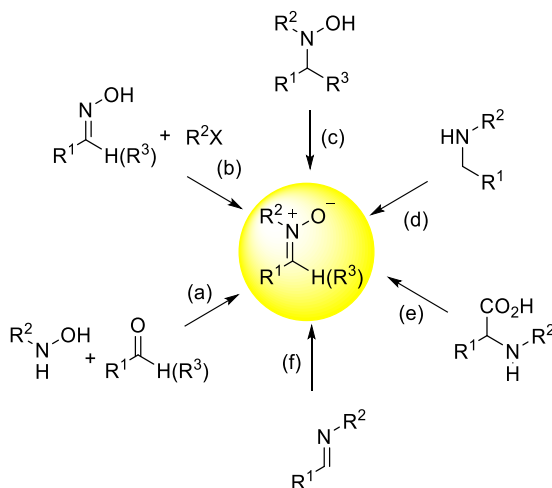
<sup>149</sup> (a) R.-H. Liu, D. Wei, B. Han, W. Yu, *ACS Catal.* **2016**, *6*, 6525; (b) X.-X. Peng, D. Wei, W.-J. Han, F. Chen, W. Yu, B. Han, *ACS Catal.* **2017**, *7*, 7830; (c) Z.-H. Wang, H.-H. Zhang, P.-F. Xu, Y.-C. Luo, *Chem. Commun.* **2018**, *54*, 10128; (d) T. Kitanosono, P. Xu, S. Kobayashi, *Science* **2018**, *362*, 311.

<sup>150</sup> (a) S. Cicchi, M. Marradi, A. Goti, A. Brandi, *Tetrahedron Lett.* **2001**, *42*, 6503; (b) C. Matassini, C. Parmeggiani, F. Cardona, A. Goti, *Org. Lett.* **2015**, *17*, 4082; (c) C. Parmeggiani, C. Matassini, F. Cardona, A. Goti, *Synthesis* **2017**, *49*, 2890.

<sup>151</sup> (a) E. Marcantoni, M. Petrini, O. Polimanti, *Tetrahedron Lett.* **1995**, *36*, 3561; (b) A. Goti, L. Nannelli, *Tetrahedron Lett.* **1996**, *37*, 6025; (c) R. W. Murray, K. Iyanar, J. Chen, J. T. Wearing, *J. Org. Chem.* **1996**, *61*, 8099; (d) A. Goti, F. Cardona, G. Soldaini, *Org. Synth.* **2005**, *81*, 204.

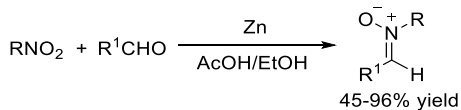
<sup>152</sup> (a) S.-I. Murahashi, Y. Imada, H. Ohtake, *J. Org. Chem.* **1994**, *59*, 6170; (b) H. Ohtake, Y. Imada, S.-I. Murahashi, *Bull. Chem. Soc. Jpn.* **1999**, *72*, 2737; (c) S.-I. Murahashi, H. Ohtake, Y. Imada, *Tetrahedron Lett.* **1998**, *39*, 2765.

<sup>153</sup> (a) F. Cardona, M. Bonanni, G. Soldaini, A. Goti, *ChemSusChem* **2008**, *1*, 327; (b) B. Singh, S. L. Jain, P. K. Khatri, B. Sain, *Green Chem.* **2009**, *11*, 1941; (c) B. Singh, S. L. Jain, B. S. Rana, P. K. Khatri, A. K. Sinha, B. Sain, *ChemCatChem* **2010**, *2*, 1260.



**Figure 7.2** Synthetic routes to nitrones.

Nitro- and nitroso compounds were successfully applied for the synthesis of nitrones. Nitro compounds can provide functionalized nitrones by reaction with aldehydes under reductive conditions, in a one-pot manner (Scheme 7.1).<sup>154</sup>

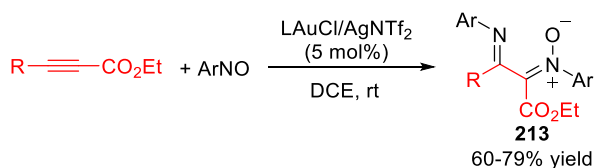


**Scheme 7.1** One-pot synthesis of functionalized nitrones from nitro compounds.

Another approach to prepare nitrones is represented by the use of nitrosoarenes as reagents, although only a few protocols are present in the literature. In 2014, Liu and colleagues reacted electron-poor alkynes and nitrosoarenes, in the presence of a gold/silver-based catalytic system, achieving the 1,2-iminonitronation of the starting

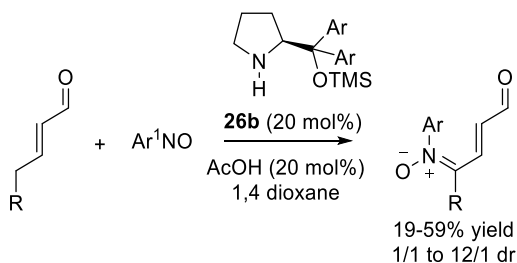
<sup>154</sup> V. Gautheron-Chapoulaud, S. U. Pandya, P. Cividino, G. Masson, S. Py, Y. Vallee, *Synlett* **2001**, 2001, 1281.

alkynes (Scheme 7.2).<sup>155</sup> The corresponding  $\alpha$ -imidoyl nitrones **213** were satisfactorily obtained, after reasonable reaction times.



**Scheme 7.2** Gold-catalyzed 1,2-iminonitration of electron-poor alkynes with nitrosoarenes.

Moyer and co-workers developed an interesting redox reaction for the nitron synthesis under organocatalytic conditions. They reacted  $\alpha,\beta$ -unsaturated aldehydes with an excess of nitrosoarene in the presence of the Jørgensen-Hayashi catalyst **26b**, thus achieving the introduction of the nitron moiety at  $\gamma$ -position of aldehyde (Scheme 7.3).<sup>156</sup>



**Scheme 7.3** Organocatalyzed nitrones formation via redox reaction.

Another interesting example for the synthesis of *N*-aryl nitrones was reported in 2014 by the Ashfeld's group. They described an *umpolung* approach to install the nitron group.<sup>157</sup> Aryl  $\alpha$ -keto esters **162** were reacted with nitrosoarenes **177**, in the presence of

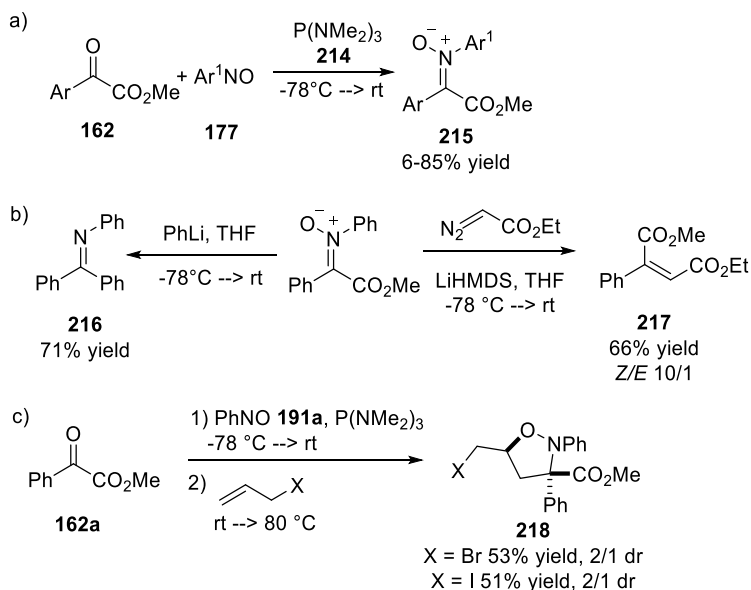
<sup>155</sup> R. R. Singh, R.-S. Liu, *Chem. Commun.* **2014**, 50, 15864.

<sup>156</sup> A. J. Fraboni, S. E. Brenner-Moyer, *Org. Lett.* **2016**, 18, 2146.

<sup>157</sup> A. P. Chavannavar, A. G. Oliver, B. L. Ashfeld, *Chem. Commun.* **2014**, 50, 10853.



stoichiometric amounts of phosphines **214**, under controlled conditions. The corresponding ketonitrones were obtained in moderate to good yields (Scheme 7.4, a). These functionalized ketonitrones **215** were consequently exploited for the synthesis of useful targets such as imines **216**, fumarates **217** (Scheme 7.4, b) and isoxazolidines **218** (Scheme 7.4, c).

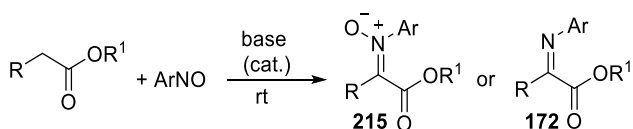


**Scheme 7.4** (a) Phosphine-mediated addition of 1,2-dicarbonyl compounds to nitroso electrophilic species, (b) Synthesis of imines, fumarates and (c) Isoxazolidines.

## 7.2 Results and discussion

The synthesis of functionalized ketonitrones **215** via the typical condensation of a ketone with hydroxylamine is not straightforward, due to the low reactivity of this class of carbonyl compounds. As demonstrated in Chapter 6, amounts of nitron were observed when reacting arylacetic acid derived pyrazoles of low acidity at the  $\alpha$ -

position (Table 6.5). Hence, we thought that further investigation on this reaction could be useful to clarify the outcome and the mechanism, by changing the nature of the starting carbonyl compound. We thought that the nitroso aldol intermediate could be eventually routed toward the nitrono product under proper conditions. Along this line, readily available arylacetic esters were chosen to perform a study on the Ehrlich-Sachs reaction under our catalytic conditions (Scheme 7.5).



**Scheme 7.5** Ehrlich-Sachs reaction of arylacetic esters under catalytic basic conditions.

A constructive collaboration with Prof. Mazzanti from University of Bologna helped us to shed light on the unknown details of the reaction mechanism through theoretical calculations.

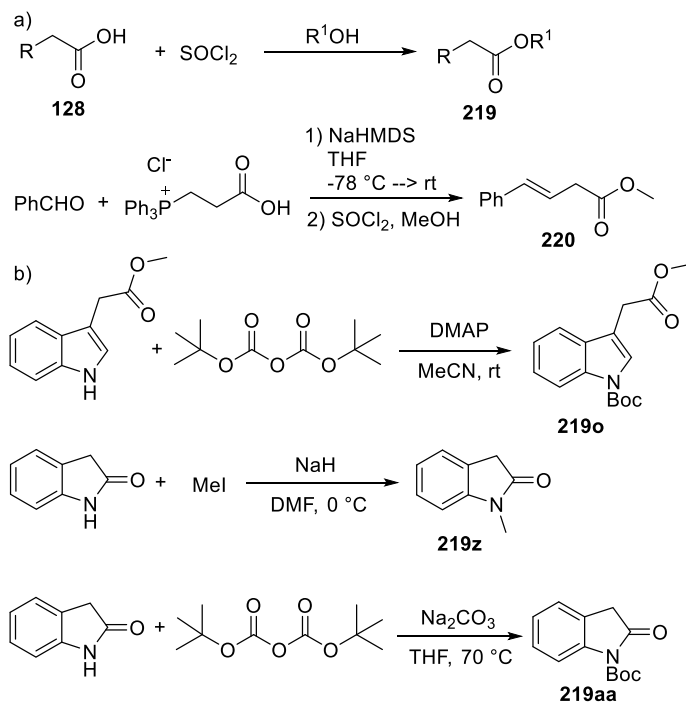
The arylacetic esters **219** have been easily synthesized through esterification of the commercially available arylacetic acids **128**, according to procedures reported in the literature,<sup>158</sup> whereas the  $\beta,\gamma$ -unsaturated ester **220** was obtained by a Wittig reaction<sup>159</sup> followed by esterification<sup>158</sup> of the corresponding *trans*-styrylacetic acid (Scheme 7.6, a). The 3-indole acetic ester and 2-oxindole were properly alkylated and acylated<sup>160</sup> at nitrogen as reported in the

<sup>158</sup> Z. Escobar, M. Johansson, A. Bjartell, R. Hellsten, O. Sterner, *Int. J. Org. Chem.*, **2014**, *4*, 225.

<sup>159</sup> C. K. Tan, J. C. Er, Y.-Y. Yeung, *Tetrahedron Lett.* **2014**, 55,1243.

<sup>160</sup> (a) W. Sun, G. Zhu, C. Wu, L. Hong, R. Wang, *Chem. Eur. J.*, **2012**, *18*, 6737; (b) J.-B. Zhao, X.-F. Ren, B.-Q. Zheng, J. Ji, Z.-B. Qiu, Y. Li, *J. Fluorine Chem.* **2018**, *215*, 44; (c) J. R. Valdéz-Camacho, J. D. Rivera-Ramírez, J. Escalante, *Int. J. Org. Chem.* **2019**, *9*, 10.

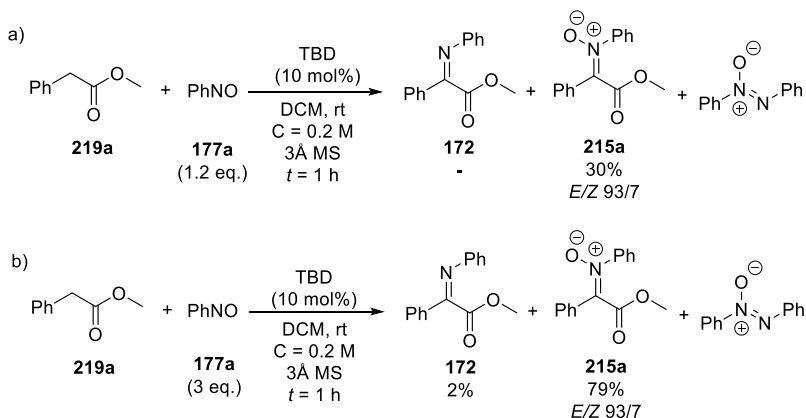
literature (Scheme 7.6, b). Finally, nitrosoarenes were synthesized as reported in Scheme 6.22, b.



**Scheme 7.6** Synthesis of esters.

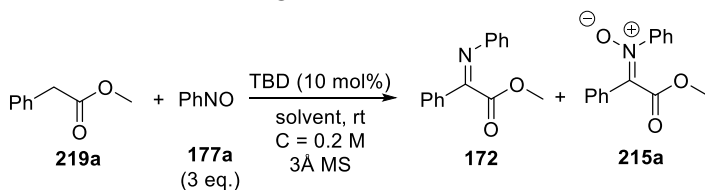
At the outset of the study, our previously reported catalytic system for the direct  $\alpha$ -imination of *N*-acylpyrazoles was checked.<sup>136</sup> Thus the commercially available methyl phenylacetate **219a** was treated with 1.2 equivalents of nitrosobenzene in the presence of 10 mol% of TBD as catalyst and 3Å molecular sieves, in dichloromethane at room temperature (Scheme 7.11, a). After 1 hour, 30% of nitrone **215a** in 93/7 *E/Z* ratio was isolated, while no traces amount of the corresponding imine **172** were observed at the end of the reaction. In order to improve the yield of the desired product **215a**, methyl

phenylacetate was then treated with an excess of nitrosobenzene. Pleasingly, under these conditions, ketonitrone **215a** was isolated in high yield and with high diastereoselectivity after a short reaction time (Scheme 7.7, b). The 19% of unreacted ester **219a** was recovered after column chromatography, while only traces amount of imine **172** were detected at the end of the reaction. Moreover, azoxybenzene was found in similar amount as nitrone, in agreement with the proposed mechanism (see Scheme 6.22).



**Scheme 7.7** Reaction of methyl phenylacetate with nitrosobenzene.

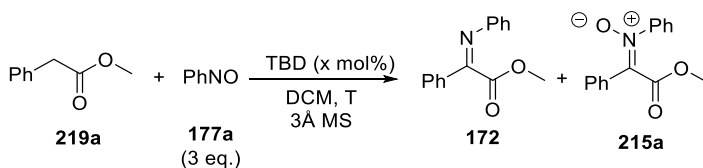
In order to improve the process, a solvent screening was carried out (Table 7.1). The yield of product **215a** dropped when more polar solvents were used, while a more pronounced amount of the undesired imine **172** was recovered at the end of the reaction (es. 2 and 4). Among the chlorinated solvents tested, dichloromethane was confirmed to be the best solvent, leading to product **215a** with the highest yield and selectivity (es. 1, 5 and 6).

**Table 7.1** Solvent screening.<sup>[a,b]</sup>

Es.	Solvent	<i>t</i> [h]	unreacted <b>219a</b> [%] <sup>[c]</sup>	Yield <b>172</b> [%] <sup>[c]</sup>	Yield <b>215a</b> [%] <sup>[c]</sup>	<i>E/Z</i> <b>215a</b> <sup>[d]</sup>
1	DCM	1	19	2	79	93/7
2	AcOEt	3	-	27	62	88/12
3	Toluene	2.5	11	14	70	87/13
4	THF	1	21	15	51	86/14
5	CHCl <sub>3</sub>	1	30	-	47	86/14
6	ClCH <sub>2</sub> CH <sub>2</sub> Cl	1	43	5	49	85/15

<sup>[a]</sup> Unless otherwise noted reactions were conducted with **219a** (0.2 mmol), **177a** (0.6 mmol), TBD (0.02 mmol), 3Å MS (~50 mg) in 1 mL of anhydrous solvent under nitrogen atmosphere. <sup>[b]</sup> After chromatography azoxybenzene was recovered in similar amounts as nitrobenzene. <sup>[c]</sup> Isolated yields. <sup>[d]</sup> Determined by <sup>1</sup>H-NMR spectroscopy of crude reaction mixture.

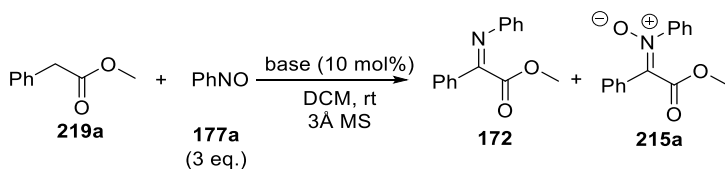
The reaction was further optimized in dichloromethane by varying temperature, reagents ratio, concentration and catalyst loading (Table 7.2). No improvement in terms of yield and selectivity was observed when decreasing the reaction temperature to 0 or -20 °C. (es. 2 and 3). Increasing either the catalyst loading or the equivalents of nitrosobenzene did not improve the outcome of the reaction (es. 4 and 5).

**Table 7.2** Effect of temperature, dilution and catalyst loading in the reaction of model compound **219a**.<sup>[a,b]</sup>

Es.	C [M]	TBD [mol%]	T [°C]	<i>t</i> [h]	Yield <b>172</b> [%] <sup>[c]</sup>	Yield <b>215a</b> [%] <sup>[c]</sup>	<i>E/Z</i> <sup>[d]</sup>
1	0.2	10	rt	1	2	79	93/7
2	0.2	10	0	1	14	77	85/15
3	0.2	10	-20	1	10	70	85/15
4 <sup>[f]</sup>	0.2	10	rt	1	4	73	84/16
5	0.1	20	rt	1	11	75	86/14

<sup>[a]</sup> Unless otherwise noted reactions were conducted with **219a** (0.2 mmol), **177a** (0.6 mmol), TBD (0.02 mmol), 3 Å MS (~50 mg) in 1 mL of anhydrous solvent under nitrogen atmosphere. <sup>[b]</sup> After chromatography azoxybenzene was recovered in similar amounts as nitron. <sup>[c]</sup> Isolated yields. <sup>[d]</sup> Determined by <sup>1</sup>H-NMR spectroscopy of crude reaction mixture. <sup>[f]</sup> 3.5 equivalents of **191a** were used.

Finally, the nature of the base was explored (Table 7.3). The yield of product **215a** drastically dropped when less basic DBU was used (es. 2). As expected, more sterically demanding tetramethylguanidine as well as the weaker proton sponge and triethylamine were not able to generate the enolate of the model methyl phenylacetate (es. 4-6). With our great delight, a marked improvement of the yield of the product was observed when using the more basic 2-tert-Butylimino-2-diethylamino-1,3-dimethylperhydro-1,3,2-diazaphosphorine, BEMP (es. 2). In this case, the product **215a** was isolated in high yield and with excellent diastereoselectivity, still observing high selectivity toward the formation of nitron.

**Table 7.3** Base screening.<sup>[a,b]</sup>

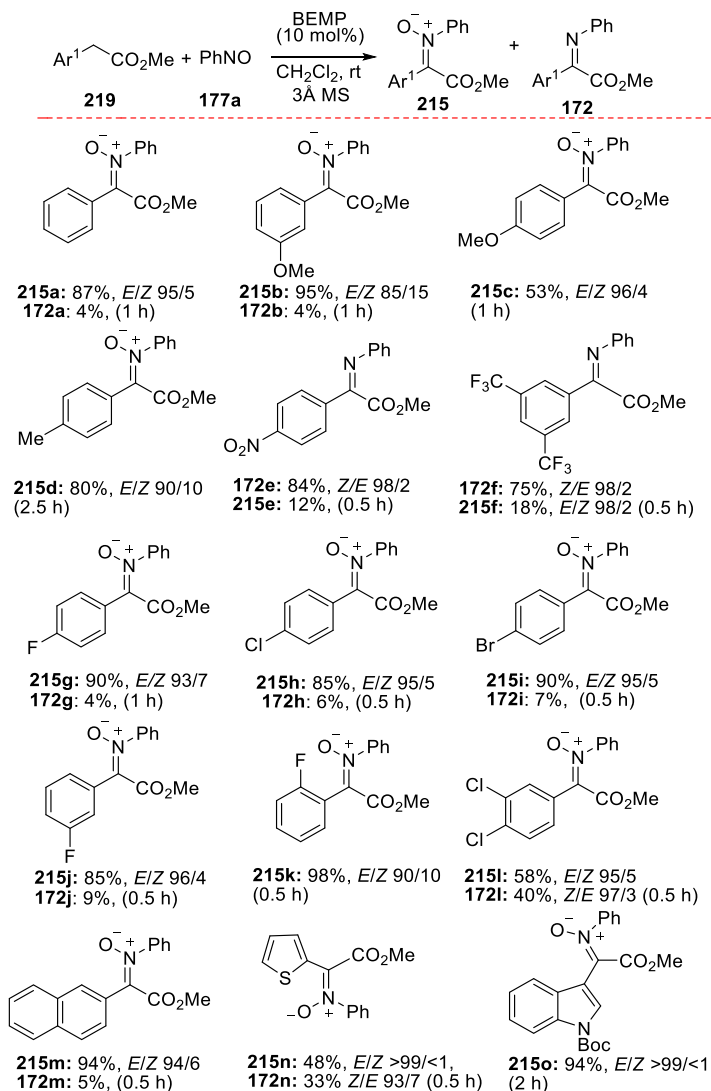
Es.	base	<i>t</i> [h]	unreacted <b>219a</b> [%] <sup>[c]</sup>	Yield <b>172</b> [%] <sup>[c]</sup>	Yield <b>215a</b> [%] <sup>[c]</sup>	<i>E/Z</i> <b>215a</b> <sup>[d]</sup>
1	TBD	1	19	2	79	93/7
2	DBU	3	28	-	61	92/8
3	BEMP	1	5	4	87	95/5
4	TMG	1	-	-	-	-
5	Proton Sponge	1	-	-	-	-
6	NEt <sub>3</sub>	1	-	-	-	-

<sup>[a]</sup> Unless otherwise noted reactions were conducted with **219a** (0.2 mmol), **177a** (0.6 mmol), TBD (0.02 mmol), 3Å MS (~50 mg) in 1 mL of anhydrous solvent under nitrogen atmosphere. <sup>[b]</sup> After chromatography azoxybenzene was recovered in similar amounts as nitrobenzene. <sup>[c]</sup> Isolated yields. <sup>[d]</sup> Determined by <sup>1</sup>H-NMR spectroscopy of crude reaction mixture.

Under the optimized reaction conditions, illustrated in Table 7.3, es. 3, the scope of the reaction was investigated (Table 7.4). The catalytic system proved to be effective with both electron-rich and electron-poor aromatic rings. As shown in Table 7.4, the starting methyl esters can be grouped into three main categories. Methyl esters bearing electron-donating (**219b-d**) and halogen substituents (**219g-k**) at different positions of the benzene ring, as well as a more sterically demanding 2-naphthyl group (**219m**) showed high to complete selectivity toward the nitron formation. In these cases, products were isolated in good to high yield and with good to excellent diastereoselectivity.

**Table 7.4** Substrate scope of arylacetic methyl esters with nitrosobenzene.

[a,b]



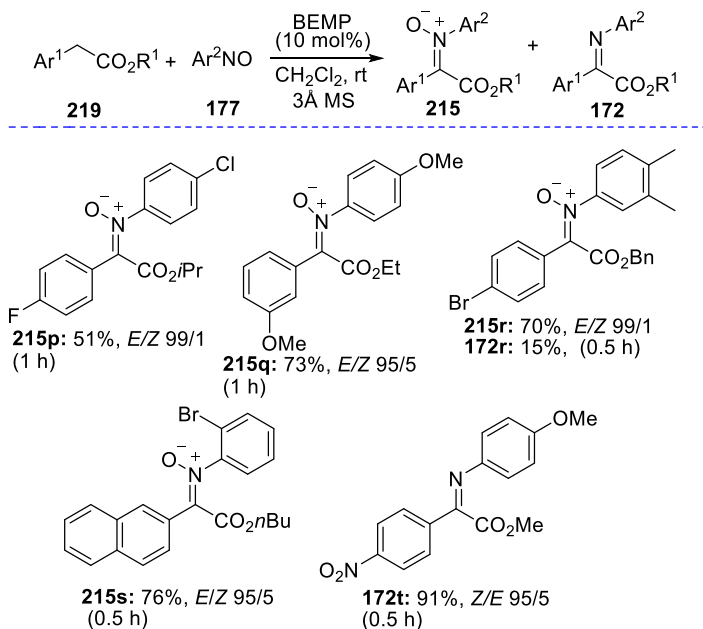
[a] Unless otherwise noted reactions were conducted with **219** (0.4 mmol), **177a** (1.2 mmol), BEMP (0.04 mmol), 3Å MS (~100 mg) in 2 mL of anhydrous dichloromethane under nitrogen atmosphere. Isolated yields after column chromatography are reported. [b] After chromatography azoxybenzene was recovered in similar amounts as nitrone.



On the contrary, electron-poor aromatic rings, bearing the nitro and CF<sub>3</sub> groups, afforded the corresponding imines in high yield and with excellent diastereoselectivity (**172e-f**). Finally, the 3,4-dichloro phenylacetate (**219l**) and 2-thiophenyl acetate (**219n**) proved to be unselective, affording nitrones and imines in comparable yields, albeit excellent diastereoselectivities for both products were recorded. Heteroaromatic moieties, such as thiophene and *N*-Boc-3-indole were well tolerated (**219n-o**).

These results have been rationalized through theoretical calculations, as clarified in section 7.2.3. Briefly, it would appear that the acidities of both  $\alpha$ -proton and NOH group of the nitrosoaldolate intermediate affect the outcome of the reaction.

Variouly substituted nitrosoarenes and different esters were then investigated (Table 7.5). Electron-donating and withdrawing substituents in the aromatic ring of nitroso compounds as well as a variety of esters moiety proved to be applicable. The corresponding nitrones were isolated in good yield, while excellent levels of diastereoselectivity were recorded in all cases (**215p-s**). When a bulkier *i*-propyl ester was used, a lower conversion to nitrone was observed (**215p**). Finally, the type of substitution on nitrosoarene significantly influenced the reactivity. For example, imine **172t** was isolated in higher yield, if compared with reaction between *p*-nitro ester **219e** and model nitrosobenzene **177a** (Table 7.4, product **172e**), when a *p*-methoxy substituted nitroso compound was used (**172t**).

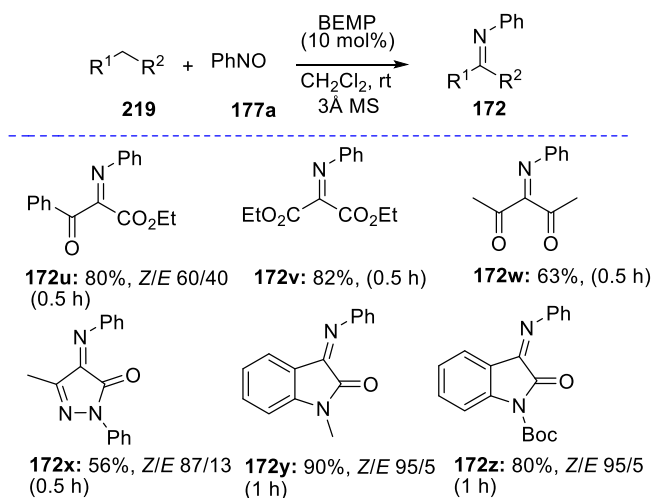
**Table 7.5** Ester and nitrosoarene scope.<sup>[a,b]</sup>

<sup>[a]</sup> Unless otherwise noted reactions were conducted with **219** (0.4 mmol), **177** (1.2 mmol), BEMP (0.04 mmol), 3Å MS (~100 mg) in 2 mL of anhydrous dichloromethane under nitrogen atmosphere. Isolated yields after column chromatography are reported. <sup>[b]</sup> After chromatography azoxyarene was recovered in similar amounts as nitron.

Finally, commercially available carbonyl compounds, ketones, and *N*-protected-2-oxindoles were reacted with model **177a**, under the optimized reaction conditions and the results are summarized in Table 7.6. Being more acidic compounds, we expected they should afford imines as the exclusive products. Indeed, 1,3-dicarbonyl compounds afforded the corresponding imines in good to high yield (**172u-v**). Commercially available 1-phenyl-3-methyl-2-pyrazolin-5-one gave access to the corresponding imine in good yield, but with moderate diastereoselectivity (**172x**). Both 2-oxindole derivatives, protected at nitrogen atom, proved to be suitable starting materials

for the synthesis of the corresponding imines, which were formed in high yield and with excellent stereocontrol (**172y** and **172z**). Hence, this catalytic system can be used as a mild, rapid and highly selective system to prepare imines, competitive to the complementary and common approach, based on isatins and anilines reacted under refluxing conditions.<sup>161</sup>

**Table 7.6** Substrate scope with 1,3-dicarbonyls and ketones.<sup>[a]</sup>



<sup>[a]</sup> Unless otherwise noted reactions were conducted with **219** (0.4 mmol), **177a** (1.2 mmol), BEMP (0.04 mmol), 3Å MS (~100 mg) in 2 mL of anhydrous dichloromethane under nitrogen atmosphere. Isolated yields after column chromatography are reported.

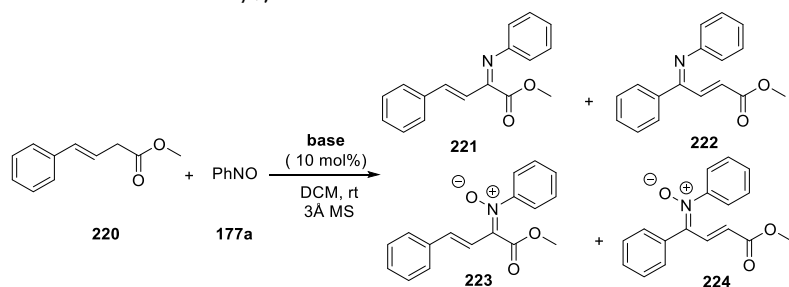
Unfortunately, our catalytic system was not effective when applied to  $\beta,\gamma$ -unsaturated esters **220** (Table 7.7). In this case, the formation of four products was observed using either BEMP or TDB as bases. Unsaturated imino esters **221** and **222** derive from the reactivity at  $\alpha$  and  $\gamma$  carbon of ester **220** respectively, whereas products **223** and **224**

<sup>161</sup> A. S. Smirnov, L. M. D. R. S. Martins, D. N. Nikolaev, R. A. Manzhos, V. V. Gurzhiy, A. G. Krivenko, K. O. Nikolaenko, A. V. Belyakov, A. V. Garabadzhiua, P. B. Davidovich, *New J. Chem.* **2019**, 43, 188.

represent regioisomers of the nitrone. Moreover *E* and *Z* stereoisomers can be observed for each compound. Unfortunately, the scarce control on the product-selectivity, regio- and stereochemistry, prevents any application of this system to prepare imines or nitrones for this class of compounds.

Firstly, BEMP was checked in the reaction of unsaturated ester **220** with nitrosobenzene **177a**, under the previously optimized reaction conditions (Table 7.7, es. 1). In this case  $\alpha$ - and  $\gamma$ -nitrone **223** and **224** were obtained in similar ratio. A less pronounced amount of imines was observed. They showed some instability on silica gel and were isolated as an inseparable mixture of the regioisomeric **221** and **222**. Unluckily, the bifunctional base TBD, was not effective in the reaction, affording all four possible products in similar ratio (es. 2).

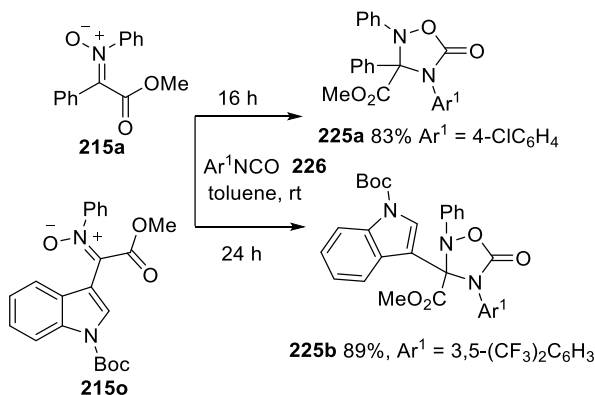
**Table 7.7** Reaction of  $\beta,\gamma$ -unsaturated esters with nitrosobenzene.<sup>[a,b]</sup>



Es.	base	<i>t</i> [h]	Yield	Yield <b>223</b>	Yield <b>224</b>	$\alpha/\gamma$ <sup>[e]</sup>
			<b>221-222</b> [%] <sup>[c,d]</sup>	[%] <sup>[c]</sup>	[%] <sup>[c]</sup>	
1	BEMP	1	20	36	39	48/52
2	TBD	1	27	36	25	60/40

<sup>[a]</sup> Unless otherwise noted reactions were conducted with **220** (0.2 mmol), **177a** (0.6 mmol), base (0.02 mmol), 3Å MS (~100 mg) in 1 mL of anhydrous dichloromethane under nitrogen atmosphere. <sup>[b]</sup> After chromatography azoxybenzene was recovered in similar amounts as nitrone. <sup>[c]</sup> Isolated yields. <sup>[d]</sup> Instable on silica gel. Isolated as inseparable mixture of the two regioisomers. <sup>[e]</sup>  $\alpha/\gamma$  ratio refers to nitrones.

Finally, ketonitrones **215** proved to be useful starting materials for the synthesis of 2,3,4-triarylsubstituted 1,2,4-oxadiazole-5-ones **225**. They were recently found to act as cytotoxic agents for the MCF-7 human breast cancer cell line.<sup>162</sup> These compounds, bearing a quaternary stereocenter, were regioselectively formed through 1,3-dipolar cycloaddition of representative ketonitrones **215a** and **215o** with arylisocyanates **226** (Scheme 7.8).



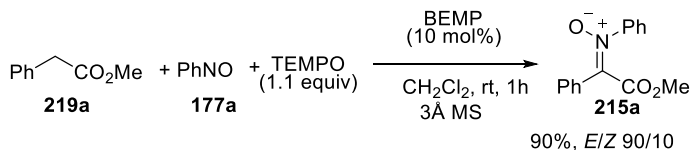
**Scheme 7.8** 1,3-Dipolar cycloaddition of ketonitrones and arylisocyanates.

### 7.2.1 Mechanistic investigations

With the aim of clarifying the mechanism of the reaction, some targeted experiments were then carried out. The model reaction of methyl phenylacetate **219a** and nitrosobenzene **177a** (Table 7.3, es. 3) was conducted in the presence of 1.1 equivalents of the radical scavenger TEMPO (Scheme 7.9). The reaction was not affected by the presence of TEMPO, since product **215a** was recovered in 90% yield and 90/10 *E/Z* ratio after 1 hour. This experiment confirmed

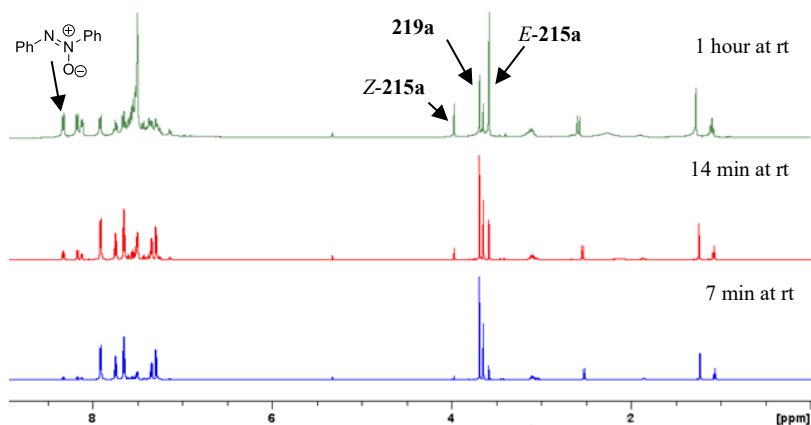
<sup>162</sup> M. A. Chiacchio, L. Legnani, A. Campisi, P. Bottino, G. Lanza, D. Iannazzo, L. Veltri, S. Giofrè, R. Romeo, *Org. Biomol. Chem.* **2019**, *17*, 4892.

that radical species are not involved in the reaction.



**Scheme 7.9** Model reaction in the presence of the radical scavenger TEMPO.

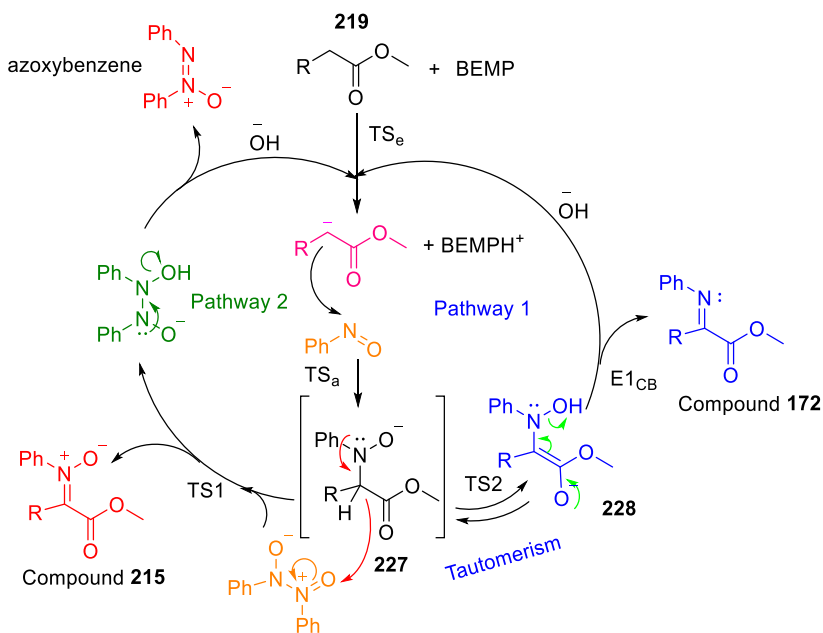
Moreover, model reaction (Table 7.3, es. 3) was monitored in deuterated dichloromethane via  $^1\text{H-NMR}$  over time (Figure 7.3).



**Figure 7.3** Monitoring of the model reaction in  $\text{CD}_2\text{Cl}_2$  via  $^1\text{H-NMR}$  over time.

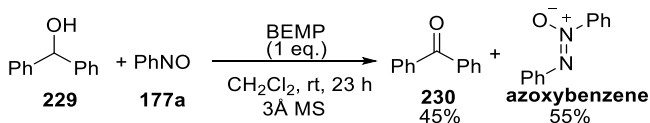
Product **215a** is rapidly formed, as demonstrated by the immediate formation of the corresponding peaks of methoxy group, at 3.59 ppm for the *E*-isomer and at 3.98 ppm for the *Z*-isomer, after 7 minutes. The gradual decrease of the intensity of the peak at 3.69 ppm, corresponding to the methoxy group of methyl phenylacetate **219a** indicates its gradual consumption as the reaction proceeds. At the same time the gradual increase of the intensity of the peak at 8.36 ppm, corresponding to the azoxybenzene, is observed.

According to experimental data, literature precedents and our previous report<sup>136</sup> we suggest a mechanistic pathway for the reaction of arylacetic esters and nitrosobenzene catalyzed by BEMP (Scheme 7.10). At the beginning of the reaction, BEMP deprotonates the ester **219** and the resulting enolate subsequently adds to nitrosobenzene to afford intermediate **227** in 10 mol% ratio. At this stage two different reaction pathways can be involved. When tautomerism, promoted by a base, takes place to yield the nitrosoenolate **228**, an E1<sub>CB</sub> elimination allows the formation of imine **172**. On the other side, the excess of nitrosobenzene can oxidize the nitrosoaldol to product **215** with the simultaneous formation of azoxybenzene. In both branches of the catalytic cycle an equivalent of hydroxyl anion OH<sup>-</sup> is generated, sustaining the catalytic cycle by deprotonating the starting ester **219**. Therefore the roles of BEMP and BEMPH<sup>+</sup> are just to trigger the formation of ester enolate at the early reaction stage, to coordinate anionic species within the catalytic cycle and to act as hydrogen bonding donor when feasible. The illustrated mechanism requires the formation of similar amounts of azoxybenzene and product **215**, as confirmed by experimental data.



**Scheme 7.10** Proposed catalytic cycle for the nitrone/imine formation.

The ability of nitrosobenzene to accept a hydride anion, thus acting as oxidizing agent, has been previously documented either under acidic or basic conditions.<sup>163</sup> In order to demonstrate the feasibility of hydride transfer under our reaction conditions, diphenyl carbinol **229** was treated with an excess of nitrosobenzene and an equimolar amount of the base in dichloromethane at room temperature (Scheme 7.11).



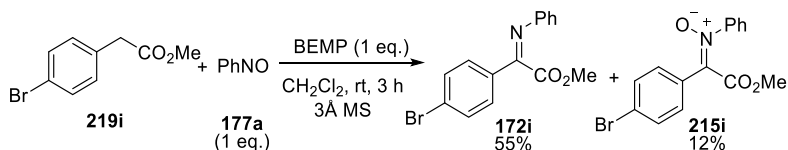
**Scheme 7.11** Oxidation of diphenyl carbinol by BEMP/PhNO system.

<sup>163</sup> a) H. Awano, T. Hirabayashi, W. Tagaki, *Tetrahedron Lett.* **1984**, 25, 2005; b) L. M. Ferreira, H. T. Chaves, A. M. Lobo, S. Prabhakar, H. S. Rzepa, *J. Chem. Soc. Chem. Commun.* **1993**, 133.



Under these conditions, the formation of benzophenone **230** was observed in 45% yield, thus supporting the occurrence of hydride migration by intermediate **227** to nitrosobenzene, which acts as hydride acceptor such as DDQ and DQ.<sup>164</sup>

Finally, we proved that by varying the reaction conditions, the reaction pathway can be reversed and the preferential formation of the imine instead of nitrone can be thus achieved. For example, *p*-bromo ester **219i**, which afforded nitrone **215i** with high selectivity under the usual reaction conditions (Table 7.4), can be driven toward the formation of the corresponding imine (Scheme 7.12).

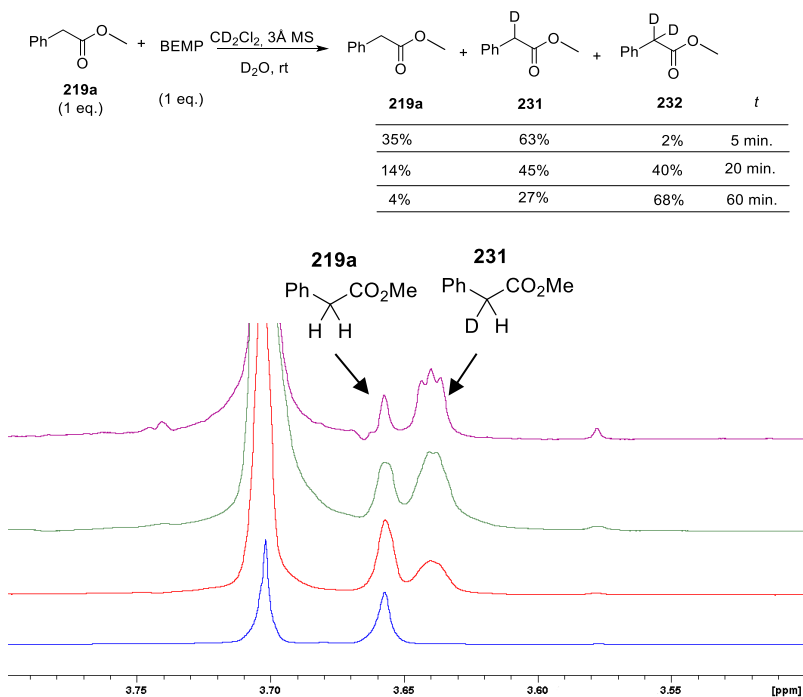


**Scheme 7.12** Reversal of reaction pathway toward the formation of imine.

In this regard, 1 equivalent of the base was slowly added to ester **219i**, followed by a one hour addition of a solution of nitrosobenzene **177a** at room temperature. In this case, the low concentration of free nitrosobenzene, together with a significant presence of the ester enolate in the reaction mixture forced the reaction pathway toward the formation of imine. Under these conditions, imine **172i** was found to be the prevalent product and was isolated in 55% yield, while only 12% of nitrone **215i** was recovered at the end of the reaction.

<sup>164</sup> a) A. E. Wendlandt, S. S. Stahl, *Angew. Chem. Int. Ed.* **2015**, *54*, 14638-14658; *Angew. Chem.* **2015**, *127*, 14848; b) S. De Sarkar, S. Grimme, A. Studer, *J. Am. Chem. Soc.* **2010**, *132*, 1190; c) M. S. Kharasch, B. S. Joshi, *J. Org. Chem.* **1957**, *22*, 1439; d) X. Li, Y. Wang, Y. Wang, M. Tang, L-B Qu, Z. Li, D. Wie, *J. Org. Chem.* **2018**, *83*, 8543.

The effectiveness of BEMP and hydroxyl anion (in the form of  $\text{BEMPH}^+\text{OH}^-$ ) in the deprotonation of model ester **219a** for the formation of the corresponding enolate was verified through  $^1\text{H}$ -NMR analysis in  $\text{CD}_2\text{Cl}_2$  at room temperature. The reaction between an equimolar amount of **219a** and BEMP was quenched after 30 minutes by adding an excess of deuterium oxide and the determination of  $\alpha$ -monodeuterated and  $\alpha,\alpha$ -dideuterated esters was examined over time. As shown in Scheme 7.13, the deuteration at the  $\alpha$  position continued even after the  $\text{D}_2\text{O}$  quenching. The formation of monodeuterated product **231** is rapidly observed, as demonstrated by the immediate formation of the triplet of CHD at 3.64 ppm after 5 minutes. The gradual decrease of the intensity of the singlet of methylene protons of ester **219a** at 3.66 ppm and the simultaneous increase of the triplet at 3.64 ppm, highlights the gradual consumption of model methyl phenylacetate as the reaction proceeds. The percentages of **219a**, **231** and **232** were estimated by integration and normalization and are reported below.



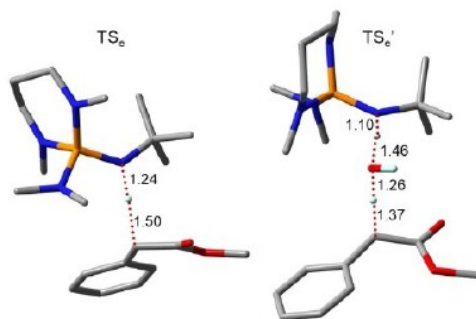
**Scheme 7.13** Monitoring of the deuteration reaction of **219a** in  $\text{CD}_2\text{Cl}_2$  via  $^1\text{H}$ -NMR over time.

### 7.2.3 Theoretical studies

A theoretical study of the catalytic cycle was performed, in collaboration with Prof. Mazzanti and Dr. Mancinelli from University of Bologna, by using DFT calculations (B3LYP/6-31G(d)), using methyl phenylacetate **219a** as the model compound. When localized, the stationary points were further optimized using M06-2X/6-311+G(d,p) DFT level.

At the beginning of the reaction, BEMP removes one of the  $\alpha$ -hydrogen from the starting ester **219a** to yield the corresponding

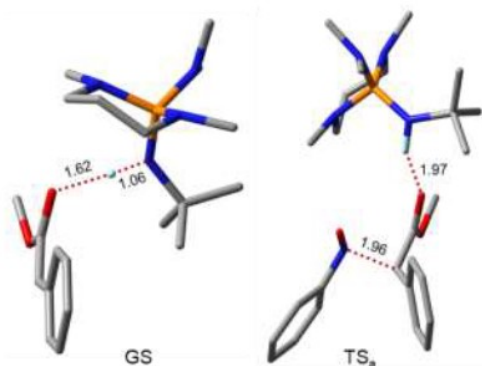
enolate.<sup>165</sup> With respect to the reagents, the activation energy for TS<sub>e</sub> is 19.0 kcal/mol (Figure 7.4, left). However, this TS is valid only in the first reaction stage, when the neutral BEMP is present. The enolization of the starting reagent has to be subsequently carried on by the OH<sup>-</sup> that is generated by both the branches of the proposed catalytic cycle (see Scheme 7.10, left). Being the presence of free and unsolvated OH<sup>-</sup> in dichloromethane not realistic, the ionic pair BEMPH<sup>+</sup>OH<sup>-</sup> was considered as the effective base for enolization. Thus, a second TS geometry was built with these requisites (TS<sub>e</sub>' , right in Figure 7.4) and after optimization it showed a calculated energy of 27.8 kcal/mol. After the formation of the enolate, the addition to nitrosobenzene yields intermediate **227a**.



**Figure 7.4.** TS<sub>e</sub> geometry for enolization of **219a** promoted by BEMP (left) and by BEMPH<sup>+</sup>OH<sup>-</sup> (TS<sub>e</sub>' ). Only the relevant hydrogens are shown. Distances in Å.

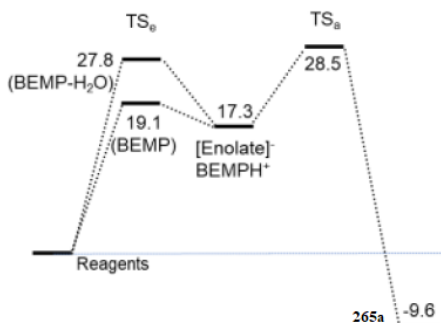
The optimized TS<sub>a</sub> geometry shows that BEMPH<sup>+</sup> is positioned between the two oxygen atoms and the calculated activation energy was 28.5 kcal/mol (Figure 7.5).

<sup>165</sup> I. Kaljurand, I. A. Koppel, A. Kütt, E.-I. Rööm, T. Rodima, I. Koppel, M. Mishima, I. Leito, *J. Phys. Chem. A* **2007**, *111*, 1245.



**Figure 7.5.** Left: GS geometry of the enolate complex of **219a** with BEMPH<sup>+</sup>. Right: TS<sub>a</sub> geometry for addition of the same enolate to nitrosobenzene. Only the relevant hydrogens are shown. Distances in Å.

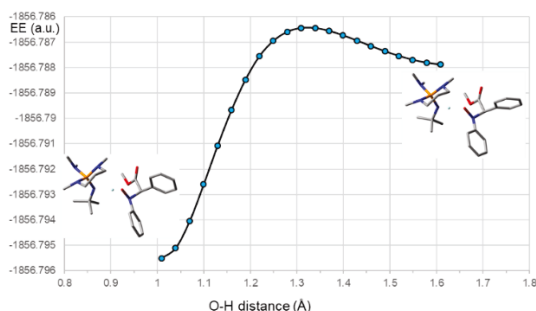
After the addition step, the formation of nitrosoaldol intermediate **227a** was observed and it showed a relative energy as low as -9.6 kcal/mol with respect to the reagents (Figure 7.6).



**Figure 7.6.** First section of the catalytic pathway for compound **219a**. Energies in kcal/mol at the M06-2X/6-311+G(d,p) level.

Since the NMR monitoring of the reaction (Figure 7.3) did not show the presence of intermediates, either the first enolization step with BEMPH<sup>+</sup>OH<sup>-</sup> or the subsequent addition to PhNO represent the

kinetically relevant TS for the whole reaction. The eventual enolate addition to the dimer of nitrosobenzene<sup>166</sup> was excluded since, the calculation of the electrophilicity index  $\omega$  as proposed by Parr,<sup>167</sup> allowed to find that the monomer had  $\omega = 1.99$  eV, whereas the dimer had  $\omega = 1.55$  eV (M06-2X/6-311+G(d,p) level). Thus, the nucleophilic attack of the enolate to the nitrosobenzene monomer is significantly favored. After the addition to nitrosobenzene, intermediate **227a** could exist in ionic pair with BEMPH<sup>+</sup> or as a nitrosoaldol/BEMP complex. The latter situation was found to be more stable by 5.2 kcal/mol. Moreover, the TS involved in the hydrogen shift from the nitrogen of BEMP to the oxygen of the nitrosoaldolate is very small, amounting to 3.0 kcal/mol starting from the ionic pair (Figure 7.7). Thus, the two forms can easily exchange into each other.

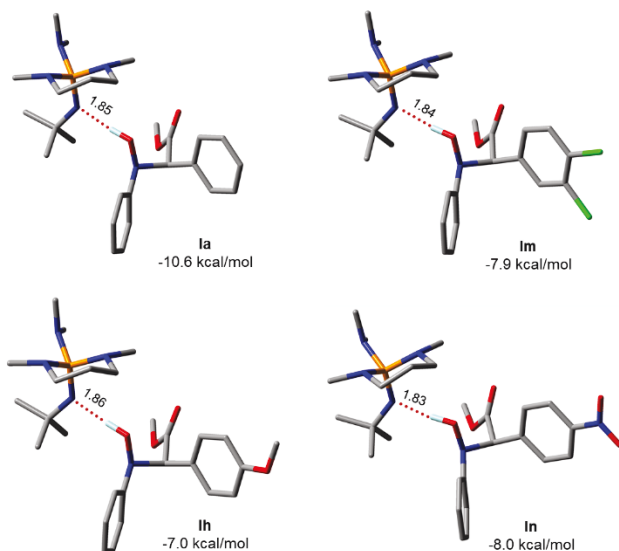


**Figure 7.7.** Energy profile for the hydrogen shift within intermediate **227a**, from oxygen (left side) to the nitrogen of BEMP (right). The relaxed scan was run by moving the hydrogen far from oxygen by 0.03 Å each step. Calculation were run at the PCM-B3LYP/6-31G(d) level using dichloromethane as the solvent.

<sup>166</sup> a) D. Beaudoin, J. D. Wuest. *Chem. Rev.* **2016**, *116*, 258; b) A. J. Fraboni, A. E. Brenner-Moyer, *Org. Lett.* **2016**, *18*, 2146.

<sup>167</sup> a) P. K. Chattaraj, U. Sarkar, D. R. Roy, *Chem. Rev.* **2006**, *106*, 2065; b) R. G. Parr, L. v. Szentpály, S. Liu, *J. Am. Chem. Soc.* **1999**, *121*, 1922.

DFT optimization of intermediate **227** with three selected substituents (4-NO<sub>2</sub>C<sub>6</sub>H<sub>4 **227e**, 4-MeOC<sub>6</sub>H<sub>4 **227c** and 3,4-Cl<sub>2</sub>C<sub>6</sub>H<sub>3 **227l**) showed very close energy profiles leading to the formation of intermediate **227** (Figure 7.8).</sub></sub></sub>



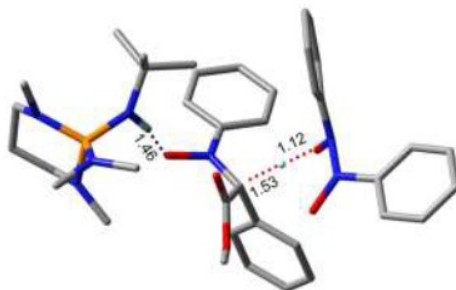
**Figure 7.8.** Optimized geometries for intermediates **227**, at the M062X/6-311+G(d,p)//B3LYP/6-31G(d) level. Reported energies are relative to the starting reagents (esters, BEMP and PhNO). Distances in Å. For clarity, only the relevant hydrogens are shown.

### 7.2.3.1 Oxidative pathway to nitrone **215**

Oxidation of the nitrosoaldolate to product **219a** can be conducted by the PhNO or by the dimer (PhNO)<sub>2</sub>, both present in the reaction mixture. First of all, the hydrogen shift to form the nitrosoaldolate/BEMPH<sup>+</sup> ionic pair has to take place, followed by the hydride abstraction.<sup>168</sup> The formed phenyl hydroxylamine anion then

<sup>168</sup> V. S. Batista, R. H. Crabtree, S. J. Konezny, O. R. Luca, J. M. Praetorius, *New. J. Chem.* **2012**, *36*, 1141.

adds to the excess of nitrosobenzene in the reaction mixture with the subsequent formation of azoxybenzene and  $\text{BEMPH}^+\text{OH}^-$ . Azoxybenzene was in fact always found in similar amounts as nitrone **215a**. Similarly, to the enolate addition step, oxidation could also be performed by the dimer of nitrosobenzene. In this case, the dehydrogenative step affords the anionic intermediate of nitrosobenzene dimer, that is finally converted to azoxybenzene thanks to the elimination of the hydroxyl anion. The optimized  $\text{TS}_1$  geometry (Figure 7.9) for the reaction with dimeric nitrosobenzene dimer is lower in energy by 8.9 kcal/mol.

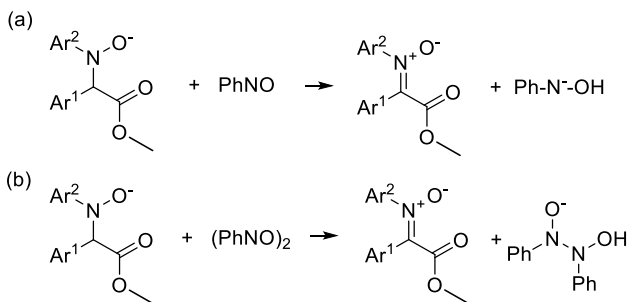


**Figure 7.9.**  $\text{TS}_1$  geometry for hydride removal from **219a** by means of  $(\text{PhNO})_2$ . Only the relevant hydrogens are shown. Distances in Å

The relative hydride affinity<sup>169</sup> of  $\text{PhNO}$  and  $(\text{PhNO})_2$  was evaluated using two isodesmic reactions with the nitrosoaldolate, that ultimately leads to a direct comparison between nitrosobenzene monomer and dimer hydride affinity (Scheme 7.14).

<sup>169</sup> X.-Q. Zhu, C.-H. Wang, *J. Phys. Chem. A* **2010**, *114*, 13244.





Calculations: SMD-B3LYP/6-311++G(d,p)

	H° (a.u.)
Nitrosoaldolate <b>227a</b>	-860.477738
Nitronium <b>215a</b>	-859.767235
PhNO	-361.547418
(PhNO) <sub>2</sub>	-723.097580
Ph-N <sup>+</sup> -OH	-362.264251
Ph-N(OH)-N(O <sup>-</sup> )-Ph	-723.823589

Reaction (a)  $\Delta H^\circ = -0.00633$  a.u. = -3.97 kcal/mol

Reaction (b)  $\Delta H^\circ = -0.01551$  a.u. = -9.74 kcal/mol

**Scheme 7.14** Isodesmic reactions for the evaluation of the hydride affinity of the monomer and dimer of nitrosobenzene.

It was found that dimeric form of nitrosobenzene was a better oxidant when compared to the monomer. When compared to intermediate **227a**, TS<sub>1</sub> has an activation energy of 29.1 kcal/mol, whereas the energy related to the starting reagents is 19.5 kcal/mol. The data are in agreement with the experimental absence of intermediates in the reaction.

### 7.2.3.2 Pathway to imine **172**

Two different mechanisms could potentially occur for the reaction pathway from nitrosoaldol to imine **172a**, that is an E2 or

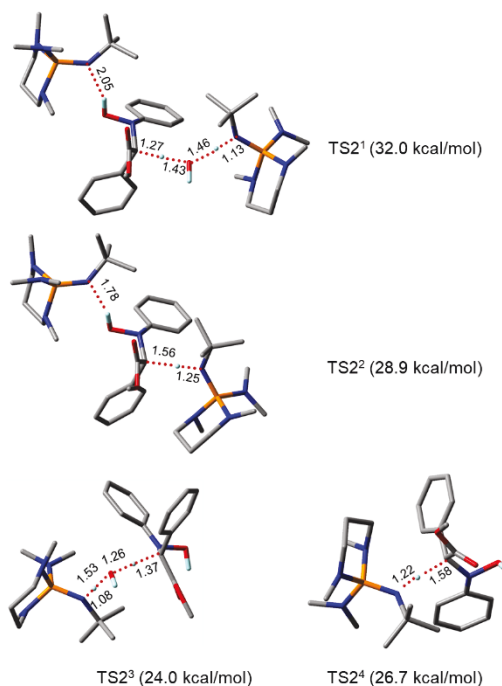
tautomerism/E1cB mechanism.<sup>170</sup> However, since the nitrosoaldol bears a poor leaving group and the carbanion is highly stabilized in non-protic solvents, the E1cB elimination pathway should be preferred. Moreover, the *anti*-stereoselectivity of the final products **172** can also be explained through an E1cB mechanism.<sup>171</sup> The reaction pathway to imine **172a** requires the formation of nitrosoenolate **228a** (Scheme 7.10, right). This first step can occur with different mechanisms. Nitrosoaldol **227a** can be converted to the nitrosoenolate **228a** thanks to the action of the bases present in the reaction mixture, namely the free BEMP and BEMPH<sup>+</sup>OH<sup>-</sup>. Two TS structures were identified and optimized starting from the BEMP-coordinated nitrosoaldol **228** (TS2<sup>1</sup> in and TS2<sup>2</sup> in Figure 7.10).<sup>172</sup> Because of the steric hindrance of BEMP it was found that the TS2<sup>1</sup>, where BEMPH<sup>+</sup>OH<sup>-</sup> removes H<sub>α</sub> from the nitrosoaldol/BEMP complex **227a**, was less stable than the corresponding TS2<sup>2</sup>, where the free BEMP acts as base. In both cases, the hydrogen atom of the nitrosoaldol is bonded to the oxygen, while BEMP is in neutral form.

---

<sup>170</sup> D. E. Ortega, R. Ormazábal-Toledo, R. Contreras, R.A. Matute, *Org. Biomol. Chem.* **2019**, *17*, 9874.

<sup>171</sup> J. R. Mohrig, B. G. Beyer, A. S. Fleischhacker, A. J. Ruthenburg, S. G. John, D. A. Snyder, P. T. Nyffeler, R. J. Noll, N. D. Penner, L. A. Phillips, H. L. S. Hurley, J. S. Jacobs, C. Treitel, T. L. James, M. P. Montgomery, *J. Org. Chem.* **2012**, *77*, 2819.

<sup>172</sup> a) H. Awano, T. Hirabayashi, W. Tagaki, *Tetrahedron Lett.* **1984**, *25*, 2005; b) L. M. Ferreira, H. T. Chaves, A. M. Lobo, S. Prabhakar, H. S. Rzepa, *J. Chem. Soc. Chem. Commun.* **1993**, 133.



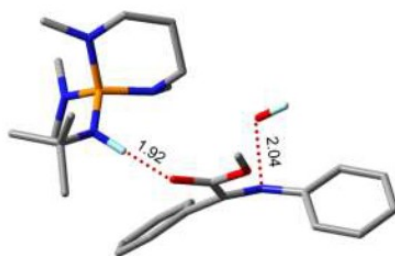
**Figure 7.10.** 3D geometries of the four TS2 related to the tautomerism from **227a** to **228a** (M06-2X/6-311+G(d,p) level). Distances in Å, energies in kcal/mol. For clarity, only the relevant hydrogens are shown.

Two more TS geometries should be therefore considered starting from the free nitrosoaldol and using BEMPH<sup>+</sup>OH<sup>-</sup> or BEMP as the base (TS2<sup>3</sup> and TS2<sup>4</sup> in Figure 7.10). In the TS geometry, the forming enolate is stabilized by intramolecular hydrogen bond of the carbonyl with the N-OH. Among the optimized TS2 geometries, the lowest energy was found for the deprotonation of the free nitrosoaldol by the action of BEMPH<sup>+</sup>OH<sup>-</sup> (TS2<sup>3</sup> in Figure 7.10), with an activation energy of 22.4 kcal/mol (vs the free nitrosoaldol). However, considering the 1.6 kcal/mol required to get the free nitrosoaldol

from complex **227a**, the overall energy of TS<sup>2</sup> with respect to intermediate **227a** is 24.0 kcal/mol.

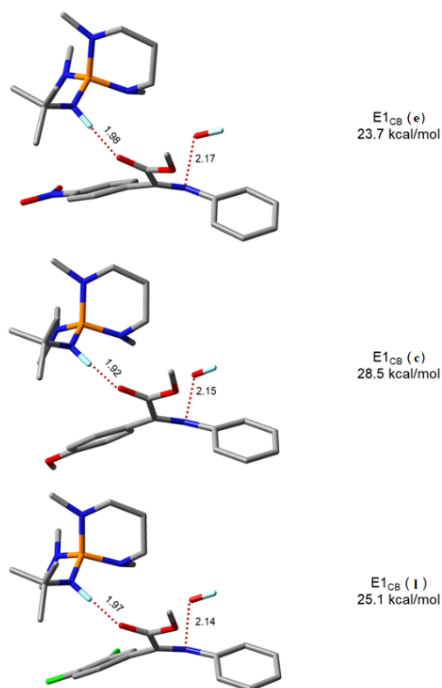
### 7.2.3.3 E1cB

The last reaction step to form imine **172** involves the E1cB elimination. The TS for the elimination step was optimized (Figure 7.11) and the calculated activation energy for compound **228a** was found to be 28.9 kcal/mol.



**Figure 7.11.** E1cB TS geometry leading to imine **172a** from nitrosoenolate **228a**. Only the relevant hydrogens are shown. Distances in Å.

According to the calculations, the pathways to nitrone **215** and imine **172** show very similar energies. Hence, the substituents on the aromatic ring of the ester play a key role in driving the reaction pathway towards the nitrone or the imine, because of the different electronic contribution to the stabilization of the negative charge of the enolate (this contribution is also dependent on the acidity of H $\alpha$ , see section 7.2.3.4). For this reason, the two TS geometries were optimized for three selected compounds, 4-NO<sub>2</sub>C<sub>6</sub>H<sub>4</sub> **e**, 4-MeOC<sub>6</sub>H<sub>4</sub> **c** and 3,4-Cl<sub>2</sub>C<sub>6</sub>H<sub>3</sub> **l** (Figure 7.12).



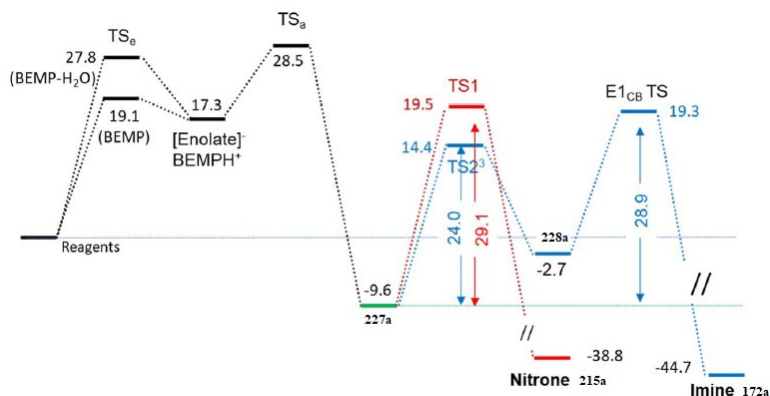
**Figure 7.12.** The three E1<sub>c</sub>B TS geometries for compounds **c**, **e**, **i**. Distances in Å. For clarity, only the relevant hydrogens are shown. Energies in kcal/mol at the M06-2X/6-311+G(d,p)//B3LYP/6-31G(d) level.

Compound **i**, which gives both nitrone **215i** and imine **172i** in similar ratio, was used as a “reference standard” to normalize the other values, in order to reduce systematic errors in the calculations. The experimental trend is in agreement with the calculations. The formation of nitrone is favoured for the *p*-methoxy substituted ester **219c**, while the formation of imine is favoured with the *p*-nitro compound **219e**. Compound **219i** is in the middle (Table 7.8).

**Table 7.8** Summary of kinetic preference for nitrone **215** or imine **172** by comparison of TS1 and E1cB TS. Energy values in kcal/mol (energy values in kcal/mol at the M06-2X/6-311+G(d,p)//B3LYP/6-31G(d) level).

Compound	Ar <sup>1</sup>	E1 <sub>CB</sub> -TS1 ( $\Delta\Delta G^\ddagger$ )	Norm. $\Delta\Delta G^\ddagger$
<b>219e</b>	4-NO <sub>2</sub> C <sub>6</sub> H <sub>4</sub>	-3.8	-3.1
<b>219l</b>	3,4-Cl <sub>2</sub> C <sub>6</sub> H <sub>3</sub>	-0.7	<b>0.0</b>
<b>219c</b>	4-MeOC <sub>6</sub> H <sub>4</sub>	+1.3	2.0

In Figure 7.13 are summarized the energies involved in the whole catalytic cycle.

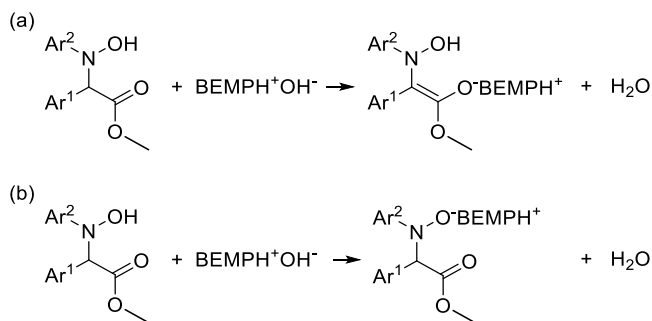


**Figure 7.13.** Full energy profile for the catalytic cycle for compound **a**. Relative energies in kcal/mol.

### 7.2.3.4 Thermodynamic approach

Previous results reveal that the acidity of the two active hydrogens of the nitrosoaldol **227** is a key factor for the selection of the preferred reaction pathway. When the N-OH is more acidic, the equilibrium with BEMP is shifted toward the ionic pair, which means that the  $\alpha$ -hydrogen is less acidic and then less prone to be removed by the bases present in the reaction mixture. In this case the oxidative pathway is preferred and the formation of nitrone **215** is observed.

When the N-OH is less acidic, the equilibrium is shifted toward the neutral aldol coordinated with BEMP. Then the  $H_\alpha$  is more acidic, thus stabilizing the intermediate **228** and the E1cB pathway is preferred. From the thermodynamic point of view, the relative acidities of  $H_\alpha$  and N-OH can be calculated by comparison of the two isodesmic reactions, illustrated in Scheme 7.15, yielding the  $\Delta pK_a$  between the two acidic hydrogens.



**Scheme 7.15** Isodesmic reactions for the calculation of the relative acidity of N-OH and  $H_\alpha$ .

Both reactions start with the same reagents, so the  $\Delta\Delta G$  for the two different pathways, which is related to the  $\Delta pK_a$ , can be determined by the calculation of the relative energies of the nitrosoaldolate and the enolate anion coordinated with BEMPH<sup>+</sup>. The  $\Delta pK_a$  can be then calculated from the following equation (1):

$$\Delta pK_a = (G_{\text{enolate}} - G_{\text{NO}^-})/RT\ln 10 \quad (1)$$

A negative value of  $\Delta pK_a$  indicates that  $H_\alpha$  is more acidic than the N-OH, thus the base affords the enolate preferentially. On the other hand, a positive value indicates the higher acidity of N-OH with respect to  $\alpha$ -hydrogen, so the base yields the nitrosoaldolate.

It was found that  $H_\alpha$  was more acidic than N-OH in three cases, that

is when the ester contains a strongly deactivated aromatic ring (Table 7.9, compounds **219e**, **219f** and **219l**). Pleasingly, for that compounds where the calculated  $\Delta pK_a$  difference is very close to zero, imine and nitron were experimentally yielded in similiar amounts (Table 7.9, compounds **219l** and **219n**).

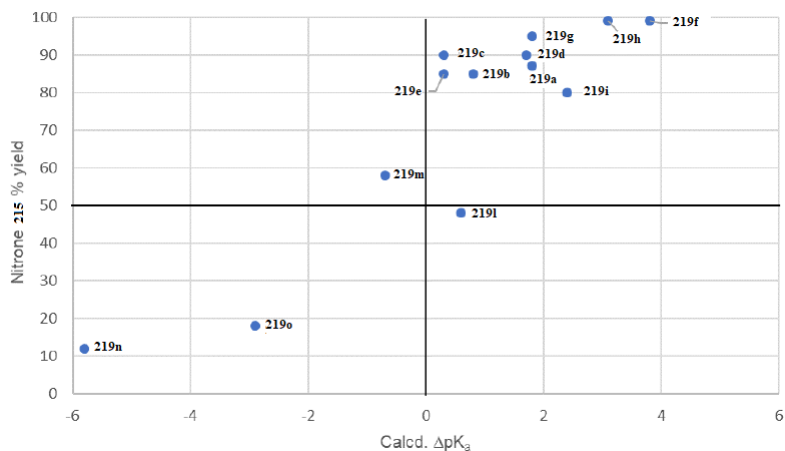
**Table 7.9** Summary of results for the  $pK_a$  calculations of **227** and **228**. Calculations at the PCM-B3LYP/6-31+G(d,p) level. Energy values in kcal/mol.

Compound	Ar <sup>1</sup>	$\Delta\Delta H$	$\Delta pK_a$	Nitron <b>215</b> [%]	Imine <b>172</b> [%]
<b>219k</b>	2-FC <sub>6</sub> H <sub>4</sub>	+5.15	+3.8	99	0
<b>219c</b>	4-MeOC <sub>6</sub> H <sub>4</sub>	+4.28	+3.1	53 <sup>a</sup>	0
<b>219d</b>	4-MeC <sub>6</sub> H <sub>4</sub>	+3.31	+2.4	80	0
<b>219a</b>	C <sub>6</sub> H <sub>5</sub>	+2.46	+1.8	87	5
<b>219b</b>	3-MeOC <sub>6</sub> H <sub>4</sub>	+2.40	+1.8	95	4
<b>219g</b>	4-FC <sub>6</sub> H <sub>4</sub>	+2.32	+1.7	90	4
<b>219h</b>	4-ClC <sub>6</sub> H <sub>4</sub>	+1.04	+0.8	85	6
<b>219n</b>	2-thiophenyl	+0.81	+0.6	48	33
<b>219i</b>	4-BrC <sub>6</sub> H <sub>4</sub>	+0.43 <sup>b</sup>	+0.3	90	8
<b>219j</b>	3-FC <sub>6</sub> H <sub>4</sub>	+0.35	+0.3	85	10
<b>219l</b>	3,4-Cl <sub>2</sub> C <sub>6</sub> H <sub>3</sub>	-0.95	-0.7	58	40
<b>219f</b>	3,5-(CF <sub>3</sub> ) <sub>2</sub> C <sub>6</sub> H <sub>3</sub>	-3.98	-2.9	18	75
<b>219e</b>	4-NO <sub>2</sub> C <sub>6</sub> H <sub>4</sub>	-7.84	-5.8	12	84

<sup>[a]</sup> 42 % reagent recovered. <sup>[b]</sup> 6-311+G(d,p) basis set.

In Figure 7.14 is illustrated the relationship that exists between the calculated  $\Delta pK_a$  and the isolated yield of nitrones **215**. With this study, our previous results, concerning the selective  $\alpha$ -imination of acylpyrazoles, can be also rationalized.<sup>136</sup> In those cases, the presence of the pyrazole moiety enhances the acidity of the  $\alpha$ -protons, so that the E1cB pathway is always energetically preferred, likewise in the case of the 1,3-dicarbonyl compounds mentioned in this Chapter.





**Figure 7.14.** Relationship between calculated  $\Delta pK_a$  and experimental yield of nitrones **215**. Positive values of  $\Delta pK_a$  means that  $H_\alpha$  is less acidic than N-OH.

## CONCLUSIONS

In conclusion we have developed a practical and mild methodology to access ketonitrone by reacting readily available arylacetic acid esters and nitroso arenes under catalytic loading of a commercial base. These products were rapidly formed in good to high yield and diastereoselectivity. Moreover, they proved to be useful starting materials to selectively obtain novel, potentially bioactive 1,2,4-oxadiazole-5-ones, via 1,3-dipolar cycloaddition. The reaction was deeply investigated to highlight the mechanism. A switch in the product selectivity has been observed, depending on the substitution pattern in the aromatic moiety of the ester. DFT calculations allowed to reproduce the whole catalytic cycle and to identify the addition of enolate to nitrosobenzene as the rate-determining step. Experimental results and DFT calculations suggested that the CH/NOH relative acidity, in the firstly formed nitroso aldol intermediate **227**, drives the reaction pathway toward nitrone or imine formation. The calculation of the relative acidity of N-OH and CH<sub>α</sub> shows the differences in the two competitive TS leading to nitrone or imine. The current methodology represents a useful way to access ketonitrone and functionalized imines, both reagents of common use in organic synthesis.

## 8. EXPERIMENTAL SECTION

### 8.1 General experimental conditions

#### General methods and material

All reactions requiring dry or inert conditions were conducted in flame-dried glassware under a positive pressure of nitrogen. Anhydrous THF, toluene, *m*-xylene, and methanol were purchased from Aldrich and used as received; all other solvents were dried over molecular sieves. Molecular sieves (Aldrich Molecular Sieves, 4 Å, 1.6 mm pellets) were activated under vacuum at 200 °C overnight. Reactions were monitored using thin layer chromatography (TLC) on Macherey–Nagel precoated silica gel plates (0.25 mm) and visualized by UV light, potassium permanganate and cerium sulfate staining solutions. Flash chromatography was performed on Merck silica gel (60, particle size: 0.040–0.063 mm). <sup>1</sup>H NMR and <sup>13</sup>C NMR spectra were recorded on a Bruker Avance III HD 600, Bruker Avance-400, Bruker Avance-300 or Bruker Avance-250 spectrometer in CDCl<sub>3</sub> or CD<sub>3</sub>OD as solvents at room temperature. Chemical shifts for protons are reported using residual solvent protons (<sup>1</sup>H NMR:  $\delta = 7.26$  ppm for CDCl<sub>3</sub>,  $\delta = 3.31$  ppm for CD<sub>3</sub>OD) as internal standard. Carbon spectra were referenced to the shift of the <sup>13</sup>C signal of CDCl<sub>3</sub> ( $\delta = 77.0$  ppm) or CD<sub>3</sub>OD ( $\delta = 49.0$  ppm). The following abbreviations are used to indicate the multiplicity in NMR spectra: s – singlet; d – doublet; t – triplet; q – quartet; dd – double doublet; m – multiplet; bs – broad signal. Optical rotation of compounds was performed on a Jasco P-2000 digital polarimeter using a WI (tungsten–halogen) lamp ( $\lambda = 589$  nm). High

resolution mass spectra (HRMS) were acquired using a Bruker solariX XR Fourier transform ion cyclotron resonance mass spectrometer (Bruker Daltonik GmbH, Bremen, Germany) equipped with a 7 T refrigerated actively shielded superconducting magnet. The samples were ionized in the positive ion mode using a MALDI ionization source. Melting points were measured with a Stuart Model SMP 30 melting point apparatus and are uncorrected. Petrol ether (PE) refers to light petroleum ether (boiling point 40-60 °C).

## 8.2 Catalytic enantioselective one-pot approach to cis- and trans-2,3-diaryl substituted 1,5-benzothiazepines

### Experimental procedures and compounds characterization

All starting materials (unless otherwise noted) were purchased from Aldrich and used as received. Enantiomeric excess of 1,5-benzothiazepines **127** and **138**, adducts **131a** and **135a** was determined using HPLC (Waters-Breeze 2487, UV dual  $\lambda$  absorbance detector and 1525 Binary HPLC Pump) using Daicel chiral columns. The absolute configuration of 1,5-benzothiazepines was determined using a hybrid NMR/ECD approach supported by DFT conformational analysis and TD-DFT calculation of ECD spectra of compound **127e**. Other configurations were assigned in analogy. Catalyst **96** was purchased from Strem Chemicals and used as received. Catalysts **71b-c**,<sup>173</sup> **25a-c**,<sup>174</sup> **83a-b**,<sup>175</sup> **132**,<sup>89</sup> and **133a**,<sup>90</sup>

---

<sup>173</sup> (a) W. Yang, D.-M. Du, *Org. Lett.* **2010**, *12*, 5450; (b) H. Y. Bae, S. Some, J. H. Lee, J.-Y. Kim, M. J. Song, S. Lee, Y. J. Zhang, C. E. Song, *Adv. Synth. Catal.* **2011**, *353*, 3196.

<sup>174</sup> B. Vakulya, S. Varga, A. Csámpai, T. Soós, *Org. Lett.* **2005**, *7*, 1967.

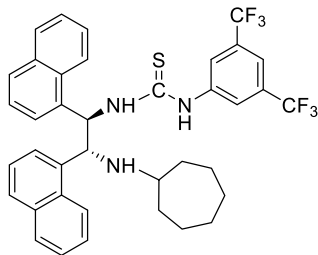
<sup>175</sup> (a) E. Sorrentino, S. J. Cannon, *Org. Lett.* **2016**, *18*, 5204; (b) R. Miyaji, K. Asano, S. Matsubara, *J. Am. Chem. Soc.* **2015**, *137*, 6766; (c) W. Wu, L. Min, L. Zhu, C.-S. Lee, *Adv. Synth. Catal.* **2011**, *353*, 1135; (d) R. Miyaji, K. Asano, S. Matsubara, *Org. Lett.* **2013**, *15*,

were prepared according to the literature. Alkenes **42** were prepared following general procedures reported in the literature.<sup>87</sup>

### Synthesis of catalyst **133b**

(1*S*,2*S*)-*N*<sup>1</sup>-cycloheptyl-1,2-di(naphthalen-1-yl)ethane-1,2-diamine (86 mg, 0.21 mmol), synthesized according to the literature,<sup>90</sup> was dissolved in anhydrous CH<sub>2</sub>Cl<sub>2</sub> (1 mL) in a flamed-dried two-necked round-bottom flask under a positive pressure of nitrogen. The solution was cooled to 0 °C and 3,5-bis(trifluoromethyl)phenyl isothiocyanate (38 μL, 0.21 mmol) was added via a syringe dropwise in 10 min. After ca. 1 h at 0 °C, the crude mixture was allowed to warm up gradually to room temperature. After reaction completion, as monitored using TLC (CHCl<sub>3</sub>/MeOH: 98/2), the solvent was removed under reduced pressure and the crude product was purified using flash chromatography (PE/EtOAc 98/2-90/10) to give the catalyst **133b** in 95% yield.

### 1-(3,5-Bis(trifluoromethyl)phenyl)-3-((1*S*,2*S*)-2-(cycloheptylamino)-1,2-di(naphthalen-1-yl)ethyl) thiourea (**133b**)



Light yellow solid, 97.2 mg, 65% yield. **mp** 95.1-98.2 °C.  $[\alpha]_{\text{D}}^{19} = +39.81$  (c 0.52, CHCl<sub>3</sub>). **<sup>1</sup>H NMR** (CD<sub>3</sub>OD, 400 MHz):  $\delta$  8.29 (d, 2H,  $J = 7.9$  Hz), 8.23 (s, 2H), 7.80–7.73 (m, 3H), 7.67–7.62 (m, 3H), 7.60 (d, 1H,  $J = 7.1$  Hz), 7.48–7.34 (m, 6H), 6.82 (bs, 1H), 5.23 (d, 1H,  $J = 4.4$  Hz), 2.50–2.43 (m, 1H), 1.72–1.63 (m, 1H), 1.62–1.52 (m, 1H), 1.50–1.41

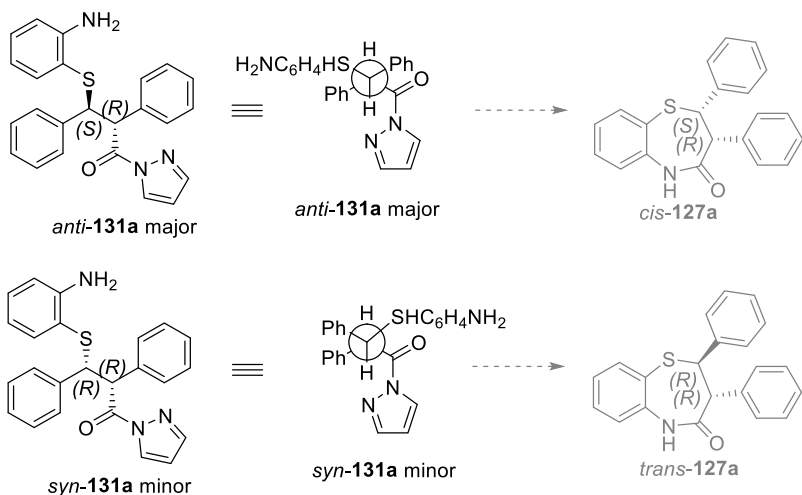
3658; (e) M. Amere, M.-C. Lasne, J. Rouden, *Org. Lett.* **2007**, *9*, 2621; (f) M. S. Manna, S. Mukherjee, *J. Am. Chem. Soc.* **2015**, *137*, 130.

(m, 1H), 1.40–1.14 (m, 8H), 1.05–0.95 (m, 1H).  $^{13}\text{C}$  NMR ( $\text{CD}_3\text{OD}$ , 100 MHz):  $\delta$  182.6, 143.1, 138.2, 137.6, 135.3, 133.0, 132.6 (q,  $^2J_{\text{CF}} = 33.1$  Hz), 132.2, 130.1, 129.8, 129.2, 129.0, 127.0, 126.9, 126.7, 126.3, 126.2, 126.0, 125.5, 124.7 (q,  $^1J_{\text{CF}} = 271.0$  Hz), 124.6, 123.8, 123.4, 117.8, 59.6, 57.0, 36.9, 34.0, 29.2, 29.0, 25.3, 24.7. **HRMS** (MALDI-FT ICR) exact mass calculated,  $[\text{M}+\text{H}]^+$  calculated for  $\text{C}_{38}\text{H}_{36}\text{F}_6\text{N}_3\text{S}$ : 680.2529, found: 680.2524.

### General procedure for preparation of aminothiols **78**

2-Aminobenzenethiol **78a** was purchased from TCI Europe N.V. and used as received. The substituted 2-aminobenzenethiols **78** were synthesized according to literature.<sup>88</sup> A solution of appropriate benzothiazole **130** (2 mmol) in a mixture of 1:1 v/v aqueous 50% NaOH and ethylene glycol ( $C = 0.5$  M) was refluxed under  $\text{N}_2$  flux until the starting material disappeared (TLC eluent: petroleum ether/ethyl acetate 8/2). The mixture was then poured into ice-water, acidified to pH 3 with 2 N HCl and extracted several times with  $\text{CH}_2\text{Cl}_2$ . The combined organic layers were washed with brine, dried over  $\text{Na}_2\text{SO}_4$  and concentrated under reduced pressure. The crude aminothiophenol derivative was quickly filtered through a short pad of flash silica-gel (eluent  $\text{CHCl}_3$ ), organic solvent was evaporated and a further purification was not necessary isolating the sufficiently pure aminothiophenols.

### Characterization of 3-((2-aminophenyl)thio)-2,3-diphenyl-1-(1H-pyrazol-1-yl)propan-1-one (**131a**)

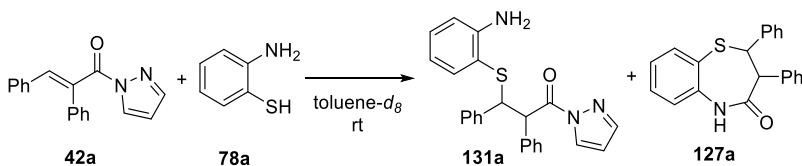


During the purification, we observed that the silica gel is able to promote the transformation of minor *syn*-131a diastereoisomer into *trans*-127a. In fact, the *syn*-127a minor diastereomer (90% ee) was recovered in small amount together with the major *anti*-131a (58% ee). Probably the silica gel during the purification by the flash chromatography eroded the enantiomeric excess of the major *anti*-131a diastereomer, catalyzing a retro-sulfa-Michael/sulfa-Michael process.

## Mechanistic investigations

### Experiment 1

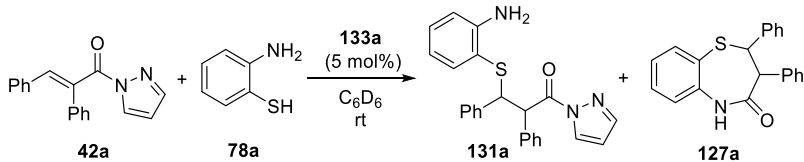
Monitoring of model reaction over time in the presence of 1,2-dichloroethane as internal standard without catalyst in toluene- $d_8$  at rt (see Figure 4.5).



Es.	<i>t</i> [h]	<b>42a</b>	Conv. <b>131a</b>	dr <b>131a</b>	Conv. <i>cis</i> - <b>127a</b>	Conv. <i>trans</i> - <b>127a</b>	Pyrazole
1	0	100	0	0	0	0	0
2	0.47	100	0	0	0	0	0
3	2.02	88	3.8	87/13	2	0	6
4	3.05	85	5.9	86/14	3.4	0	9
5	4.08	79	8.6	86/14	5.8	0	13
6	5.1	72	10	83/17	8	1	18
7	5.8	68	10	84/16	8.3	1	22
8	7.2	61	12	83/17	10	1.3	27
9	8	54	14	81/19	11	1	32
10	9.5	44	17	81/19	12	2	40
11	14	29	20	81/19	15	2	51
12	16.5	26	20	80/20	16	1	54
13	19.7	14	23	83/17	14	2	63

## Experiment 2

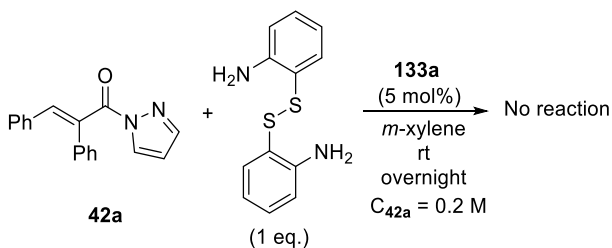
Table 4.8. Monitoring of model reaction over time in the presence of 1,2-dichloroethane as internal standard with 5 mol% **133a** in C<sub>6</sub>D<sub>6</sub> at room temperature (see Figure 4.6, a).



Es.	<i>t</i> [h]	<b>42a</b>	Conv. <b>131a</b>	dr <b>131a</b>	Conv. <i>cis</i> - <b>127a</b>	Conv. <i>trans</i> - <b>127a</b>	Pyrazole
1	0	100	0	0	0	0	0
2	0.23	82	14	65/35	0	0	4
3	0.77	58	30	63/37	0	0	12
4	1.3	43	39	66/34	0	0	18
5	2.4	26	45	67/33	0	0	27
6	3.4	17	50	64/36	0	0	31
7	4.5	13	55	65/35	0	0	32
8	5.6	10	57	64/36	0	0	32
9	6.6	7	61	65/35	0	0	32
10	7.7	5	63	65/35	0	0	32
11	8.8	4	64	65/5	0	0	32

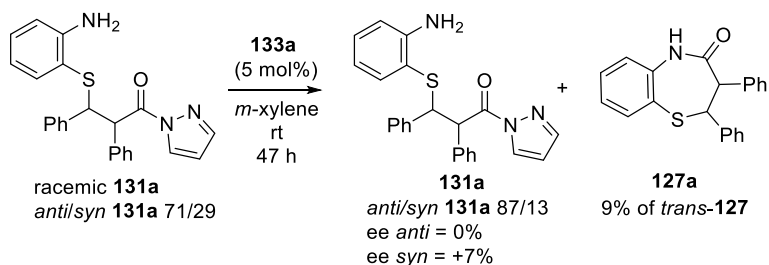


## Experiment 3



**Experimental procedure:**  $\alpha,\beta$ -Unsaturated pyrazolamide **42a** (27.4 mg, 0.1 mmol) and catalyst **133a** (3.3 mg, 0.005 mmol) were dissolved in *m*-xylene (0.5 mL) and 2-aminophenyl disulfide (24.8 mg, 0.10 mmol) was added. The reaction was stirred at room temperature for 15 h.  $^1\text{H}$  NMR analysis of the crude reaction mixture showed only the presence of reagents. This experiment shows that even if the oxidation product of **78a** was formed in small amount, it would not react with **42a**.

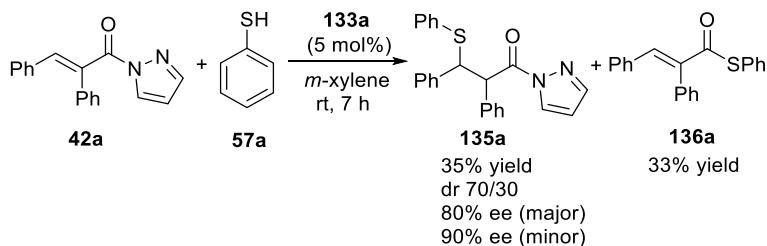
## Experiment 4



**Experimental procedure:** Racemic 3-((2-aminophenyl)thio)-2,3-diphenyl-1-(1H-pyrazol-1-yl)propan-1-one **131a** (31.9 mg, 0.08 mmol, *anti/syn* 71/29) and catalyst **133a** (2.7 mg, 0.004 mmol) were dissolved in dry *m*-xylene (0.4 mL) and the mixture was stirred at room temperature for 47 h. After this time, the diastereoisomeric

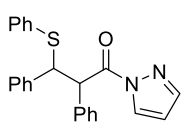
ratio of diastereomers of **131a** was determined by  $^1\text{H-NMR}$  analysis. 9% of *trans*-**127a** was detected respect to **131a**. Compound **131a** was recovered in racemic form for the major *anti* diastereomer and 7% ee for the minor *syn* diastereomer. By comparison of HPLC retention times, the *syn* (*2R,3R*)-adduct was preferentially recovered. This experiment confirmed that organocatalyzed amidation reactions are negligible processes within the reaction times reported in Table 4.5.

### Asymmetric sulfa-Michael reaction of **42a** with thiophenol



**Experimental procedure:** (*E*)- $\alpha,\beta$ -unsaturated *N*-acylpyrazole **42a** (41.1 mg, 0.15 mmol) and catalyst **133a** (5.3 mg, 0.008 mmol) were dissolved in dry *m*-xylene (770  $\mu\text{L}$ ) and thiophenol **57a** (18  $\mu\text{L}$ , 0.165 mmol) was added under nitrogen atmosphere at room temperature. The reaction was stirred at room temperature for 7 hours (PE/EtOAc 8/2). The crude product was purified by flash chromatography (hexane/EtOAc 100/0.1-90/10) to afford adduct **135a** as inseparable mixture of diastereoisomers in 35% yield and product **136a**<sup>176</sup> in 33% yield.

<sup>176</sup> H. Yoshida, T. Ogata, *Nippon Kagaku Kaishi* **1982**, 534.

**2,3-diphenyl-3-(phenylthio)-1-(1H-pyrazol-1-yl)propan-1-one  
(135a)**

Mixture of diastereoisomers in 70/30 ratio. White solid, 20.2 mg, 35% yield. 80 % ee major, 90% ee minor.  $^1\text{H NMR}$  ( $\text{CDCl}_3$ , 400 MHz):  $\delta$  8.30 (d, 0.6H,  $J = 2.8$  Hz, minor), 7.93 (d, 1H,  $J = 2.8$  Hz), 7.79 (s, 0.6H, minor), 7.67-7.65 (m, 3H), 7.38-7.34 (m, 2H), 7.32-7.28 (m, 4H), 7.24-7.17 (m, 3H, minor), 7.15-7.08 (m, 5H), 7.07-7.01 (m, 8H), 6.48-6.47 (m, 0.6H, minor), 6.28-6.27 (m, 1H), 5.86 (d, 1H,  $J = 12.1$  Hz) major overlapped with 5.82 (d, 0.6H,  $J = 12.2$  Hz) minor, 5.03 (d, 0.6H,  $J = 11.5$  Hz) minor overlapped with 5.00 (d, 1H,  $J = 11.7$  Hz) major.  $^{13}\text{C NMR}$  ( $\text{CDCl}_3$ , 100 MHz):  $\delta$  171.0 (minor), 170.2, 144.1 (minor), 144.0, 140.4, 139.2 (minor), 135.7, 135.5 (minor), 134.0, 133.9 (minor), 133.6, 133.4 (minor), 129.5, 129.2 (minor), 128.8 (minor), 128.7, 128.64 (minor), 128.59 (minor), 128.44, 128.35 (minor), 128.21, 128.16, 128.07, 127.9 (minor), 127.6, 127.5 (minor), 127.2, 126.69 (minor), 110.30 (minor), 109.96, 57.1, 56.4 (minor), 53.7. HPLC analysis major diastereoisomer: with Chiralpak AD column, 95:5 *n*-hexane:2-propanol, 1 mL/min, 254 nm; minor enantiomer  $t_R = 14.8$  min, major enantiomer  $t_R = 9.8$  min; minor diastereoisomer: with Chiralpak IC column, 95:5 *n*-hexane:2-propanol, 1 mL/min, 254 nm; minor enantiomer  $t_R = 5.2$  min, major enantiomer  $t_R = 5.7$  min.

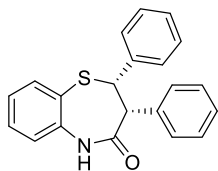
**General procedure for the synthesis of racemic 2,3-substituted-1,5-benzothiazepines (127)**

To a suspension of (*E*)- $\alpha,\beta$ -unsaturated *N*-acylpyrazole **42** (0.1 mmol) and aluminum oxide (aluminium oxide Fluka for

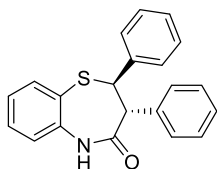
chromatography 17 994, pH =  $10 \pm 0.5$ , 101.96 mg) in dry diethyl ether (500  $\mu$ L) 2-aminothiophenol **78** (0.11 mmol) was added under a N<sub>2</sub> atmosphere. The reaction mixture was stirred at room temperature for 5–24 h. After completion, the reaction mixture was filtered through a short pad of flash silica-gel and the organic solvent was evaporated. Then, the crude mixture was dissolved in dry toluene (500  $\mu$ L), *p*-toluenesulfonic acid monohydrate (0.02 mmol) was added and the suspension was stirred at 80 °C for 20 h. The crude product was purified using flash chromatography (hexane/EtOAc 100/1 – 70/30) to afford racemic 1,5-benzothiazepines **127**.

**General procedure for the enantioselective synthesis of *cis*- and *trans*-2,3-substituted-1,5-benzothiazepine (**127**)**

(*E*)- $\alpha,\beta$ -unsaturated *N*-acylpyrazole **42** (0.2 mmol) and catalyst **133a** or **83b** (0.01 mmol) were dissolved in dry *m*-xylene (1 mL) and 2-aminothiophenol **78** (0.11 + 0.10 mmol) was added in two portions (the second portion added after 2 hours) under a nitrogen atmosphere at room temperature. After completion, *p*-toluenesulfonic acid monohydrate (0.04 mmol) was added. The suspension was stirred at 80 °C until completion. The crude mixture was analysed using <sup>1</sup>H-NMR to determine the diastereoisomeric ratio. The crude product was purified using flash chromatography (hexane/EtOAc: 100/1-70/30) to afford product **127**.

**(2*S*,3*R*)-2,3-Diphenyl-2,3-dihydrobenzo[*b*][1,4]thiazepin-4(5*H*)-one (127a)**

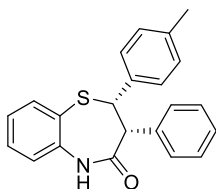
White solid, 41.1 mg, 62% yield. **mp** 187.6–189.7 °C.  $[\alpha]_D^{17} = +17.4$  (c 0.66, CHCl<sub>3</sub>), 81% ee. **<sup>1</sup>H NMR** (CDCl<sub>3</sub>, 400 MHz):  $\delta$  8.14 (bs, 1H), 7.73 (d, 1H,  $J = 7.6$  Hz), 7.43 (t, 1H,  $J = 7.6$  Hz), 7.32–7.20 (m, 6H), 7.13–7.11 (d, 2H,  $J = 7.6$  Hz), 7.07–7.03 (m, 2H), 6.92 (d, 2H,  $J = 7.5$  Hz), 4.98 (d, 1H,  $J = 6.3$  Hz), 4.22 (d, 1H,  $J = 6.3$  Hz). **<sup>13</sup>C NMR** (CDCl<sub>3</sub>, 100 MHz):  $\delta$  172.1, 142.3, 136.2, 135.0, 134.6, 130.8, 130.2, 130.1, 128.9, 128.6, 128.0, 127.4, 127.3, 126.6, 123.2, 61.3, 51.1. **HRMS** (MALDI-FT ICR) exact mass calculated,  $[M+H]^+$  calculated for C<sub>21</sub>H<sub>18</sub>NOS: 332.1104, found: 332.1110. HPLC analysis with Chiralpak IC column, 95:5 *n*-hexane:2-propanol, 1 mL/min, 254 nm; minor enantiomer  $t_R = 17.4$  min, major enantiomer  $t_R = 21.4$  min.

**(2*R*,3*R*)-2,3-Diphenyl-2,3-dihydrobenzo[*b*][1,4]thiazepin-4(5*H*)-one (127a)**

White solid, 21.9 mg, 33% yield. **mp** 190.2–193.7 °C.  $[\alpha]_D^{17} = -318.54$  (c 0.68, CHCl<sub>3</sub>), 94% ee. **<sup>1</sup>H NMR** (CDCl<sub>3</sub>, 300 MHz):  $\delta$  7.65 (d, 1H,  $J = 7.9$  Hz), 7.53–7.48 (m, 2H), 7.30 (t, 1H,  $J = 7.7$  Hz), 7.26–7.07 (m, 9H), 6.96–6.93 (m, 2H), 4.89 (d, 1H,  $J = 12.2$  Hz), 4.17 (d, 1H,  $J = 12.2$  Hz). **<sup>13</sup>C NMR** (CDCl<sub>3</sub>, 75 MHz):  $\delta$  172.6, 142.7, 141.5, 136.3, 135.4, 130.5, 129.9, 128.4, 128.0, 127.4, 127.0, 126.6, 126.4, 123.4, 58.3, 54.4. **HRMS** (MALDI-FTICR) exact mass calculated,  $[M+H]^+$  calculated for C<sub>21</sub>H<sub>18</sub>NOS: 332.1104, found: 332.1110. HPLC analysis with Chiralpak IC column, 80:20 *n*-

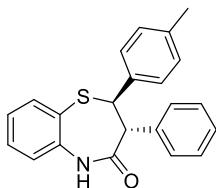
hexane:2-propanol, 1 mL/min, 254 nm; minor enantiomer  $t_R = 9.6$  min, major enantiomer  $t_R = 14.2$  min.

**(2*S*,3*R*)-3-Phenyl-2-(*p*-tolyl)-2,3-dihydrobenzo[*b*][1,4]thiazepine-4(5*H*)-one (127*b*)**



White solid, 26.2 mg, 38% yield. **mp** 189 °C (Decomp.).  $[\alpha]_D^{18} = +36.4$  (c 0.54, CHCl<sub>3</sub>), 74% ee. **<sup>1</sup>H NMR** (CDCl<sub>3</sub>, 400 MHz):  $\delta$  7.99 (bs, 1H), 7.72 (d, 1H,  $J = 7.2$  Hz), 7.42 (t, 1H,  $J = 7.5$  Hz), 7.29–7.26 (m, 1H), 7.21–7.19 (m, 2H), 7.16–7.03 (m, 6H), 6.93–6.91 (m, 2H), 4.94 (d, 1H,  $J = 6.2$  Hz), 4.20 (d, 1H,  $J = 6.2$  Hz), 2.34 (s, 3H). **<sup>13</sup>C NMR** (CDCl<sub>3</sub>, 100 MHz):  $\delta$  172.0, 142.2, 138.4, 134.9, 134.7, 133.1, 130.8, 130.1, 130.0, 129.0, 128.7, 127.4, 127.3, 126.5, 123.1, 60.9, 51.0, 21.2. **HRMS** (MALDI-FT ICR) exact mass calculated,  $[M+H]^+$  calculated for C<sub>22</sub>H<sub>20</sub>NOS: 346.1260, found: 346.1265. HPLC analysis with Chiralpak IC column, 95:5 *n*-hexane:2-propanol, 1 mL/min, 254 nm; minor enantiomer  $t_R = 31.0$  min, major enantiomer  $t_R = 25.1$  min.

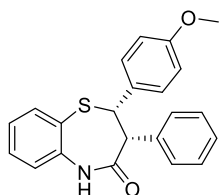
**(2*R*,3*R*)-3-Phenyl-2-(*p*-tolyl)-2,3-dihydrobenzo[*b*][1,4]thiazepine-4(5*H*)-one (127*b*)**



White solid, 22.8 mg, 33% yield. **mp** 146.0–150.0 °C.  $[\alpha]_D^{18} = -233.72$  (c 0.60, CHCl<sub>3</sub>), 93% ee. **<sup>1</sup>H NMR** (CDCl<sub>3</sub>, 400 MHz):  $\delta$  7.63 (d, 1H,  $J = 7.7$  Hz), 7.49 (t, 1H,  $J = 7.6$  Hz), 7.29 (t, 1H,  $J = 7.6$  Hz), 7.24–7.08 (m, 7H), 6.90 (d, 2H,  $J = 8.0$  Hz), 6.84 (d, 2H,  $J = 8.1$  Hz), 4.88 (d, 1H,  $J = 12.2$  Hz), 4.17 (d, 1H,  $J = 12.2$  Hz), 2.19 (s, 3H). **<sup>13</sup>C NMR** (CDCl<sub>3</sub>, 100 MHz):  $\delta$  173.0, 141.6, 139.8, 137.0, 136.2, 135.6, 130.4, 129.9, 129.1, 127.9, 127.3, 126.8,

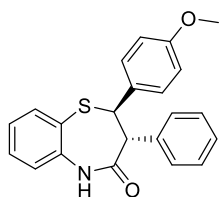
126.5, 126.1, 123.3, 58.0, 54.3, 21.0. **HRMS** (MALDI-FT ICR) exact mass calculated,  $[M+H]^+$  calculated for  $C_{22}H_{20}NOS$ : 346.1260, found: 346.1265. HPLC analysis with Chiralpak IC column, 80:20 *n*-hexane:2-propanol, 1 mL/min, 254 nm; minor enantiomer  $t_R = 10.6$  min, major enantiomer  $t_R = 15.8$  min.

**(2*S*,3*R*)-2-(4-Methoxyphenyl)-3-phenyl-2,3-dihydrobenzo[*b*][1,4]thiazepine-4(5*H*)-one (127c)**



Yellow solid, 11.6 mg, 16% yield. **mp** 68.7–73.7 °C.  $[\alpha]_D^{19} = +47.1$  (c 0.44,  $CHCl_3$ ), 75% ee. **<sup>1</sup>H NMR** ( $CDCl_3$ , 400 MHz):  $\delta$  7.95 (bs, 1H), 7.72 (d, 1H,  $J = 7.2$  Hz), 7.43 (t, 1H,  $J = 7.5$  Hz), 7.29–7.26 (m, 1H), 7.23 (d, 2H,  $J = 8.4$  Hz), 7.15–7.12 (m, 2H), 7.09–7.05 (m, 2H), 6.93 (d, 2H,  $J = 7.5$  Hz), 6.77 (d, 2H,  $J = 8.1$  Hz), 4.94 (d, 1H,  $J = 6.0$  Hz), 4.19 (d, 1H,  $J = 6.0$  Hz), 3.80 (s, 3H). **<sup>13</sup>C NMR** ( $CDCl_3$ , 100 MHz):  $\delta$  172.0, 159.8, 142.2, 134.9, 134.7, 131.2, 130.8, 130.1, 129.2, 128.1, 127.4, 127.3, 126.6, 123.1, 113.4, 60.6, 55.2, 51.1. **HRMS** (MALDI-FT ICR) exact mass calculated,  $[M+H]^+$  calculated for  $C_{22}H_{20}NO_2S$ : 362.1209, found: 362.1206. HPLC analysis with Chiralpak IC column, 70:30 *n*-hexane:2-propanol, 1 mL/min, 254 nm; minor enantiomer  $t_R = 17.8$  min, major enantiomer  $t_R = 7.4$  min.

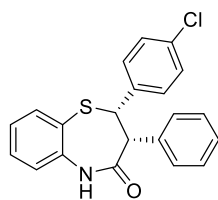
**(2*R*,3*R*)-2-(4-Methoxyphenyl)-3-phenyl-2,3-dihydrobenzo[*b*][1,4]thiazepin-4(5*H*)-one (127c)**



White solid, 21.7 mg, 30% yield. **mp** 142.2–144.1 °C.  $[\alpha]_D^{20} = -165.0$  (c 0.58,  $CHCl_3$ ), 82% ee. **<sup>1</sup>H NMR** ( $CDCl_3$ , 600 MHz):  $\delta$  7.64 (dd, 1H,  $J = 7.6, 1.1$  Hz), 7.62 (bs, 1H), 7.49 (td, 1H,  $J =$

7.6, 1.4 Hz), 7.29 (td, 1H,  $J = 7.6, 1.1$  Hz), 7.22 (d, 1H,  $J = 7.7$  Hz), 7.19–7.17 (m, 2H), 7.16–7.14 (m, 2H), 7.12–7.11 (m, 1H), 6.87 (d, 2H,  $J = 8.7$  Hz), 6.62 (d, 2H,  $J = 8.7$  Hz), 4.87 (d, 1H,  $J = 12.2$  Hz), 4.13 (d, 1H,  $J = 12.2$  Hz), 3.68 (s, 3H).  $^{13}\text{C}$  NMR ( $\text{CDCl}_3$ , 100 MHz):  $\delta$  172.7, 158.6, 141.5, 136.3, 135.6, 135.1, 130.5, 129.9, 128.0, 127.4, 127.3, 126.9, 126.5, 123.3, 113.7, 57.9, 55.1, 54.6. **HRMS** (MALDI-FT ICR) exact mass calculated,  $[\text{M}+\text{H}]^+$  calculated for  $\text{C}_{22}\text{H}_{20}\text{NO}_2\text{S}$ : 362.1209, found: 362.1206. HPLC analysis with Chiralpak IC column, 70:30 *n*-hexane:2-propanol, 1 mL/min, 254 nm; minor enantiomer  $t_R = 10.1$  min, major enantiomer  $t_R = 14.7$  min.

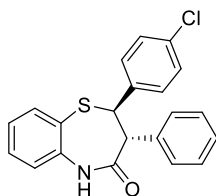
**(2*S*,3*R*)-2-(4-Chlorophenyl)-3-phenyl-2,3-dihydrobenzo[*b*][1,4]thiazepin-4(5*H*)-one (127d)**



Brown solid, 25.6 mg, 35% yield. **mp** 193 °C (Decomp.).  $[\alpha]_D^{17} = +34.00$  (c 0.50,  $\text{CHCl}_3$ ), 59% ee.  $^1\text{H}$  NMR ( $\text{CDCl}_3$ , 400 MHz):  $\delta$  7.72 (d, 1H,  $J = 7.8$  Hz), 7.52–7.44 (m, 2H), 7.31–7.27 (m, 1H), 7.26–7.23 (m, 4H), 7.17–7.13 (m, 2H), 7.10–7.07 (m, 2H), 6.94 (d, 2H,  $J = 7.7$  Hz), 4.93 (d, 1H,  $J = 6.3$  Hz), 4.19 (d, 1H,  $J = 6.3$  Hz).  $^{13}\text{C}$  NMR ( $\text{CDCl}_3$ , 100 MHz):  $\delta$  171.7, 142.1, 135.1, 134.8, 134.4, 134.3, 131.4, 130.7, 130.4, 128.6, 128.2, 127.6, 127.5, 126.8, 123.2, 60.5, 50.8. **HRMS** (MALDI-FT ICR) exact mass calculated,  $[\text{M}+\text{H}]^+$  calculated for  $\text{C}_{21}\text{H}_{17}\text{ClNOS}$ : 366.0714, found: 366.0718. HPLC analysis with Chiralpak IC column, 95:5 *n*-hexane:2-propanol, 1 mL/min, 254 nm; minor enantiomer  $t_R = 22.8$  min, major enantiomer  $t_R = 11.7$  min.

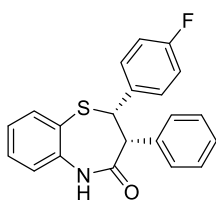


**(2*R*,3*R*)-2-(4-Chlorophenyl)-3-phenyl-2,3-dihydrobenzo[*b*][1,4]thiazepin-4(5*H*)-one (127*d*)**



Light brown solid, 27.8 mg, 38% yield. **mp** 76.1–78.6 °C.  $[\alpha]_D^{17} = -247.83$  (c 0.46, CHCl<sub>3</sub>), 92% ee. **<sup>1</sup>H NMR** (CDCl<sub>3</sub>, 400 MHz):  $\delta$  7.63 (d, 1H,  $J = 7.4$  Hz), 7.52 (td, 1H,  $J = 7.6, 1.3$  Hz), 7.31 (t, 1H,  $J = 7.8$  Hz), 7.26–7.23 (m, 2H), 7.18–7.12 (m, 5H), 7.06 (d, 2H,  $J = 8.0$  Hz), 6.88 (d, 2H,  $J = 8.0$  Hz), 4.86 (d, 1H,  $J = 12.2$  Hz), 4.09 (d, 1H,  $J = 12.2$  Hz). **<sup>13</sup>C NMR** (CDCl<sub>3</sub>, 100 MHz):  $\delta$  172.7, 141.6, 141.3, 136.1, 135.1, 133.0, 130.7, 129.9, 128.6, 128.2, 128.1, 127.7, 127.5, 127.0, 123.5, 57.6, 54.3. **HRMS** (MALDI-FT ICR) exact mass calculated,  $[M+H]^+$  calculated for C<sub>21</sub>H<sub>17</sub>ClNOS: 366.0714, found: 366.0717. HPLC analysis with Chiralpak IC column, 80:20 *n*-hexane:2-propanol, 1 mL/min, 254 nm; minor enantiomer  $t_R = 9.8$  min, major enantiomer  $t_R = 13.9$  min.

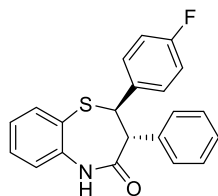
**(2*S*,3*R*)-2-(4-Fluorophenyl)-3-phenyl-2,3-dihydrobenzo[*b*][1,4]thiazepin-4(5*H*)-one (127*e*)**



Brown solid, 28.0 mg, 40% yield. **mp** 174 °C (Decomp.).  $[\alpha]_D^{22} = +37.9$  (c 0.87, CHCl<sub>3</sub>), 81% ee. **<sup>1</sup>H NMR** (CDCl<sub>3</sub>, 400 MHz):  $\delta$  8.03 (bs, 1H), 7.73 (d, 1H,  $J = 7.6$  Hz), 7.46 (t, 1H,  $J = 7.7$  Hz), 7.31–7.25 (m, 3H), 7.17–7.13 (m, 2H), 7.09–7.06 (m, 2H), 6.94–6.90 (m, 4H), 4.96 (d, 1H,  $J = 6.3$  Hz), 4.20 (d, 1H,  $J = 6.3$  Hz). **<sup>13</sup>C NMR** (CDCl<sub>3</sub>, 100 MHz):  $\delta$  172.4, 162.8 (d,  $^1J_{CF} = 245.9$  Hz), 142.3, 134.9, 134.5, 132.0 (d,  $^4J_{CF} = 3.0$  Hz), 131.8 (d,  $^3J_{CF} = 8.2$  Hz), 130.7, 130.3, 128.6, 127.5, 127.4, 126.6, 123.3, 114.8 (d, 2 JCF = 21.3 Hz), 60.6, 50.9. **HRMS** (MALDI-FT

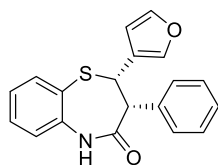
ICR) exact mass calculated,  $[M+H]^+$  calculated for  $C_{21}H_{17}FNOS$ : 350.1009, found: 350.1006. HPLC analysis with Chiralpak IC column, 95:5 *n*-hexane:2-propanol, 1 mL/min, 254 nm; minor enantiomer  $t_R = 13.6$  min, major enantiomer  $t_R = 12.6$  min.

**(2*R*,3*R*)-2-(4-Fluorophenyl)-3-phenyl-2,3-dihydrobenzo[*b*][1,4]thiazepin-4(5*H*)-one (127e)**



White solid, 26.6 mg, 38% yield. **mp** 182.0–184.1 °C.  $[\alpha]_D^{22} = -322.3$  (c 0.99,  $CHCl_3$ ), 94% ee.  $^1H$  NMR ( $CDCl_3$ , 300 MHz):  $\delta$  7.90 (bs, 1H), 7.65–7.60 (m, 1H), 7.50 (td, 1H,  $J = 7.6$ , 1.3 Hz), 7.33–7.11 (m, 7H), 6.94–6.89 (m, 2H), 6.80–6.74 (m, 2H), 4.88 (d, 1H,  $J = 12.2$  Hz), 4.09 (d, 1H,  $J = 12.2$  Hz).  $^{13}C$  NMR ( $CDCl_3$ , 62.5 MHz):  $\delta$  172.7, 161.7 (d,  $^1J_{CF} = 245.0$  Hz), 141.6, 138.7 (d,  $^4J_{CF} = 3.1$  Hz), 136.1, 135.3, 130.6, 129.9, 128.0, 127.9, 127.5, 126.9, 126.0, 123.4, 115.3 (d,  $^2J_{CF} = 21.4$  Hz), 57.6, 54.7. **HRMS** (MALDI-FT ICR) exact mass calculated,  $[M+H]^+$  calculated for  $C_{21}H_{17}FNOS$ : 350.1009, found: 350.1006. HPLC analysis with Chiralpak IC column, 80:20 *n*-hexane:2-propanol, 1 mL/min, 254 nm; minor enantiomer  $t_R = 9.7$  min, major enantiomer  $t_R = 13.8$  min.

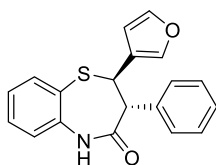
**(2*S*,3*R*)-2-(Furan-3-yl)-3-phenyl-2,3-dihydrobenzo[*b*][1,4]thiazepin-4(5*H*)-one (127f)**



Ochre yellow solid, 19.3 mg, 30% yield. **mp** 76.4–79.6 °C.  $[\alpha]_D^{21} = +1.1$  (c 0.60,  $CHCl_3$ ), 67% ee.  $^1H$  NMR ( $CDCl_3$ , 250 MHz):  $\delta$  7.72–7.69 (dd, 1H,  $J = 7.5$ , 1.2 Hz), 7.54 (bs, 2H), 7.45–7.41 (dd, 1H,  $J = 7.4$ , 1.7), 7.20–7.13 (m, 8H), 6.62 (s, 1H),

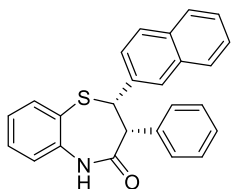
4.95 (d, 1H,  $J = 6.3$  Hz), 4.17 (d, 1H,  $J = 6.1$  Hz).  $^{13}\text{C}$  NMR ( $\text{CDCl}_3$ , 100 MHz):  $\delta$  171.9, 143.1, 142.2, 142.0, 135.0, 134.7, 130.6, 130.3, 128.6, 127.6, 127.5, 126.7, 123.1, 121.0, 111.0, 51.7, 50.3. HRMS (MALDI-FT ICR) exact mass calculated,  $[\text{M}+\text{H}]^+$  calculated for  $\text{C}_{19}\text{H}_{16}\text{NO}_2\text{S}$ : 322.0896, found: 322.0892. HPLC analysis with Chiralpak IC column, 90:10 *n*-hexane:2-propanol, 1 mL/min, 254 nm; minor enantiomer  $t_R = 15.0$  min, major enantiomer  $t_R = 11.8$  min.

**(2*R*,3*R*)-2-(Furan-3-yl)-3-phenyl-2,3-dihydrobenzo[*b*][1,4]thiazepin-4(5*H*)-one (127f)**



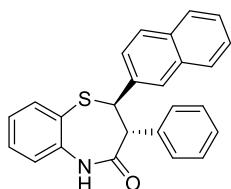
Brown solid, 10.9 mg, 17% yield. mp 151.8 °C (Decomp.).  $[\alpha]_D^{19} = -175.9$  (c 0.51,  $\text{CHCl}_3$ ), 99% ee.  $^1\text{H}$  NMR ( $\text{CDCl}_3$ , 400 MHz):  $\delta$  7.92 (s, 1H), 7.67 (d, 1H,  $J = 7.6$  Hz), 7.48 (t, 1H,  $J = 7.2$  Hz), 7.30–7.28 (m, 1H), 7.23–7.19 (m, 6H), 7.15 (s, 1H), 6.97 (s, 1H), 6.00 (s, 1H), 4.84 (d, 1H,  $J = 11.9$  Hz), 3.88 (d, 1H,  $J = 11.8$  Hz).  $^{13}\text{C}$  NMR ( $\text{CDCl}_3$ , 100 MHz):  $\delta$  172.7, 143.1, 141.6, 138.8, 136.3, 135.8, 130.6, 129.8, 128.1, 127.7, 126.89, 126.80, 126.0, 123.3, 108.5, 54.5, 50.0. HRMS (MALDI-FT ICR) exact mass calculated,  $[\text{M}+\text{H}]^+$  calculated for  $\text{C}_{19}\text{H}_{16}\text{NO}_2\text{S}$ : 322.0896, found: 322.0892. HPLC analysis with Chiralpak IC column, 80:20 *n*-hexane:2-propanol, 1 mL/min, 254 nm; minor enantiomer  $t_R = 10.7$  min, major enantiomer  $t_R = 17.4$  min.

**(2*S*,3*R*)-2-(Naphthalen-2-yl)-3-phenyl-2,3-dihydrobenzo[*b*][1,4]thiazepin-4(5*H*)-one (127g)**



Yellow solid, 25.9 mg, 34% yield. **mp** 205 °C (Decomp.).  $[\alpha]_D^{17} = +36.1$  (c 0.69, CHCl<sub>3</sub>), 45% ee. **<sup>1</sup>H NMR** (CDCl<sub>3</sub>, 400 MHz):  $\delta$  7.84 (d, 1H,  $J = 7.5$  Hz), 7.79 (d, 1H,  $J = 8.4$  Hz), 7.75 (t, 2H,  $J = 6.5$  Hz), 7.69 (s, 1H), 7.60–7.57 (m, 2H), 7.50–7.44 (m, 3H), 7.30 (t, 1H,  $J = 7.6$  Hz), 7.19 (d, 1H,  $J = 7.4$  Hz), 7.11–7.07 (m, 1H), 7.01–6.97 (m, 2H), 6.94–6.92 (m, 2H), 5.15 (d, 1H,  $J = 6.4$  Hz), 4.29 (d, 1H,  $J = 6.4$  Hz). **<sup>13</sup>C NMR** (CDCl<sub>3</sub>, 62.5 MHz):  $\delta$  171.9, 142.2, 135.0, 134.6, 133.8, 133.4, 132.8, 130.8, 130.3, 129.7, 128.9, 128.2, 127.7, 127.6, 127.5, 127.42, 127.39, 126.7, 126.3, 126.0, 123.1, 61.4, 51.1. **HRMS** (MALDI-FT ICR) exact mass calculated,  $[M+H]^+$  calculated for C<sub>25</sub>H<sub>20</sub>NOS: 382.1260, found: 382.1283. HPLC analysis with Chiralpak IC column, 80:20 *n*-hexane:2-propanol, 1 mL/min, 254 nm; minor enantiomer  $t_R = 13.6$  min, major enantiomer  $t_R = 7.9$  min.

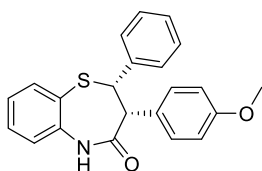
**(2*R*,3*R*)-2-(Naphthalen-2-yl)-3-phenyl-2,3-dihydrobenzo[*b*][1,4]thiazepin-4(5*H*)-one (127g)**



Yellow solid, 28.2 mg, 37% yield. **mp** 210 °C (Decomp.).  $[\alpha]_D^{18} = -82.0$  (c 0.42, CHCl<sub>3</sub>), 55% ee. **<sup>1</sup>H NMR** (CDCl<sub>3</sub>, 400 MHz):  $\delta$  7.73–7.61 (m, 5H), 7.53 (td, 1H,  $J = 7.6, 1.3$  Hz), 7.39–7.27 (m, 5H), 7.26–7.22 (m, 2H), 7.16–7.05 (m, 4H), 5.09 (d, 1H,  $J = 12.2$  Hz), 4.33 (d, 1H,  $J = 12.2$  Hz). **<sup>13</sup>C NMR** (CDCl<sub>3</sub>, 75 MHz):  $\delta$  172.7, 141.5, 139.9, 136.4, 135.3, 133.0, 132.5, 130.6, 129.8, 128.7, 128.5, 128.0, 127.8, 127.5, 127.0, 126.5, 126.1, 125.9,

125.4, 123.9, 123.4, 58.3, 53.9. **HRMS** (MALDI-FT ICR) exact mass calculated,  $[M+H]^+$  calculated for  $C_{25}H_{20}NOS$ : 382.1260, found: 382.1263. HPLC analysis with Chiralpak IC column, 80:20 *n*-hexane:2-propanol, 1 mL/min, 254 nm; minor enantiomer  $t_R$  = 8.1 min, major enantiomer  $t_R$  = 10.7 min.

**(2*S*,3*R*)-3-(4-Methoxyphenyl)-2-phenyl-2,3-dihydrobenzo[*b*][1,4] thiazepin-4(5*H*)-one (127h)**



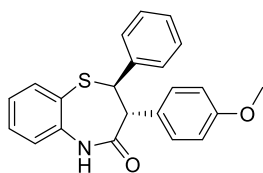
Ochre yellow solid, 28.9 mg, 40% yield. **mp** 167.4–172.0 °C.  $[\alpha]_D^{19}$  = +57.4 (c 0.51,  $CHCl_3$ ), 55% ee.  **$^1H$  NMR** ( $CDCl_3$ , 400 MHz):  $\delta$  8.18 (bs, 1H), 7.72 (d, 1H,  $J$  = 7.7

Hz), 7.44–7.40 (m, 1H), 7.33–7.22 (m, 6H), 7.12 (d, 1H,  $J$  = 7.8 Hz), 6.80 (d, 2H,  $J$  = 8.7 Hz), 6.60 (d, 2H,  $J$  = 8.8 Hz), 4.94 (d, 1H,  $J$  = 6.3 Hz), 4.17 (d, 1H,  $J$  = 6.3 Hz), 3.70 (s, 3H).  **$^{13}C$  NMR** ( $CDCl_3$ , 100 MHz):  $\delta$  172.3, 158.8, 142.3, 136.3, 135.0, 131.9, 130.2, 130.1, 128.9, 128.6, 128.0, 126.6, 126.5, 123.1, 112.8, 61.3, 55.1, 50.3.

**HRMS** (MALDI-FT ICR) exact mass calculated,  $[M+H]^+$  calculated for  $C_{22}H_{20}NO_2S$ : 362.1209, found: 362.1206. HPLC analysis with Chiralpak IC column, 80:20 *n*-hexane:2-propanol, 1 mL/min, 254 nm; minor enantiomer  $t_R$  = 13.8 min, major enantiomer  $t_R$  = 10.0 min.

**(2*R*,3*R*)-3-(4-Methoxyphenyl)-2-phenyl-2,3-dihydrobenzo[*b*][1,4] thiazepin-4(5*H*)-one (127h)**

Ochre yellow solid, 28.9 mg, 40% yield. **mp** 157.8 °C (Decomp.).  $[\alpha]_D^{19}$  = –245.3 (c 0.54,  $CHCl_3$ ), 99% ee.  **$^1H$  NMR** ( $CDCl_3$ , 400 MHz):  $\delta$  7.65–7.62 (dd, 1H,  $J$  = 7.7, 1.1 Hz), 7.55 (bs, 1H), 7.52–7.48 (td, 1H,  $J$  = 7.7, 1.3 Hz), 7.32–7.28 (td, 1H,  $J$  = 7.5, 1.1 Hz),

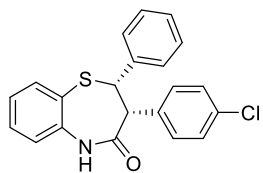


7.23 (d, 1H,  $J = 7.8$  Hz), 7.11–7.09 (m, 5H), 6.95–6.93 (m, 2H), 6.67 (d, 2H,  $J = 8.7$  Hz), 4.83 (d, 1H,  $J = 12.2$  Hz), 4.12 (d, 1H,  $J = 12.2$  Hz), 3.69 (s, 3H).  $^{13}\text{C}$  NMR ( $\text{CDCl}_3$ ,

100 MHz):  $\delta$  173.3, 158.6, 142.9, 141.7, 136.2, 130.9, 130.4, 128.4, 127.5, 127.3, 126.8, 126.42, 126.35, 123.3, 113.4, 58.4, 55.0, 53.5.

**HRMS** (MALDI-FT ICR) exact mass calculated,  $[\text{M}+\text{H}]^+$  calculated for  $\text{C}_{22}\text{H}_{20}\text{NO}_2\text{S}$ : 362.1209, found: 362.1206. HPLC analysis with Chiralpak IC column, 70:30 *n*-hexane:2-propanol, 1 mL/min, 220 nm; minor enantiomer  $t_R = 14.1$  min, major enantiomer  $t_R = 25.1$  min.

**(2*S*,3*R*)-3-(4-Chlorophenyl)-2-phenyl-2,3-dihydrobenzo[*b*][1,4]thiazepin-4(5*H*)-one (127)**

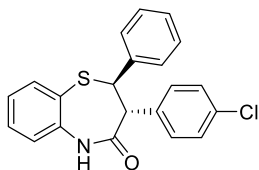


Yellow solid, 22.0 mg, 30% yield. **mp** 158 °C (Decomp.).  $[\alpha]_D^{20} = +63.07$  (c 0.56,  $\text{CHCl}_3$ ), 81% ee.  $^1\text{H}$  NMR ( $\text{CDCl}_3$ , 250 MHz):  $\delta$  7.75–7.72 (dd, 1H,  $J = 7.2, 0.7$  Hz),

7.51 (bs, 1H), 7.47–7.43 (dd, 1H,  $J = 7.7, 1.3$  Hz), 7.32–7.30 (m, 6H), 7.18–7.15 (m, 1H), 7.02 (d, 2H,  $J = 8.5$  Hz), 6.85 (d, 2H,  $J = 8.7$  Hz), 4.92 (d, 1H,  $J = 6.4$  Hz), 4.17 (d, 1H,  $J = 6.3$  Hz).  $^{13}\text{C}$  NMR ( $\text{CDCl}_3$ , 100 MHz):  $\delta$  171.5, 141.9, 135.8, 135.1, 133.4, 133.0, 132.1, 130.3,

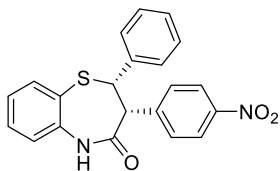
130.1, 128.8, 128.7, 128.1, 127.6, 126.8, 123.2, 61.0, 50.4. **HRMS** (MALDI-FT ICR) exact mass calculated,  $[\text{M}+\text{H}]^+$  calculated for  $\text{C}_{21}\text{H}_{17}\text{ClNOS}$ : 366.0714, found: 366.0711. HPLC analysis with Chiralpak IC column, 95:5 *n*-hexane:2-propanol, 1 mL/min, 254 nm; minor enantiomer  $t_R = 17.4$  min, major enantiomer  $t_R = 15.7$  min.

**(2*R*,3*R*)-3-(4-Chlorophenyl)-2-phenyl-2,3-dihydrobenzo[*b*][1,4]thiazepin-4(5*H*)-one (127*i*)**



White solid, 30.7 mg, 42% yield. **mp** 182.8–185.2 °C.  $[\alpha]_{\text{D}}^{19} = -282.2$  (c 0.60, CHCl<sub>3</sub>), 95% ee. **<sup>1</sup>H NMR** (CDCl<sub>3</sub>, 600 MHz):  $\delta$  7.86 (s, 1H), 7.64 (d, 1H,  $J = 7.3$  Hz), 7.50 (t, 1H,  $J = 7.3$  Hz), 7.31 (t, 1H,  $J = 7.5$  Hz), 7.21 (d, 1H,  $J = 7.8$  Hz), 7.14–7.10 (m, 7H), 6.93–6.92 (m, 2H), 4.81 (d, 1H,  $J = 12.2$  Hz), 4.14 (d, 1H,  $J = 12.2$  Hz). **<sup>13</sup>C NMR** (CDCl<sub>3</sub>, 150 MHz):  $\delta$  172.3, 142.5, 141.4, 136.3, 134.1, 133.3, 131.3, 130.6, 128.6, 128.2, 127.6, 127.1, 126.4, 126.3, 123.4, 58.3, 53.8. **HRMS** (MADI-FT ICR) exact mass calculated,  $[M+H]^+$  calculated for C<sub>21</sub>H<sub>17</sub>ClNOS: 366.0714, found: 366.0711. HPLC analysis with Chiralpak IC column, 80:20 *n*-hexane:2-propanol, 1 mL/min, 254 nm; minor enantiomer  $t_R = 7.6$  min, major enantiomer  $t_R = 10.7$  min.

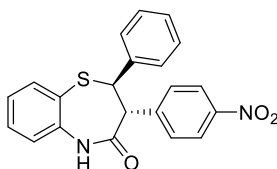
**(2*S*,3*R*)-3-(4-Nitrophenyl)-2-phenyl-2,3-dihydrobenzo[*b*][1,4]thiazepin-4(5*H*)-one (127*j*)**



Pale yellow solid, 23.3 mg, 31% yield. **mp** 207.4–211.8 °C.  $[\alpha]_{\text{D}}^{19} = +71.3$  (c 0.58, CHCl<sub>3</sub>), 73% ee. **<sup>1</sup>H NMR** (CDCl<sub>3</sub>, 300 MHz):  $\delta$  8.02 (bs, 1H), 7.90 (d, 2H,  $J = 8.0$  Hz), 7.75 (d, 1H,  $J = 7.5$  Hz), 7.49 (t, 1H,  $J = 7.7$  Hz), 7.35–7.24 (m, 6H), 7.16 (d, 1H,  $J = 7.7$  Hz), 7.13 (d, 2H,  $J = 8.7$  Hz), 4.96 (d, 1H,  $J = 6.5$  Hz), 4.31 (d, 1H,  $J = 6.5$  Hz). **<sup>13</sup>C NMR** (CDCl<sub>3</sub>, 75 MHz):  $\delta$  170.9, 147.0, 142.0, 141.8, 135.2, 131.7, 130.6, 129.9, 129.1, 128.5, 128.3, 127.0, 123.4, 122.4, 60.9, 50.7. **HRMS** (MALDI-FT ICR) exact mass calculated,  $[M+H]^+$  calculated for C<sub>21</sub>H<sub>17</sub>N<sub>2</sub>O<sub>3</sub>S:

377.0954, found: 377.0951. HPLC analysis with Chiralpak IC column, 90:10 *n*-hexane:2-propanol, 1 mL/min, 254 nm; minor enantiomer  $t_R = 31.0$  min, major enantiomer  $t_R = 24.7$  min.

**(2*R*,3*R*)-3-(4-Nitrophenyl)-2-phenyl-2,3-dihydrobenzo[*b*][1,4]thiazepin-4(5*H*)-one (127j)**

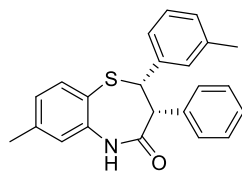


Ochre yellow solid, 15.1 mg, 20% yield.

**mp** 175.5–177.5 °C.  $[\alpha]_D^{19} = -132.7$  (c 0.42, CHCl<sub>3</sub>), 77% ee. **<sup>1</sup>H NMR** (CDCl<sub>3</sub>, 400 MHz):  $\delta$  8.01–7.99 (m, 3H), 7.68 (d, 1H,  $J = 8.0$  Hz), 7.54 (t, 1H,  $J = 7.4$  Hz), 7.40–7.33 (m, 3H), 7.11–

7.10 (m, 3H), 6.92–6.91 (m, 2H), 4.86 (d, 1H,  $J = 12.2$  Hz), 4.28 (d, 1H,  $J = 12.3$  Hz). **<sup>13</sup>C NMR** (CDCl<sub>3</sub>, 100 MHz):  $\delta$  171.4, 147.0, 142.9, 142.0, 141.1, 136.3, 131.0, 130.8, 128.7, 127.9, 127.4, 126.2, 126.1, 123.6, 123.0, 58.2, 54.1. **HRMS** (MALDI-FT ICR) exact mass calculated,  $[M+H]^+$  calculated for C<sub>21</sub>H<sub>17</sub>N<sub>2</sub>O<sub>3</sub>S: 377.0954, found: 377.0951. HPLC analysis with Chiralpak IC column, 90:10 *n*-hexane:2-propanol, 1 mL/min, 254 nm; minor enantiomer  $t_R = 31.0$  min, major enantiomer  $t_R = 25.1$  min.

**(2*S*,3*R*)-7-Methyl-3-phenyl-2-(*m*-tolyl)-2,3-dihydrobenzo[*b*][1,4]thiazepin-4(5*H*)-one (127k)**



White solid, 18.7 mg, 26% yield. **mp** 181.5–183.8 °C.  $[\alpha]_D^{19} = +17.3$  (c 0.54, CHCl<sub>3</sub>), 70% ee. **<sup>1</sup>H NMR** (CDCl<sub>3</sub>, 400 MHz):  $\delta$  7.70 (s, 1H), 7.58 (d, 1H,  $J = 7.7$  Hz), 7.11–7.04

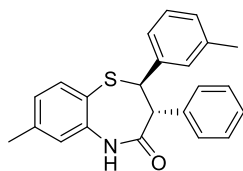
(m, 8H), 6.93–6.90 (m, 3H), 4.89 (d, 1H,  $J = 6.2$  Hz), 4.81 (d, 1H,  $J = 6.2$  Hz), 2.39 (s, 3H), 2.29 (s, 3H). **<sup>13</sup>C NMR** (CDCl<sub>3</sub>, 100 MHz):  $\delta$  172.0, 142.0, 140.7, 137.5, 136.2, 134.7, 130.8, 130.7, 129.3,



127.8, 127.34, 127.28, 127.2, 125.4, 123.7, 61.1, 51.1, 21.4, 21.2.

**HRMS** (MALDI-FT ICR) exact mass calculated,  $[M+H]^+$  calculated for  $C_{23}H_{22}NOS$ : 360.1417, found: 360.1413. HPLC analysis with Chiralpak IE-3 column, 70:30 *n*-hexane : 2-propanol, 0.6 mL/min, 254 nm; minor enantiomer  $t_R = 30.6$  min, major enantiomer  $t_R = 15.2$  min.

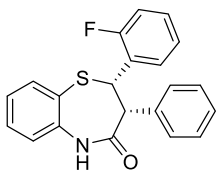
**(2*R*,3*R*)-7-Methyl-3-phenyl-2-(*m*-tolyl)-2,3-dihydrobenzo[*b*][1,4] thiazepin-4(5*H*)-one (127k)**



White solid, 12.2 mg, 17% yield. **mp** 199.6–201.9 °C.  $[\alpha]_D^{20} = -333.2$  (c 0.60,  $CHCl_3$ ), 95% ee.  **$^1H$  NMR** ( $CDCl_3$ , 600 MHz):  $\delta$  7.50 (d, 1H,  $J = 7.8$  Hz), 7.20–7.18 (m, 2H), 7.14 (t, 2H,  $J = 7.4$  Hz), 7.11–7.10 (m, 2H), 7.04 (s, 1H), 6.97 (t, 1H,  $J = 7.9$  Hz), 6.87 (d, 1H,  $J = 7.3$  Hz), 6.75–6.74 (m, 2H), 4.82 (d, 1H,  $J = 12.2$  Hz), 4.17 (d, 1H,  $J = 12.2$  Hz), 2.45 (s, 3H), 2.17 (s, 3H).  **$^{13}C$  NMR** ( $CDCl_3$ , 150 MHz):  $\delta$  172.8, 142.7, 141.4, 141.1, 138.0, 136.1, 135.6, 129.9, 128.2, 128.1, 127.9, 127.8, 127.30, 127.27, 124.0, 123.2, 123.1, 58.1, 54.3, 21.32, 21.28. **HRMS** (MALDI-FT ICR) exact mass calculated,  $[M+H]^+$  calculated for  $C_{23}H_{22}NOS$ : 360.1417, found: 360.1413. HPLC analysis with Chiralpak IE-3 column, 70:30 *n*-hexane:2-propanol, 0.6 mL/min, 254 nm; minor enantiomer  $t_R = 24.3$  min, major enantiomer  $t_R = 22.9$  min.

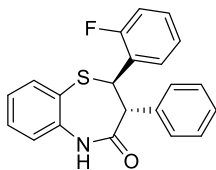
**(2*S*,3*R*)-2-(2-Fluorophenyl)-3-phenyl-2,3-dihydrobenzo[*b*][1,4] thiazepin-4(5*H*)-one (127l)**

White solid, 16.7 mg, 23% yield. **mp** 214.6–218.4 °C.  $[\alpha]_D^{18} = +5.4$  (0.59,  $CHCl_3$ ), 66% ee.  **$^1H$  NMR** ( $CDCl_3$ , 400 MHz):  $\delta$  8.20 (s, 1H), 8.08–8.04 (td, 1H,  $J = 7.5, 1.3$  Hz), 7.61 (d, 1H,  $J = 7.8$  Hz), 7.26–



7.25 (m, 1H), 7.17–7.13 (m, 2H), 7.10–7.06 (m, 3H), 6.99 (d, 2H,  $J = 7.5$  Hz), 6.91 (s, 1H), 6.80 (t, 1H,  $J = 8.9$ ), 5.48 (d, 1H,  $J = 6.6$  Hz), 4.21 (d, 1H,  $J = 6.6$  Hz), 2.38 (s, 3H).  $^{13}\text{C}$  NMR ( $\text{CDCl}_3$ , 100 MHz):  $\delta$  172.3, 160.8 (d,  $^1J_{\text{CF}} = 245.8$  Hz), 142.0, 141.0, 135.0, 134.4, 131.1, 130.4, 129.9 (d,  $^2J_{\text{CF}} = 8.4$  Hz), 127.5, 127.4, 124.9, 124.1 (d,  $^4J_{\text{CF}} = 2.9$  Hz), 123.9, 123.7, 123.6, 114.6 (d,  $^3J_{\text{CF}} = 22.8$  Hz), 51.0, 50.6, 21.2. **HRMS** (MALDI-FT ICR) exact mass calculated,  $[\text{M}+\text{H}]^+$  calculated for  $\text{C}_{22}\text{H}_{19}\text{FNOS}$ : 364.1166, found: 364.1163. HPLC analysis with Chiralpak IC column, 95:5 *n*-hexane:2-propanol, 1 mL/min, 254 nm; minor enantiomer  $t_R = 16.4$  min, major enantiomer  $t_R = 12.1$  min.

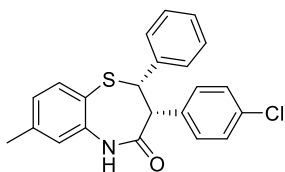
**(2*R*,3*R*)-2-(2-Fluorophenyl)-3-phenyl-2,3-dihydrobenzo[*b*][1,4]thiazepin-4(5*H*)-one (127I)**



Cream coloured solid, 18.2 mg, 25% yield. **mp** 201.0–205.9 °C.  $[\alpha]_{\text{D}}^{18} = -369.0$  (c 0.62,  $\text{CHCl}_3$ ), 94% ee.  $^1\text{H}$  NMR ( $\text{CDCl}_3$ , 400 MHz):  $\delta$  7.89 (bs, 1H), 7.46 (d, 1H,  $J = 7.8$  Hz), 7.24–7.22 (m, 2H), 7.17–7.13 (m, 3H), 7.11–7.05 (m, 2H), 7.03–6.98 (m, 2H), 6.89 (t, 1H,  $J = 7.5$  Hz), 6.82 (t, 1H,  $J = 9.3$  Hz), 5.30 (d, 1H,  $J = 12.5$  Hz), 4.24 (d, 1H,  $J = 12.4$  Hz), 2.43 (s, 3H).  $^{13}\text{C}$  NMR ( $\text{CDCl}_3$ , 100 MHz):  $\delta$  172.8, 158.9 (d,  $^1J_{\text{CF}} = 245.4$  Hz), 141.23, 141.20, 135.9, 135.2, 129.7, 128.7 (d,  $^3J_{\text{CF}} = 8.3$  Hz), 128.0, 127.6 (d,  $^2J_{\text{CF}} = 23.9$  Hz), 127.18, 127.15, 124.1 (d, 4 JCF = 3.4 Hz), 124.0, 122.6, 115.5 (d,  $^2J_{\text{CF}} = 22.4$  Hz), 52.9, 50.0, 21.3. **HRMS** (MALDI-FT ICR) exact mass calculated,  $[\text{M}+\text{H}]^+$  calculated for  $\text{C}_{22}\text{H}_{19}\text{FNOS}$ : 364.1166, found: 364.1163. HPLC analysis with Chiralpak IC column, 90:10

*n*-hexane:2-propanol, 1 mL/min, 254 nm; minor enantiomer  $t_R = 17.8$  min, major enantiomer  $t_R = 18.9$  min.

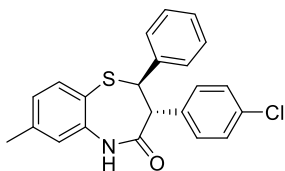
**(2*S*,3*R*)-3-(4-Chlorophenyl)-7-methyl-2-phenyl-2,3-dihydrobenzo[*b*][1,4]thiazepin-4(5*H*)-one (127*m*)**



White solid, 20.5 mg, 27% yield. **mp** 192.8–194.0 °C.  $[\alpha]_D^{17} = +47.0$  (c 0.52, CHCl<sub>3</sub>), 73% ee. **<sup>1</sup>H NMR** (CDCl<sub>3</sub>, 600 MHz):  $\delta$  7.78 (s, 1H), 7.59 (d, 1H,  $J = 7.8$

Hz), 7.32–7.25 (m, 5H), 7.09 (d, 1H,  $J = 7.1$  Hz), 7.02 (d, 2H,  $J = 8.5$  Hz), 6.94 (s, 1H), 6.85 (d, 2H,  $J = 8.5$  Hz), 4.89 (d, 1H,  $J = 6.5$  Hz), 4.16 (d, 1H,  $J = 6.4$  Hz), 2.40 (s, 3H). **<sup>13</sup>C NMR** (CDCl<sub>3</sub>, 150 MHz):  $\delta$  171.6, 141.8, 140.9, 136.0, 134.8, 133.4, 133.2, 132.1, 130.1, 128.7, 128.1, 127.59, 127.57, 125.3, 123.8, 61.0, 50.5, 21.2. **HRMS** (MALDI-FT ICR) exact mass calculated,  $[M+H]^+$  calculated for C<sub>22</sub>H<sub>19</sub>ClNOS: 380.0870, found: 380.0866. HPLC analysis with Chiralpak IC column, 95:5 *n*-hexane:2-propanol, 1 mL/min, 254 nm; minor enantiomer  $t_R = 21.6$  min, major enantiomer  $t_R = 13.8$  min.

**(2*R*,3*R*)-3-(4-Chlorophenyl)-7-methyl-2-phenyl-2,3-dihydrobenzo[*b*][1,4]thiazepin-4(5*H*)-one (127*m*)**

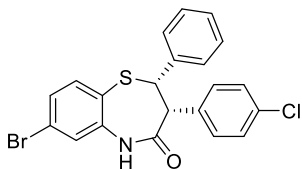


White solid, 16.7 mg, 22% yield. **mp** 180.6 °C (Decomp.).  $[\alpha]_D^{20} = -518.8$  (c 0.98, CHCl<sub>3</sub>), 95% ee. **<sup>1</sup>H NMR** (CDCl<sub>3</sub>, 400 MHz):  $\delta$  7.71 (s, 1H), 7.51 (d, 1H,  $J$

$= 7.8$  Hz), 7.12–7.09 (m, 8H), 7.03 (s, 1H), 6.94–6.91 (m, 2H), 4.77 (d, 1H,  $J = 12.2$  Hz), 4.13 (d, 1H,  $J = 12.2$  Hz), 2.44 (s, 3H). **<sup>13</sup>C NMR** (CDCl<sub>3</sub>, 100 MHz):  $\delta$  172.4, 142.6, 141.3, 141.1, 136.0, 134.1, 133.2, 131.2, 128.5, 128.1, 128.0, 127.5, 126.3, 124.1, 122.8, 58.2,

53.8, 21.3. **HRMS** (MALDI-FT ICR) exact mass calculated,  $[M+H]^+$  calculated for  $C_{22}H_{19}ClNOS$ : 380.0870, found: 380.0866. HPLC analysis with Chiralpak IC column, 80:20 *n*-hexane:2-propanol, 1 mL/min, 254 nm; minor enantiomer  $t_R = 8.4$  min, major enantiomer  $t_R = 10.9$  min.

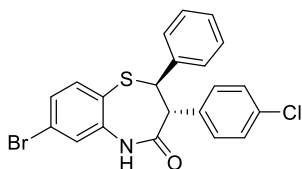
**(2*S*,3*R*)-7-Bromo-3-(4-chlorophenyl)-2-phenyl-2,3-dihydrobenzo[b][1,4]thiazepin-4(5*H*)-one (127*n*)**



White solid, 32.9 mg, 37% yield. **mp** 60.4–65.4 °C.  $[\alpha]_D^{25} = +23.38$  (c 0.61,  $CHCl_3$ ), 72% ee. **<sup>1</sup>H NMR** ( $CDCl_3$ , 400 MHz):  $\delta$  8.32 (bs, 1H), 7.57 (d, 1H,  $J =$

8.2 Hz), 7.42–7.39 (dd, 1H,  $J = 8.3, 1.9$ ), 7.314–7.309 (m, 1H), 7.22–7.21 (m, 4H), 7.15 (d, 1H,  $J = 7.4$  Hz), 7.10 (m, 2H), 6.93 (d, 2H,  $J = 7.5$  Hz), 4.92 (d, 1H,  $J = 6.3$  Hz), 4.16 (d, 1H,  $J = 6.3$  Hz). **<sup>13</sup>C NMR** ( $CDCl_3$ , 75 MHz):  $\delta$  172.0, 136.0, 134.6, 134.4, 134.0, 131.4, 130.6, 129.6, 129.4, 128.9, 128.3, 127.7, 127.4, 126.2, 123.9, 60.6, 50.9. **HRMS** (MALDI-FT ICR) exact mass calculated,  $[M+H]^+$  calculated for  $C_{21}H_{16}BrClNOS$ : 442.9640, found: 442.9637. HPLC analysis with Chiralpak IE3 column, 70:30 *n*-hexane:2-propanol, 0.6 mL/min, 220 nm; minor enantiomer  $t_R = 17.1$  min, major enantiomer  $t_R = 10.7$  min.

**(2*R*,3*R*)-7-Bromo-3-(4-chlorophenyl)-2-phenyl-2,3-dihydrobenzo [b][1,4]thiazepin-4(5*H*)-one (127*n*)**



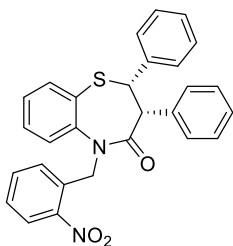
White solid, 26.7 mg, 30% yield. **mp** 206.2–210.7 °C.  $[\alpha]_D^{18} = -405.1$  (c 0.77,  $CHCl_3$ ), 99% ee. **<sup>1</sup>H NMR** ( $CDCl_3$ , 400 MHz):  $\delta$  8.26 (bs, 1H), 7.47–7.41 (m,

2H), 7.385–7.381 (m, 1H), 7.18–7.13 (m, 5H), 7.07 (d, 2H,  $J = 8.4$  Hz), 6.86 (d, 2H,  $J = 8.4$  Hz), 4.86 (d, 1H,  $J = 12.2$  Hz), 4.07 (d, 1H,  $J = 12.2$  Hz).  $^{13}\text{C}$  NMR ( $\text{CDCl}_3$ , 100 MHz):  $\delta$  172.6, 142.9, 140.9, 137.1, 134.7, 133.2, 130.0, 129.8, 128.7, 128.2, 127.7, 127.6, 126.4, 124.9, 124.3, 57.6, 54.3. **HRMS** (MALDI-FT ICR) exact mass calculated,  $[\text{M}+\text{H}]^+$  calculated for  $\text{C}_{21}\text{H}_{16}\text{BrCINOS}$ : 442.9640, found: 442.9637. HPLC analysis with Chiralpak IC column, 70:30 *n*-hexane:2-propanol, 1 mL/min, 254 nm; minor enantiomer  $t_R = 10.5$  min, major enantiomer  $t_R = 7.9$  min.

### Synthesis of *N*-*o*-nitrobenzyl-1,5-benzothiazepines (**138**)

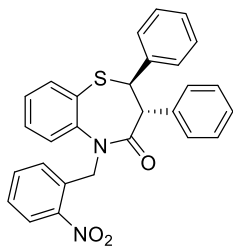
*trans*- or *cis*-1,5-benzothiazepine **138a** (33.1 mg, 0.1 mmol) was dissolved in ethyl acetate (770  $\mu\text{L}$ ); then, 1-(iodomethyl)-2-nitrobenzene **137** (52.6 mg, 0.2 mmol) and potassium carbonate (27.6 mg, 0.2 mmol) were added and the mixture was stirred at 85  $^\circ\text{C}$  for 48 hours. After completion, the mixture was cooled to room temperature and diluted with ethyl acetate. The aqueous phase was extracted with ethyl acetate (50 mL  $\times$  3); then, the combined organic phases were washed with saturated aqueous NaCl and dried over anhydrous  $\text{Na}_2\text{SO}_4$ . After concentration under reduced pressure, the crude mixture was purified using flash chromatography (hexane/ethyl acetate 100/0 – 90/10) to give pure *trans*-**138** or *cis*-**138**.

**(2*S*,3*R*)-5-(2-Nitrobenzyl)-2,3-diphenyl-2,3-dihydrobenzo[*b*][1,4] thiazepin-4(5*H*)-one (*cis*-138)**



White solid, 34.1 mg, 73% yield. **mp** 142.8–146.4 °C.  $[\alpha]_D^{24} = -118.1$  (c 0.74, CHCl<sub>3</sub>), 74% ee. **<sup>1</sup>H NMR** (CDCl<sub>3</sub>, 400 MHz): δ 8.04–8.00 (m, 2H), 7.78–7.75 (dd, 1H, *J* = 7.6, 1.5 Hz), 7.63–7.59 (td, 1H, *J* = 7.6, 1.2 Hz), 7.50–7.46 (m, 1H), 7.44–7.39 (m, 1H), 7.37–7.29 (m, 3H), 7.25–7.22 (m, 2H), 7.17–7.15 (m, 2H), 7.13–7.10 (m, 1H), 7.05–7.01 (m, 2H), 6.92–6.90 (m, 2H), 5.61 and 5.57 (ABq, 2H, *J* = 17.3 Hz), 4.87 (d, 1H, *J* = 6.8 Hz) 4.29 (d, 1H, *J* = 6.8 Hz). **<sup>13</sup>C NMR** (CDCl<sub>3</sub>, 100 MHz): δ 171.1, 148.1, 146.8, 135.8, 134.6, 133.6, 133.0, 130.8, 130.7, 130.1, 129.83, 129.79, 128.6, 128.0, 127.5, 127.41, 127.39, 125.0, 123.6, 61.1, 51.6, 50.5. **HRMS** (MALDI-FT ICR) exact mass calculated,  $[M+H]^+$  calculated for C<sub>28</sub>H<sub>22</sub>N<sub>2</sub>KO<sub>3</sub>S: 505.0983, found: 505.0978. HPLC analysis with Chiralpak IC column, 95:5 *n*-hexane:2-propanol, 1 mL/min, 220 nm; minor enantiomer *t<sub>R</sub>* = 39.8 min, major enantiomer *t<sub>R</sub>* = 25.5 min.

**(2*R*,3*R*)-5-(2-Nitrobenzyl)-2,3-diphenyl-2,3-dihydrobenzo[*b*][1,4] thiazepin-4(5*H*)-one (*trans*-138)**



White solid, 34.5 mg, 74% yield. **mp** 188.8–191.5 °C.  $[\alpha]_D^{22} = -466.5$  (c 0.78, CHCl<sub>3</sub>), 91% ee. **<sup>1</sup>H NMR** (CDCl<sub>3</sub>, 400 MHz): δ 7.96 (d, 1H, *J* = 8.2 Hz), 7.90 (d, 1H, *J* = 7.8 Hz), 7.62–7.51 (m, 3H), 7.42 (d, 1H, *J* = 8.0 Hz), 7.37 (t, 1H, *J* = 7.8 Hz), 7.31 (t, 1H, *J* = 7.5 Hz), 7.23–7.21 (m, 2H), 7.16–7.08 (m, 6H), 6.91–6.88 (m, 2H), 5.54 and 5.50 (ABq, 2H, *J* =

17.2 Hz), 4.95 (d, 1H,  $J = 12.2$  Hz), 4.28 (d, 1H,  $J = 12.2$  Hz).  $^{13}\text{C}$  NMR ( $\text{CDCl}_3$ , 100 MHz):  $\delta$  172.3, 148.0, 145.9, 142.2, 137.0, 135.5, 133.6, 132.6, 131.0, 129.9, 129.7, 128.4, 127.99, 127.95, 127.5, 127.4, 127.0, 126.3, 124.8, 123.5, 57.9, 54.8, 49.9. HRMS (MALDI-FT ICR) exact mass calculated,  $[\text{M}+\text{H}]^+$  calculated for  $\text{C}_{28}\text{H}_{22}\text{N}_2\text{K}_2\text{O}_3\text{S}$ : 505.0983, found: 505.0978. HPLC analysis with Chiralpak AD column, 70:30 *n*-hexane:2-propanol, 1 mL/min, 254 nm; minor enantiomer  $t_R = 22.6$  min, major enantiomer  $t_R = 27.7$  min.

### 8.3 1,5,7-Triazabicyclo[4.4.0]-dec-5-ene (TBD) Triggered diastereoselective [3+2] cycloaddition of azomethine imines and pyrazoleamides (TBD)

#### Experimental procedures and compounds characterization

Catalyst **96** was purchased from Strem Chemicals and used as received. Quinine and catalyst **149** were purchased from Aldrich and used as received. Catalysts **25a-b**<sup>177</sup>, **71a**<sup>178</sup>, **133a**<sup>179</sup>, **155a-b**<sup>32</sup> are known compounds, they were prepared according to the literature. The pyrazolamides **81** were prepared by using general procedures reported in the literature.<sup>180</sup> The ylides **139** were prepared by using general procedures reported in the literature.<sup>181</sup>

<sup>177</sup> B. Vakulya, S. Varga, A. Csámpai, T. Soós *Org. Lett.* **2005**, *7*, 1967.

<sup>178</sup> a) H. Jiang, M. W. Paixão, D. Monge, K. A. Jørgensen *J. Am. Chem. Soc.* **2010**, *132*, 2775; b) J. George, B. Sridhar, B. V. S. Reddy *Org. Biomol. Chem.* **2014**, *12*, 1595.

<sup>179</sup> S. Meninno, J. Overgaard, A. Lattanzi *Synthesis* **2017**, *49*, 1509

<sup>180</sup> J. Zhang, X. Liu, R. Wang *Chem. Eur. J.* **2014**, *20*, 4911.

<sup>181</sup> (a) S. T. Perri, S. C. Slater, S. G. Toske, J. D. White *J. Org. Chem.* **1990**, *55*, 6037; (b) E. Gould, T. Lebl, A. M. Z. Slawin, M. Reid, A. D. Smith *Tetrahedron* **2010**, *66*, 8992; (c) R. Shintani, G. C. Fu *J. Am. Chem. Soc.* **2003**, *125*, 10778.

**General procedure for the synthesis of bicyclic pyrazolidinones (145)**

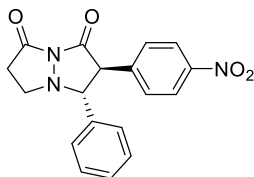
In an oven-dried vial *N*-acylpyrazole **81** (0.15 mmol), ylide **139** (0.18 mmol), 4Å molecular sieves (~150 mg) and dry dichloromethane (750 μL) were introduced. To this solution 1,5,7-triazabicyclo[4.4.0]dec-5-ene (0.015 mmol) was added under nitrogen atmosphere. The reaction mixture was stirred at room temperature and monitored by TLC. After completion, the crude reaction mixture was purified by flash chromatography (eluent: hexane, hexane/dichloromethane 1/1, dichloromethane/ethyl acetate 100/0 to 95/5) to afford products **145** as an inseparable mixture of *trans* or *trans,cis* predominating diastereomers in 49-93% yield.

**General procedure for the enantioselective synthesis of bicyclic pyrazolidinone 145a**

In an oven-dried vial *N*-acylpyrazole **81a** (0.1 mmol), ylide **139a** (0.12 mmol), 4Å molecular sieves (~100 mg) and dry mesitylene (500 μL) were introduced. To this solution catalyst **25b** (0.02 mmol) was added under nitrogen atmosphere. The reaction mixture was stirred at room temperature and monitored by TLC. After completion, the crude reaction mixture was purified by flash chromatography (eluent: hexane, hexane/dichloromethane 1/1, dichloromethane/ethyl acetate 100/0 to 95/5) to afford product **145a** in 60% yield, 96/4 dr and 70% ee .

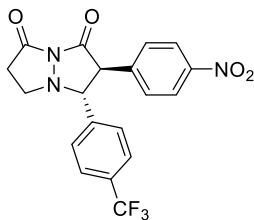


**(2*S*\*,3*R*\*)-2-(4-nitrophenyl)-3-phenyltetrahydro-1*H*,7*H*-pyrazolo[1,2-*a*]pyrazole-1,7-dione (145a)**



Light yellow solid, 20.2 mg, 60% yield. **mp** 176.4-180.5 °C.  $[\alpha]_D^{27} = +9.6$  (c 0.39, CHCl<sub>3</sub>), 70% ee. **FTIR**<sub>v<sub>max</sub></sub>(KBr)/cm<sup>-1</sup>: 1783, 1700, 1525, 1349, 1319. **<sup>1</sup>H NMR** (CDCl<sub>3</sub>, 400 MHz):  $\delta$  8.17 (d, 2H, *J* = 8.6 Hz), 8.02 (d, 0.08H, *J* = 8.6 Hz, minor), 7.38-7.37 (m, 3H), 7.28-7.26 (m, 4H), 7.20-7.18 (m, 0.19H, minor), 7.08-7.06 (m, 0.1H, minor), 4.60 (d, 0.04H, *J* = 7.8 Hz, minor), 4.36 (d, 0.04H, *J* = 7.8 Hz, minor), 4.29 (d, 1H, *J* = 12.5 Hz), 4.00 (d, 1H, *J* = 12.5 Hz), 3.64-3.60 (m, 1H), 3.19-3.09 (m, 1H), 2.98-2.86 (m, 2H). **<sup>13</sup>C NMR** (CDCl<sub>3</sub>, 100 MHz):  $\delta$  164.8, 162.9, 147.7, 139.6, 133.7, 130.3, 129.5, 129.1, 127.3, 123.9, 78.9, 61.8, 52.0, 36.4. **HRMS (ESI-FT ICR)** exact mass calculated [M+H]<sup>+</sup> calculated for C<sub>18</sub>H<sub>16</sub>N<sub>3</sub>O<sub>4</sub>: 338.1140, found: 338.1173. HPLC analysis with Chiralpak AD column, 50:50 *n*-hexane:2-propanol, 0.6 mL/min, 254 nm; minor enantiomer *t<sub>R</sub>* = 34.1 min, major enantiomer *t<sub>R</sub>* = 19.8 min.

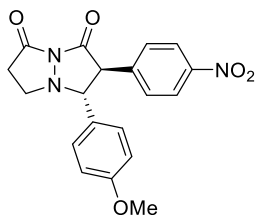
**(2*S*\*,3*R*\*)-2-(4-nitrophenyl)-3-(4-(trifluoromethyl)phenyl)tetrahydro-1*H*,7*H*-pyrazolo[1,2-*a*]pyrazole-1,7-dione (145b)**



White solid, 46.2 mg, 76% yield. **mp** 188.0-189.9 °C. **FTIR**<sub>v<sub>max</sub></sub>(KBr)/cm<sup>-1</sup>: 1783, 1708, 1603, 1525, 1349, 1326, 1285, 1168, 1127, 1070. **<sup>1</sup>H NMR** (CDCl<sub>3</sub>, 400 MHz):  $\delta$  8.19 (d, 2H, *J* = 8.2 Hz), 7.63 (d, 2H, *J* = 8.0 Hz), 7.38 (d, 2H, *J* = 8.0 Hz), 7.25 (d, 2H, *J* = 8.2 Hz), 4.62 (d, 0.04H, *J* = 7.3 Hz, minor), 4.37 (d, 0.04H, *J* = 7.3 Hz, minor), 4.23 (d, 1H, *J*

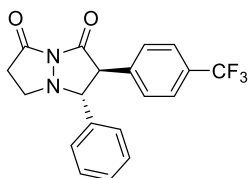
= 12.4 Hz), 4.03 (d, 1H,  $J = 12.4$  Hz), 3.63-3.59 (m, 1H), 3.19-3.07 (m, 1H), 2.96-2.87 (m, 2H).  $^{13}\text{C}$  NMR ( $\text{CDCl}_3$ , 100 MHz):  $\delta$  164.4, 162.3, 148.0, 139.1, 138.0, 131.8 (q,  $^2J_{\text{CF}} = 32.7$  Hz), 130.4, 127.7, 126.2 (q,  $^3J_{\text{CF}} = 3.4$  Hz), 124.2, 123.6 (q,  $^1J_{\text{CF}} = 272.6$  Hz), 78.3, 62.0, 52.1, 36.4. **HRMS (ESI-FT ICR)** exact mass calculated  $[\text{M}+\text{Na}]^+$  calculated for  $\text{C}_{19}\text{H}_{14}\text{F}_3\text{N}_3\text{NaO}_4$ : 428.0829, found: 428.0836.

**(2*S*\*,3*R*\*)-3-(4-methoxyphenyl)-2-(4-nitrophenyl)tetrahydro-1*H*,7*H*-pyrazolo[1,2-*a*]pyrazole-1,7-dione (145c)**



Yellow solid, 51.2 mg, 93% yield. **mp** 171.6-173.4 °C. **FTIR** $\nu_{\text{max}}$ (KBr)/ $\text{cm}^{-1}$ : 1783, 1706, 1612, 1517, 1348, 1314, 1287, 1252.  $^1\text{H}$  NMR ( $\text{CDCl}_3$ , 400 MHz):  $\delta$  8.14 (d, 2H,  $J = 8.6$  Hz), 8.02 (d, 0.06H,  $J = 8.6$  Hz, minor), 7.24 (d, 2H,  $J = 8.6$  Hz), 7.17 (d, 2H,  $J = 8.6$  Hz), 6.94 (d, 0.06H,  $J = 8.6$  Hz, minor), 6.86 (d, 2H,  $J = 8.6$  Hz), 6.68 (d, 0.06H,  $J = 8.6$  Hz, minor), 4.49 (d, 0.03H,  $J = 7.6$  Hz, minor), 4.27 (d, 0.03H,  $J = 7.6$  Hz, minor), 4.23 (d, 1H,  $J = 12.4$  Hz), 3.88 (d, 1H,  $J = 12.4$  Hz), 3.80 (s, 3H), 3.71 (s, 0.1H, minor), 3.58-3.54 (m, 1H), 3.10-3.05 (m, 1H), 2.92-2.82 (m, 2H).  $^{13}\text{C}$  NMR ( $\text{CDCl}_3$ , 100 MHz):  $\delta$  164.8, 163.0, 160.4, 147.7, 139.8, 130.3, 128.6, 125.4, 123.9, 114.5, 78.7, 61.7, 55.3, 51.9, 36.4. **HRMS (ESI-FT ICR)** exact mass calculated  $[\text{M}+\text{Na}]^+$  calculated for  $\text{C}_{19}\text{H}_{17}\text{N}_3\text{NaO}_5$ : 390.1060, found: 390.1067.

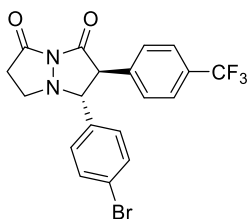
**(2*S*\*,3*R*\*)-3-phenyl-2-(4-(trifluoromethyl)phenyl)tetrahydro-1*H*,7*H*-pyrazolo[1,2-*a*]pyrazole-1,7-dione (145d)<sup>99</sup>**



Data for this compound are consistent with those reported in the literature.

White solid, 39.5 mg, 73% yield. **mp** 171.1-173.3 °C. **FTIR**<sub>v<sub>max</sub></sub>(KBr)/cm<sup>-1</sup>: 1784, 1706, 1322, 1171, 1126, 1070. **<sup>1</sup>H NMR** (CDCl<sub>3</sub>, 400 MHz): δ 7.54 (d, 2H, *J* = 8.1 Hz), 7.35-7.33 (m, 3H), 7.26-7.24 (m, 2H), 7.20 (d, 2H, *J* = 8.1 Hz), 7.10-7.08 (m, 0.06H, minor), 7.04-7.02 (m, 0.06H, minor), 4.55 (d, 0.03H, *J* = 7.6 Hz, minor), 4.28 (d, 0.03H, *J* = 7.6 Hz, minor), 4.21 (d, 1H, *J* = 12.5 Hz), 3.98 (d, 1H, *J* = 12.5 Hz), 3.60-3.56 (m, 1H), 3.13-3.04 (m, 1H), 2.96-2.83 (m, 2H). **<sup>13</sup>C NMR** (CDCl<sub>3</sub>, 100 MHz): δ 164.9, 163.5, 136.5, 134.0, 130.3 (q, <sup>2</sup>*J*<sub>CF</sub> = 32.5 Hz), 129.7, 129.2, 128.9, 127.3, 125.7 (q, <sup>3</sup>*J*<sub>CF</sub> = 3.4 Hz), 123.8 (q, <sup>1</sup>*J*<sub>CF</sub> = 270.6 Hz), 78.9, 61.9, 52.0, 36.4. **HRMS (ESI-FT ICR)** exact mass calculated [M+Na]<sup>+</sup> calculated for C<sub>19</sub>H<sub>15</sub>F<sub>3</sub>N<sub>2</sub>NaO<sub>2</sub>: 383.0978, found: 383.0982.

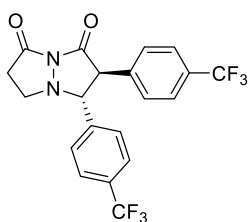
**(2*S*\*,3*R*\*)-3-(4-bromophenyl)-2-(4-(trifluoromethyl)phenyl)tetrahydro-1*H*,7*H*-pyrazolo[1,2-*a*]pyrazole-1,7-dione (145e)**



White solid, 46.6 mg, 71% yield. **mp** 177.4-179.5 °C. **FTIR**<sub>v<sub>max</sub></sub>(KBr)/cm<sup>-1</sup>: 1783, 1320, 1129, 1070. **<sup>1</sup>H NMR** (CDCl<sub>3</sub>, 400 MHz): δ 7.55 (d, 2H, *J* = 8.1 Hz), 7.47 (d, 2H, *J* = 8.4 Hz), 7.18 (d, 2H, *J* = 8.1 Hz), 7.12 (d, 2H, *J* = 8.4 Hz), 6.92 (d, 0.07H, *J* = 8.4 Hz, minor), 4.50 (d, 0.03H, *J* = 7.5 Hz, minor), 4.26 (d, 0.03H, *J* = 7.5 Hz, minor), 4.13 (d, 1H, *J* = 12.5 Hz), 3.94 (d, 1H, *J* = 12.5 Hz), 3.58-3.54 (m, 1H), 3.14-3.04 (m, 1H),

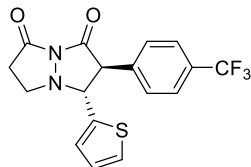
2.94-2.83 (m, 2H).  $^{13}\text{C}$  NMR ( $\text{CDCl}_3$ , 100 MHz):  $\delta$  164.8, 163.2, 136.1, 133.2, 132.2, 130.5 (q,  $^2J_{\text{CF}} = 32.4$  Hz), 129.7, 128.9, 125.8 (q,  $^3J_{\text{CF}} = 3.5$  Hz), 123.7 (q,  $^1J_{\text{CF}} = 270.8$  Hz), 123.3, 78.2, 62.0, 52.0, 36.3. **HRMS (ESI-FT ICR)** exact mass calculated  $[\text{M}+\text{Na}]^+$  calculated for  $\text{C}_{19}\text{H}_{14}^{79}\text{BrF}_3\text{N}_2\text{NaO}_2$ : 461.0083, found: 461.0089; exact mass calculated  $[\text{M}+\text{Na}]^+$  calculated for  $\text{C}_{19}\text{H}_{14}^{81}\text{BrF}_3\text{N}_2\text{NaO}_2$ : 463.0063, found: 463.0069.

**(2*S*\*,3*R*\*)-2,3-bis(4-(trifluoromethyl)phenyl)tetrahydro-1*H*,7*H*-pyrazolo[1,2-*a*]pyrazole-1,7-dione (145f)**



White solid, 46.9 mg, 73% yield. **mp** 175.8-177.8 °C. **FTIR** $_{\text{vmax}}(\text{KBr})/\text{cm}^{-1}$ : 1783, 1710, 1675, 1622, 1559, 1507, 1456, 1325, 1169, 1125, 1071.  $^1\text{H}$  NMR ( $\text{CDCl}_3$ , 400 MHz):  $\delta$  7.61 (d, 2H,  $J = 8.3$  Hz) overlapped with 7.58 (d, 2H,  $J = 8.3$  Hz), 7.37 (d, 2H,  $J = 8.1$  Hz), 7.19 (d, 2H,  $J = 8.1$  Hz), 7.11 (d, 0.05H,  $J = 8.2$  Hz, minor), 4.59 (d, 0.02H,  $J = 7.7$  Hz, minor), 4.31 (d, 0.02H,  $J = 7.7$  Hz, minor), 4.16 (d, 1H,  $J = 12.4$  Hz), 4.02 (d, 1H,  $J = 12.4$  Hz), 3.61-3.57 (m, 1H), 3.17-3.05 (m, 1H), 2.95-2.85 (m, 2H).  $^{13}\text{C}$  NMR ( $\text{CDCl}_3$ , 100 MHz):  $\delta$  164.6, 162.9, 138.4, 136.0, 131.6 (q,  $^2J_{\text{CF}} = 32.6$  Hz), 130.8 (q,  $^2J_{\text{CF}} = 32.5$  Hz), 129.8, 127.7, 126.0 (q,  $^3J_{\text{CF}} = 3.7$  Hz), 123.8 (q,  $^1J_{\text{CF}} = 270.4$  Hz), 123.7 (q,  $^1J_{\text{CF}} = 269.6$  Hz), 78.3, 62.1, 52.1, 36.4. **HRMS (ESI-FT ICR)** exact mass calculated  $[\text{M}+\text{Na}]^+$  calculated for  $\text{C}_{20}\text{H}_{14}\text{F}_6\text{N}_2\text{NaO}_2$ : 451.0852, found: 451.0867.

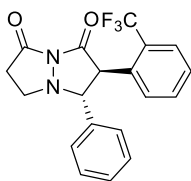
**(2*S*\*,3*R*\*)-3-(thiophen-2-yl)-2-(4-(trifluoromethyl)phenyl)tetrahydro-1*H*,7*H*-pyrazolo[1,2-*a*]pyrazole-1,7-dione (145g)**



White solid, 31.3 mg, 57% yield. **mp** 188.8-190.5 °C. **FTIR** $\nu_{\max}$ (KBr)/ $\text{cm}^{-1}$ : 1785, 1705, 1324, 1173, 1126, 1070.  **$^1\text{H NMR}$**  ( $\text{CDCl}_3$ , 400 MHz):  $\delta$  7.60 (d, 2H,  $J = 7.9$  Hz), 7.39-

7.38 (m, 1H), 7.28 (d, 2H,  $J = 7.9$  Hz), 6.97-6.94 (m, 1H), 6.78-6.77 (m, 1H), 4.31 (d, 1H,  $J = 12.2$  Hz), 4.23 (d, 1H,  $J = 12.2$  Hz), 3.74-3.70 (m, 1H), 3.17-3.08 (m, 1H), 3.02-2.95 (m, 1H), 2.92-2.86 (m, 1H).  **$^{13}\text{C NMR}$**  ( $\text{CDCl}_3$ , 100 MHz):  $\delta$  164.7, 163.0, 136.9, 136.1, 130.5 (q,  $^2J_{\text{CF}} = 32.5$  Hz), 129.6, 127.2, 127.0, 126.7, 125.8 (q,  $^3J_{\text{CF}} = 3.4$  Hz), 123.8 (q,  $^1J_{\text{CF}} = 270.6$  Hz), 74.3, 62.5, 52.0, 36.3. **HRMS (MALDI-FT ICR)** exact mass calculated  $[\text{M}+\text{K}]^+$  calculated for  $\text{C}_{17}\text{H}_{13}\text{F}_3\text{N}_2\text{KO}_2\text{S}$ : 405.0281, found: 405.0280.

**(2*S*\*,3*R*\*)-3-phenyl-2-(2-(trifluoromethyl)phenyl)tetrahydro-1*H*,7*H*-pyrazolo[1,2-*a*]pyrazole-1,7-dione (145h)**

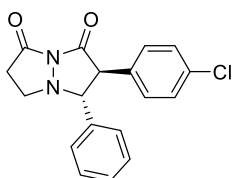


White solid, 38.4 mg, 71% yield. **mp** 177.4-180.2 °C. **FTIR** $\nu_{\max}$ (KBr)/ $\text{cm}^{-1}$ : 1785, 1703, 1698, 1669, 1653, 1617, 1559, 1506, 1315, 1219, 1129, 772.  **$^1\text{H NMR}$**  ( $\text{CDCl}_3$ , 400 MHz):  $\delta$  7.69-7.68

(m, 2H), 7.59 (d, 1H,  $J = 7.9$  Hz), 7.44-7.41 (m, 1H), 7.30-7.29 (m, 3H), 7.24-7.22 (m, 2H), 4.77 (d, 0.04H,  $J = 8.0$  Hz, minor), 4.63 (d, 1H,  $J = 12.2$  Hz), 4.56 (d, 0.04H,  $J = 8.0$  Hz, minor), 4.22 (d, 1H,  $J = 12.2$  Hz), 3.63-3.59 (m, 1H), 3.15-3.06 (m, 1H), 3.00-2.85 (m, 2H).  **$^{13}\text{C NMR}$**  ( $\text{CDCl}_3$ , 100 MHz):  $\delta$  164.9, 163.7, 133.7, 132.2, 131.4, 130.6, 129.0, 128.7, 128.3, 128.0, 127.0, 126.2 (q,  $^3J_{\text{CF}} = 4.3$  Hz), 123.4 (q,  $^1J_{\text{CF}} = 272.6$  Hz), 79.6, 58.2, 52.0, 36.3. **HRMS (MALDI-**

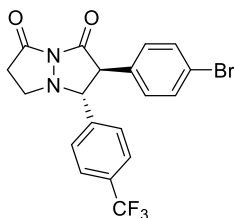
**FT ICR)** exact mass calculated  $[M+Na]^+$  calculated for  $C_{19}H_{15}F_3N_2NaO_2$ : 383.0978, found: 383.0979.

**(2*S*\*,3*R*\*)-2-(4-chlorophenyl)-3-phenyltetrahydro-1*H*,7*H*-pyrazolo[1,2-*a*]pyrazole-1,7-dione (145i)**



White solid, 39.2 mg, 80% yield. **mp** 187.1-188.0 °C. **FTIR** $v_{max}$ (KBr)/ $cm^{-1}$ : 1782, 1709, 1496, 1318. **<sup>1</sup>H NMR** ( $CDCl_3$ , 400 MHz):  $\delta$  7.33-7.32 (m, 3H), 7.26-7.22 (m, 4H), 6.99 (d, 2H,  $J = 8.3$  Hz), 4.48 (d, 0.04H, minor,  $J = 7.3$  Hz), 4.17 (d, 0.04H, minor,  $J = 7.3$  Hz), 4.09 (d, 1H,  $J = 12.5$  Hz), 3.92 (d, 1H,  $J = 12.5$  Hz), 3.58-3.54 (m, 1H), 3.13-3.02 (m, 1H), 2.93-2.81 (m, 2H). **<sup>13</sup>C NMR** ( $CDCl_3$ , 100 MHz):  $\delta$  164.9, 163.9, 134.2, 134.1, 131.0, 130.6, 129.1, 128.94, 128.85, 127.3, 79.0, 61.7, 52.0, 36.4. **HRMS (MALDI-FT ICR)** exact mass calculated  $[M+Na]^+$  calculated for  $C_{18}H_{15}^{35}ClN_2NaO_2$ : 349.0714, found: 349.0713; exact mass calculated  $[M+Na]^+$  calculated for  $C_{18}H_{15}^{37}ClN_2NaO_2$ : 351.0685, found: 351.0684.

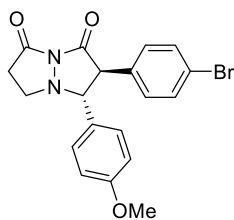
**(2*S*\*,3*R*\*)-2-(4-bromophenyl)-3-(4-(trifluoromethyl)phenyl)tetrahydro-1*H*,7*H*-pyrazolo[1,2-*a*]pyrazole-1,7-dione (145j)**



White solid, 42.8 mg, 65% yield. **mp** 206.3-208.3 °C. **FTIR** $v_{max}$ (KBr)/ $cm^{-1}$ : 1784, 1733, 1717, 1706, 1663, 1620, 1545, 1533, 1506, 1494, 1437, 1385, 1324, 1168. **<sup>1</sup>H NMR** ( $CDCl_3$ , 400 MHz):  $\delta$  7.60 (d, 2H,  $J = 7.9$  Hz), 7.45 (d, 2H,  $J = 8.0$  Hz), 7.36 (d, 2H,  $J = 7.9$  Hz), 7.29 (d, 0.06H,  $J = 8.0$  Hz, minor), 7.20 (d, 0.06H,  $J = 8.0$  Hz, minor), 6.93 (d, 2H,  $J = 8.0$  Hz), 6.86 (d, 0.06H,  $J = 8.0$  Hz), 4.53 (d, 0.03H,  $J = 7.5$  Hz,

minor), 4.20 (d, 0.03H,  $J = 7.5$  Hz, minor), 4.04 (d, 1H,  $J = 12.4$  Hz), 3.97 (d, 1H,  $J = 12.4$  Hz), 3.60-3.56 (m, 1H), 3.15-3.04 (m, 1H), 2.93-2.84 (m, 2H).  $^{13}\text{C}$  NMR ( $\text{CDCl}_3$ , 100 MHz):  $\delta$  164.6, 163.2, 138.6, 132.2, 131.4 (q,  $^2J_{\text{CF}} = 32.8$  Hz), 131.1, 130.9, 127.7, 126.0 (q,  $^3J_{\text{CF}} = 3.5$  Hz), 123.7 (q,  $^1J_{\text{CF}} = 270.7$  Hz), 122.8, 78.3, 62.0, 52.1, 36.3. **HRMS (ESI-FT ICR)** exact mass calculated  $[\text{M}+\text{Na}]^+$  calculated for  $\text{C}_{19}\text{H}_{14}^{79}\text{BrF}_3\text{N}_2\text{NaO}_2$ : 461.0083, found: 461.0088; exact mass calculated  $[\text{M}+\text{Na}]^+$  calculated for  $\text{C}_{19}\text{H}_{14}^{81}\text{BrF}_3\text{N}_2\text{NaO}_2$ : 463.0063, found: 463.0069.

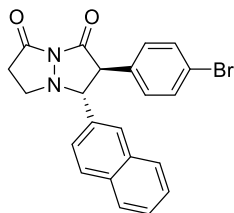
**(2*S*\*,3*R*\*)-2-(4-bromophenyl)-3-(4-methoxyphenyl) tetrahydro-1*H*,7*H*-pyrazolo[1,2-*a*]pyrazole-1,7-dione (145k)**



Light yellow solid, 43.3 mg, 72% yield. **mp** 165.0-167.5 °C. **FTIR** $\nu_{\text{max}}$ (KBr)/ $\text{cm}^{-1}$ : 1782, 1701, 1546, 1313, 1289, 1250.  $^1\text{H}$  NMR ( $\text{CDCl}_3$ , 400 MHz):  $\delta$  7.40 (d, 2H,  $J = 8.4$  Hz), 7.16 (d, 2H,  $J = 8.6$  Hz), 6.93 (d, 2H,  $J = 8.4$  Hz), 6.84 (d, 2H,  $J = 8.6$  Hz), 6.69-6.67 (m, 0.04H, minor), 4.39 (d, 0.02H,  $J = 7.4$  Hz, minor), 4.05 (d, 1H,  $J = 12.4$  Hz), 3.85 (d, 1H,  $J = 12.4$  Hz), 3.78 (s, 3H), 3.72 (s, 0.07H, minor), 3.55-3.51 (m, 1H), 3.10-2.98 (m, 1H), 2.89-2.79 (m, 2H).  $^{13}\text{C}$  NMR ( $\text{CDCl}_3$ , 100 MHz):  $\delta$  164.9, 163.9, 160.0, 131.9, 131.6, 130.9, 128.5, 125.9, 122.2, 114.2, 78.6, 61.6, 55.2, 51.9, 36.4. **HRMS (MALDI-FT ICR)** exact mass calculated  $[\text{M}+\text{Na}]^+$  calculated for  $\text{C}_{19}\text{H}_{17}^{79}\text{BrN}_2\text{NaO}_3$ : 423.0315, found: 423.0313; exact mass calculated  $[\text{M}+\text{Na}]^+$  calculated for  $\text{C}_{19}\text{H}_{17}^{81}\text{BrN}_2\text{NaO}_3$ : 425.0294, found: 425.0293.

**(2*S*\*,3*R*\*)-2-(4-bromophenyl)-3-(naphthalen-2-yl)tetrahydro-1*H*,7*H*-pyrazolo[1,2-*a*]pyrazole-1,7-dione (145l)**

White solid, 49.9 mg, 79% yield. **mp** 233.7-236.8 °C.

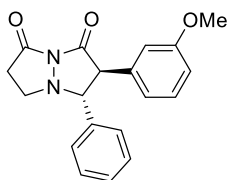


**FTIR** $\nu_{\max}$ (KBr)/ $\text{cm}^{-1}$ : 1782, 1700, 1331, 1292. **<sup>1</sup>H NMR** ( $\text{CDCl}_3$ , 400 MHz):  $\delta$  7.85 (d, 2H,  $J = 8.4$  Hz), 7.80-7.77 (m, 1H), 7.69 (s, 1H), 7.53-7.51 (m, 2H), 7.41 (d, 2H,  $J = 8.4$  Hz), 7.38-7.37 (m, 1H), 6.93 (d, 2H,  $J = 8.4$

Hz), 4.60 (d, 0.03H,  $J = 7.5$  Hz), 4.25 (d, 0.03H,  $J = 7.5$  Hz), 4.22 (d, 1H,  $J = 12.4$  Hz), 4.04 (d, 1H,  $J = 12.4$  Hz), 3.61-5.57 (m, 1H), 3.18-3.08 (m, 1H), 2.96-2.84 (m, 2H). **<sup>13</sup>C NMR** ( $\text{CDCl}_3$ , 100 MHz):  $\delta$  164.7, 163.7, 133.7, 133.1, 132.1, 131.7, 131.6, 130.9, 129.0, 128.0, 127.8, 127.2, 126.8, 126.7, 124.3, 122.5, 79.4, 61.7, 52.1, 36.5.

**HRMS (ESI-FT ICR)** exact mass calculated  $[\text{M}+\text{Na}]^+$  calculated for  $\text{C}_{22}\text{H}_{17}^{79}\text{BrN}_2\text{NaO}_2$ : 443.0366, found: 443.0367; exact mass calculated  $[\text{M}+\text{Na}]^+$  calculated for  $\text{C}_{22}\text{H}_{17}^{81}\text{BrN}_2\text{NaO}_2$ : 445.0345, found: 445.0346.

**(2*S*\*,3*R*\*)-2-(3-methoxyphenyl)-3-phenyltetrahydro-1*H*,7*H*-pyrazolo[1,2-*a*]pyrazole-1,7-dione (145m)**

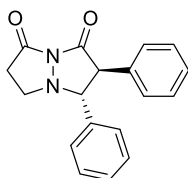


White solid, 35.8 mg, 74% yield. **mp** 142.5-144.0 °C. **FTIR** $\nu_{\max}$ (KBr)/ $\text{cm}^{-1}$ : 1785, 1708, 1601, 1587, 1495, 1455, 1316, 1300. **<sup>1</sup>H NMR** ( $\text{CDCl}_3$ , 400 MHz):  $\delta$  7.32-7.31 (m, 3H), 7.25-7.23 (m, 2H), 7.19 (t, 1H,  $J = 7.7$  Hz), 6.83-6.80 (m, 1H), 6.63 (d, 1H,  $J = 7.7$  Hz), 6.60 (s, 1H), 4.46 (d, 0.03H,  $J = 7.6$  Hz, minor), 4.16 (d, 0.03H,  $J = 7.6$  Hz, minor), 4.08 (d, 1H,  $J = 12.4$  Hz), 3.97 (d, 1H, = 12.4 Hz), 3.71 (s, 3H), 3.57-3.53 (m, 1H), 3.12-2.99



(m, 1H), 2.92-2.81 (m, 2H).  $^{13}\text{C}$  NMR ( $\text{CDCl}_3$ , 100 MHz):  $\delta$  164.9, 164.2, 159.6, 134.6, 133.8, 129.7, 128.9, 128.7, 127.3, 121.5, 114.7, 113.7, 78.8, 62.2, 55.1, 52.0, 36.4. **HRMS (MALDI-FT ICR)** exact mass calculated  $[\text{M}+\text{Na}]^+$  calculated for  $\text{C}_{19}\text{H}_{18}\text{N}_2\text{NaO}_3$ : 345.1210, found: 345.1210.

**(2*S*\*,3*R*\*)-2,3-diphenyltetrahydro-1*H*,7*H*-pyrazolo[1,2-*a*]pyrazole-1,7-dione (145*n*)<sup>99</sup>**

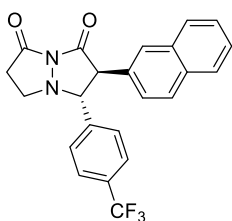


Data for this compound are consistent with those reported in the literature.

White solid, 29.4 mg, 67% yield. **mp** 191.1-192.8 °C. **FTIR**<sub>vmax</sub>(KBr)/ $\text{cm}^{-1}$ : 1785, 1706,

1318, 1301  $^1\text{H}$  NMR ( $\text{CDCl}_3$ , 400 MHz):  $\delta$  7.33-7.23 (m, 8H), 7.06-7.05 (m, 2H), 4.46 (d, 0.03H,  $J = 7.5$  Hz, minor), 4.20 (d, 0.03H,  $J = 7.5$  Hz, minor), 4.11 (d, 1H,  $J = 12.4$  Hz), 3.96 (d, 1H,  $J = 12.4$  Hz), 3.58-3.54 (m, 1H), 3.13-3.00 (m, 1H), 2.92-2.81 (m, 2H).  $^{13}\text{C}$  NMR ( $\text{CDCl}_3$ , 100 MHz):  $\delta$  164.9, 164.3, 134.6, 132.5, 129.2, 128.9, 128.73, 128.70, 128.1, 127.3, 79.0, 62.3, 52.0, 36.4. **HRMS (MALDI-FT ICR)** exact mass calculated  $[\text{M}+\text{Na}]^+$  calculated for  $\text{C}_{18}\text{H}_{16}\text{N}_2\text{NaO}_2$ : 315.1104, found: 315.1103.

**(2*S*\*,3*R*\*)-2-(naphthalen-2-yl)-3-(4-(trifluoromethyl)phenyl)tetrahydro-1*H*,7*H*-pyrazolo[1,2-*a*]pyrazole-1,7-dione (145*o*)**

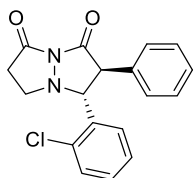


White solid, 46.8 mg, 76% yield. **mp** 124.1-130.8 °C. **FTIR**<sub>vmax</sub>(KBr)/ $\text{cm}^{-1}$ : 1783, 1705, 1324, 1170, 1130, 1069.  $^1\text{H}$  NMR ( $\text{CDCl}_3$ , 400 MHz):  $\delta$  7.81-7.78 (m, 2H), 7.72 (d, 1H,  $J = 7.7$  Hz), 7.56-7.54 (m, 3H), 7.50-7.44 (m,

2H), 7.35 (d, 2H,  $J = 7.7$  Hz), 7.20 (d, 1H,  $J = 8.4$  Hz), 4.55 (d, 0.03H,

$J = 7.6$  Hz, minor), 4.39 (d, 0.03H,  $J = 7.6$  Hz, minor), 4.24 (d, 1H,  $J = 12.4$  Hz), 4.18 (d, 1H,  $J = 12.4$  Hz), 3.61-3.57 (m, 1H), 3.16-3.07 (m, 1H), 2.99-2.86 (m, 2H).  $^{13}\text{C}$  NMR ( $\text{CDCl}_3$ , 100 MHz):  $\delta$  164.8, 163.9, 138.9, 133.2, 132.9, 131.0 (q,  $^2J_{\text{CF}} = 32.4$  Hz), 129.5, 129.1, 128.9, 127.8, 127.6, 126.5, 126.4, 126.2, 125.8 (q,  $^3J_{\text{CF}} = 3.6$  Hz), 123.7 (q,  $^1J_{\text{CF}} = 270.8$  Hz), 78.1, 62.7, 52.1, 36.4. **HRMS (MALDI-FT ICR)** exact mass calculated  $[\text{M}+\text{Na}]^+$  calculated for  $\text{C}_{23}\text{H}_{17}\text{F}_3\text{N}_2\text{NaO}_2$ : 433.1134, found: 433.1133.

**(2*S*\*,3*R*\*)-3-(2-chlorophenyl)-2-phenyltetrahydro-1*H*,7*H*-pyrazolo[1,2-*a*]pyrazole-1,7-dione (145p)<sup>99</sup>**



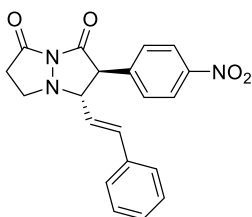
Data for this compound are consistent with those reported in the literature.

Light yellow solid, 35.3 mg, 72% yield.

**FTIR**<sub>vmax</sub>(KBr)/ $\text{cm}^{-1}$ : 1787, 1710, 1306, 1271.  **$^1\text{H}$  NMR** ( $\text{CDCl}_3$ , 400 MHz):  $\delta$  7.85 (d, 1H,  $J = 7.8$  Hz), 7.39-7.35 (m, 1H), 7.27-7.24 (m, 4H), 7.19-7.17 (m, 0.27H, minor), 7.09-7.07 (m, 3H), 7.03-7.01 (m, 0.54H, minor), 6.97-6.94 (m, 0.28H, minor), 4.76 (d, 0.27H,  $J = 7.6$  Hz, minor), 4.70 (d, 1H,  $J = 12.4$  Hz), 4.56 (d, 0.27H,  $J = 7.6$  Hz, minor), 4.16 (d, 1H,  $J = 12.4$  Hz), 3.65-3.61 (m, 0.27H, minor), 3.50-3.46 (m, 1H), 3.22-3.11 (m, 0.27H, minor), 3.07-2.79 (m, 3H major + 0.54H minor).  $^{13}\text{C}$  NMR ( $\text{CDCl}_3$ , 100 MHz):  $\delta$  165.1 (minor), 164.9 (minor), 164.8, 163.9, 134.4, 132.6 (minor), 132.4 (minor), 132.3, 132.0, 131.6 (minor), 129.8, 129.7, 129.1 (minor), 129.02, 128.95 (minor), 128.65, 128.58, 128.5 (minor), 128.4 (minor), 128.2 (minor), 128.1, 127.6 (minor), 127.4, 126.5 (minor), 73.6, 71.4 (minor), 62.0, 57.4 (minor), 52.4 (minor), 51.9, 36.5 (minor), 36.3. **HRMS (MALDI-FT ICR)** exact mass

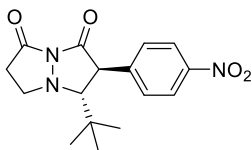
calculated  $[M+Na]^+$  calculated for  $C_{18}H_{15}^{35}ClN_2NaO_2$ : 349.0714, found: 349.0713; exact mass calculated  $[M+Na]^+$  calculated for  $C_{18}H_{15}^{37}ClN_2NaO_2$ : 351.0685, found: 351.0684.

**(2*S*\*,3*S*\*)-2-(4-nitrophenyl)-3-((*E*)-styryl)tetrahydro-1*H*,7*H*-pyrazolo[1,2-*a*]pyrazole-1,7-dione (145q)**



Yellow solid, 33.8 mg, 62% yield. **mp** 191.9-193.7 °C. **FTIR** $v_{max}$ (KBr)/ $cm^{-1}$ : 1781, 1706, 1685, 1654, 1601, 1522, 1387, 1340, 1219, 772.  **$^1H$  NMR** ( $CDCl_3$ , 400 MHz):  $\delta$  8.21 (dd, 2H,  $J = 8.7, 1.7$  Hz), 7.53 (dd, 0.09H,  $J = 8.6, 1.6$  Hz, minor), 7.44 (dd, 2H,  $J = 8.6, 1.6$  Hz), 7.34-7.30 (m, 5H), 6.68 (d, 0.04H,  $J = 16.0$  Hz), 6.49 (d, 1H,  $J = 16.0$  Hz), 6.15 (ddd, 1H,  $J = 16, 8.0, 1.5$  Hz), 5.63-5.57 (m, 0.04H, minor), 4.18 (dd, 1H,  $J = 12.2, 1.3$  Hz), 3.73 (td, 1H,  $J = 8.0, 1.0$  Hz), 3.64 (ddd, 1H,  $J = 12.2, 8.0, 0.9$  Hz), 3.13-3.04 (m, 1H), 2.97-2.84 (m, 2H).  **$^{13}C$  NMR** ( $CDCl_3$ , 100 MHz):  $\delta$  164.7, 163.0, 147.8, 139.7, 136.8, 134.9, 130.3, 128.9, 128.8, 126.7, 124.0, 121.9, 77.5, 59.5, 52.1, 36.4. **HRMS (ESI-FT ICR)** exact mass calculated  $[M+Na]^+$  calculated for  $C_{20}H_{17}N_3NaO_4$ : 386.1111, found: 386.1116.

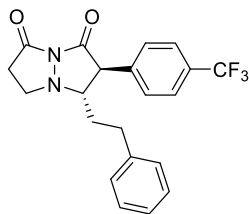
**(2*S*\*,3*R*\*)-3-(tert-butyl)-2-(4-nitrophenyl)tetrahydro-1*H*,7*H*-pyrazolo[1,2-*a*]pyrazole-1,7-dione (145r)**



Yellow solid, 24.7 mg, 51% yield. **mp** 196.0-202.0 °C. **FTIR** $v_{max}$  (KBr)/ $cm^{-1}$ : 1783, 1694, 1521, 1347, 1334, 1308.  **$^1H$  NMR** ( $CDCl_3$ , 400 MHz):  $\delta$  8.21 (d, 2H,  $J = 8.6$  Hz), 7.47 (d, 2H,  $J = 8.6$  Hz), 4.15 (d, 1H,  $J = 11.5$  Hz), 3.83-3.77 (m, 1H), 3.16 (d, 1H,  $J = 11.5$  Hz), 3.10-2.98 (m, 2H), 2.84-2.77

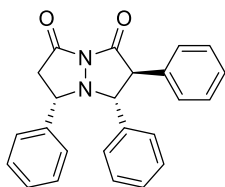
(m, 1H), 0.90 (s, 9H).  $^{13}\text{C}$  NMR ( $\text{CDCl}_3$ , 100 MHz):  $\delta$  165.3, 164.2, 147.4, 143.9, 130.2, 124.1, 81.5, 56.9, 55.6, 36.3, 34.3, 27.4. **HRMS (MALDI-FT ICR)** exact mass calculated  $[\text{M}+\text{Na}]^+$  calculated for  $\text{C}_{16}\text{H}_{19}\text{N}_3\text{NaO}_4$ : 340.1268, found: 340.1266.

**(2S\*,3S\*)-3-phenethyl-2-(4-(trifluoromethyl)phenyl)tetrahydro-1H,7H-pyrazolo[1,2-a]pyrazole-1,7-dione (145s)**



White solid, 28.5 mg, 49% yield. **mp** 159.6-163.8 °C. **FTIR** $_{\text{v}_{\text{max}}}(\text{KBr})/\text{cm}^{-1}$ : 1785, 1325, 1166, 1125, 1069, 1019.  $^1\text{H}$  NMR ( $\text{CDCl}_3$ , 400 MHz):  $\delta$  7.63 (d, 2H,  $J = 7.8$  Hz), 7.49 (d, 0.10H,  $J = 7.8$  Hz, minor), 7.32 (d, 2H,  $J = 7.8$  Hz), 7.28-7.20 (m, 3H), 7.04 (d, 2H,  $J = 7.0$  Hz), 6.96 (d, 0.11H,  $J = 7.0$  Hz, minor), 4.03 (d, 0.05H,  $J = 7.4$  Hz, minor), 3.99 (d, 1H,  $J = 12.6$  Hz), 3.76 (t, 1H,  $J = 8.3$  Hz), 3.18-3.03 (m, 2H), 2.94-2.80 (m, 2H), 2.67-2.61 (m, 2H), 2.53-2.49 (m, 0.10H, minor), 2.02-1.94 (m, 2H).  $^{13}\text{C}$  NMR ( $\text{CDCl}_3$ , 100 MHz):  $\delta$  165.1 (minor), 164.9 (minor), 164.7, 164.2, 140.3, 140.0 (minor), 137.3, 136.8 (minor), 130.5 (q,  $^2J_{\text{CF}} = 32.5$  Hz), 129.9 (minor), 129.8, 128.6, 128.05, 127.98 (minor), 126.4, 125.9 (q,  $^3J_{\text{CF}} = 3.5$  Hz), 123.8 (q,  $^1J_{\text{CF}} = 270.6$  Hz), 73.9, 70.2 (minor), 59.0, 57.7 (minor), 53.3, 52.9 (minor), 36.6 (minor), 36.4, 32.0, 31.9 (minor), 31.5, 29.1 (minor). **HRMS (ESI-FT ICR)** exact mass calculated  $[\text{M}+\text{Na}]^+$  calculated for  $\text{C}_{21}\text{H}_{19}\text{F}_3\text{N}_2\text{NaO}_2$ : 411.1291, found: 411.1294.

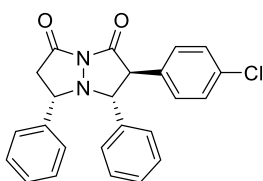
**(2*S*\*,3*R*\*,5*S*\*)-2,3,5-triphenyltetrahydro-1*H*,7*H*-pyrazolo[1,2-*a*]pyrazole-1,7-dione (145t)<sup>99</sup>**



Data for this compound are consistent with those reported in the literature.

White solid, 32.6 mg, 59% yield. **mp** 215.6–218.2 °C. **FTIR**<sub>vmax</sub>(KBr)/cm<sup>-1</sup>: 1789, 1700, 1498 1457, 1372, 1337, 1118, 759, 696. **<sup>1</sup>H NMR** (CDCl<sub>3</sub>, 400 MHz): δ 7.27–7.26 (m, 3H), 7.19–7.17 (m, 2H), 7.07–7.02 (m, 6H), 6.98–6.96 (m, 4H), 4.23–4.19 (m, 2H), 4.08 (d, 1H, *J* = 12.4 Hz), 3.21–3.08 (m, 2H). **<sup>13</sup>C NMR** (CDCl<sub>3</sub>, 100 MHz): δ 164.2, 163.8, 135.7, 134.4, 132.5, 129.1, 128.7, 128.4, 128.3, 128.2, 128.1, 127.9, 127.7, 127.5, 79.6, 71.2, 62.2, 45.2. **HRMS (MALDI-FT ICR)** exact mass calculated [M+K]<sup>+</sup> calculated for C<sub>24</sub>H<sub>20</sub>KN<sub>2</sub>O<sub>2</sub>: 407.1156, found: 407.1172.

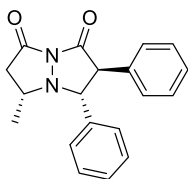
**(2*S*\*,3*R*\*,5*S*\*)-2-(4-chlorophenyl)-3,5-diphenyltetrahydro-1*H*,7*H*-pyrazolo[1,2-*a*]pyrazole-1,7-dione (145u)**



White solid, 43.4 mg, 72% yield. **mp** 244.8–247.7 °C. **FTIR**<sub>vmax</sub>(KBr)/cm<sup>-1</sup>: 1786, 1701, 1496, 1369, 1318, 1271, 773, 698. **<sup>1</sup>H NMR** (CDCl<sub>3</sub>, 400 MHz): δ 7.25–7.22 (m, 2H), 7.18–7.16 (m, 2H), 7.06–7.04 (m, 3H), 7.02–6.99 (m, 1H), 6.97–6.95 (m, 6H), 4.23–4.16 (m, 2H), 4.03 (d, 1H, *J* = 12.5 Hz), 3.20–3.07 (m, 2H). **<sup>13</sup>C NMR** (CDCl<sub>3</sub>, 100 MHz): δ 163.9, 163.8, 135.6, 134.2, 134.1, 131.0, 130.5, 129.0, 128.5, 128.4, 128.2, 128.0, 127.6, 127.5, 79.6, 71.1, 61.5, 45.1. **HRMS (MALDI-FT ICR)** exact mass calculated [M+K]<sup>+</sup> calculated for C<sub>24</sub>H<sub>19</sub><sup>35</sup>ClKN<sub>2</sub>O<sub>2</sub>: 441.0767, found: 441.0782; exact mass calculated [M+K]<sup>+</sup>

calculated for  $C_{24}H_{19}^{37}ClKN_2O_2$ : 443.0737, found: 443.0752.

**(2*S*\*,3*R*\*,5*R*\*)-5-methyl-2,3-diphenyltetrahydro-1*H*,7*H*-  
pyrazolo[1,2-*a*]pyrazole-1,7-dione (145v)<sup>99</sup>**

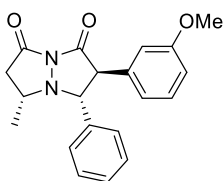


Data for major diastereomer are consistent with those reported in the literature.

White solid, 29.4 mg, 64% yield.

**FTIR**<sub>vmax</sub>(KBr)/cm<sup>-1</sup>: 1783, 1700, 1560, 1541, 1507, 1387, 1314. **<sup>1</sup>H NMR** (CDCl<sub>3</sub>, 400 MHz): δ 7.34-7.25 (m, 8H) overlapped with (m, 2H, minor), 7.10-7.08 (m, 1.9 H, minor), 7.02-6.99 (m, 2H), 4.34 (d, 0.52H, *J* = 10.9 Hz, minor), 4.11 (m, 1.52H, major + minor), 3.97 (d, 1H, *J* = 12.4 Hz), 3.72-3.69 (m, 0.51H, minor), 3.35-3.29 (m, 1H), 3.26-3.20 (m, 0.50H, minor), 2.89-2.83 (m, 1H), 2.75-2.68 (m, 1H), 2.54-2.49 (m, 0.51H, minor), 1.19 (d, 1.53H, *J* = 6.6 Hz, minor), 0.92 (d, 3H, *J* = 6.1 Hz). **<sup>13</sup>C NMR** (CDCl<sub>3</sub>, 100 MHz): δ 164.6, 164.2 (minor), 164.0, 136.1, 134.9 (minor), 133.4 (minor), 132.6, 129.2, 129.0 (minor), 128.9, 128.8 (minor), 128.72, 128.70, 128.12 (minor), 128.10, 127.6, 79.0, 69.3 (minor), 63.2, 62.81, 62.75 (minor), 52.0 (minor), 44.1, 44.0 (minor), 18.1, 13.8 (minor). **HRMS (ESI-FT ICR)** exact mass calculated [M+Na]<sup>+</sup> calculated for C<sub>19</sub>H<sub>18</sub>N<sub>2</sub>NaO<sub>2</sub>: 329.1261, found: 329.1264.

**(2*S*\*,3*R*\*,5*R*\*)-2-(3-methoxyphenyl)-5-methyl-3-  
phenyltetrahydro-1*H*,7*H*-pyrazolo[1,2-*a*]pyrazole-1,7-dione  
(145w)**

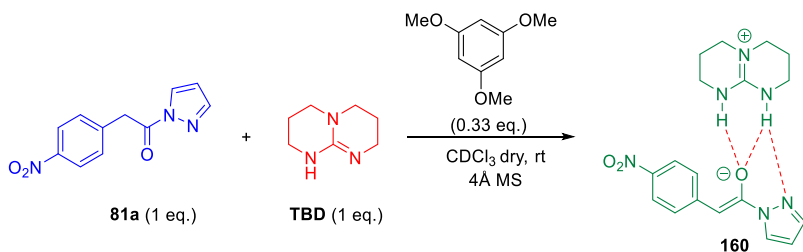


White solid, 25.2 mg, 50% yield.

**FTIR**<sub>vmax</sub>(KBr)/cm<sup>-1</sup>: 1783, 1703, 1697, 1600, 1558, 1506, 1492, 1455, 1317, 1299, 1155, 1043, 751, 697. **<sup>1</sup>H NMR** (CDCl<sub>3</sub>, 400 MHz):

$\delta$  7.33-7.23 (m, 7.5H, major + minor), 7.21-7.15 (m, 1.5H, major + minor), 6.84-6.79 (m, 1.5H, major + minor), 6.68-6.54 (m, 3H, major + minor), 4.35 (d, 0.5H,  $J = 10.8$  Hz, minor), 4.09-4.05 (m, 1.5H, major + minor), 3.98 (d, 1H,  $J = 12.4$  Hz), 3.73 (s, 1.5H, minor), 3.70 (s, 3H), 3.35-3.29 (m, 1H), 3.24-3.18 (m, 0.5H, minor), 2.88-2.82 (m, 1H), 2.74-2.70 (m, 1H), 2.53-2.48 (m, 1H, minor), 1.19 (d, 1.5H,  $J = 6.5$  Hz, minor), 0.92 (d, 3H,  $J = 6.0$  Hz).  $^{13}\text{C}$  NMR ( $\text{CDCl}_3$ , 100 MHz):  $\delta$  164.63, 164.60 (minor), 164.1 (minor), 163.9, 159.8 (minor), 159.7, 136.2, 135.0 (minor), 134.8 (minor), 133.9, 129.8 (minor), 129.7, 128.91 (minor), 128.87, 128.7, 127.6, 121.4, 121.3 (minor), 114.7, 113.8, 113.6 (minor), 78.8, 69.1 (minor), 63.1, 62.7, 62.6 (minor), 55.21 (minor), 55.17, 52.0 (minor), 44.1, 44.0 (minor), 18.1, 13.8 (minor). HRMS (ESI-FT ICR) exact mass calculated  $[\text{M}+\text{H}]^+$  calculated for  $\text{C}_{20}\text{H}_{21}\text{N}_2\text{O}_3$ : 337.1547, found: 337.1563.

### Mechanistic investigations



**Experimental procedure:** In an oven-dried vial 2-(4-nitrophenyl)-1-(1H-pyrazol-1-yl)ethan-1-one **81a** (18.5 mg, 0.08 mmol), **TBD** (11.1 mg, 0.08 mmol), 1,3,5-trimethoxybenzene (0.33 eq.), 4Å molecular sieves (~50 mg) and  $\text{CDCl}_3$  dry (0.4 mL) were introduced under nitrogen atmosphere. The reaction was stirred at room temperature for 30 min.  $^1\text{H}$  NMR of crude reaction mixture reveals the disappearance of the two methylene protons singlet at 4.58 ppm,

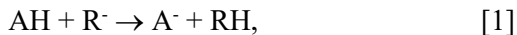
whereas one proton singlet appears at 7.58 ppm, attesting the formation of guanidinium-enolate complex **160** (see Figure 5.5).

### Scale-up synthesis of bicyclic pyrazolidinone **145i**

In an oven-dried vial, pyrazolamide **81i** (441.3 mg, 2 mmol), ylide **139a** (418.1 mg, 2.4 mmol), 4Å molecular sieves (~1.5 g) and dry dichloromethane (10 mL) were introduced. To this solution **TBD** (0.2 mmol) was added under nitrogen atmosphere. The reaction mixture was stirred at room temperature and monitored by TLC. After completion, the crude product was purified by flash chromatography (eluent: hexane, hexane/dichloromethane 1/1, dichloromethane/ethyl acetate 100/0 to 95/5) to afford bicyclic pyrazolidinone **145i** as an inseparable mixture of diastereomers in 64% yield (417.9 mg) and 97/3 dr, with the *trans* product predominating.

### Computational details

Predictions of  $pK_a$  in water were carried out at the density functional level of theory (DFT), by following the procedure based on the isodesmic reaction:



where RH is the reference, whose  $pK_a$  is experimentally known, and AH is the species whose acidic strength has to be determined. The  $pK_a$  of AH is thus computed according to:

$$pK_a(AH) = pK_a(RH) + \Delta G/(RT \ln 10),$$

in which the experimental  $pK_a$  of RH is employed,  $T$  is taken as 298.15 K and  $\Delta G$  is the predicted Gibbs free energy of reaction. For isoseismic reactions, the same reference carbon acid ( $pK_a$  17) was



adopted (see Figure 8.2).<sup>182,183</sup>

Only vibrational effects (evaluated in harmonic approximation) were included in free energy estimates, under the reasonable assumption that librational contributions elide in reaction [1].<sup>184,185</sup> The B3LYP functional in conjunction with the 6-311++G(d,p) basis set was used throughout. Effects due to solvent polarization were included in all computations via the density based solvation model (SMD) proposed by Truhlar and coworkers.<sup>186</sup> NMR computations were carried out by following the literature procedure.<sup>187</sup> In brief, geometry optimizations and frequency computations were carried out at the M06-2X/6-31+G(d,p) level; shielding tensors were computed at the B3LYP/6-311+G(2d,p) level by using M06-2X predicted geometries and the gauge independent atomic orbitals approach. Solvent (chloroform) effects were included via the polarizable continuum model.<sup>188</sup>

DFT computations were carried out by using the Gaussian 09 package.<sup>189</sup>

---

<sup>182</sup> R. Casasnovas, M. Adrover, J. Ortega-Castro, J. Frau, J. Donoso, F. Muñoz *J. Phys. Chem. B* **2012**, *116*, 10665.

<sup>183</sup> R. Casasnovas, J. Ortega-Castro, J. Frau, J. Donoso, F. Muñoz *Int. J. Quantum Chem.* **2014**, *114*, 1350.

<sup>184</sup> R. F. Ribeiro, A. V. Marenich, C. J. Cramer, D. G. Truhlar *J. Phys. Chem. B* **2011**, *115*, 14556.

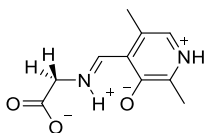
<sup>185</sup> S. Sastre, R. Casasnovas, F. Muñoz, J. Frau *Theor. Chem. Acc.* **2013**, *132*, 1310.

<sup>186</sup> A. V. Marenich, C. J. Cramer, D. G. Truhlar *J. Phys. Chem. B* **2009**, *113*, 6378.

<sup>187</sup> P. H. Willoughby, M. J. Jansma, T. R. Hoye *Nat. Protoc.* **2014**, *9*, 643.

<sup>188</sup> S. Miertuš, E. Scrocco, J. Tomasi *Chem. Phys.* **1981**, *55*, 117.

<sup>189</sup> M. J. Frisch *et al.*, Gaussian 09 rev D.01, Gaussian, Inc., Wallingford CT, **2016**.

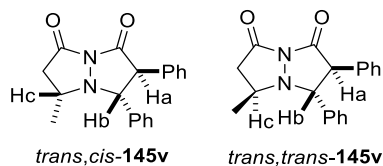


**Figure 8.2.** Carbon acid used as the reference (RH) in the computations of Gibbs free energy of isodesmic reactions [1].

**Table 8.1** Calculated acidity in water.

Compound	Predicted $pK_a$ in water
	20.4
	19.5
	16.2
	15.5
	12.0

The product *trans*-**145v** is predicted to be more stable than the *cis*-**145v** in dichloromethane by 3.0 kcal/mol both in terms of potential energy and Gibbs free energy at 298.15 K by SMD/B3LYP computations. That is mainly due to unfavourable steric repulsions between phenyl rings occurring in the *cis* stereoisomer.

**Table 8.2** Predicted  $^1\text{H-NMR}$ .

set of protons for <b>145v</b>	<i>trans,trans</i> - <b>145v</b>	<i>trans,cis</i> - <b>145v</b>
Ha	3.89	3.95
Hb	4.15	3.71
Hc	3.65	3.15
CH <sub>3</sub>	1.10	0.86

Chemical shift (ppm, vs TMS).

The *trans,cis* isomer **161v** is predicted to be more stable than the *trans,trans* **145v** by 2.0 kcal/mol.

### Biological Evaluations

The antimicrobial activity of the selected compounds **145b**, **145e**, **145f**, **145g**, **145i**, **145j**, **145k**, **145n**, was preliminarily tested on *Escherichia coli* and the human pathogen *Staphylococcus aureus*, belonging respectively to the Gram-negative and Gram-positive group of bacteria. *E. coli* (strain JM109) was purchased from Promega (<http://www.promega.com/products>, accessed December 4, 2015). The *S. aureus* strain was obtained from the collection deposited in the microbiology laboratory directed by Dr. Vigliotta at University of Salerno and derives from an hospitalized patient. Ethanol (purity 99.9%) and chloroform (purity 99.9%) were from Carlo Erba, trypton, yeast extract and agar (n. 1) from Oxoid, NaCl from Sigma Aldrich. The compounds were solubilized in stock solutions of 5mg/mL, using ethanol as solvent for **145b**, **145e**, **145f**, **145g**, **145i**, **145j**, **145k** and chloroform for the more hydrophobic **145n**.

The minimal inhibitory concentration (MIC) of each compound was estimated using protocols recommended by the Clinical and Laboratory Standards Institute (CLSI), formerly the National Committee for Clinical Laboratory Standards (NCCLS).<sup>190,191</sup> Bacteria strains were spread on Luria-Bertani (LB) agarized medium (10g/L trypton, 5g/L yeast extract, 10g/L NaCl, 15 g/L agar) and grown for 24 hours at 37 °C. Subsequently, the microorganisms were resuspended at a density of  $5 \times 10^5$  CFU (colony forming units)/mL in liquid LB medium containing increasing concentration of each compound (0, 5, 10, 100  $\mu\text{g}/\text{mL}$ ) and grown at 37 °C for 16 hours, with constant shaking (250 rpm/min). The microbial growth was measured by turbidity, by measuring optical density at 600 nm ( $\text{OD}_{600}$ ). To evaluate the action of the solvent, control populations were introduced by incubating each bacterial strains in the presence of the same volume of ethanol or chloroform used for the MIC determination, in absence of compounds. The inhibitory action was calculated as the percentage value obtained by comparing the  $\text{OD}_{600}$  value reached at 16 hours for each concentration of compound tested, with that of the corresponding control.

---

<sup>190</sup> M. De Rosa, G. Vigliotta, G. Palma, C. Saturnino, A. Soriente *Molecules* **2015**, *20*, 22044.

<sup>191</sup> National Committee for Clinical Laboratory Standards. Methods for dilution antimicrobial susceptibility tests for bacteria that grow aerobically; approved standard. 5th ed. Document M07-A5. Wayne, PA, USA; **2001**.

**Table 8.3** Antimicrobial activity of tested compounds.

Sample (100 µg/mL)	Growth rate [%] <sup>[a]</sup>	
	<i>Staphylococcus aureus</i>	<i>Escherichia coli</i>
<b>145b</b>	74.9 (±19.0)	104.0 (±21.1)
<b>145e</b>	14.3 (±12.8)	111.0 (±11.6)
<b>145f</b>	68.6 (±7.3)	93.1 (±13.1)
<b>145g</b>	98.3 (± 14.0)	93.7 (±11.9)
<b>145i</b>	86.0 (±2.0)	95.0 (±10.4)
<b>145j</b>	36.7 (±5.3)	101.4 (±13.4)
<b>145k</b>	73.2 (±27.7)	93.7 (±10.3)
<b>145n</b>	98.8 (±13.0)	116.7 (±13.8)

<sup>[a]</sup> As a percentage of growth compared to the untreated sample.

#### 8.4 Direct $\alpha$ -imination of *N*-acylpyrazoles with nitrosoarenes

##### Experimental procedures and compounds characterization

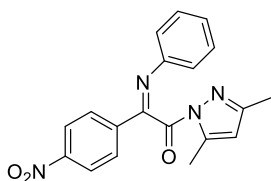
TBD and nitrosobenzene **177a** were purchased from TCI and used as received. Nitrosoarenes **177b-e** are known compounds, they were prepared according to the literature.<sup>138</sup> The pyrazoleamides **81** and **204** were prepared by using general procedures reported in the literature.<sup>87b,137</sup>

##### General procedure for the synthesis of imines **202** and **206**

In an oven-dried vial *N*-acylpyrazole **81** or **204** (0.2 mmol), nitrosoarene **177** (0.24 mmol), 3Å molecular sieves (45 mg) and anhydrous dichloromethane (1 mL) were introduced. To this solution TBD (0.02 or 0.04 mmol) was added under nitrogen atmosphere. The reaction mixture was stirred at room temperature and monitored by TLC. After completion, the crude reaction mixture was purified by flash chromatography (eluent: hexane/ethyl acetate 100/0 to 90/10) to afford products **202** in 40-92% yield and products **206** in 26-76% yield. Nitron of imine **206a** was isolated in mixture with unidentified products and it was identified by HRMS spectrometry

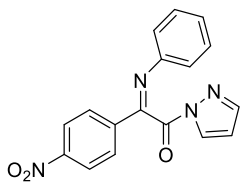
(see Figure 6.2). To evaluate the  $\alpha/\gamma$ -regioselectivity, the crude reaction mixture of model compound **206a**, was directly subjected to acid hydrolysis followed by  $^1\text{H-NMR}$  analysis. The expected  $\alpha$ - and  $\gamma$ -ketoacids were found to be in 95/5 ratio respectively.

**(Z)-1-(3,5-dimethyl-1H-pyrazol-1-yl)-2-(4-nitrophenyl)-2-(phenylimino)ethan-1-one (202a)**



Yellow solid, 62.0 mg, 89% yield. **mp** 100.8-102.2 °C. **FTIR** $\nu_{\text{max}}$ (KBr)/ $\text{cm}^{-1}$ : 1715, 1602, 1558, 1523, 1486, 1380, 1348, 1201, 917, 852, 786, 764, 695.  **$^1\text{H NMR}$**  ( $\text{CDCl}_3$ , 400 MHz):  $\delta$  8.30 (d, 2H,  $J = 8.9$  Hz), 8.04 (d, 2H,  $J = 8.9$  Hz), 7.25-7.21 (m, 2H), 7.08-7.04 (m, 1H), 6.88 (d, 2H,  $J = 8.1$  Hz), 5.90 (s, 1H), 2.42 (s, 3H), 2.11 (s, 3H).  **$^{13}\text{C NMR}$**  ( $\text{CDCl}_3$ , 100 MHz):  $\delta$  165.3, 159.6, 154.9, 143.3, 149.0, 143.6, 140.1, 128.9, 128.6, 125.3, 123.8, 119.3, 112.0, 13.7, 13.3. **HRMS (MALDI-FT ICR)** exact mass  $[\text{M}+\text{H}]^+$  calculated for  $\text{C}_{19}\text{H}_{17}\text{N}_4\text{O}_3$ : 349.1295, found: 349.1294.

**(Z)-2-(4-nitrophenyl)-2-(phenylimino)-1-(1H-pyrazol-1-yl)ethan-1-one (202A)**



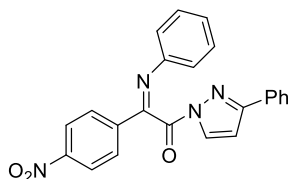
Yellow solid, 50.6 mg, 79% yield. **mp** 109.8-110.8 °C. **FTIR** $\nu_{\text{max}}$ (KBr)/ $\text{cm}^{-1}$ : 1722, 1602, 1523, 1484, 1422, 1388, 1347, 1196, 909, 881, 850, 770, 695.  **$^1\text{H NMR}$**  ( $\text{CDCl}_3$ , 400 MHz):  $\delta$  8.30 (d, 2H,  $J = 8.5$  Hz), 8.13 (s, 1H), 8.04 (d, 2H,  $J = 8.4$  Hz), 7.68 (s, 1H), 7.23 (t, 2H,  $J = 7.6$  Hz), 7.07 (t, 1H,  $J = 7.3$  Hz), 6.90 (d, 2H,  $J = 7.6$  Hz), 6.44 (s, 1H).  **$^{13}\text{C NMR}$**  ( $\text{CDCl}_3$ , 100 MHz):  $\delta$  164.0, 158.4, 149.5, 148.7, 146.2, 139.7, 128.9, 128.7,

127.9, 125.7, 124.0, 119.3, 111.2. **HRMS (MALDI-FT ICR)** exact mass  $[M+H]^+$  calculated for  $C_{17}H_{13}N_4O_3$ : 321.0982, found: 321.0983.

**(Z)-2-(4-nitrophenyl)-1-(3-phenyl-1H-pyrazol-1-yl)-2-(phenylimino)ethan-1-one (202B)**

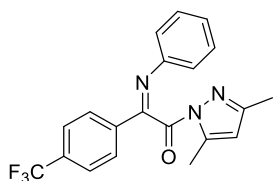
Yellow solid, 61.2 mg, 78% yield. **mp** 123.3-124.9 °C.

**FTIR** $_{v_{max}}$ (KBr)/ $cm^{-1}$ : 1719, 1523, 1415, 1346, 883, 850, 760, 691.  **$^1H$  NMR** ( $CDCl_3$ , 400 MHz):  $\delta$  8.32 (d, 2H,  $J = 8.6$  Hz), 8.153-8.147 (m, 1H), 8.08 (d, 2H,  $J = 8.6$  Hz), 7.74-7.72 (m, 2H), 7.41-7.39 (m, 3H), 7.21 (t, 2H,  $J = 7.6$  Hz), 7.05 (t, 1H,  $J = 7.4$  Hz), 6.94 (d, 2H,  $J = 8.0$  Hz), 6.772-6.765 (m, 1H).  **$^{13}C$  NMR** ( $CDCl_3$ , 100 MHz):  $\delta$  163.8, 158.6, 157.4, 149.5, 148.9, 140.0, 130.7, 129.8, 129.1, 128.9, 128.8, 128.7, 126.4, 125.6, 123.9, 119.3, 109.1. **HRMS (MALDI-FT ICR)** exact mass  $[M+H]^+$  calculated for  $C_{23}H_{17}N_4O_3$ : 397.1295, found: 397.1294.



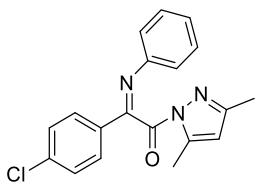
**(Z)-1-(3,5-dimethyl-1H-pyrazol-1-yl)-2-(phenylimino)-2-(4-(trifluoromethyl)phenyl)ethan-1-one (202b)**

Yellow solid, 68.3 mg, 92% yield. **mp** 65.0-69.1 °C. **FTIR** $_{v_{max}}$ (KBr)/ $cm^{-1}$ : 1714, 1627, 1595, 1485, 1383, 1355, 1325, 1170, 1127, 1070, 915, 785.  **$^1H$  NMR** ( $CDCl_3$ , 400 MHz):  $\delta$  7.99 (d, 2H,  $J = 8.3$  Hz), 7.71 (d, 2H,  $J = 8.3$  Hz), 7.23-7.19 (m, 2H), 7.04 (t, 1H,  $J = 7.4$  Hz), 6.89-6.87 (m, 2H), 5.88 (s, 1H), 2.41 (s, 3H), 2.12 (s, 3H).  **$^{13}C$  NMR** ( $CDCl_3$ , 100 MHz):  $\delta$  165.6, 160.3, 154.6, 149.3, 143.5, 137.7, 132.8 (q,  $^2J_{CF} = 32.4$  Hz), 128.5, 128.3, 125.6 (q,  $^3J_{CF} = 3.5$  Hz), 124.9, 123.8 (q,  $^1J_{CF} = 270.8$  Hz).



Hz), 119.3, 111.9, 13.7, 13.3. **HRMS (MALDI-FT ICR)** exact mass  $[M+H]^+$  calculated for  $C_{20}H_{17}F_3N_3O$ : 372.1258, found: 372.1259.

**(Z)-2-(4-chlorophenyl)-1-(3,5-dimethyl-1H-pyrazol-1-yl)-2-(phenylimino)ethan-1-one (202c)**



Light yellow solid, 50.7 mg, 75% yield. **mp**

87.6-92.2 °C. **FTIR** $v_{max}$ (KBr)/ $cm^{-1}$ : 1715,

1591, 1492, 1379, 1355, 1201, 1092, 914,

765, 696.  **$^1H$  NMR** ( $CDCl_3$ , 400 MHz):  $\delta$

7.82 (d, 2H,  $J = 8.6$  Hz), 7.43 (d, 2H,  $J = 8.6$  Hz), 7.22-7.18 (m, 2H),

7.02 (t, 1H,  $J = 7.4$  Hz), 8.87 (m, 2H), 5.86 (s, 1H), 2.39 (s, 3H), 2.12

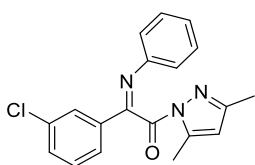
(s, 3H).  **$^{13}C$  NMR** ( $CDCl_3$ , 100 MHz):  $\delta$  165.9, 160.4, 154.4, 149.4,

143.4, 137.6, 133.1, 129.3, 128.9, 128.4, 124.6, 119.4, 111.7, 13.7,

13.3. **HRMS (MALDI-FT ICR)** exact mass  $[M+H]^+$  calculated for

$C_{19}H_{17}ClN_3O$ : 338.1055, found: 338.1058.

**(Z)-2-(3-chlorophenyl)-1-(3,5-dimethyl-1H-pyrazol-1-yl)-2-(phenylimino)ethan-1-one (202d)**



Light yellow solid, 53.4 mg, 79% yield. **mp**

66.7-71.7 °C. **FTIR** $v_{max}$ (KBr)/ $cm^{-1}$ : 1715,

1626, 1594, 1487, 1380, 1355, 1247, 1203,

963, 924, 782, 696.  **$^1H$  NMR** ( $CDCl_3$ , 400

MHz):  $\delta$  7.96 (t, 1H,  $J = 1.6$  Hz), 7.70 (dd, 1H,  $J = 7.8, 1.2$  Hz), 7.48-

7.45 (m, 1H), 7.37 (t, 1H,  $J = 7.9$  Hz), 7.22-7.18 (m, 2H), 7.02 (t,

1H,  $J = 7.4$  Hz), 6.88 (d, 2H,  $J = 7.4$  Hz), 5.86 (s, 1H), 2.40 (s, 3H),

2.12 (s, 3H).  **$^{13}C$  NMR** ( $CDCl_3$ , 100 MHz):  $\delta$  165.6, 160.2, 154.5,

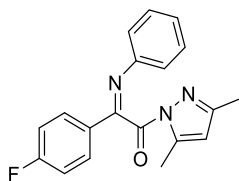
149.3, 143.4, 136.3, 134.8, 131.4, 129.8, 128.4, 127.8, 126.3, 124.7,

119.4, 111.8, 13.7, 13.3. **HRMS (MALDI-FT ICR)** exact mass

$[M+H]^+$  calculated for  $C_{19}H_{17}ClN_3O$ : 338.1055, found: 338.1058.

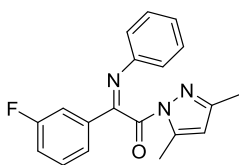


**(Z)-1-(3,5-dimethyl-1H-pyrazol-1-yl)-2-(4-fluorophenyl)-2-(phenylimino)ethan-1-one (202e)**



Light yellow solid, 48.2 mg, 75% yield. **mp** 74.5-78.4 °C. **FTIR**<sub>vmax</sub>(KBr)/cm<sup>-1</sup>: 1715, 1585, 1489, 1445, 1380, 1355, 1296, 1205, 942, 856, 780, 696. **<sup>1</sup>H NMR** (CDCl<sub>3</sub>, 400 MHz): δ 7.91-7.87 (m, 2H), 7.21-7.12 (m, 4H), 7.01 (t, 1H, *J* = 7.2 Hz), 6.87 (d, 2H, *J* = 7.5 Hz), 5.85 (s, 1H), 2.39 (s, 3H), 2.12 (s, 3H). **<sup>13</sup>C NMR** (CDCl<sub>3</sub>, 100 MHz): δ 166.0, 164.7 (d, <sup>1</sup>*J*<sub>CF</sub> = 251.0 Hz), 160.3, 154.4, 149.5, 143.4, 130.8 (d, <sup>4</sup>*J*<sub>CF</sub> = 2.8 Hz), 130.2 (d, <sup>3</sup>*J*<sub>CF</sub> = 8.8 Hz), 128.4, 124.5, 119.4, 115.8 (d, <sup>2</sup>*J*<sub>CF</sub> = 21.9 Hz), 111.7, 13.7, 13.4. **HRMS (MALDI-FT ICR)** exact mass [M+H]<sup>+</sup> calculated for C<sub>19</sub>H<sub>17</sub>FN<sub>3</sub>O: 322.1366, found: 322.1360.

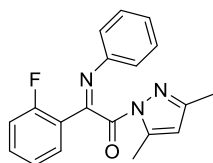
**(Z)-1-(3,5-dimethyl-1H-pyrazol-1-yl)-2-(3-fluorophenyl)-2-(phenylimino)ethan-1-one (202f)**



Light yellow solid, 50.1 mg, 78% yield. **mp** 64.9-66.9 °C. **FTIR**<sub>vmax</sub>(KBr)/cm<sup>-1</sup>: 1715, 1629, 1587, 1489, 1445, 1380, 1355, 1290, 1205, 942, 860, 786, 696. **<sup>1</sup>H NMR** (CDCl<sub>3</sub>, 400 MHz): δ 7.67 (m, 1H), 7.59 (dd, 1H, *J* = 7.8, 0.8 Hz), 7.44-7.38 (m, 1H), 7.22-7.18 (m, 3H), 7.02 (td, 1H, *J* = 7.4, 1.0 Hz), 6.88 (dd, 2H, *J* = 8.2 Hz), 5.86 (s, 1H), 2.40 (s, 3H), 2.13 (s, 3H). **<sup>13</sup>C NMR** (CDCl<sub>3</sub>, 100 MHz): δ 165.7, 162.9 (d, <sup>1</sup>*J*<sub>CF</sub> = 245.3 Hz), 160.3, 154.5, 149.3, 143.4, 136.8 (d, <sup>3</sup>*J*<sub>CF</sub> = 7.4 Hz), 130.2 (d, <sup>3</sup>*J*<sub>CF</sub> = 8.0 Hz), 128.5, 124.7, 123.9 (d, <sup>4</sup>*J*<sub>CF</sub> = 2.5 Hz), 119.4, 118.4 (d, <sup>2</sup>*J*<sub>CF</sub> = 21.3 Hz), 114.6 (d, <sup>2</sup>*J*<sub>CF</sub> = 23.1 Hz), 111.8, 13.7, 13.4. **HRMS (MALDI-FT ICR)** exact mass [M+H]<sup>+</sup> calculated for C<sub>19</sub>H<sub>17</sub>FN<sub>3</sub>O: 322.1366, found:

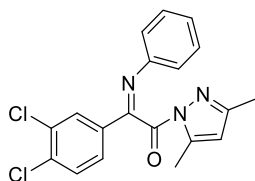
322.1350.

**(Z)-1-(3,5-dimethyl-1H-pyrazol-1-yl)-2-(2-fluorophenyl)-2-(phenylimino)ethan-1-one (202g)**



Light yellow solid, 41.8 mg, 66% yield. **mp** 64.1-66.0 °C. **FTIR**<sub>vmax</sub>(KBr)/cm<sup>-1</sup>: 1722, 1612, 1594, 1489, 1456, 1380, 1355, 1213, 913, 762, 697. **<sup>1</sup>H NMR** (CDCl<sub>3</sub>, 400 MHz): δ 8.24 (td, 1H, *J* = 7.7, 1.7 Hz), 7.50-7.45 (m, 1H), 7.31-7.26 (m, 1H), 7.20 (t, 2H, *J* = 7.9 Hz), 7.08-7.00 (m, 2H), 6.88 (dd, 2H, *J* = 7.5, 0.9 Hz), 5.83 (s, 1H), 2.38 (s, 3H), 2.12 (s, 3H). **<sup>13</sup>C NMR** (CDCl<sub>3</sub>, 100 MHz): δ 165.6, 161.6 (d, <sup>1</sup>*J*<sub>CF</sub> = 251.6 Hz), 157.1, 153.8, 149.2, 143.4, 133.3 (d, <sup>3</sup>*J*<sub>CF</sub> = 8.8 Hz), 129.7 (d, <sup>4</sup>*J*<sub>CF</sub> = 1.8 Hz), 128.3, 124.63, 124.58, 123.1 (d, <sup>3</sup>*J*<sub>CF</sub> = 9.7 Hz), 119.4, 116.1 (d, <sup>2</sup>*J*<sub>CF</sub> = 22.1), 111.2, 13.7, 13.3. **HRMS (MALDI-FT ICR)** exact mass [M+H]<sup>+</sup> calculated for C<sub>19</sub>H<sub>17</sub>FN<sub>3</sub>O: 322.1366, found: 322.1367.

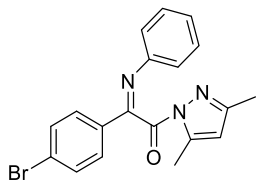
**(Z)-2-(3,4-dichlorophenyl)-1-(3,5-dimethyl-1H-pyrazol-1-yl)-2-(phenylimino)ethan-1-one (202h)**



Yellow solid, 60.3 mg, 81% yield. **mp** 72.3-75.8 °C. **FTIR**<sub>vmax</sub>(KBr)/cm<sup>-1</sup>: 1717, 1624, 1589, 1558, 1487, 1379, 1355, 1202, 1030, 922, 784, 697. **<sup>1</sup>H NMR** (CDCl<sub>3</sub>, 400 MHz): δ 8.04 (s, 1H), 7.71 – 7.59 (m, 1H), 7.56 – 7.46 (m, 1H), 7.20 (t, 2H, *J* = 6.9 Hz), 7.03 (t, 1H, *J* = 7.3 Hz), 6.86 (d, 2H, *J* = 7.5 Hz), 5.87 (s, 1H), 2.40 (s, 3H), 2.12 (s, 3H). **<sup>13</sup>C NMR** (CDCl<sub>3</sub>, 100 MHz): δ 165.4, 159.3, 154.7, 149.1, 143.5, 135.7, 134.5, 133.2, 130.6, 129.6, 128.5, 127.1, 124.9, 119.4, 111.9, 13.7, 13.3. **HRMS (MALDI-FT ICR)** exact mass [M+H]<sup>+</sup> calculated for C<sub>19</sub>H<sub>16</sub>Cl<sub>2</sub>N<sub>3</sub>O: 372.0665,

found: 372.06678.

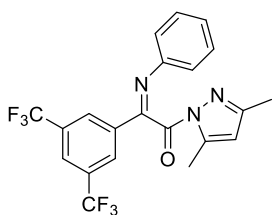
**(Z)-2-(4-bromophenyl)-1-(3,5-dimethyl-1H-pyrazol-1-yl)-2-(phenylimino)ethan-1-one (202i)**



Pale yellow solid, 57.3 mg, 75% yield. **mp** 90.1-92.5 °C. **FTIR**<sub>vmax</sub>(KBr)/cm<sup>-1</sup>: 1716, 1586, 1489, 1379, 1354, 1201, 1072, 1010, 913, 783, 696. **<sup>1</sup>H NMR** (CDCl<sub>3</sub>, 400 MHz):

δ 7.75 (d, 2H, *J* = 8.4 Hz), 7.59 (d, 2H, *J* = 8.4 Hz), 7.19 (t, 2H, *J* = 7.6 Hz), 7.02 (t, 1H, *J* = 7.0 Hz), 6.87 (d, 2H, *J* = 8.1 Hz), 5.86 (s, 1H), 2.39 (s, 3H), 2.12 (s, 3H). **<sup>13</sup>C NMR** (CDCl<sub>3</sub>, 100 MHz): δ 165.8, 160.5, 154.5, 149.4, 143.4, 133.5, 131.9, 129.4, 128.4, 126.2, 124.7, 119.4, 111.7, 13.7, 13.4. **HRMS (MALDI- mFT ICR)** exact mass [M+H]<sup>+</sup> calculated for C<sub>19</sub>H<sub>17</sub>BrN<sub>3</sub>O: 382.0550, found: 382.0549.

**(Z)-2-(3,5-bis(trifluoromethyl)phenyl)-1-(3,5-dimethyl-1H-pyrazol-1-yl)-2-(phenylimino)ethan-1-one (202j)**

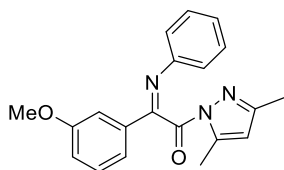


White solid, 72.9 mg, 83% yield. **mp** 78.4-84.3 °C. **FTIR**<sub>vmax</sub>(KBr)/cm<sup>-1</sup>: 2120, 1718, 1593, 1487, 1385, 1356, 1279, 1238, 1174, 1138, 841, 784, 697, 682. **<sup>1</sup>H NMR** (CDCl<sub>3</sub>, 400 MHz): δ 8.34 (s, 2H), 8.01 (s,

1H), 7.23 (t, 2H, *J* = 7.7 Hz), 7.09-7.05 (m, 1H), 6.89 (d, 2H, *J* = 8.2 Hz), 5.90 (s, 1H), 2.42 (s, 3H), 2.12 (s, 3H). **<sup>13</sup>C NMR** (CDCl<sub>3</sub>, 100 MHz): δ 164.9, 158.7, 155.1, 148.7, 143.6, 136.7, 132.2 (q, <sup>2</sup>*J*<sub>CF</sub> = 33.6 Hz), 128.6, 128.0 (q, <sup>4</sup>*J*<sub>CF</sub> = 2.3 Hz), 125.4, 124.7 (q, <sup>3</sup>*J*<sub>CF</sub> = 3.4 Hz), 123.0 (q, <sup>1</sup>*J*<sub>CF</sub> = 271.3 Hz), 119.3, 112.1, 13.7, 13.3. **HRMS (MALDI-FT ICR)** exact mass [M+H]<sup>+</sup> calculated for C<sub>21</sub>H<sub>16</sub>F<sub>6</sub>N<sub>3</sub>O:

440.1120, found: 440.1118.

**(Z)-1-(3,5-dimethyl-1H-pyrazol-1-yl)-2-(3-methoxyphenyl)-2-(phenylimino)ethan-1-one (202k)**



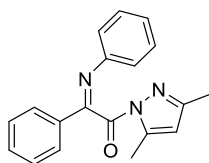
Light yellow solid, 54.0 mg, 81% yield.

**mp** 81.0-82.1 °C. **FTIR**<sub>vmax</sub>(KBr)/cm<sup>-1</sup>:

1715, 1600, 1592, 1508, 1485, 1378,  
1352, 1315, 1259, 1200, 1167, 1023, 913,

785, 697. **<sup>1</sup>H NMR** (CDCl<sub>3</sub>, 400 MHz): δ 7.58 (s, 1H), 7.38 – 7.27 (m, 2H), 7.21-7.18 (m, 2H), 7.08-6.96 (m, 2H), 6.92-6.84 (m, 2H), 5.84 (s, 1H), 3.87 (s, 3H), 2.39 (s, 3H), 2.13 (s, 3H). **<sup>13</sup>C NMR** (CDCl<sub>3</sub>, 100 MHz): δ 166.1, 161.4, 159.8, 154.2, 149.6, 143.3, 135.8, 129.6, 128.4, 124.4, 121.1, 119.4, 118.2, 111.8, 111.6, 55.4, 13.7, 13.4. **HRMS (MALDI-FT ICR)** exact mass [M+H]<sup>+</sup> calculated for C<sub>20</sub>H<sub>20</sub>N<sub>3</sub>O<sub>2</sub>: 334.1550, found: 334.1559.

**(Z)-1-(3,5-dimethyl-1H-pyrazol-1-yl)-2-phenyl-2-(phenylimino)ethan-1-one (202l)**



Light yellow solid, 39.4 mg, 65% yield. **mp**

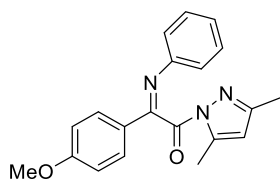
91.7-94.0 °C. **FTIR**<sub>vmax</sub>(KBr)/cm<sup>-1</sup>: 3089, 3051,

3025, 2971, 2364, 1715, 1591, 1485, 1377,

1353, 694. **<sup>1</sup>H NMR** (CDCl<sub>3</sub>, 400 MHz): δ 7.89-

7.87 (m, 2H), 7.52-7.43 (m, 3H), 7.19 (t, 2H, *J* = 7.8 Hz), 7.01 (t, 1H, *J* = 7.4 Hz), 6.89 (d, 2H, *J* = 7.6 Hz), 5.85 (s, 1H), 2.40 (s, 3H), 2.12 (s, 3H). **<sup>13</sup>C NMR** (CDCl<sub>3</sub>, 100 MHz): δ 166.3, 161.6, 154.2, 149.7, 143.4, 134.5, 131.4, 128.6, 128.4, 128.0, 124.4, 119.5, 111.6, 13.7, 13.4. **HRMS (MALDI-FT ICR)** exact mass [M+H]<sup>+</sup> calculated for C<sub>19</sub>H<sub>18</sub>N<sub>3</sub>O: 304.1444, found: 304.1446.

**(Z)-1-(3,5-dimethyl-1H-pyrazol-1-yl)-2-(4-methoxyphenyl)-2-(phenylimino)ethan-1-one (202m)**



Light yellow solid, 36.0 mg, 54% yield.

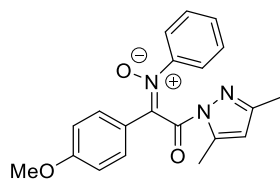
**mp** 87.0-88.0 °C. **FTIR**<sub>vmax</sub>(KBr)/cm<sup>-1</sup>:

1713, 1603, 1592, 1513, 1485, 1378, 1354,

1315, 1259, 1201, 1167, 1027, 913, 785,

698. **<sup>1</sup>H NMR** (CDCl<sub>3</sub>, 400 MHz): δ 7.83 (d, 2H, *J* = 8.8 Hz), 7.19-7.15 (m, 2H), 7.00-6.94 (m, 3H), 6.86 (d, 2H, *J* = 7.8 Hz), 5.83 (s, 1H), 3.85 (s, 3H), 2.38 (s, 3H), 2.12 (s, 3H). **<sup>13</sup>C NMR** (CDCl<sub>3</sub>, 100 MHz): δ 166.5, 162.3, 160.9, 154.1, 149.9, 143.3, 129.8, 128.3, 127.3, 124.2, 119.6, 114.0, 111.5, 55.4, 13.8, 13.4. **HRMS (MALDI-FT ICR)** exact mass [M+H]<sup>+</sup> calculated for C<sub>20</sub>H<sub>20</sub>N<sub>3</sub>O<sub>2</sub>: 334.1550, found: 334.1557.

**(E)-2-(3,5-dimethyl-1H-pyrazol-1-yl)-1-(4-methoxyphenyl)-2-oxo-N-phenylethan-1-imine oxide (205m)**



Brown solid, 11.2 mg, 16% yield. **mp**

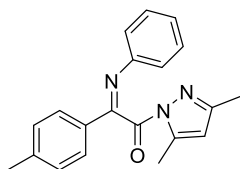
111.7-116.9 °C. **FTIR**<sub>vmax</sub>(KBr)/cm<sup>-1</sup>:

1703, 1603, 1508, 1380, 1360, 1253,

1180, 1026, 873, 774, 694. **<sup>1</sup>H NMR**

(CDCl<sub>3</sub>, 400 MHz): δ 8.28 (d, 2H, *J* = 9.1 Hz), 7.43-7.41 (m, 2H), 7.28-7.26 (m, 3H), 6.95 (d, 2H, *J* = 9.1), 5.81 (s, 1H), 3.85 (s, 3H), 2.27 (s, 3H), 2.12 (s, 3H). **<sup>13</sup>C NMR** (CDCl<sub>3</sub>, 100 MHz): δ 163.4, 161.2, 154.0, 147.3, 144.0, 142.5, 130.4, 129.7, 128.6, 123.7, 122.3, 113.8, 111.8, 55.3, 13.7, 13.4. **HRMS (MALDI-FT ICR)** exact mass [M+H]<sup>+</sup> calculated for C<sub>20</sub>H<sub>20</sub>N<sub>3</sub>O<sub>3</sub>: 350.1499, found: 350.1492.

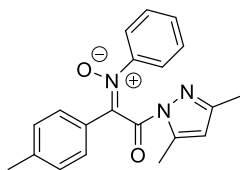
**(Z)-1-(3,5-dimethyl-1H-pyrazol-1-yl)-2-(phenylimino)-2-(p-tolyl)ethan-1-one (202n)**



Light yellow solid, 36.8 mg, 58% yield. **mp** 99.8-104.3 °C. **FTIR**<sub>vmax</sub>(KBr)/cm<sup>-1</sup>: 1715, 1600, 1592, 1515, 1485, 1379, 1355, 1315, 1259, 1200, 1167, 1027, 913, 785, 697. **<sup>1</sup>H NMR** (CDCl<sub>3</sub>, 400 MHz): δ 7.77 (d, 2H, *J* = 7.0 Hz), 7.26 (d, 2H, *J* = 7.7 Hz), 7.20-7.16 (m, 2H), 6.99 (t, 1H, *J* = 7.3 Hz), 6.88 (d, 2H, *J* = 7.7 Hz), 5.84 (s, 1H), 2.41 (s, 3H), 2.39 (s, 3H), 2.12 (s, 3H). **<sup>13</sup>C NMR** (CDCl<sub>3</sub>, 100 MHz): δ 166.4, 161.5, 154.1, 149.8, 143.3, 141.9, 131.9, 129.4, 128.3, 128.0, 124.3, 119.6, 111.5, 21.6, 13.8, 13.4.

**HRMS (MALDI-FT ICR)** exact mass [M+H]<sup>+</sup> calculated for C<sub>20</sub>H<sub>20</sub>N<sub>3</sub>O: 318.1529, found: 318.1535.

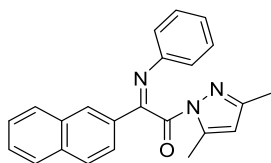
**(E)-2-(3,5-dimethyl-1H-pyrazol-1-yl)-2-oxo-N-phenyl-1-(p-tolyl)ethan-1-imine oxide (205n)**



Brown rubber, 12.7 mg, 19% yield. **FTIR**<sub>vmax</sub>(KBr)/cm<sup>-1</sup>: 1709, 1592, 1483, 1378, 1359, 1333, 1273, 1232, 962, 874, 774, 693, 515. **<sup>1</sup>H NMR** (CDCl<sub>3</sub>, 400 MHz): δ 8.16

(d, 2H, *J* = 8.4 Hz), 7.45-7.43 (m, 2H), 7.30-7.27 (m, 4H), 7.25 (s, 1H), 5.82 (s, 1H), 2.39 (s, 3H), 2.29 (s, 3H), 2.13 (s, 3H). **<sup>13</sup>C NMR** (CDCl<sub>3</sub>, 100 MHz): δ 163.4, 154.0, 147.5, 144.0, 142.8, 141.3, 129.8, 129.2, 128.7, 128.4, 126.9, 123.7, 111.8, 21.7, 13.8, 13.4. **HRMS (MALDI-FT ICR)** exact mass [M+H]<sup>+</sup> calculated for C<sub>20</sub>H<sub>20</sub>N<sub>3</sub>O<sub>2</sub>: 334.1489, found: 333.1476.

**(Z)-1-(3,5-dimethyl-1H-pyrazol-1-yl)-2-(naphthalen-2-yl)-2-(phenylimino)ethan-1-one (202o)**



Yellow solid, 56.5 mg, 80% yield. **mp**

117.3-121.2 °C **FTIR**<sub>vmax</sub>(KBr)/cm<sup>-1</sup>:

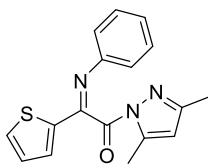
1713, 1615, 1591, 1485, 1379, 1350, 1294,

1194, 1126, 956, 916, 867, 785, 752, 696,

476. **<sup>1</sup>H NMR** (CDCl<sub>3</sub>, 400 MHz): δ 8.20-8.18 (m, 2H), 7.94 (d, 1H, *J* = 9.0 Hz), 7.88 (d, 2H, *J* = 7.7 Hz), 7.57-7.49 (m, 2H), 7.22 (t, 2H, *J* = 7.4 Hz), 7.05-7.01 (m, 1H), 6.92 (d, 2H, *J* = 7.7 Hz), 5.86 (s, 1H), 2.45 (s, 3H), 2.11 (s, 3H). **<sup>13</sup>C NMR** (CDCl<sub>3</sub>, 100 MHz): δ 166.3, 161.7, 154.3, 149.8, 143.4, 134.9, 132.8, 132.0, 129.5, 129.1, 128.6, 128.4, 127.8, 127.7, 126.5, 124.5, 123.9, 119.5, 111.6, 13.7, 13.4.

**HRMS (MALDI-FT ICR)** exact mass [M+H]<sup>+</sup> calculated for C<sub>23</sub>H<sub>20</sub>N<sub>3</sub>O: 354.1601, found: 354.1599.

**(E)-1-(3,5-dimethyl-1H-pyrazol-1-yl)-2-(phenylimino)-2-(thiophen-2-yl)ethan-1-one (202p)**



Light yellow solid, 52.6 mg, 85% yield. **mp**

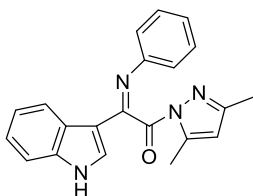
101.6-104.5 °C **FTIR**<sub>vmax</sub>(KBr)/cm<sup>-1</sup>: 1714,

1615, 1592, 1485, 1424, 1379, 1353, 1200, 961,

851, 783, 760, 696. **<sup>1</sup>H NMR** (CDCl<sub>3</sub>, 400

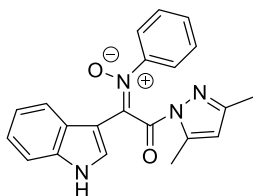
MHz): δ 7.54 (dd, 1H, *J* = 4.4, 0.7 Hz), 7.28 (dd, 1H, *J* = 4.4, 0.7 Hz), 7.18 (t, 2H, *J* = 7.8 Hz), 7.08-7.06 (m, 1H), 7.00 (t, 1H, *J* = 7.4 Hz), 6.91 (d, 2H, *J* = 7.4 Hz), 5.85 (s, 1H), 2.41 (s, 3H), 2.13 (s, 3H). **<sup>13</sup>C NMR** (CDCl<sub>3</sub>, 100 MHz): δ 165.1, 155.7, 154.3, 149.0, 143.5, 141.0, 131.1, 130.8, 128.4, 127.8, 124.7, 120.0, 111.8, 13.7, 13.4. **HRMS (MALDI-FT ICR)** exact mass [M+H]<sup>+</sup> calculated for C<sub>17</sub>H<sub>16</sub>N<sub>3</sub>OS: 310.1009, found: 310.1007.

**(Z)-1-(3,5-dimethyl-1H-pyrazol-1-yl)-2-(1H-indol-3-yl)-2-(phenylimino)ethan-1-one (202q)**



Light brown solid, 34.2 mg, 50% yield. **mp** 168.6-172.6 °C **FTIR** $v_{\max}$ (KBr)/ $\text{cm}^{-1}$ : 1717, 1591, 1533, 1485, 1436, 1384, 1344, 749. **<sup>1</sup>H NMR** ( $\text{CDCl}_3$ , 400 MHz):  $\delta$  8.88 (bs, 1H), 8.49-8.47 (m, 1H), 7.37-7.35 (m, 1H), 7.27-7.21 (m, 3H), 7.17 (t, 2H,  $J = 7.8$  Hz), 6.98-6.92 (m, 3H), 5.81 (s, 1H), 2.38 (s, 3H), 2.09 (s, 3H). **<sup>13</sup>C NMR** ( $\text{CDCl}_3$ , 100 MHz):  $\delta$  166.3, 157.2, 153.9, 150.4, 143.6, 136.7, 129.9, 128.2, 125.1, 123.8, 123.6, 122.7, 121.9, 120.1, 113.7, 111.4, 111.3, 13.7, 13.5. **HRMS (MALDI-FT ICR)** exact mass  $[\text{M}+\text{H}]^+$  calculated for  $\text{C}_{21}\text{H}_{19}\text{N}_4\text{O}$ : 343.1553, found: 343.1576.

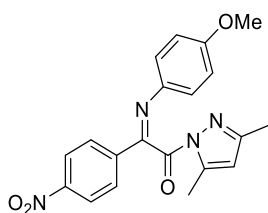
**(E)-2-(3,5-dimethyl-1H-pyrazol-1-yl)-1-(1H-indol-3-yl)-2-oxo-N-phenylethan-1-imine oxide (205q)**



Yellow solid, 14.3 mg, 20% yield. **mp** 133.5-136.7 °C **FTIR** $v_{\max}$ (KBr)/ $\text{cm}^{-1}$ : 1711, 1483, 1439, 1385, 1345, 1226, 874, 745, 693, 588. **<sup>1</sup>H NMR** ( $\text{CDCl}_3$ , 400 MHz):  $\delta$  10.7-10.5 (m, 1H), 9.54 (d, 1H,  $J = 2.9$  Hz), 7.50-7.48 (m, 2H), 7.30-7.28 (m, 3H), 7.20 (t, 2H,  $J = 8.0$  Hz), 7.12-7.08 (m, 1H), 7.02-6.99 (m, 1H), 5.85 (s, 1H), 2.41 (s, 3H), 2.05 (s, 3H). **<sup>13</sup>C NMR** ( $\text{CDCl}_3$ , 100 MHz):  $\delta$  163.2, 154.3, 146.2, 143.9, 140.1, 136.1, 132.4, 129.5, 128.7, 124.4, 124.3, 122.7, 121.1, 118.8, 112.4, 112.1, 106.2, 13.73, 13.66. **HRMS (MALDI-FT ICR)** exact mass  $[\text{M}+\text{H}]^+$  calculated for  $\text{C}_{21}\text{H}_{19}\text{N}_4\text{O}_2$ : 359.1503, found: 359.1516.

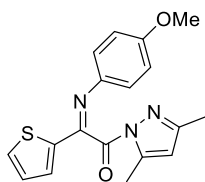


**(Z)-1-(3,5-dimethyl-1H-pyrazol-1-yl)-2-((4-methoxyphenyl)imino)-2-(4-nitrophenyl)ethan-1-one (202r)**

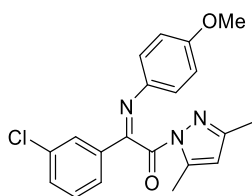


Orange solid, 66.6 mg, 88% yield. **mp** 93.5-96.2 °C. **FTIR**<sub>vmax</sub>(KBr)/cm<sup>-1</sup>: 1715, 1600, 1592, 1515, 1485, 1379, 1355, 1315, 1259, 1200, 1167, 1027, 913, 785, 697. **<sup>1</sup>H NMR** (CDCl<sub>3</sub>, 400 MHz): δ 8.28 (d, 2H, *J* = 8.8 Hz), 8.01 (d, 2H *J* = 8.8 Hz), 6.90 (d, 2H, *J* = 8.8 Hz), 6.77 (d, 2H, *J* = 8.9 Hz), 5.93 (s, 1H), 3.76 (s, 3H), 2.50 (s, 3H), 2.09 (s, 3H). **<sup>13</sup>C NMR** (CDCl<sub>3</sub>, 100 MHz): δ 166.0, 158.4, 157.6, 154.9, 149.1, 143.6, 142.1, 140.5, 128.6, 123.8, 121.4, 114.0, 112.2, 55.3, 13.7, 13.5. **HRMS (MALDI-FT ICR)** exact mass [M+H]<sup>+</sup> calculated for C<sub>20</sub>H<sub>19</sub>N<sub>4</sub>O<sub>4</sub> 379.1406, found: 379.1400.

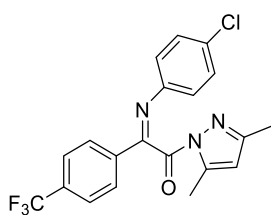
**(E)-1-(3,5-dimethyl-1H-pyrazol-1-yl)-2-((4-methoxyphenyl)imino)-2-(thiophen-2-yl)ethan-1-one (202s)**



Yellow solid, 59.7 mg, 88% yield. **mp** 95.3-96.3 °C. **FTIR**<sub>vmax</sub>(KBr)/cm<sup>-1</sup>: 1714, 1609, 1501, 1425, 1379, 1353, 1246, 1201, 1033, 880, 853, 764. **<sup>1</sup>H NMR** (CDCl<sub>3</sub>, 400 MHz): δ 7.50 (dd, 1H, *J* = 5.0, 0.6 Hz), 7.22 (dd, 1H, *J* = 3.7, 0.9 Hz), 7.05 (dd, 1H, *J* = 4.9, 3.9 Hz), 6.90 (d, 2H, *J* = 8.9 Hz), 6.72 (d, 2H, *J* = 8.9 Hz), 5.88 (s, 1H), 3.73 (s, 3H), 2.47 (s, 3H), 2.11 (s, 3H). **<sup>13</sup>C NMR** (CDCl<sub>3</sub>, 100 MHz): δ 165.7, 157.0, 155.0, 154.3, 143.5, 142.3, 141.4, 130.6, 130.4, 127.7, 121.6, 113.7, 111.9, 55.3, 13.8, 13.5. **HRMS (MALDI-FT ICR)** exact mass [M+H]<sup>+</sup> calculated for C<sub>18</sub>H<sub>18</sub>N<sub>3</sub>O<sub>2</sub>S: 340.11142, found: 340.11299.

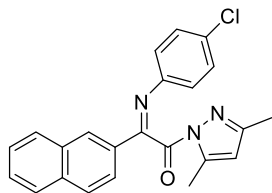
**(Z)-2-(3-chlorophenyl)-1-(3,5-dimethyl-1H-pyrazol-1-yl)-2-((4-methoxyphenyl)imino)ethan-1-one (202t)**

Yellow solid, 57.4 mg, 78% yield. **mp** 81.0-84.4 °C. **FTIR**<sub>vmax</sub>(KBr)/cm<sup>-1</sup>: 1715, 1600, 1592, 1515, 1485, 1379, 1355, 1315, 1259, 1200, 1167, 1027, 913, 785, 697. **<sup>1</sup>H NMR** (CDCl<sub>3</sub>, 400 MHz): δ 7.93 (s, 1H), 7.66 (d, 1H, *J* = 7.7 Hz), 7.44 (d, 1H, *J* = 8.0 Hz), 7.35 (t, 1H, *J* = 7.9 Hz), 6.87 (d, 2H, *J* = 8.7 Hz), 6.75 (d, 2H, *J* = 8.7 Hz), 5.89 (s, 1H), 3.74 (s, 3H), 2.47 (s, 3H), 2.11 (s, 3H). **<sup>13</sup>C NMR** (CDCl<sub>3</sub>, 100 MHz): δ 166.3, 159.5, 157.1, 154.5, 143.4, 142.5, 136.6, 134.8, 131.1, 129.8, 127.6, 126.1, 121.1, 113.8, 111.9, 55.3, 13.8, 13.5. **HRMS (MALDI-FT ICR)** exact mass [M+H]<sup>+</sup> calculated for C<sub>20</sub>H<sub>19</sub>ClN<sub>3</sub>O<sub>2</sub>: 368.11603, found: 368.11641.

**(Z)-2-((4-chlorophenyl)imino)-1-(3,5-dimethyl-1H-pyrazol-1-yl)-2-(4-(trifluoromethyl)phenyl)ethan-1-one (202u)**

Yellow solid, 70.6 mg, 87% yield. **mp** 122.0-126.4 °C. **FTIR**<sub>vmax</sub>(KBr)/cm<sup>-1</sup>: 1715, 1610, 1590, 1513, 1480, 1375, 1355, 1312, 1259, 1200, 1163, 1026, 915, 785, 696. **<sup>1</sup>H NMR** (CDCl<sub>3</sub>, 400 MHz): δ 7.97 (d, 2H, *J* = 8.0 Hz), 7.71 (d, 2H, *J* = 8.0 Hz), 7.18 (d, 2H, *J* = 8.4 Hz), 6.83 (d, 2H, *J* = 8.4 Hz), 5.92 (s, 1H), 2.45 (s, 3H), 2.12 (s, 3H). **<sup>13</sup>C NMR** (CDCl<sub>3</sub>, 100 MHz): δ 165.3, 160.9, 154.9, 147.8, 143.6, 137.5, 133.1 (q, <sup>2</sup>*J*<sub>CF</sub> = 32.5 Hz), 130.4, 128.7, 128.3, 125.7 (q, <sup>3</sup>*J*<sub>CF</sub> = 3.6 Hz), 123.8 (q, <sup>1</sup>*J*<sub>CF</sub> = 271.7 Hz), 120.9, 112.1, 13.8, 13.4. **HRMS (MALDI-FT ICR)** exact mass [M+H]<sup>+</sup> calculated for C<sub>20</sub>H<sub>16</sub>ClF<sub>3</sub>N<sub>3</sub>O: 406.0856, found: 406.0848.

**(Z)-2-((4-chlorophenyl)imino)-1-(3,5-dimethyl-1H-pyrazol-1-yl)-2-(naphthalen-2-yl)ethan-1-one (202v)**



Light yellow solid, 67.5 mg, 87% yield.

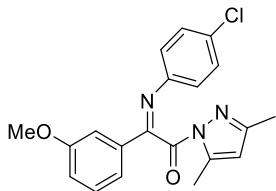
**mp** 134.6-137.4 °C. **FTIR**<sub>vmax</sub>(KBr)/cm<sup>-1</sup>:

1713, 1615, 1591, 1485, 1379, 1350, 1294,

1194, 1126, 956, 916, 867, 785, 752, 696,

476. **<sup>1</sup>H NMR** (CDCl<sub>3</sub>, 400 MHz): δ 8.20-8.09 (m, 2H), 7.93 (d, 1H, *J* = 9.1 Hz), 7.87 (d, 2H, *J* = 9.1 Hz), 7.62-7.42 (m, 2H), 7.18 (d, 2H, *J* = 8.7 Hz), 6.87 (d, 2H, *J* = 8.7 Hz), 5.91 (s, 1H), 2.49 (s, 3H), 2.10 (s, 3H). **<sup>13</sup>C NMR** (CDCl<sub>3</sub>, 100 MHz): δ 166.0, 162.2, 154.6, 148.4, 143.5, 135.0, 132.8, 131.8, 129.8, 129.6, 129.1, 128.7, 128.6, 127.84, 128.82, 126.6, 123.8, 121.0, 112.0, 13.8, 13.6. **HRMS (MALDI-FT ICR)** exact mass [M+H]<sup>+</sup> calculated for C<sub>23</sub>H<sub>19</sub>ClN<sub>3</sub>O: 388.1211, found: 388.1215.

**(Z)-2-((4-chlorophenyl)imino)-1-(3,5-dimethyl-1H-pyrazol-1-yl)-2-(3-methoxyphenyl)ethan-1-one (202w)**



Light yellow solid, 51.5 mg, 70% yield.

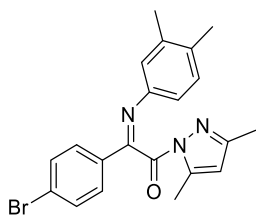
**mp** 124.5-127.2 °C. **FTIR**<sub>vmax</sub>(KBr)/cm<sup>-1</sup>:

1715, 1600, 1592, 1508, 1485, 1378, 1352,

1315, 1259, 1200, 1167, 1023, 913, 785,

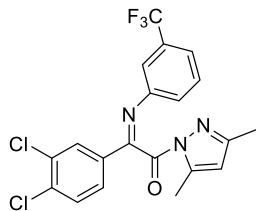
697. **<sup>1</sup>H NMR** (CDCl<sub>3</sub>, 400 MHz): δ 7.54 (s, 1H), 7.35-7.28 (m, 2H), 7.17-7.15 (m, 2H), 7.06 (d, 1H, *J* = 7.8 Hz), 6.83 (dd, 2H, *J* = 8.5, 2.1 Hz), 5.89 (s, 1H), 3.87 (s, 3H), 2.43 (s, 3H), 2.12 (s, 3H). **<sup>13</sup>C NMR** (CDCl<sub>3</sub>, 100 MHz): δ 165.8, 162.0, 159.8, 154.5, 148.2, 143.5, 135.6, 129.8, 129.6, 128.5, 121.1, 121.0, 118.4, 111.9, 55.4, 13.8, 13.5. **HRMS (MALDI-FT ICR)** exact mass [M+H]<sup>+</sup> calculated for C<sub>20</sub>H<sub>19</sub>ClN<sub>3</sub>O<sub>2</sub>: 368.1160, found: 368.1164.

**(Z)-2-(4-bromophenyl)-1-(3,5-dimethyl-1H-pyrazol-1-yl)-2-((3,4-dimethylphenyl)imino)ethan-1-one (202x)**



Yellow solid, 59.1 mg, 72% yield. **mp** 83.8-87.6 °C. **FTIR**<sub>vmax</sub>(KBr)/cm<sup>-1</sup>: 1715, 1600, 1592, 1508, 1485, 1378, 1352, 1315, 1259, 1200, 1167, 1023, 913, 785, 697. **<sup>1</sup>H NMR** (CDCl<sub>3</sub>, 400 MHz):  $\delta$  7.72 (d, 2H,  $J$  = 8.5 Hz), 7.57 (d, 2H,  $J$  = 8.5 Hz), 6.93 (d, 1H,  $J$  = 8.0 Hz), 6.69 (s, 1H), 6.58 (d, 1H,  $J$  = 7.9 Hz), 5.89 (s, 1H), 2.43 (s, 3H), 2.16 (s, 3H), 2.13 (s, 3H), 2.13 (s, 3H). **<sup>13</sup>C NMR** (CDCl<sub>3</sub>, 100 MHz):  $\delta$  166.4, 159.9, 154.4, 147.2, 143.4, 136.8, 133.8, 133.1, 131.8, 129.6, 129.3, 125.9, 121.1, 116.6, 111.7, 19.7, 19.2, 13.8, 13.5. **HRMS (MALDI-FT ICR)** exact mass [M+H]<sup>+</sup> calculated for C<sub>21</sub>H<sub>21</sub>BrN<sub>3</sub>O: 410.0790, found: 410.0778.

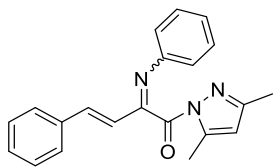
**(Z)-2-(3,4-dichlorophenyl)-1-(3,5-dimethyl-1H-pyrazol-1-yl)-2-((3-(trifluoromethyl)phenyl)imino)ethan-1-one (202y)**



Yellow solid, 70.4 mg, 80% yield. **mp** 74.8-78.3 °C. **FTIR**<sub>vmax</sub>(KBr)/cm<sup>-1</sup>: 1715, 1600, 1592, 1508, 1485, 1378, 1352, 1315, 1259, 1200, 1167, 1023, 913, 785, 697. **<sup>1</sup>H NMR** (CDCl<sub>3</sub>, 400 MHz):  $\delta$  8.04 (d, 1H,  $J$  = 2.0 Hz), 7.68 (dd, 1H,  $J$  = 8.4, 2.0 Hz), 7.54 (d, 1H,  $J$  = 8.4 Hz), 7.33 (t, 1H,  $J$  = 7.7 Hz), 7.27 (d, 1H,  $J$  = 7.9 Hz), 7.08 (s, 1H), 7.04 (d, 1H,  $J$  = 7.9 Hz), 5.87 (s, 1H), 2.37 (s, 3H), 2.12 (s, 3H). **<sup>13</sup>C NMR** (CDCl<sub>3</sub>, 100 MHz):  $\delta$  164.7, 160.8, 155.3, 149.6, 143.7, 136.3, 133.9, 133.4, 130.84 (q, <sup>2</sup>J<sub>CF</sub> = 32.3 Hz), 130.77, 129.8, 129.0, 127.3, 123.7 (q, <sup>1</sup>J<sub>CF</sub> = 270.9 Hz), 122.8, 121.4 (q, <sup>3</sup>J<sub>CF</sub> = 3.5 Hz), 116.3 (q, <sup>3</sup>J<sub>CF</sub> =

3.5 Hz), 112.1, 13.6, 13.2. **HRMS (MALDI-FT ICR)** exact mass  $[M+H]^+$  calculated for  $C_{20}H_{15}Cl_2F_3N_3O$ : 440.0539, found: 440.0571.

**(3E)-1-(3,5-dimethyl-1H-pyrazol-1-yl)-4-phenyl-2-(phenylimino)but-3-en-1-one (206a)**



Mixture of diastereomers in 70:30 ratio.

Yellow oil, 50.1 mg, 76% yield.

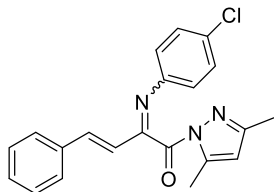
**FTIR** $v_{max}$ (KBr)/ $cm^{-1}$ : 1710, 1588, 1480, 1443, 1379, 1352, 1240, 1196, 1090, 1011,

954, 846, 754, 699.  **$^1H$  NMR** ( $CDCl_3$ , 400 MHz):  $\delta$  (major+minor) 7.53 (dd, 2H,  $J = 7.8, 1.5$  Hz), 7.46 – 7.29 (m, 6H), 7.25-7.14 (m, 3H), 7.12 – 6.95 (m, 3H), 6.92 – 6.82 (m, 2H), 5.86 (s, 1H) [6.08 (s, 1H)]<sub>minor</sub>, 2.42 (s, 3H), 2.18 (s, 3H) [2.73 (s, 3H), 2.25 (s, 3H)]<sub>minor</sub>.

**$^{13}C$  NMR** ( $CDCl_3$ , 75 MHz):  $\delta$  (major+minor) 165.8 [165.9]<sub>minor</sub>, 162.3 [162.2]<sub>minor</sub>, 154.3 [154.1]<sub>minor</sub>, 149.6 [148.6]<sub>minor</sub>, 143.5 [144.6]<sub>minor</sub>, 141.2 [141.8]<sub>minor</sub>, 135.3 [135.0]<sub>minor</sub>, 130.0, 129.7, 128.9, 128.8, 128.7, 128.4, 127.9, 127.7, 126.5, [124.8]<sub>minor</sub>, 124.7, 120.6, 119.6, 117.7, [112.0]<sub>minor</sub>, 111.7, [14.1]<sub>minor</sub>, 13.8, 13.5.

**HRMS (MALDI-FT ICR)** exact mass  $[M+H]^+$  calculated for  $C_{21}H_{20}N_3O$ : 330.1529, found: 330.1517.

**(3E)-2-((4-chlorophenyl)imino)-1-(3,5-dimethyl-1H-pyrazol-1-yl)-4-phenylbut-3-en-1-one (206b)**



Mixture of diastereomers in 70:30 ratio.

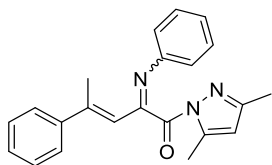
Yellow wax, 50.9 mg, 70% yield.

**FTIR** $v_{max}$ (KBr)/ $cm^{-1}$ : 1714, 1591, 1483, 1449, 1380, 1357, 1241, 1195, 1092, 1011,

954, 847, 754, 699.  **$^1H$  NMR** ( $CDCl_3$ , 400 MHz):  $\delta$  (major+minor) 7.52 (dd, 2H,  $J = 7.6, 1.6$  Hz), 7.42-7.28 (m, 7H), 7.19 – 7.11 (m,

3H), 7.06-6.98 (m, 2H), 6.81 (d, 2H,  $J = 8.5$  Hz), [6.07 (s, 1H)]<sub>minor</sub> 5.89 (s, 1H), [2.71 (s, 3H), 2.22 (s, 3H)]<sub>minor</sub>, 2.44 (s, 3H), 2.16 (s, 3H). <sup>13</sup>C NMR (CDCl<sub>3</sub>, 100 MHz):  $\delta$  (major+minor) 165.5 [165.6]<sub>minor</sub>, 162.79 [162.84]<sub>minor</sub>, 154.5 [154.2]<sub>minor</sub>, 148.1 [147.1]<sub>minor</sub>, 143.5 [144.6]<sub>minor</sub>, 141.6 [142.4]<sub>minor</sub>, 135.1 [134.8, 130.2, 130.0]<sub>minor</sub>, 129.8, 129.1, 128.8, 128.5, 127.9, 127.7, 126.2, 122.0, 121.1, [117.3, 112.0]<sub>minor</sub> 111.9, [14.0]<sub>minor</sub>, 13.8, 13.5. **HRMS (MALDI-FT ICR)** exact mass [M+H]<sup>+</sup> calculated for C<sub>21</sub>H<sub>19</sub>ClN<sub>3</sub>O: 364.1140, found: 364.1127.

**(3E)-1-(3,5-dimethyl-1H-pyrazol-1-yl)-4-phenyl-2-(phenylimino)pent-3-en-1-one (206c)**



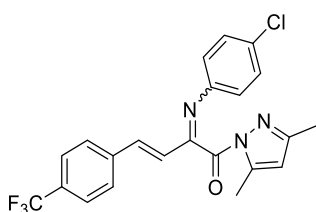
Mixture of diastereomers in 65:35 ratio.

Yellow oil, 42.6 mg, 62% yield.

**FTIR**<sub>v<sub>max</sub></sub>(KBr)/cm<sup>-1</sup>: 1718, 1590, 1485, 1447, 1380, 1354, 1027, 963, 931, 861,

797. <sup>1</sup>H NMR (CDCl<sub>3</sub>, 400 MHz):  $\delta$  (major+minor) 7.54 (d, 2H,  $J = 6.9$  Hz), 7.42 – 7.27 (m, 7H), 7.21-7.11 (m, 2H), 7.09 – 6.95 (m, 2H), 6.84 (d, 2H,  $J = 7.5$  Hz), 6.65 (s, 1H), 5.85 (s, 1H) [6.39 (s, 1H), 6.05 (s, 1H)]<sub>minor</sub>, 2.45 (s, 3H), 2.35 (s, 3H), 2.20 (s, 3H) [2.67 (s, 3H), 2.25 (s, 3H), 2.06 (s, 3H)]<sub>minor</sub>. <sup>13</sup>C NMR (CDCl<sub>3</sub>, 75 MHz):  $\delta$  (major+minor) 166.7, 161.3, 154.1, 149.7, 148.8, 143.4, 143.0 [166.9, 161.9, 153.9, 148.6, 146.2, 144.6, 142.2]<sub>minor</sub>, 128.7, 128.5, 128.4, 128.3, 126.4, 126.2, 124.3, 123.4, 120.9, 119.4 [124.9, 111.7]<sub>minor</sub>, 111.5, 18.5, 13.8, 13.4 [18.3, 14.03, 13.98]<sub>minor</sub>. **HRMS (MALDI-FT ICR)** exact mass [M+H]<sup>+</sup> calculated for C<sub>22</sub>H<sub>22</sub>N<sub>3</sub>O: 344.1695, found: 344.1687.

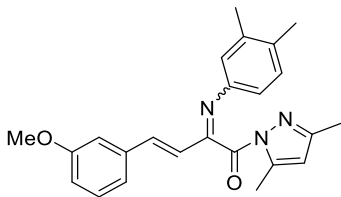
**(3E)-2-((4-chlorophenyl)imino)-1-(3,5-dimethyl-1H-pyrazol-1-yl)-4-(4-(trifluoromethyl) phenyl)but-3-en-1-one (206d)**



Mixture of diastereomers in 77:23 ratio. Yellow oil, 57.0 mg; 66% yield. **FTIR**<sub>vmax</sub>(KBr)/cm<sup>-1</sup>: 1716, 1618, 1485, 1382, 1359, 1325, 1168, 1128, 1069, 1017, 957, 829, 757. **<sup>1</sup>H NMR**

(CDCl<sub>3</sub>, 300 MHz): δ (major+minor) 7.63 (s, 4H), 7.57 (d, 1H, *J* = 8.4 Hz), 7.45 (d, 1H, *J* = 8.4 Hz), 7.38 (d, 1H, *J* = 8.3 Hz), 7.23-7.09 (m, 4H), 7.04-6.98 (m, 1H), [6.86 (d, 1H, *J* = 16.7 Hz)]<sub>minor</sub>, 6.80 (d, 2H, *J* = 8.4 Hz), [6.08 (s, 1H)]<sub>minor</sub>, 5.91 (s, 1H), 2.45 (s, 3H), 2.16 (s, 3H) [2.71 (s, 3H), 2.22 (s, 3H)]<sub>minor</sub>. **<sup>13</sup>C NMR** (CDCl<sub>3</sub>, 75 MHz): δ (major+minor) 165.3, 162.2, 154.8, [154.5]<sub>minor</sub>, 147.9, [146.8, 144.8]<sub>minor</sub>, 143.6, [140.4]<sub>minor</sub>, 139.5, 138.5, [138.2]<sub>minor</sub>, 131.2 (q, <sup>2</sup>*J*<sub>CF</sub> = 33.0 Hz), 130.6, 130.3, 129.2, 128.6, [128.5]<sub>minor</sub>, 128.0, 127.8, 125.8 (q, <sup>3</sup>*J*<sub>CF</sub> = 3.4 Hz), [122.0]<sub>minor</sub>, 121.9, 121.0, 119.4, [112.2]<sub>minor</sub>, 112.1, [14.0]<sub>minor</sub>, 13.8, 13.6. **HRMS (MALDI-FT ICR)** exact mass [M+H]<sup>+</sup> calculated for C<sub>22</sub>H<sub>18</sub>ClF<sub>3</sub>N<sub>3</sub>O: 432.1085, found: 432.1067.

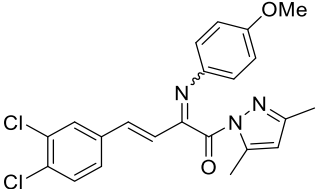
**(3E)-1-(3,5-dimethyl-1H-pyrazol-1-yl)-2-((3,4-dimethylphenyl)imino)-4-(3-methoxyphenyl)but-3-en-1-one (206e)**



Mixture of diastereomers in 70:30 ratio. Yellow oil, 50.4 mg, 65% yield. **FTIR**<sub>vmax</sub>(KBr)/cm<sup>-1</sup>: 1716, 1598, 1495, 1455, 1381, 1357, 1291, 1226, 1160, 1043, 961, 829, 757. **<sup>1</sup>H NMR** (CDCl<sub>3</sub>, 400 MHz): δ (major+minor) 7.29-7.68 (m, 11H), 6.58 (d, 1H, *J* = 7.8 Hz), 6.67 (s, 1H), [6.05 (s, 1H)]<sub>minor</sub> 5.88 (s, 1H), 3.82 (s, 3H) [3.77 (s, 3H)]<sub>minor</sub>,

[2.67 (s, 3H)]<sub>minor</sub> 2.44 (s, 3H), 2.28 (s, 3H) [2.22 (s, 3H)]<sub>minor</sub>, 2.15 (s, 3H), 2.13 (s, 3H) [2.17 (s, 3H) overlapped with 2.16 (s, 3H)]<sub>minor</sub>. <sup>13</sup>C NMR (CDCl<sub>3</sub>, 100 MHz): δ (major+minor) 166.3, 161.6, 159.8, 154.2, 147.3, 143.5, 140.5 [166.0, 161.7, 159.7, 154.1, 146.2, 144.6, 141.1]<sub>minor</sub>, 136.8, 136.7, 133.1, 129.72, 129.56, 127.1, 121.3, 120.5 [137.2, 136.6, 133.2, 129.9, 129.68, 122.0, 120.4, 118.3, 118.1]<sub>minor</sub>, 117.0, 115.8 112.0, 111.6 [115.2, 113.3, 111.9]<sub>minor</sub>, 55.25, 19.7, 19.2, 13.8, 13.6 [55.30, 19.9, 19.3, 14.10, 14.05]<sub>minor</sub>. **HRMS (MALDI-FT ICR)** exact mass [M+H]<sup>+</sup> calculated for C<sub>24</sub>H<sub>26</sub>N<sub>3</sub>O<sub>2</sub>: 388.1947, found: 388.1943.

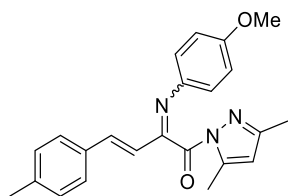
**(3E)-4-(3,4-dichlorophenyl)-1-(3,5-dimethyl-1H-pyrazol-1-yl)-2-((4-methoxyphenyl)imino)but-3-en-1-one (206f)**

 Mixture of diastereomers in 75:25 ratio. Yellow oil, 47.1 mg, 55% yield. **FTIR**<sub>vmax</sub>(KBr)/cm<sup>-1</sup>: 1715, 1605, 1502, 1379, 1356, 1246, 1030, 955, 757. <sup>1</sup>H NMR (CDCl<sub>3</sub>, 400 MHz): δ 7.57 (d, 1H, *J* = 1.9 Hz), 7.43 (s, 1H), 7.35 (dd, 1H, *J* = 8.4, 2.0 Hz), 7.13 (d, 1H, *J* = 16.5 Hz) [7.45 (s, 1H), 7.19 (dd, 1H, *J* = 8.4, 2.0 Hz), 7.02 (d, 2H, *J* = 8.8 Hz), 6.95 (d, 2H, *J* = 8.9 Hz)]<sub>minor</sub>, 6.89 (d, 1H, *J* = 16.5 Hz) overlapped with [6.89 (s, 1H)]<sub>minor</sub>, 6.84 (d, 2H, *J* = 8.8 Hz), 6.73 (d, 2H, *J* = 8.9 Hz), 5.89 (s, 1H) [6.06 (s, 1H)]<sub>minor</sub>, 3.74 (m, 3H), 2.47 (s, 3H), 2.14 (s, 3H) [3.85 (s, 3H), 2.69 (s, 3H), 2.21 (s, 3H)]<sub>minor</sub>. <sup>13</sup>C NMR (CDCl<sub>3</sub>, 100 MHz): δ (major+minor) 166.3, 160.6, 157.3, 154.5 [165.8, 161.1, 157.5, 154.3, 144.7, 141.4]<sub>minor</sub>, 143.5, 142.6, 137.4, 135.5, 130.8, 129.4, 128.6, 126.3 [138.3, 135.3, 133.2, 133.0, 130.7, 126.6, 119.4]<sub>minor</sub>, 122.5, 121.4, 113.8, 111.9 [114.3, 112.1]<sub>minor</sub>, 55.3, 13.8,



13.7. [55.5, 14.0]<sub>minor</sub>. **HRMS (MALDI-FT ICR)** exact mass  $[M+H]^+$  calculated for  $C_{22}H_{20}Cl_2N_3O_2$ : 428.0856, found: 428.0850.

**(3E)-1-(3,5-dimethyl-1H-pyrazol-1-yl)-2-((4-methoxyphenyl)imino)-4-(p-tolyl)but-3-en-1-one (206g)**



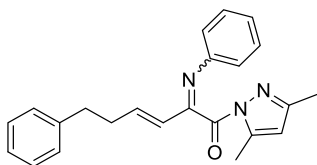
Mixture of diastereomers in 73:27 ratio.

Yellow oil, 44.8 mg, 60% yield.

**FTIR**<sub>vmax</sub>(KBr)/cm<sup>-1</sup>: 1715, 1605, 1502, 1379, 1356, 1246, 1030, 955, 757. **<sup>1</sup>H**

**NMR** (CDCl<sub>3</sub>, 400 MHz): δ 7.40 (d, 2H, *J* = 8.1 Hz), 7.14 (d, 2H, *J* = 8.1 Hz), 7.14 (d, 1H, *J* = 16.8 Hz), 6.97 (d, 1H, *J* = 16.8 Hz), 6.84 (d, 2H, *J* = 8.9 Hz), 6.72 (d, 2H, *J* = 8.9 Hz), 5.87 (s, 1H) [7.24 (s, 1H), 7.04 (d, 2H, *J* = 8.9 Hz), 6.94 – 6.90 (m, 2H), 6.05 (s, 1H)]<sub>minor</sub>, 3.74 (s, 3H), 2.46 (s, 3H), 2.36 (s, 3H), 2.14 (s, 3H) [3.85 (s, 3H), 2.70 (s, 3H), 2.33 (s, 3H), 2.21 (s, 3H)]<sub>minor</sub>. **<sup>13</sup>C** **NMR** (CDCl<sub>3</sub>, 100 MHz): δ (major+minor) 166.6, 161.8, 156.9, 154.2, 143.4, 141.3, 140.6 [166.1, 162.1, 157.1, 154.0, 144.6, 142.9, 141.8, 140.2]<sub>minor</sub>, 139.9, 132.7, 129.50, 127.6, 125.9, 121.3, 113.7, 111.8 [132.4, 129.46, 127.8, 122.5, 117.0, 114.1, 111.9]<sub>minor</sub>, 55.3, 21.4, 13.8, 13.7 [55.4, 23.8, 14.09, 14.03]<sub>minor</sub>. **HRMS (MALDI-FT ICR)** exact mass  $[M+H]^+$  calculated for  $C_{23}H_{24}N_3O_2$ : 374.1790, found: 374.1780.

**(3E)-1-(3,5-dimethyl-1H-pyrazol-1-yl)-6-phenyl-2-(phenylimino)hex-3-en-1-one (206h)**



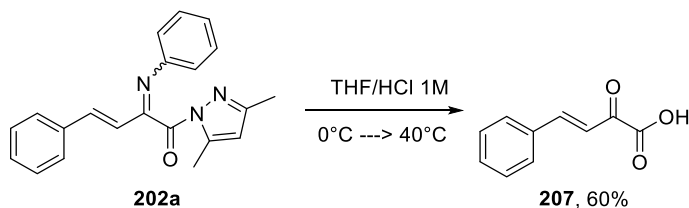
Mixture of diastereomers in 65:35 ratio. Yellow oil, 18.6 mg, 26% yield.

**FTIR**<sub>vmax</sub>(KBr)/cm<sup>-1</sup>: 1710, 1586, 1470, 1442, 1379, 1352, 1240, 1196,

1090, 1011, 954, 846, 754, 699.  $^1\text{H NMR}$  ( $\text{CDCl}_3$ , 400 MHz):  $\delta$  (major+minor) 7.48-6.91 (m, 10H) overlapped with [(m, 10H)]<sub>minor</sub>, 6.81 (d, 1H,  $J=7.4$  Hz), 6.57 (dt, 1H,  $J=16.4, 1.2$  Hz) [6.38 – 6.08 (m, 2H), 6.05 (s, 1H)]<sub>minor</sub>, 5.84 (s, 1H), 2.84 – 2.75 (m, 2H), [2.65 (s, 3H)]<sub>minor</sub>, 2.62-2.56 (m, 2H) overlapped with [2.69-2.56 (m, 2H)]<sub>minor</sub>, [2.48 – 2.39 (m, 2H)]<sub>minor</sub>, 2.34 (s, 3H), [2.26 (s, 3H)]<sub>minor</sub>, 2.20 (s, 3H).  $^{13}\text{C NMR}$  ( $\text{CDCl}_3$ , 100 MHz):  $\delta$  (major+minor) 165.9 [166.0]<sub>minor</sub>, 162.3 [162.2]<sub>minor</sub>, 154.1 [154.0]<sub>minor</sub>, 149.5 [148.5]<sub>minor</sub>, 145.4 [144.6]<sub>minor</sub>, 144.7 [143.4]<sub>minor</sub>, 141.0 [140.6]<sub>minor</sub>, 129.6 [129.4, 129.2]<sub>minor</sub>, 128.8, 128.46, 128.40, 128.33, 128.27, 126.1, 124.5 [122.7, 121.6]<sub>minor</sub>, 120.4, 119.6 [116.6]<sub>minor</sub>, 111.5 [111.8]<sub>minor</sub>, 35.0, 34.6 [34.5]<sub>minor</sub>, 13.8, 13.4 [14.05, 14.01]<sub>minor</sub>. **HRMS (MALDI-FT ICR)** exact mass  $[\text{M}+\text{H}]^+$  calculated for  $\text{C}_{23}\text{H}_{24}\text{N}_3\text{O}$ : 358.1841, found: 358.1837.

### Scale up synthesis of imine **202a**

In an oven-dried round-bottomed flask, pyrazoleamide **81b** (1.0370 g, 4 mmol), nitrosobenzene **177a** (514.1 mg, 4.8 mmol), 3 Å molecular sieves (900 mg) and anhydrous dichloromethane (20 mL) were introduced. Under nitrogen atmosphere, **TBD** (0.4 mmol) was added to this solution. The reaction mixture was stirred at room temperature for 15 minutes. After completion, the solvent was evaporated and the crude product was purified by flash chromatography (eluent: hexane/ethyl acetate 100/0 to 90/10) to afford imine **202a** in 87% yield (1.212 g) and 99/1 *Z/E*.

**General procedure for the hydrolysis of imine 206a**

To a stirred solution of **202a** (0.1 mmol, mixture of diastereoisomers in 70:30 ratio) in THF (0.4 mL) 1M aqueous HCl (0.4 mL) was added at 0°C. Then, the mixture was stirred at 40°C for 17 h. After completion the mixture was diluted with EtOAc and water and extracted with EtOAc (x4). The combined organic layers were dried over Na<sub>2</sub>SO<sub>4</sub>, filtered and concentrated. The crude reaction mixture was purified by flash chromatography (eluent: hexane/ethyl acetate 80/20 to 50/50 and ethyl acetate/methanol 100/0 to 70/30) to afford the corresponding  $\alpha$ -ketoacid in 60% yield (The same hydrolysis conditions applied to the crude reaction mixture allowed to determine the  $\alpha/\gamma$  regioselectivity, that was found to be in 95/5 ratio respectively). Data for this compound are consistent with those reported in the literature.<sup>192</sup>

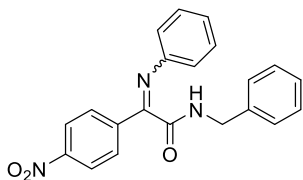
**General procedures for the one-pot synthesis of  $\alpha$ -imino amides 209**

In an oven-dried vial *N*-acylpyrazole **81** or **204** (0.2 mmol), nitrosoarene **177** (0.24 mmol), 3Å molecular sieves (45 mg) and anhydrous dichloromethane (1 mL) were introduced (for product **209b** the first step was conducted in 1 mL of anhydrous toluene). Under nitrogen atmosphere, **TBD** (0.02 mmol) was added to this

<sup>192</sup> C. Allais, T. Constantieux, J. Rodriguez, *Synthesis* **2009**, 15, 2523.

solution. The reaction mixture was stirred at room temperature and monitored by TLC. For products **209a**, **209b** and **209d**, after completion of the first step, the opportune amine (0.6 mmol) was added and the mixture was stirred for the time and at the temperature reported in Table 6.7; for products **209c** and **209e**, after completion of the imination step, dichloromethane was evaporated and anhydrous toluene (1 mL) together with the opportune amine (0.6 mmol) were added to the reaction mixture that was stirred until completion (see conditions reported in Table 6.7). After completion, the solvent was evaporated and the crude reaction mixture was purified by flash chromatography (eluent: hexane/ethyl acetate 100/0 to 70/30) to afford products **209** in 65-97% yield.

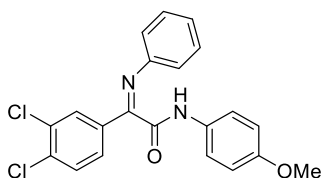
#### ***N*-benzyl-2-(4-nitrophenyl)-2-(phenylimino)acetamide (209a)**



Mixture of diastereomers. A third species is observed in  $^1\text{H}$  and  $^{13}\text{C}$  NMR spectra, hypothesized to be a conformational isomer. Yellow wax, 69.7 mg, 97% yield. **FTIR** $_{\text{vmax}}$ (KBr)/ $\text{cm}^{-1}$ : 1715, 1604, 1498, 1376, 1353, 1245, 1026, 957, 757.  **$^1\text{H}$  NMR** ( $\text{CDCl}_3$ , 400 MHz):  $\delta$  8.55 (d, 0.3H,  $J = 8.9$  Hz), 8.32-8.28 (m, 1H), 8.15 (d, 0.6H,  $J = 8.9$  Hz), 8.11 (d, 2H,  $J = 8.9$  Hz), 8.03-8.00 (m, 1H), 7.40-7.34 (m, 6H), 7.22-7.18 (m, 3H), 7.09-7.02 (m, 2H), 6.79 (d, 0.5H,  $J = 7.3$  Hz), 6.67 (d, 2H,  $J = 8.4$  Hz), 5.70-5.67 (m, 0.3H), 4.61 (d, 2H,  $J = 6.0$  Hz), 4.58 (d, 0.3H,  $J = 6.0$  Hz), 4.37 (d, 0.6H,  $J = 6.0$  Hz).  **$^{13}\text{C}$  NMR** ( $\text{CDCl}_3$ , 100 MHz):  $\delta$  164.2, 162.7, 160.8, 160.3, 159.3, 149.5, 148.9, 147.9, 147.2, 139.9, 138.3, 137.9, 137.6, 136.6, 136.3, 132.4, 130.9, 129.4, 129.2, 129.1, 129.0, 128.8, 128.7, 128.1, 127.9, 127.79, 127.76,

127.6, 125.9, 125.8, 123.8, 123.5, 122.9, 120.7, 119.7, 43.9, 43.7, 43.4. **HRMS (MALDI-FT ICR)** exact mass  $[M+H]^+$  calculated for  $C_{21}H_{18}N_3O_3$ : 360.1343, found: 360.1369.

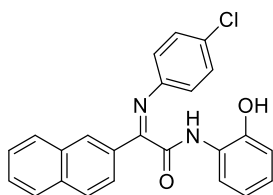
**(Z)-2-(3,4-dichlorophenyl)-N-(4-methoxyphenyl)-2-(phenylimino)acetamide (209b)**



Yellow solid, 71.1 mg, 89% yield. **mp** 89.3-92.5 °C. **FTIR** $v_{max}$ (KBr)/ $cm^{-1}$ : 1654, 1510, 1248, 695.  **$^1H$  NMR** ( $CDCl_3$ , 400 MHz):  $\delta$  9.50 (s, 1H),

7.64 (d, 2H,  $J = 9.0$  Hz), 7.42 (d, 1H,  $J = 1.8$  Hz), 7.34-7.27 (m, 3H), 7.14-7.12 (m, 1H), 7.01 (dd, 1H,  $J = 8.3$  1.9 Hz), 6.92 (d, 2H,  $J = 9.0$  Hz), 6.76 (d, 2H,  $J = 7.4$  Hz), 3.82 (s, 3H).  **$^{13}C$  NMR** ( $CDCl_3$ , 100 MHz):  $\delta$  160.2, 159.1, 156.6, 147.2, 134.1, 132.4, 132.0, 131.0, 130.5, 130.0, 129.2, 129.1, 125.8, 121.1, 120.8, 114.3, 55.5. **HRMS (MALDI-FT ICR)** exact mass  $[M+H]^+$  calculated for  $C_{21}H_{17}Cl_2N_2O_2$ : 399.0662, found: 399.0666.

**(Z)-2-((4-chlorophenyl)imino)-N-(2-hydroxyphenyl)-2-(naphthalen-2-yl)acetamide (209c)**

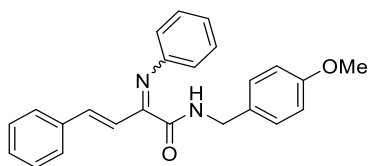


Yellow oil, 52.1 mg, 65% yield. **FTIR** $v_{max}$ (KBr)/ $cm^{-1}$ : 3360, 1751, 1655, 1381, 1280, 1184, 1137, 682, 732.  **$^1H$  NMR** ( $CDCl_3$ , 400 MHz):  $\delta$  8.50-8.43 (m, 1H), 8.09 (s, 1H), 7.82-7.73 (m, 3H),

7.49-7.46 (m, 2H), 7.20 (d, 1H,  $J = 8.0$  Hz), 7.06-7.01 (m, 3H), 6.91 (t, 1H,  $J = 7.4$  Hz), 6.82 (d, 2H,  $J = 8.6$  Hz), 9.79-6.75 (m, 1H), 6.69 (d, 1H,  $J = 7.4$  Hz) 5.18 (s, 1H).  **$^{13}C$  NMR** ( $CDCl_3$ , 100 MHz):  $\delta$  164.4, 142.8, 141.6, 133.8, 133.5, 132.7, 128.9, 128.8, 128.5, 127.6,

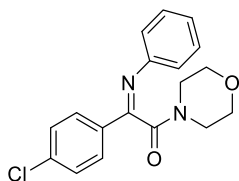
127.1, 126.7, 126.5, 125.6, 125.0, 124.7, 123.7, 122.9, 117.7, 117.6, 115.6, 90.8. **HRMS (MALDI-FT ICR)** exact mass  $[M+H]^+$  calculated for  $C_{24}H_{18}ClN_2O_2$ : 401.0978, found: 401.0979.

**(3E)-N-(4-methoxybenzyl)-4-phenyl-2-(phenylimino)but-3-enamide (209d)**



Mixture of diastereomers in 86:14 ratio. Yellow oil, 51.9 mg, 70% yield. **FTIR** $v_{max}$ (KBr)/ $cm^{-1}$ : 1715, 1603, 1499, 1378, 1352, 1248, 1029, 956, 756.  **$^1H$  NMR** ( $CDCl_3$ , 400 MHz):  $\delta$  (major + minor) 8.11 (d, 1H,  $J = 16.5$  Hz), [7.95 (d, 1H,  $J = 16.5$  Hz)]<sub>minor</sub>, 7.83-7.78 (m, 1H), [7.68 (d, 1H,  $J = 7.7$  Hz)]<sub>minor</sub>, 7.44-7.30 (m, 8H), 7.262-7.255 (m, 1H), 7.20-7.16 (m, 1H), 6.92-6.86 (m, 4H), 6.68 (dd, 2H,  $J = 16.4$  2.9 Hz), 4.55 (d, 2H,  $J = 5.9$  Hz), [4.48 (d, 2H,  $J = 5.9$  Hz)]<sub>minor</sub>, 3.81 (s, 3H), [3.77 (s, 3H)]<sub>minor</sub>.  **$^{13}C$  NMR** ( $CDCl_3$ , 75 MHz):  $\delta$  164.2, 159.0, 158.0, 148.6, 143.8, 136.0, 130.0, 129.7, 129.3, 129.0, 128.7, 127.8, 124.9, 120.1, 117.1, 114.1, 55.3, 43.0. **HRMS (MALDI-FT ICR)** exact mass  $[M+H]^+$  calculated for  $C_{24}H_{23}N_2O_2$ : 371.1682, found: 371.1675.

**(Z)-2-(4-chlorophenyl)-1-morpholino-2-(phenylimino)ethan-1-one (209e)**



Pale yellow solid, 48.0 mg, 73% yield. **mp** 91.1-95.0 °C. **FTIR** $v_{max}$ (KBr)/ $cm^{-1}$ : 1716, 1602, 1500, 1375, 1350, 1246, 1030, 957, 757.  **$^1H$  NMR** ( $CDCl_3$ , 400 MHz):  $\delta$  7.87 (d, 2H,  $J = 8.3$  Hz), 7.44 (d, 2H,  $J = 8.3$  Hz), 7.37 (t, 2H,  $J = 7.6$  Hz), 7.20 (t, 1H,  $J = 7.6$  Hz), 7.11 (d, 2H,  $J = 7.6$  Hz), 3.70-3.59 (m, 2H),

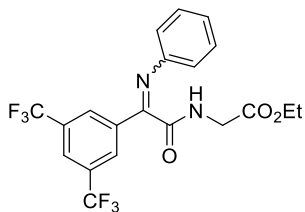
3.46-3.33 (m, 2H), 3.23-3.12 (m, 2H), 3.00-2.97 (m, 1H), 2.67-2.63 (m, 1H).  $^{13}\text{C}$  NMR ( $\text{CDCl}_3$ , 75 MHz):  $\delta$  164.6, 160.4, 148.7, 138.0, 133.0, 129.3, 129.1, 129.0, 125.8, 120.6, 66.3, 66.2, 46.0, 41.1.

**HRMS (MALDI-FT ICR)** exact mass  $[\text{M}+\text{H}]^+$  calculated for  $\text{C}_{18}\text{H}_{18}\text{ClN}_2\text{O}_2$ : 329.0980, found: 329.0974.

### **General procedure for one-pot synthesis of $\alpha$ -imino dipeptides 210**

In an oven-dried vial *N*-acylpyrazole **81** (0.2 mmol), nitrosobenzene **177a** (0.24 mmol), 3 Å molecular sieves (45 mg) and anhydrous dichloromethane (1 mL) were introduced. Under nitrogen atmosphere, **TBD** (0.02 mmol) was added to this solution. The reaction mixture was stirred at room temperature and monitored by TLC. After completion, for product **210a** glycine ethylester hydrochloride (0.3 mmol) and triethylamine (0.3 mmol) were added and the mixture was stirred at 30°C for 2 hours; for compound **210b**, after completion of the first step dichloromethane was evaporated, anhydrous toluene (1 mL), alanine methyl ester hydrochloride (0.3 mmol) and triethylamine (0.3 mmol) were added and the mixture was stirred at 50°C for 12 hours. After completion, the solvent was evaporated and the crude reaction mixture was purified by flash chromatography (eluent: hexane/diethyl ether 100/0 to 70/30) to afford product **210a** in 78% yield and product **210b** in 67% yield.

**Ethyl(2-(3,5-bis(trifluoromethyl)phenyl)-2-(phenylimino)acetyl)glycinate (210a)**



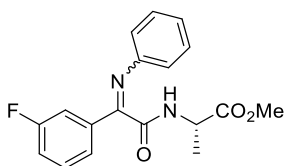
Mixture of diastereomers in 73:27 ratio.

Pale yellow solid, 69.6 mg, 78% yield.

**mp** 128.2-130.7 °C. **FTIR**<sub>vmax</sub> (KBr)/cm<sup>-1</sup>: 1751, 1655, 1381, 1280, 1184, 1137, 982, 732. **<sup>1</sup>H NMR** (CDCl<sub>3</sub>,

400 MHz):  $\delta$  (major + minor) 8.47 (s, 1H), 8.14 (s, 1H), [8.00 (s, 1H), 7.79 (s, 2H)]<sub>minor</sub>, 7.64 (s, 2H), [7.37 (t, 2H,  $J = 7.4$  Hz)]<sub>minor</sub>, 7.26-7.18 (m, 2.6H), 7.12-7.08 (m, 1H), [7.04 (d, 2H,  $J = 7.4$  Hz)]<sub>minor</sub>, 6.69 (d, 2H,  $J = 7.4$  Hz), [5.98 (s, 1H)]<sub>minor</sub>, 4.28 (qd, 2H,  $J = 7.1, 1.0$  Hz), 4.21 (d, 2H,  $J = 5.6$  Hz) overlapped with [4.17 (q, 2H,  $J = 7.1$  Hz)]<sub>minor</sub>, [3.92 (d, 2H,  $J = 5.1$  Hz)]<sub>minor</sub>, 1.35 (td, 3H,  $J = 7.1, 1.0$  Hz), [1.26-1.22 (m, 3H)]<sub>minor</sub>. **<sup>13</sup>C NMR** (CDCl<sub>3</sub>, 100 MHz):  $\delta$  (major + minor) 169.3, [168.5, 164.1]<sub>minor</sub>, 162.8, [159.3]<sub>minor</sub>, 157.4, [148.4, 147.0]<sub>minor</sub>, 136.5, 133.2, 131.2 (q,  $^2J_{CF} = 33.5$  Hz), 130.30, 130.28, 129.3, 129.2, 128.47, 128.45, 126.1, 126.0, 123.2 (q,  $^3J_{CF} = 3.7$  Hz), 122.8 (q,  $^1J_{CF} = 271.2$  Hz), 120.5, 119.7, [61.9]<sub>minor</sub>, 61.8, 41.6, [41.1]<sub>minor</sub>, 14.1, [14.0]<sub>minor</sub>. **HRMS (MALDI-FT ICR)** exact mass [M+Na]<sup>+</sup> calculated for C<sub>20</sub>H<sub>16</sub>F<sub>6</sub>NaN<sub>2</sub>O<sub>3</sub>: 469.0957, found: 469.0965.

**Methyl (2-(3-fluorophenyl)-2-(phenylimino)acetyl)-L-alaninate (210b)**



Mixture of diastereomers in 63:37 ratio.

Ochre yellow solid, 44.0 mg, 68% yield.

**mp** 97.3-101.0 °C.  $[\alpha]_D^{16} = -83.8$  (c 0.58, CHCl<sub>3</sub>). **FTIR**<sub>vmax</sub>(KBr)/cm<sup>-1</sup>: 1754,



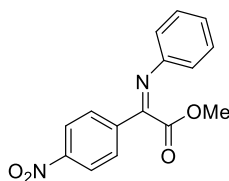
1656, 1380, 1283, 1184, 1135, 983, 732, 696. **<sup>1</sup>H NMR** (CDCl<sub>3</sub>, 400 MHz):  $\delta$  (major + minor) 8.10 (d, 1H,  $J = 7.3$  Hz), 7.71 (d, 1H,  $J = 8.3$  Hz), 7.45-7.40 (m, 1H), 7.33 (t, 1H,  $J = 7.8$  Hz), 7.23-7.18 (m, 3H), 7.14 (t, 1H,  $J = 7.4$  Hz), 7.06 (t, 1H,  $J = 7.4$  Hz), 6.99 (d, 1H,  $J = 8.0$  Hz), 6.93 (d, 1H,  $J = 8.0$  Hz), 6.73 (d, 2H,  $J = 7.5$  Hz), [5.99 (d, 1H,  $J = 6.7$  Hz)]<sub>minor</sub>, 4.69 (m, 1H), [4.51 (m, 1H)]<sub>minor</sub>, 3.80 (s, 3H), [3.68 (s, 3H)]<sub>minor</sub>, 1.55 (d, 3H,  $J = 7.2$  Hz), [1.03 (d, 3H,  $J = 7.2$  Hz)]<sub>minor</sub>. **<sup>13</sup>C NMR** (CDCl<sub>3</sub>, 100 MHz):  $\delta$  173.0, [172.3, 162.9 (d,  $^1J_{CF} = 245.4$  Hz)]<sub>minor</sub>, 164.0, 162.9, 162.0 (d,  $^1J_{CF} = 245.4$  Hz), 159.34, 159.33, 149.4, 147.6, 136.4 (d,  $^3J_{CF} = 7.5$  Hz), 133.5 (d,  $^3J_{CF} = 7.5$  Hz), 130.2 (d,  $^3J_{CF} = 7.9$  Hz), 129.4 (d,  $^3J_{CF} = 7.9$  Hz), 129.0, 128.9, 125.5 (d,  $^4J_{CF} = 3.0$  Hz), 125.3, 125.2, 124.2 (d,  $^4J_{CF} = 2.7$  Hz), 120.8, 119.7, 118.7 (d,  $^2J_{CF} = 21.4$  Hz), 116.9 (d,  $^2J_{CF} = 22.8$  Hz), 116.6 (d,  $^2J_{CF} = 20.9$  Hz), 114.9 (d,  $^2J_{CF} = 23.1$  Hz), [52.6]<sub>minor</sub>, 52.5, 48.4, [47.7]<sub>minor</sub>, 18.3, [17.7]<sub>minor</sub>. **HRMS (MALDI-FT ICR)** exact mass [M+H]<sup>+</sup> calculated for C<sub>18</sub>H<sub>18</sub>FN<sub>2</sub>O<sub>3</sub>: 329.12960, found: 329.12991. HPLC analysis with Chiralpak IC column, 80:20 *n*-hexane:2-propanol, 1 mL/min, 220 nm; minor enantiomer  $t_R = 11.5$  min, major enantiomer  $t_R = 7.5$  min.

### General procedure for one-pot synthesis of $\alpha$ -imino esters **172**

In an oven-dried vial *N*-acylpyrazole **81** or **204** (0.2 mmol), nitrosoarene **177** (0.24 mmol), 3Å molecular sieves (45 mg) and anhydrous dichloromethane (1 mL) were introduced. To this solution **TBD** (0.02 mmol) was added under nitrogen atmosphere. The reaction mixture was stirred at room temperature and monitored by TLC. After completion, for product **172a**, anhydrous methanol (10 mmol) was added and the mixture was stirred at room temperature

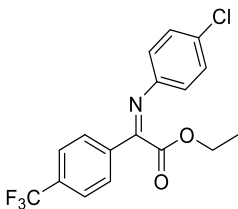
for 29 hours; for products **172b-c** dichloromethane was evaporated, DMAP (0.04 mmol) and anhydrous alcohol (2 mL) were added and the mixture was stirred at 70°C (for indicative reaction times see Table 6.7). After completion solvent was evaporated and the crude reaction mixture was purified by flash chromatography (eluent: hexane/diethyl ether 100/0 to 90/10) to afford products **172** in 56-70% yield.

#### Methyl (Z)-2-(4-nitrophenyl)-2-(phenylimino)acetate (**172a**)



Yellow solid, 37.0 mg, 65% yield. **mp** 89.3-93.0 °C. **FTIR**<sub>v<sub>max</sub></sub>(KBr)/cm<sup>-1</sup>: 1736, 1602, 1524, 1485, 1348, 1309, 1227, 1197, 1168, 1010, 857, 764, 696. **<sup>1</sup>H NMR** (CDCl<sub>3</sub>, 300 MHz): δ 8.32 (d, 2H, *J* = 9.0 Hz), 8.07 (d, 2H, *J* = 9.0 Hz), 7.38 (t, 2H, *J* = 7.7 Hz), 7.21 (td, 1H, *J* = 7.2, 1.1 Hz), 6.98 (dd, 2H, *J* = 7.4, 1.0 Hz), 3.68 (s, 3H). **<sup>13</sup>C NMR** (CDCl<sub>3</sub>, 75 MHz): δ 164.7, 157.5, 149.5, 149.3, 139.2, 129.1, 129.0, 125.9, 123.9, 119.3, 52.4. **HRMS (MALDI-FT ICR)** exact mass [M+Na]<sup>+</sup> calculated for C<sub>15</sub>H<sub>12</sub>NaN<sub>2</sub>O<sub>4</sub>: 307.0689, found: 307.0703.

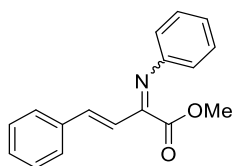
#### Ethyl(Z)-2-((4-chlorophenyl)imino)-2-(4-(trifluoromethyl)phenyl)acetate (**172b**)



Yellow oil, 49.8 mg, 70% yield. **mp** 89.3-93.0 °C. **FTIR**<sub>v<sub>max</sub></sub>(KBr)/cm<sup>-1</sup>: 1732, 1605, 1525, 1485, 1346, 1310, 1226, 1197, 1165, 1011, 854, 763, 695. **<sup>1</sup>H NMR** (CDCl<sub>3</sub>, 400 MHz): δ 8.00 (d, 2H, *J* = 8.3 Hz), 7.73 (d, 2H, *J* = 8.3 Hz), 7.32 (d, 2H, *J* = 8.6 Hz), 6.91 (d, 2H, *J* = 8.6 Hz), 4.18 (q, 2H, *J* = 7.1 Hz), 1.07 (t, 3H, *J* = 7.1 Hz). **<sup>13</sup>C NMR** (CDCl<sub>3</sub>, 100 MHz):

$\delta$  164.1, 159.4, 148.1, 136.7, 133.4 (q,  $^2J_{CF} = 32.6$  Hz), 130.8, 129.0, 128.4, 125.7 (q,  $^3J_{CF} = 3.4$  Hz), 123.6 (q,  $^1J_{CF} = 268.4$  Hz), 120.9, 61.9, 13.8. **HRMS (MALDI-FT ICR)** exact mass  $[M+H]^+$  calculated for  $C_{17}H_{14}ClF_3NO_2$ : 356.0587, found: 356.0580.

### Methyl (3*E*)-4-phenyl-2-(phenylimino)but-3-enoate (**172c**)



Mixture of diastereomers in 60:40 ratio.

Yellow oil, 29.7 mg, 56% yield.

**FTIR** $v_{max}$ (KBr)/ $cm^{-1}$ : 1732, 1600, 1527, 1486, 1348, 1310, 1223, 1197, 1168, 1009, 855, 764,

696.  **$^1H$  NMR** ( $CDCl_3$ , 400 MHz):  $\delta$  (major+minor) 7.54 (dd, 1H,  $J = 7.8, 1.7$  Hz), 7.46 (d, 1H,  $J = 16.5$  Hz), 7.41-7.38 (m, 2H), 7.36-7.31 (m, 6H), 7.21-7.12 (m, 2H), 7.03 (d, 1H,  $J = 16.5$  Hz), 6.93 (d, 3H,  $J = 7.5$  Hz), 6.70 (d, 1H,  $J = 16.5$  Hz), 4.01 (s, 3H), [3.62 (s, 3H)]<sub>minor</sub>.  **$^{13}C$  NMR** ( $CDCl_3$ , 100 MHz):  $\delta$  (major+minor) 165.2, [165.0, 160.5]<sub>minor</sub>, 158.4, [150.0]<sub>minor</sub>, 148.6, 142.6, [141.5]<sub>minor</sub>, 135.3, [135.1]<sub>minor</sub>, 130.1, 130.0, 129.0, 128.91, 128.87, 128.8, 127.9, 127.7, 125.7, 125.1, 125.0, 120.2, 119.6, 117.1, 53.0, [52.0]<sub>minor</sub>.

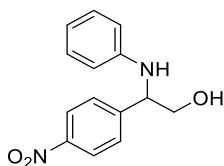
**HRMS (MALDI-FT ICR)** exact mass  $[M+H]^+$  calculated for  $C_{17}H_{16}NO_2$ : 266.11756, found: 266.11780.

### General procedure for one-pot synthesis of $\beta$ -amino alcohols **211**

In an oven-dried round-bottomed flask, *N*-acylpyrazole **81** or **204** (0.2 mmol), nitrosoarene **177** (0.24 mmol), 3Å molecular sieves (45 mg) and anhydrous dichloromethane (1 mL) were introduced. To this solution **TBD** (0.02 mmol) was added under nitrogen atmosphere. The reaction mixture was stirred at room temperature and monitored by TLC. After completion solvent was evaporated and THF (1 or 4 mL) was added.  $NaBH_4$  (0.4 mmol for product **211a**, 0.2 mmol for

product **211b**) or  $\text{LiBH}_4$  (0.6 mmol for products **211c-e**) was added at  $0^\circ\text{C}$  and the mixture was stirred while warming up to room temperature (see Scheme 6.21). After completion,  $\text{NaBH}_4$  or  $\text{LiAlH}_4$  was quenched with water and the aqueous phase was extracted with  $\text{EtOAc}$  (x4). The organic layers were dried over  $\text{Na}_2\text{SO}_4$ , filtered and evaporated. The crude reaction mixture was purified by flash chromatography (eluent: hexane/ethyl acetate 100/0 to 70/30) to afford products **211** in 53-92% yield.

### 2-(4-nitrophenyl)-2-(phenylamino)ethan-1-ol (**211a**)

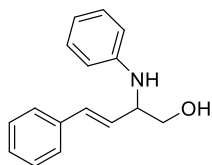


Yellow oil, 47.5 mg, 92% yield.

**FTIR** $v_{\text{max}}$ (KBr)/ $\text{cm}^{-1}$ : 3412, 2936, 1602, 1518, 1346, 1066, 855, 751, 694.  **$^1\text{H}$  NMR** ( $\text{CDCl}_3$ , 400 MHz):  $\delta$  8.19 (d, 2H,  $J = 7.9$  Hz),

7.57 (d, 2H,  $J = 8.4$  Hz), 7.11 (t, 2H,  $J = 7.7$  Hz), 6.72 (t, 1H,  $J = 7.2$  Hz), 6.51 (d, 2H,  $J = 8.3$  Hz), 4.59 (dd, 1H,  $J = 6.8, 4.0$  Hz), 4.01 (dd, 1H,  $J = 11.0, 4.0$  Hz), 3.78 (dd, 1H,  $J = 11.0, 6.8$  Hz).  **$^{13}\text{C}$  NMR** ( $\text{CDCl}_3$ , 100 MHz):  $\delta$  148.2, 147.4, 146.4, 129.3, 127.7, 124.0, 118.4, 113.8, 66.7, 59.5. **HRMS (MALDI-FT ICR)** exact mass  $[\text{M}+\text{H}]^+$  calculated for  $\text{C}_{14}\text{H}_{15}\text{N}_2\text{O}_3$ : 259.10772, found: 259.10853.

### (*E*)-4-phenyl-2-(phenylamino)but-3-en-1-ol (**211b**)



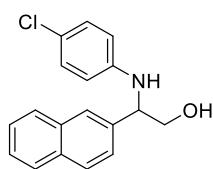
Yellow oil, 25.4 mg, 53% yield.

**FTIR** $v_{\text{max}}$ (KBr)/ $\text{cm}^{-1}$ : 3429, 2935, 1654, 1602, 1499, 1319, 1030, 969, 749, 692.  **$^1\text{H}$  NMR** ( $\text{CDCl}_3$ , 400 MHz):  $\delta$  7.41 – 7.10 (m, 7H), 6.80

– 6.61 (m, 4H), 6.18 (dd, 1H,  $J = 16.0, 5.9$  Hz), 4.19 (dd, 1H,  $J = 8.1, 3.9$  Hz), 3.88 (dd, 1H,  $J = 10.9, 4.4$  Hz), 3.73 (dd, 1H,  $J = 10.9, 6.4$  Hz).  **$^{13}\text{C}$  NMR** ( $\text{CDCl}_3$ , 75 MHz):  $\delta$  147.3, 136.4, 132.2, 129.3,

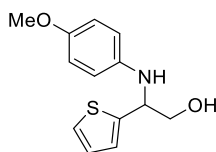
128.6, 127.9, 127.7, 126.4, 118.1, 113.9, 65.3, 57.5. **HRMS (MALDI-FT ICR)** exact mass  $[M+H]^+$  calculated for  $C_{16}H_{18}NO$ : 240.1320, found: 240.1317.

**2-((4-chlorophenyl)amino)-2-(naphthalen-2-yl)ethan-1-ol (211c)**

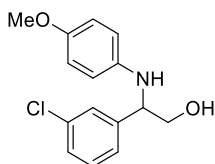


White solid, 53.6 mg, 90% yield. **mp** 130.0–133.7 °C. **FTIR** $v_{max}$ (KBr)/ $cm^{-1}$ : 3441, 1653, 1600, 1498, 1318, 1220, 1068, 816, 722.  **$^1H$  NMR** ( $CDCl_3$ , 400 MHz):  $\delta$  7.86–7.79 (m, 4H), 7.54 – 7.39 (m, 3H), 7.02 (d, 2H,  $J = 8.6$  Hz), 6.51 (d, 2H,  $J = 8.6$  Hz), 4.61 (dd, 1H,  $J = 6.5, 4.0$  Hz), 4.03 (dd, 1H,  $J = 11.1, 4.0$  Hz), 3.85 (dd, 1H,  $J = 11.1, 6.5$  Hz).  **$^{13}C$  NMR** ( $CDCl_3$ , 75 MHz):  $\delta$  145.7, 137.0, 133.4, 133.0, 129.0, 128.8, 127.8, 127.7, 126.4, 126.0, 125.6, 124.5, 122.5, 114.9, 67.2, 60.1. **HRMS (MALDI-FT ICR)** exact mass  $[M+H]^+$  calculated for  $C_{18}H_{17}ClNO$ : 297.0920, found: 297.0919.

**2-((4-methoxyphenyl)amino)-2-(thiophen-2-yl)ethan-1-ol (211d)**



Brown oil, 42.9 mg, 86% yield. **FTIR** $v_{max}$ (KBr)/ $cm^{-1}$ : 3424, 2934, 1653, 1513, 1240, 1036, 822, 707.  **$^1H$  NMR** ( $CDCl_3$ , 400 MHz):  $\delta$  7.36 (s, 1H), 7.29 – 7.19 (m, 3H), 6.71 (d, 2H,  $J = 8.7$  Hz), 6.51 (d, 2H,  $J = 8.7$  Hz), 4.40–4.34 (m, 1H), 3.89 (dd, 1H,  $J = 11.1, 4.0$  Hz), 3.70 (s, 3H), 3.67 (dd, 1H,  $J = 11.1, 7.6$  Hz).  **$^{13}C$  NMR** ( $CDCl_3$ , 100 MHz):  $\delta$  152.9, 144.9, 140.8, 127.0, 124.5, 124.3, 115.8, 114.8, 66.9, 57.1, 55.7. **HRMS (MALDI-FT ICR)** exact mass  $[M+H]^+$  calculated for  $C_{13}H_{16}NO_2S$ : 250.0824, found: 250.0815.

**2-(3-chlorophenyl)-2-((4-methoxyphenyl)amino)ethan-1-ol****(211e)**

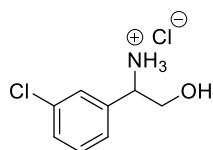
Light pink oil, 45.6 mg, 82% yield.

**FTIR** $v_{\max}$ (KBr)/ $\text{cm}^{-1}$ : 3400, 2933, 1575, 1514, 1464, 1239, 1181, 1075, 1036, 821, 787, 697.

**$^1\text{H}$  NMR** ( $\text{CDCl}_3$ , 400 MHz):  $\delta$  7.36 (s, 1H), 7.29 – 7.19 (m, 3H), 6.71 (d, 2H,  $J = 8.7$  Hz), 6.51 (d, 2H,  $J = 8.7$  Hz), 4.40–4.34 (m, 1H), 3.89 (dd, 1H,  $J = 11.1, 4.0$  Hz), 3.70 (s, 3H), 3.67 (dd, 1H,  $J = 11.1, 7.6$  Hz).  **$^{13}\text{C}$  NMR** ( $\text{CDCl}_3$ , 75 MHz):  $\delta$  152.4, 142.8, 141.0, 134.6, 130.0, 127.7, 126.9, 124.9, 115.2, 114.8, 67.0, 60.4, 55.7. **HRMS (MALDI-FT ICR)** exact mass  $[\text{M}+\text{H}]^+$  calculated for  $\text{C}_{15}\text{H}_{17}\text{ClNO}_2$ : 277.0870, found: 277.0872.

**General procedure for the synthesis of  $\beta$ -amino alcohol 212**

To a stirred solution of **211e** (0.15 mmol) in  $\text{CH}_3\text{CN}/\text{H}_2\text{O}$  (2.7 mL, 1/1), TCCA (0.08 mmol) and 1M aqueous  $\text{H}_2\text{SO}_4$  (0.15 mL) were added. The mixture was stirred at room temperature for 12 h and then washed with dichloromethane (x3). The resulting aqueous phase was basified to pH 9 by adding 5M aqueous KOH and then extracted with EtOAc (x4). The combined organic layers were dried over  $\text{Na}_2\text{SO}_4$ , concentrated, and treated with 1M aqueous HCl stirring at room temperature for 1 h. The aqueous phase was concentrated under reduced pressure to afford the HCl salt **212** in 62% yield.

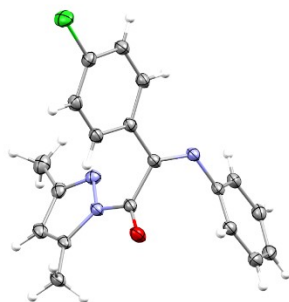
**1-(3-chlorophenyl)-2-hydroxyethan-1-aminium chloride (212)**Ochre yellow solid, 19.4 mg, 62% yield.  **$^1\text{H}$** **NMR** (MeOD, 300 MHz):  $\delta$  7.36 (s, 1H), 7.46 – 7.40 (m, 3H), 4.39–4.35 (m, 1H), 3.90 (dd, 1H,  $J = 11.5, 4.2$  Hz), (dd, 1H,  $J = 11.5, 7.7$  Hz).  **$^{13}\text{C}$**

NMR (MeOD, 75 MHz):  $\delta$  138.3, 136.0, 131.8, 130.4, 128.6, 126.9, 64.0, 57.5. HRMS (MALDI-FT ICR) exact mass  $[M+H]^+$  calculated for  $C_8H_{12}Cl_2NO$ : 208.0219, found: 208.0210.

### Computational details

Conformer search was carried out by using the MMFF force field as implemented in the Spartan software.<sup>193</sup> Equilibrium geometries and vibrational frequencies were computed at the density functional level of theory, by using the M06-2X functional in conjunction with the 6-31+G(d,p) basis set.<sup>194</sup> Solvent (dichloromethane) effects were included via the polarizable continuum model.<sup>195</sup> The Gaussian package was employed for quantum chemical computations.<sup>196</sup>

### X-ray structure of compound 202c (Figure 8.3)



<sup>193</sup> Spartan'04, Wavefunction, Inc., Irvine, CA.

<sup>194</sup> Y. Zhao, D. G. Truhlar, *Theor. Chem. Acc.* **2008**, *120*, 215.

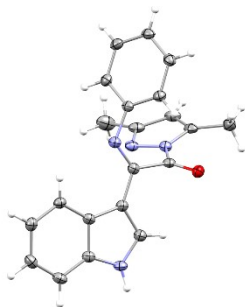
<sup>195</sup> S. Miertuš, E. Scrocco, J. Tomasi, *Chem. Phys.* **1981**, *55*, 117.

<sup>196</sup> M. J. Frisch et al., Gaussian 09 Revision D.01, Gaussian Inc., Wallingford CT, **2009**.

**Table 8.4** Crystallographic data for compound **202c**

Crystal data	
Chemical formula	C <sub>19</sub> H <sub>16</sub> ClN <sub>3</sub> O
$M_r$	337.80
Crystal system, space group	Monoclinic, $P2_1/c$
Temperature (K)	100
$a, b, c$ (Å)	11.5354 (3), 16.8698 (5), 16.9455 (7)
$\beta$ (°)	92.822 (3)
$V$ (Å <sup>3</sup> )	3293.60 (19)
$Z$	8
Radiation type	Mo $K\alpha$
$\mu$ (mm <sup>-1</sup> )	0.24
Crystal size (mm)	0.24 × 0.21 × 0.13
Data collection	
Diffractometer	SuperNova, Single source at offset/far, Atlas
Absorption correction	Multi-scan <i>CrysAlis PRO</i> 1.171.39.46 (Rigaku Oxford Diffraction, 2018) Empirical absorption correction using spherical harmonics, implemented in SCALE3 ABSPACK scaling algorithm.
$T_{\min}, T_{\max}$	0.580, 1.000
No. of measured, independent and observed [ $I > 2\sigma(I)$ ] reflections	33882, 7746, 5699
$R_{\text{int}}$	0.044
$(\sin \theta/\lambda)_{\text{max}}$ (Å <sup>-1</sup> )	0.675
Refinement	
$R[F^2 > 2\sigma(F^2)], wR(F^2), S$	0.047, 0.124, 1.05
No. of reflections	7746
No. of parameters	437
H-atom treatment	H-atom parameters constrained
$\Delta\rho_{\text{max}}, \Delta\rho_{\text{min}}$ (e Å <sup>-3</sup> )	0.35, -0.36



X-ray structure of compound **202q** (Figure 8.4)**Table 8.5.** Crystallographic data for compound **202q**

Crystal data	
Chemical formula	C <sub>21</sub> H <sub>18</sub> N <sub>4</sub> O
$M_r$	342.39
Crystal system, space group	Monoclinic, $P2_1/c$
Temperature (K)	100
$a, b, c$ (Å)	9.02920 (18), 10.0497 (3), 19.3137 (4)
$\beta$ (°)	98.739 (2)
$V$ (Å <sup>3</sup> )	1732.20 (7)
$Z$	4
Radiation type	Mo $K\alpha$
$\mu$ (mm <sup>-1</sup> )	0.08
Crystal size (mm)	0.33 × 0.28 × 0.21
Data collection	
Diffractometer	SuperNova, Single source at offset/far, Atlas
Absorption correction	Gaussian <i>CrysAlis PRO</i> 1.171.39.46 (Rigaku Oxford Diffraction, 2018) Numerical absorption correction based on gaussian integration over a multifaceted crystal model Empirical absorption correction using spherical harmonics, implemented in SCALE3 ABSPACK scaling algorithm.
$T_{\min}, T_{\max}$	0.583, 1.000
No. of measured, independent and observed [ $I > 2\sigma(I)$ ] reflections	20194, 4073, 3328
$R_{\text{int}}$	0.031
$(\sin \theta/\lambda)_{\text{max}}$ (Å <sup>-1</sup> )	0.675

Refinement	
$R[F^2 > 2\sigma(F^2)], wR(F^2), S$	0.039, 0.096, 1.03
No. of reflections	4073
No. of parameters	237
H-atom treatment	H-atom parameters constrained
$\Delta\rho_{\max}, \Delta\rho_{\min}$ ( $e \text{ \AA}^{-3}$ )	0.29, -0.26

## 8.5 Nitron/imine selectivity switch in the base catalyzed reaction of arylacetic esters with nitrosoarenes

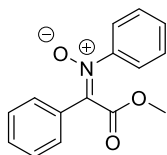
### Experimental procedures and compounds characterization

TBD and nitrosobenzene **177a** were purchased from TCI and used as received. All other bases and methylphenylacetate **219a** were purchased from Aldrich and used as received. Nitrosoarenes **177b-e** are known compounds, they were prepared according to the literature.<sup>197</sup> The esters **219** were prepared by using general procedures reported in the literature.

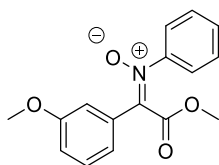
### General procedures for the synthesis of imines **172** and nitrones **215**

In an oven-dried vial ester **219** (0.4 mmol), nitrosoarene **177** (1.2 mmol), 3Å molecular sieves (~90 mg) and anhydrous dichloromethane (2 mL) were introduced. To this solution **BEMP** (0.04 mmol) was added under nitrogen atmosphere. The reaction mixture was stirred at room temperature and monitored by TLC (eluent: hexane/ethyl acetate 9/1). After completion, the crude reaction mixture was purified by flash chromatography (eluent: hexane/ethyl acetate 100/0 to 50/50) to afford products **172** in 20-91% yield and products **215** in 48-99% yield.

<sup>197</sup> W. Hu, Q. Zheng, S. Sun, J. Cheng, *Chem. Commun.* **2017**, 53, 6263.

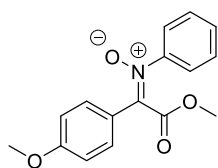
**(E)-2-methoxy-2-oxo-N,1-diphenylethan-1-imine oxide (215a)**

Ochre yellow solid, 91.9 mg, 87% yield. **mp** 90.3-91.6 °C. **FTIR**<sub>vmax</sub>(KBr)/cm<sup>-1</sup>: 3061, 2952, 1730, 1714, 1592, 1575, 1492, 1432, 1348, 1306. **<sup>1</sup>H NMR** (CDCl<sub>3</sub>, 400 MHz): δ 8.15-8.13 (m, 2H), 7.50-7.46 (m, 8H), 3.56 (s, 3H). **<sup>13</sup>C NMR** (CDCl<sub>3</sub>, 100 MHz): δ 164.4, 148.4, 140.5, 130.9, 130.1, 129.2, 129.1, 128.6, 128.5, 123.1, 52.9. **HRMS (MALDI-FT ICR)** exact mass [M+H]<sup>+</sup> C<sub>15</sub>H<sub>14</sub>NO<sub>3</sub>: 256.0968, found: 256.0952.

**(E)-2-methoxy-1-(3-methoxyphenyl)-2-oxo-N-phenylethan-1-imine oxide (215b)**

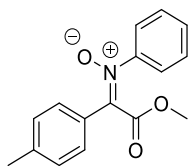
Yellow wax, 108.4 mg, 95% yield. **FTIR**<sub>vmax</sub>(KBr)/cm<sup>-1</sup>: 2963, 1730, 1577, 1488, 1255, 1124, 1037, 795, 693. **<sup>1</sup>H NMR** (CDCl<sub>3</sub>, 300 MHz): δ 8.02-8.01 (m, 1H), 7.52-7.44 (m, 6H, Major + minor), 7.37 (t, 2H, *J* = 8.1 Hz), 7.13 (t, 1H, *J* = 7.9 Hz, minor), 7.03 (dd, 1H, *J* = 8.1, 2.5 Hz), 6.80 (dd, 1H, *J* = 7.9, 2.5 Hz, minor), 6.70 (d, 1H, *J* = 7.9, minor), 6.61-6.60 (m, 1H, minor), 3.98 (s, 3H, minor), 3.85 (s, 3H), 3.60 (s, 3H, minor), 3.56 (s, 3H). **<sup>13</sup>C NMR** (CDCl<sub>3</sub>, 75 MHz): δ 164.4, 163.4 (minor), 159.4, 148.3, 140.6, 130.2, 129.8 (minor), 129.4, 129.2, 129.1 (minor), 124.3 (minor), 123.1, 121.3 (minor), 121.2, 117.5, 115.8 (minor), 114.0 (minor), 113.2, 55.4, 55.1 (minor), 53.2 (minor), 52.9. **HRMS (MALDI-FT ICR)** exact mass [M+H]<sup>+</sup> calculated for C<sub>16</sub>H<sub>16</sub>NO<sub>4</sub>: 286.1074, found: 286.1082.

**(E)-2-methoxy-1-(4-methoxyphenyl)-2-oxo-N-phenylethan-1-imine oxide (215c)**



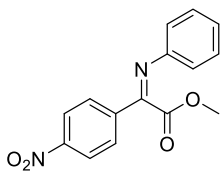
Pale brown solid, 68.5 mg, 60% yield. **mp** 100.4-103.0 °C. **FTIR** $v_{\max}$ (KBr)/ $\text{cm}^{-1}$ : 1717, 1604, 1248, 1071, 777.  **$^1\text{H NMR}$**  ( $\text{CDCl}_3$ , 400 MHz):  $\delta$  8.20 (d, 2H,  $J = 9.0$  Hz), 7.49-7.47 (m, 2H), 7.43-7.41 (m, 3H), 6.96 (d, 2H,  $J = 9.0$  Hz), 3.85 (s, 3H), 3.53 (s, 3H).  **$^{13}\text{C NMR}$**  ( $\text{CDCl}_3$ , 150 MHz):  $\delta$  164.7, 161.4, 148.3, 140.4, 130.5, 129.9, 129.1, 123.3, 121.7, 113.8, 55.4, 52.8. **HRMS (MALDI-FT ICR)** exact mass  $[\text{M}+\text{H}]^+$  calculated for  $\text{C}_{16}\text{H}_{16}\text{NO}_4$ : 286.1074, found: 286.1091.

**(E)-2-methoxy-2-oxo-N-phenyl-1-(p-tolyl)ethan-1-imine oxide (215d)**



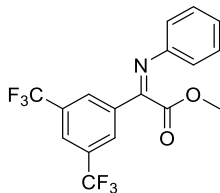
Yellow solid, 86.2 mg, 80% yield. **mp** 90.8-94.0 °C. **FTIR** $v_{\max}$ (KBr)/ $\text{cm}^{-1}$ : 1794, 1685, 1462, 1138, 519.  **$^1\text{H NMR}$**  ( $\text{CDCl}_3$ , 600 MHz):  $\delta$  8.06 (d, 2H,  $J = 8.4$  Hz), 7.51-7.50 (m, 2H), 7.46-7.44 (m, 3H), 7.28 (d, 2H,  $J = 8.4$  Hz), 3.56 (s, 3H), 2.41 (s, 3H).  **$^{13}\text{C NMR}$**  ( $\text{CDCl}_3$ , 150 MHz):  $\delta$  164.6, 148.4, 141.5, 140.6, 130.0, 129.2, 129.1, 128.5, 126.3, 123.2, 52.9, 21.7. **HRMS (MALDI-FT ICR)** exact mass  $[\text{M}+\text{H}]^+$  calculated for  $\text{C}_{16}\text{H}_{16}\text{NO}_3$ : 270.1125, found: 270.1120.

**(Z)-1-(3,5-dimethyl-1H-pyrazol-1-yl)-2-(4-nitrophenyl)-2-(phenylimino)ethan-1-one (172e)**



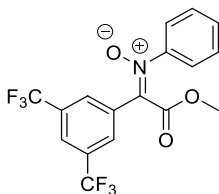
Yellow solid, 95.5 mg, 84% yield. **mp** 89.3-93.0 °C. **FTIR** $v_{\max}$ (KBr)/ $\text{cm}^{-1}$ : 1736, 1602, 1524, 1485, 1348, 1309, 1227, 1197, 1168, 1010, 857, 764, 696.  **$^1\text{H}$  NMR** ( $\text{CDCl}_3$ , 300 MHz):  $\delta$  8.32 (d, 2H,  $J = 9.2$  Hz), 8.07 (d, 2H,  $J = 9.2$  Hz), 7.38 (t, 2H,  $J = 7.4$  Hz), 7.21 (td, 1H,  $J = 7.4, 1.3$  Hz), 6.98 (dd, 2H,  $J = 7.4, 1.3$  Hz), 3.68 (s, 3H).  **$^{13}\text{C}$  NMR** ( $\text{CDCl}_3$ , 75 MHz):  $\delta$  164.7, 157.5, 149.5, 149.3, 139.2, 129.1, 129.0, 125.9, 123.9, 119.3, 52.4. **HRMS (MALDI-FT ICR)** exact mass  $[\text{M}+\text{Na}]^+$  calculated for  $\text{C}_{15}\text{H}_{12}\text{NaN}_2\text{O}_4$ : 307.0689, found: 307.0703.

**Methyl(Z)-2-(3,5-bis(trifluoromethyl)phenyl)-2-(phenylimino)acetate (172f)**



Yellow oil, 112.6 mg, 75% yield. **FTIR** $v_{\max}$ (KBr)/ $\text{cm}^{-1}$ : 1730, 1382, 1291, 1207, 1131, 771, 683.  **$^1\text{H}$  NMR** ( $\text{CDCl}_3$ , 600 MHz):  $\delta$  8.34 (s, 2H), 8.02 (s, 1H), 7.38 (t, 2H,  $J = 7.6$  Hz), 7.21 (t, 1H,  $J = 7.6$  Hz), 6.97 (d, 2H,  $J = 7.6$  Hz), 3.68 (s, 3H).  **$^{13}\text{C}$  NMR** ( $\text{CDCl}_3$ ,  $y$  MHz):  $\delta$ . **HRMS (MALDI-FT ICR)** exact mass  $[\text{M}+\text{H}]^+$  calculated for  $\text{C}_{17}\text{H}_{12}\text{F}_6\text{NO}_2$ : 376.0767, found: 376.0760.

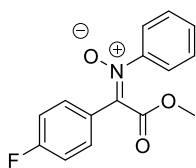
**(E)-1-(3,5-bis(trifluoromethyl)phenyl)-2-methoxy-2-oxo-N-phenylethan-1-imine oxide (215f)**



Pale brown solid, 28.2 mg, 18% yield. **mp** 133.2-135.5 °C. **FTIR** $v_{\max}$ (KBr)/ $\text{cm}^{-1}$ : 1735, 1385, 1280, 1219, 1134, 772, 682.  **$^1\text{H}$  NMR**

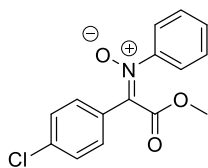
(CDCl<sub>3</sub>, 600 MHz):  $\delta$  8.58 (s, 2H), 7.95 (s, 1H), 7.52-7.50 (m, 5H), 3.59 (s, 3H). <sup>13</sup>C NMR (CDCl<sub>3</sub>, 150 MHz):  $\delta$  163.3, 148.4, 137.6, 131.9 (q, <sup>2</sup>J<sub>CF</sub> = 33.5 Hz), 131.3, 130.8, 129.4, 128.7 (q, <sup>3</sup>J<sub>CF</sub> = 3.5 Hz), 123.9 (q, <sup>3</sup>J<sub>CF</sub> = 3.5 Hz), 123.0 (q, <sup>1</sup>J<sub>CF</sub> = 271.3 Hz), 122.9, 53.3. **HRMS (MALDI-FT ICR)** exact mass [M+H]<sup>+</sup> calculated for C<sub>17</sub>H<sub>12</sub>F<sub>6</sub>NO<sub>3</sub>: 392.0716, found: 392.0734.

**(E)-1-(4-fluorophenyl)-2-methoxy-2-oxo-N-phenylethan-1-imine oxide (215g)**



Ochre yellow solid, 98.4 mg, 90% yield. **mp** 89.5-92.4 °C. **FTIR**<sub>v<sub>max</sub></sub>(KBr)/cm<sup>-1</sup>: 3061, 2952, 1730, 1714, 1592, 1575, 1492, 1432, 1348, 1306. <sup>1</sup>H NMR (CDCl<sub>3</sub>, 400 MHz):  $\delta$  8.21-8.18 (m, 2H), 7.49-7.47 (m, 2H), 7.44-7.43 (m, 3H), 7.14 (t, 2H, *J* = 8.6 Hz), 3.96 (s, 3H, minor), 3.54 (s, 3H). <sup>13</sup>C NMR (CDCl<sub>3</sub>, 150 MHz):  $\delta$  164.2, 163.4 (d, <sup>1</sup>J<sub>CF</sub> = 252.3 Hz), 148.3, 139.5, 131.0 (d, <sup>3</sup>J<sub>CF</sub> = 8.5 Hz), 130.2, 129.2, 125.3 (d, <sup>4</sup>J<sub>CF</sub> = 3.3 Hz), 123.1, 115.6 (d, <sup>2</sup>J<sub>CF</sub> = 21.8 Hz), 52.9. **HRMS (MALDI-FT ICR)** exact mass [M+H]<sup>+</sup> calculated for C<sub>15</sub>H<sub>13</sub>FNO<sub>3</sub>: 274.0874, found: 274.0862.

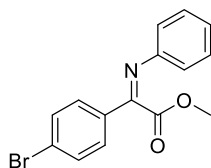
**(E)-1-(4-chlorophenyl)-2-methoxy-2-oxo-N-phenylethan-1-imine oxide (215h)**



Ochre yellow solid, 98.5 mg, 85% yield. **mp** 76.6-79.0 °C. **FTIR**<sub>v<sub>max</sub></sub>(KBr)/cm<sup>-1</sup>: 3455, 1727, 1491, 1213, 1133, 1041, 768, 691. <sup>1</sup>H NMR (CDCl<sub>3</sub>, 300 MHz):  $\delta$  8.11 (d, 2H, *J* = 9.0 Hz), 7.50-7.41 (m, 7H), 3.97 (s, 3H, minor), 3.55 (s, 3H). <sup>13</sup>C NMR (CDCl<sub>3</sub>, 75 MHz):  $\delta$  164.1, 148.3, 139.5, 136.5, 130.3, 129.9, 129.3, 128.7, 127.5, 123.0, 53.0. **HRMS (MALDI-FT ICR)** exact mass

$[M+H]^+$  calculated for  $C_{15}H_{13}ClNO_3$ : 290.0579, found: 290.0586.

**Methyl (Z)-2-(4-bromophenyl)-2-(phenylimino)acetate (172i)**

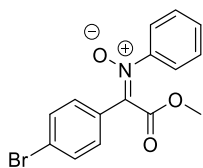


Yellow oil, 70.0 mg, 55% yield.

**FTIR** $v_{max}$ (KBr)/ $cm^{-1}$ : 1734, 1600, 1521, 1342, 1248, 842, 744.  **$^1H$  NMR** ( $CDCl_3$ , 300 MHz):  $\delta$  7.92 (d, 2H,  $J = 8.6$  Hz, minor), 7.75 (d, 2H,  $J =$

8.4 Hz), 7.66 (d, 2H,  $J = 8.6$  Hz, minor), 7.61 (d, 2H,  $J = 8.4$  Hz), 7.34 (t, 2H,  $J = 7.5$  Hz), 7.16 (t, 1H,  $J = 7.5$  Hz), 6.95 (d, 2H,  $J = 7.5$  Hz), 3.98 (s, 3H, minor), 3.63 (s, 3H).  **$^{13}C$  NMR** ( $CDCl_3$ , 75 MHz):  $\delta$  165.0, 158.7, 149.7, 132.6, 131.9, 129.4, 128.9, 126.6, 125.2, 119.3, 52.0. **HRMS (MALDI-FT ICR)** exact mass  $[M+H]^+$  calculated for  $C_{15}H_{13}BrNO_2$ : 318.0124, found: 318.0115.

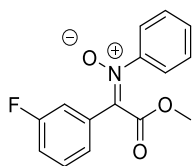
**(E)-1-(4-bromophenyl)-2-methoxy-2-oxo-N-phenylethan-1-imine oxide (215i)**



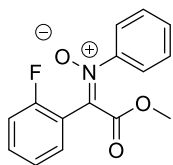
Pale brown solid, 120.3 mg, 90% yield. **mp**

116.8-119.0 °C. **FTIR** $v_{max}$ (KBr)/ $cm^{-1}$ : 1734, 1535, 1207, 1077, 771.  **$^1H$  NMR** ( $CDCl_3$ , 400 MHz):  $\delta$  8.04 (d, 2H,  $J = 8.6$  Hz), 7.60 (d, 2H,  $J =$

8.6 Hz), 7.50-7.45 (m, 5H), 7.37-7.35 (m, 10H, minor), 6.97 (d, 2H,  $J = 8.6$  Hz, minor), 3.98 (s, 3H, minor), 3.56 (s, 3H).  **$^{13}C$  NMR** ( $CDCl_3$ , 75 MHz):  $\delta$  164.1, 148.3, 139.6, 132.0 (minor), 131.7, 130.41 (minor), 130.36 (minor), 130.3, 130.1, 129.3, 128.0, 125.0, 124.3 (minor), 123.0, 53.0. **HRMS (MALDI-FT ICR)** exact mass  $[M+H]^+$  calculated for  $C_{15}H_{13}BrNO_3$ : 334.0073, found: 334.0050.

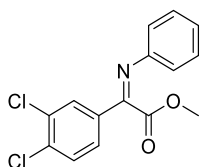
**(E)-1-(3-fluorophenyl)-2-methoxy-2-oxo-N-phenylethan-1-imine oxide (215j)**

Yellow solid, 92.9 mg, 85% yield. **mp** 71.7-73.6 °C. **FTIR** $\nu_{\max}$ (KBr)/ $\text{cm}^{-1}$ : 1731, 1580, 1487, 1244, 1122, 771, 692.  **$^1\text{H}$  NMR** ( $\text{CDCl}_3$ , 300 MHz):  $\delta$  8.11 (d, 1H,  $J = 10.7$  Hz), 7.76 (d, 1H,  $J = 8.2$  Hz), 7.51-7.39 (m, 6H), 7.16 (td, 1H,  $J = 8.2, 1.8$  Hz), 3.97 (s, 3H, minor), 3.56 (s, 3H).  **$^{13}\text{C}$  NMR** ( $\text{CDCl}_3$ , 75 MHz):  $\delta$  164.0, 162.3 (d,  $^1J_{\text{CF}} = 244.3$  Hz), 148.3, 139.5, 130.8 (d,  $^3J_{\text{CF}} = 8.8$  Hz), 130.3, 129.9 (d,  $^3J_{\text{CF}} = 8.0$  Hz), 129.2, 124.3 (d,  $^4J_{\text{CF}} = 2.8$  Hz), 123.0, 117.8 (d,  $^2J_{\text{CF}} = 21.2$  Hz), 115.4 (d,  $^2J_{\text{CF}} = 25.0$  Hz), 53.0. **HRMS (MALDI-FT ICR)** exact mass  $[\text{M}+\text{H}]^+$  calculated for  $\text{C}_{15}\text{H}_{13}\text{FNO}_3$ : 274.0874, found: 274.0904.

**(E)-1-(2-fluorophenyl)-2-methoxy-2-oxo-N-phenylethan-1-imine oxide (215k)**

Pale yellow solid, 108.2 mg, 99% yield. **mp** 65.1-71.4 °C. **FTIR** $\nu_{\max}$ (KBr)/ $\text{cm}^{-1}$ : 1726, 1473, 1340, 1260, 1211, 1135, 1051, 769, 693.  **$^1\text{H}$  NMR** ( $\text{CDCl}_3$ , 600 MHz):  $\delta$  7.98 (td, 1H,  $J = 7.4, 1.4$  Hz), 7.49-7.44 (m, 6H), 7.28 (td, 1H,  $J = 7.7, 1.0$  Hz), 7.18-7.15 (m, 1H), 3.60 (s, 3H).  **$^{13}\text{C}$  NMR** ( $\text{CDCl}_3$ , 150 MHz):  $\delta$  163.2, 160.3 (d,  $^1J_{\text{CF}} = 250.7$  Hz), 148.5, 135.1, 132.2 (d,  $^3J_{\text{CF}} = 8.7$  Hz), 130.6 (d,  $^4J_{\text{CF}} = 1.6$  Hz), 130.3, 129.2, 124.2 (d,  $^3J_{\text{CF}} = 3.0$  Hz), 123.0, 118.9 (d,  $^2J_{\text{CF}} = 13.0$  Hz), 116.0 (d,  $^2J_{\text{CF}} = 21.2$  Hz), 52.9. **HRMS (MALDI-FT ICR)** exact mass  $[\text{M}+\text{H}]^+$  calculated for  $\text{C}_{15}\text{H}_{13}\text{FNO}_3$ : 274.0874, found: 274.0915.



**Methyl (Z)-2-(3,4-dichlorophenyl)-2-(phenylimino)acetate (172l)**

Yellow solid, 49.3 mg, 40% yield. **mp** 52.2-54.7 °C. **FTIR**<sub>v<sub>max</sub></sub>(KBr)/cm<sup>-1</sup>: 1790, 1524, 1239,

1208, 1173, 607. **<sup>1</sup>H NMR**

(CDCl<sub>3</sub>, 600 MHz): δ 8.01 (d, 1H, *J* = 2.0 Hz),

7.69 (dd, 1H, *J* = 8.4, 2.0 Hz), 7.54 (d, 1H, *J* = 8.4 Hz), 7.36 (d, 1H,

*J* = 7.5 Hz) overlapped with 7.34 (d, 1H, *J* = 7.5 Hz), 7.17 (t, 1H, *J*

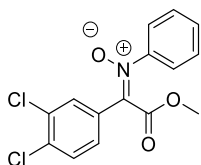
= 7.5 Hz), 6.95 (dd, 2H, *J* = 8.3, 0.9 Hz), 3.99 (s, 0.1H, minor), 3.64

(s, 3H). **<sup>13</sup>C NMR** (CDCl<sub>3</sub>, 150 MHz): δ 164.7, 157.4, 149.4, 136.1,

133.7, 133.3, 130.7, 129.7, 129.0, 127.1, 125.5, 119.4, 52.2. **HRMS**

**(MALDI-FT ICR)** exact mass [M+H]<sup>+</sup> calculated for

C<sub>15</sub>H<sub>12</sub>Cl<sub>2</sub>NO<sub>2</sub>: 308.0240, found: 308.0259.

**(E)-1-(3,4-dichlorophenyl)-2-methoxy-2-oxo-*N*-phenylethan-1-imine oxide (215l)**

Ochre yellow solid, 75.2 mg, 58% yield. **mp**

59.3-63.3 °C. **FTIR**<sub>v<sub>max</sub></sub>(KBr)/cm<sup>-1</sup>: 3450, 1733,

1589, 1485, 1335, 1278, 1212, 1134, 1045, 802,

785, 787, 693. **<sup>1</sup>H NMR** (CDCl<sub>3</sub>, 600 MHz): δ

8.39 (d, 1H, *J* = 2.2 Hz), 7.93 (dd, 1H, *J* = 8.8, 2.2 Hz), 7.53 (d, 1H,

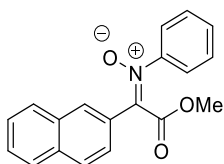
*J* = 8.8 Hz), 7.49-7.47 (m, 5H), 3.56 (s, 3H). **<sup>13</sup>C NMR** (CDCl<sub>3</sub>, 150

MHz): δ 163.8, 148.3, 138.5, 134.6, 132.9, 130.5, 130.3, 130.2,

129.3, 128.9, 127.7, 53.1. **HRMS (MALDI-FT ICR)** exact mass

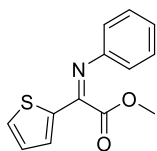
[M+K]<sup>+</sup> calculated for C<sub>15</sub>H<sub>11</sub>KCl<sub>2</sub>NO<sub>3</sub>: 361.9748, found: 361.9747.

**(*E*)-2-methoxy-1-(naphthalen-2-yl)-2-oxo-*N*-phenylethan-1-imine oxide (215m)**



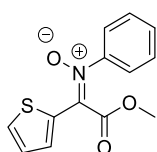
Ochre yellow solid, 114.8 mg, 94% yield. **mp** 92.6-95.2 °C. **FTIR**<sub>v<sub>max</sub></sub>(KBr)/cm<sup>-1</sup>: 1739, 1668, 1463, 1422, 1233, 667. **<sup>1</sup>H NMR** (CDCl<sub>3</sub>, 600 MHz): δ 8.97 (s, 1H), 7.97 (dd, 1H, *J* = 8.7, 1.8 Hz), 7.93 (d, 1H, *J* = 8.0 Hz), 7.90 (d, 1H, *J* = 8.7 Hz), 7.85 (d, 1H, *J* = 8.0 Hz), 7.58-7.55 (m, 3H), 7.54-7.51 (m, 1H), 7.49-7.47 (m, 3H), 3.61 (s, 3H). **<sup>13</sup>C NMR** (CDCl<sub>3</sub>, 150 MHz): δ 164.6, 148.4, 140.6, 134.1, 132.8, 130.2, 129.4, 129.2, 127.9, 127.8, 127.5, 126.6, 126.4, 124.8, 123.2, 53.0. **HRMS (MALDI-FT ICR)** exact mass [M+H]<sup>+</sup> calculated for C<sub>19</sub>H<sub>16</sub>NO<sub>3</sub>: 306.1125, found: 306.1162.

**Methyl (*E*)-2-(phenylimino)-2-(thiophen-2-yl)acetate (172n)**



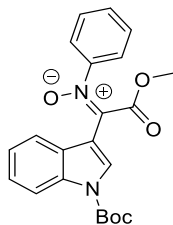
Ochre yellow solid, 32.4 mg, 33% yield. **mp** 52.2-54.7 °C. **FTIR**<sub>v<sub>max</sub></sub>(KBr)/cm<sup>-1</sup>: 1735, 1424, 1219, 1197, 1169, 819, 772, 695. **<sup>1</sup>H NMR** (CDCl<sub>3</sub>, 600 MHz): δ 7.55 (dd, 1H, *J* = 5.1, 1.1 Hz), 7.44 (dd, 1H, *J* = 3.8, 1.1 Hz), 7.33 (d, 1H, *J* = 7.8 Hz) overlapped with 7.32 (d, 1H, *J* = 7.8 Hz), 7.14 (t, 1H, *J* = 7.8 Hz), 7.11 (dd, 1H, *J* = 5.1, 3.8 Hz), 6.96 (dd, 2H, *J* = 7.8, 1.1 Hz), 6.85 (d, 2H, *J* = 7.3 Hz, minor), 4.02 (s, 3H, minor), 3.65 (s, 3H). **<sup>13</sup>C NMR** (CDCl<sub>3</sub>, 150 MHz): δ 165.4 (minor), 164.3, 153.9, 152.5 (minor), 149.5, 149.4 (minor), 140.6, 134.5 (minor), 132.5 (minor), 131.49, 131.46, 129.7 (minor), 128.9, 127.9, 126.5 (minor), 125.2, 124.8 (minor), 119.9, 118.5 (minor), 53.3 (minor), 52.2. **HRMS (MALDI-FT ICR)** exact mass [M+H]<sup>+</sup> calculated for C<sub>13</sub>H<sub>12</sub>NO<sub>2</sub>S: 246.0583, found: 246.0590.

**(Z)-2-methoxy-2-oxo-N-phenyl-1-(thiophen-2-yl)ethan-1-imine oxide (215n)**



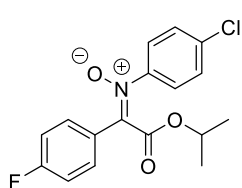
Ochre yellow solid, 50.2 mg, 48% yield. **mp** 105.4-108.7 °C. **FTIR**<sub>v<sub>max</sub></sub>(KBr)/cm<sup>-1</sup>: 3455, 1733, 1417, 1362, 1264, 1204, 1127, 1003, 795, 693. **<sup>1</sup>H NMR** (CDCl<sub>3</sub>, 400 MHz): δ 7.67 (d, 1H, *J* = 4.6 Hz), 7.58 (d, 1H, *J* = 4.6 Hz), 7.53-7.50 (m, 2H), 7.47-7.46 (m, 3H), 7.23 (t, 1H, *J* = 4.6 Hz), 3.63 (s, 3H). **<sup>13</sup>C NMR** (CDCl<sub>3</sub>, 100 MHz): δ 163.0, 146.8, 136.4, 131.0, 130.9, 130.2, 130.1, 129.2, 126.9, 123.1, 53.1. **HRMS (MALDI-FT ICR)** exact mass [M+H]<sup>+</sup> calculated for C<sub>13</sub>H<sub>12</sub>NO<sub>3</sub>S: 262.0532, found: 262.0564.

**(E)-1-(1-(tert-butoxycarbonyl)-1H-indol-3-yl)-2-methoxy-2-oxo-N-phenylethan-1-imine oxide (215o)**



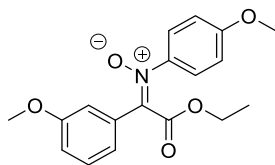
Pale brown solid, 148.3 mg, 94% yield. **mp** 134.7-137.9 °C. **FTIR**<sub>v<sub>max</sub></sub>(KBr)/cm<sup>-1</sup>: 3455, 1738, 1382, 1233, 1148, 1093, 759. **<sup>1</sup>H NMR** (CDCl<sub>3</sub>, 400 MHz): δ 9.61 (s, 1H), 8.33 (d, 1H, *J* = 8.4 Hz), 7.53-7.50 (m, 2H), 7.48-7.46 (m, 3H), 7.41-7.37 (m, 1H), 7.31-7.24 (m, 2H), 3.68 (s, 3H), 1.68 (s, 9H). **<sup>13</sup>C NMR** (CDCl<sub>3</sub>, 100 MHz): δ 164.0, 149.0, 147.2, 135.8, 135.2, 131.3, 130.0, 129.2, 126.5, 125.2, 123.5, 123.4, 119.2, 115.7, 109.4, 84.8, 53.1, 28.1. **HRMS (MALDI-FT ICR)** exact mass [M+H]<sup>+</sup> calculated for C<sub>22</sub>H<sub>23</sub>N<sub>2</sub>O<sub>5</sub>: 395.1602, found: 395.1615.

**(E)-N-(4-chlorophenyl)-1-(4-fluorophenyl)-2-isopropoxy-2-oxoethan-1-imine oxide (215p)**



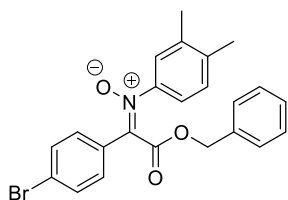
Pale yellow solid, 68.5 mg, 51% yield. **mp** 70.6-74.4 °C. **FTIR**<sub>vmax</sub>(KBr)/cm<sup>-1</sup>: 1724, 1601, 1505, 1236, 1165, 1236, 1165, 1098, 1036, 837, 773. **<sup>1</sup>H NMR** (CDCl<sub>3</sub>, 600 MHz): δ 8.24 (dd, 2H, *J* = 9.0, 5.4 Hz), 7.46 (d, 2H, *J* = 8.9 Hz), 7.42 (d, 2H, *J* = 8.9 Hz), 7.15 (t, 2H, *J* = 9.0 Hz), 4.94 (sep, 1H), 1.02 (d, 6H, *J* = 6.2 Hz). **<sup>13</sup>C NMR** (CDCl<sub>3</sub>, 150 MHz): δ 163.6 (d, <sup>1</sup>*J*<sub>CF</sub> = 252.7 Hz), 163.0, 146.5, 140.4, 136.2, 131.1 (d, <sup>3</sup>*J*<sub>CF</sub> = 8.7 Hz), 129.4, 125.2 (d, <sup>4</sup>*J*<sub>CF</sub> = 3.2 Hz), 124.9, 115.7 (d, <sup>2</sup>*J*<sub>CF</sub> = 21.5 Hz), 71.0, 21.1. **HRMS (MALDI-FT ICR)** exact mass [M+H]<sup>+</sup> calculated for C<sub>17</sub>H<sub>16</sub>ClFNO<sub>3</sub>: 336.0797, found: 336.0795.

**(E)-2-ethoxy-1-(3-methoxyphenyl)-N-(4-methoxyphenyl)-2-oxoethan-1-imine oxide (215q)**



Yellow wax, 96.2 mg, 73% yield. **FTIR**<sub>vmax</sub>(KBr)/cm<sup>-1</sup>: 1733, 1505, 1249, 1108, 1030, 772. **<sup>1</sup>H NMR** (CDCl<sub>3</sub>, 300 MHz): δ 8.06-8.05 (m, 1H), 7.52-7.44 (m, 3H), 7.35 (t, 1H, *J* = 8.3 Hz), 7.01 (dd, 1H, *J* = 8.3, 2.6 Hz), 6.91 (d, 2H, *J* = 8.3 Hz), 4.46 (q, 2H, *J* = 7.1 Hz, minor), 4.07 (q, 2H, *J* = 7.1 Hz), 3.85 (s, 3H), 3.84 (s, 3H), 3.78 (s, 3H, minor), 3.63 (s, 3H, minor), 1.39 (t, 3H, *J* = 7.1 Hz, minor), 1.00 (t, 3H, *J* = 7.1 Hz). **<sup>13</sup>C NMR** (CDCl<sub>3</sub>, 75 MHz): δ 164.0, 160.7, 159.3, 141.7, 140.5, 130.3, 129.3, 124.7, 121.1, 117.4, 114.0, 113.0, 62.3, 55.6, 55.3, 13.6. **HRMS (MALDI-FT ICR)** exact mass [M+H]<sup>+</sup> calculated for C<sub>18</sub>H<sub>20</sub>NO<sub>5</sub>: 330.1336, found: 330.1350.

**(E)-1-(4-bromophenyl)-N-(3,4-dimethylphenyl)-2-oxo-2-phenoxyethan-1-imine oxide (215r)**



Yellow solid, 122.7 mg, 70% yield. **mp**

79.5-82.4 °C. **FTIR** $v_{\max}$ (KBr)/ $\text{cm}^{-1}$ :

1696, 1654, 1507, 1220, 1144, 772. **<sup>1</sup>H**

**NMR** ( $\text{CDCl}_3$ , 400 MHz):  $\delta$  8.01 (d, 2H,

$J = 8.8$  Hz), 7.56 (d, 2H,  $J = 8.8$  Hz),

7.33-7.22 (m, 4H), 7.22 (s, 1H), 7.13 (dd, 1H,  $J = 8.0, 1.7$  Hz), 7.05-

7.02 (m, 3H), 5.01 (s, 2H), 2.25 (s, 3H), 2.19 (s, 3H). **<sup>13</sup>C**

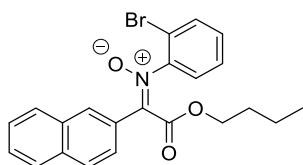
**NMR** ( $\text{CDCl}_3$ , 100 MHz):  $\delta$  163.6, 146.2, 139.2, 139.1, 138.0, 133.8, 131.6,

130.0, 129.9, 128.9, 128.7, 128.4, 128.2, 124.7, 124.0, 120.1, 68.2,

19.7. **HRMS (MALDI-FT ICR)** exact mass  $[M+H]^+$  calculated for

$\text{C}_{23}\text{H}_{21}\text{BrNO}_3$ : 438.0699, found: 438.0680.

**(E)-N-(2-bromophenyl)-2-butoxy-1-(naphthalen-2-yl)-2-oxoethan-1-imine oxide (215s)**



Yellow oil, 129.6 mg, 76% yield.

**FTIR** $v_{\max}$ (KBr)/ $\text{cm}^{-1}$ : **<sup>1</sup>H**

**NMR** ( $\text{CDCl}_3$ , 400 MHz):  $\delta$  8.97 (s, 1H), 8.55

(s, 1H, minor), 7.94 (d, 1H,  $J = 8.0$  Hz),

7.91 (s, 2H), 7.86 (d, 1H,  $J = 8.0$  Hz), 7.69 (dd, 1H,  $J = 1.0, 8.0$  Hz),

7.59-7.51 (m, 3H), 7.43 (td, 1H,  $J = 1.2, 7.7$  Hz), 7.33 (td, 1H,  $J =$

1.2, 7.7 Hz), 4.46 (t, 2H,  $J = 7.0$  Hz, minor), 4.04 (t, 2H,  $J = 7.0$  Hz),

1.82-1.76 (m, 2H, minor), 1.51-1.44 (m, 2H, minor), 1.39-1.33 (m,

2H), 1.26-1.17 (m, 2H), 0.99 (t, 3H,  $J = 7.0$  Hz), 0.83 (t, 3H,  $J = 7.0$

Hz). **<sup>13</sup>C**

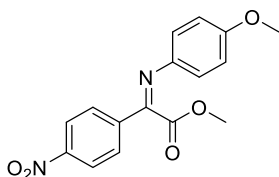
**NMR** ( $\text{CDCl}_3$ , 100 MHz):  $\delta$  162.9, 146.9, 142.1, 134.2,

133.7, 132.8, 130.8, 130.0, 129.3, 128.2, 127.9, 127.6, 126.6, 126.0,

125.6, 125.2, 117.2, 66.4, 30.0, 18.9, 13.5. **HRMS (MALDI-FT**

**ICR)** exact mass  $[M+H]^+$  calculated for  $C_{22}H_{21}BrNO_3$ : 426.0699, found: 426.0703.

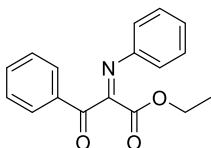
**Methyl(Z)-2-((4-methoxyphenyl)imino)-2-(4-nitrophenyl) acetate (172t)**



Orange solid, 114.4 mg, 91% yield. **mp** 72.7-75.9 °C. **FTIR** $_{\text{vmax}}$ (KBr)/ $\text{cm}^{-1}$ : 3451, 1735, 1602, 1522, 1503, 1347, 1248, 842.

**$^1\text{H NMR}$**  ( $\text{CDCl}_3$ , 300 MHz):  $\delta$  8.30 (d, 2H,  $J = 9.0$  Hz), 8.04 (d, 2H,  $J = 9.0$  Hz), 7.01 (d, 2H,  $J = 8.9$  Hz), 6.91 (d, 2H,  $J = 8.9$  Hz), 4.02 (s, 3H, minor), 3.97 (s, 3H, minor), 3.83 (s, 3H), 3.74 (s, 3H).  **$^{13}\text{C NMR}$**  ( $\text{CDCl}_3$ , 75 MHz):  $\delta$  165.4, 158.2, 156.0, 149.3, 142.1, 139.6, 128.7, 123.8, 121.4, 114.3, 55.4, 52.4. **HRMS (MALDI-FT ICR)** exact mass  $[M+H]^+$  calculated for  $C_{16}H_{15}N_2O_5$ : 315.0976, found: 315.0970.

**Ethyl (Z)-3-oxo-3-phenyl-2-(phenylimino)propanoate (172u)**

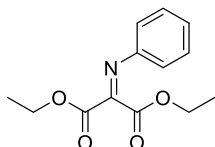


Yellow oil, 90.0 mg, 80% yield. **FTIR** $_{\text{vmax}}$ (KBr)/ $\text{cm}^{-1}$ : 3402, 1669, 1536, 1449, 1242, 1100, 766, 688.  **$^1\text{H NMR}$**  ( $\text{CDCl}_3$ , 400

MHz):  $\delta$  8.20 (dd, 1H,  $J = 8.3, 1.2$  Hz), 7.71 (dd, 2H,  $J = 8.3, 1.2$  Hz), 7.64 (t, 1H,  $J = 7.3$  Hz, minor), 7.49 (d, 1H,  $J = 7.7$  Hz), 7.53 (d, 1H,  $J = 7.7$  Hz), 7.38 (t, 3H,  $J = 7.7$  Hz), 7.23 (t, 1H,  $J = 7.3$  Hz, minor), 7.17 (t, 2H,  $J = 7.7$  Hz), 7.06-7.02 (m, 2H), 6.96-6.94 (m, 2H), 4.42 (q, 2H,  $J = 7.1$  Hz), 4.19 (q, 2H,  $J = 7.1$  Hz, minor), 1.34 (t, 3H,  $J = 7.1$  Hz), 1.08 (t, 3H,  $J = 7.1$  Hz, minor).  **$^{13}\text{C NMR}$**  ( $\text{CDCl}_3$ , 100 MHz):  $\delta$  194.1, 189.1 (minor), 162.9 (minor), 162.0, 158.6, 157.3 (minor), 147.8 (minor), 146.8, 134.6, 134.3 (minor), 134.0, 133.6 (minor), 130.8 (minor), 129.0 (minor), 128.94, 128.91, 128.8, 128.4

(minor), 126.8, 126.7 (minor), 120.5, 119.4 (minor), 62.9, 62.0 (minor), 14.0, 13.7 (minor). **HRMS (MALDI-FT ICR)** exact mass  $[M+H]^+$  calculated for  $C_{17}H_{16}NO_3$ : 282.1125, found: 282.1115.

### Diethyl 2-(phenylimino)malonate (172v)



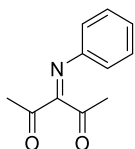
Yellow oil, 81.8 mg, 82% yield.

**FTIR** $v_{\max}$ (KBr)/ $cm^{-1}$ : 1781, 1676, 1617,

1071, 1256, 695, 666. **<sup>1</sup>H NMR** ( $CDCl_3$ , 400

MHz):  $\delta$  7.34 (t, 2H,  $J = 7.6$  Hz), 7.21 (t, 1H,  $J = 7.6$  Hz), 6.98 (d, 2H,  $J = 7.6$  Hz), 5.94 (q, 2H,  $J = 7.1$  Hz), 4.16 (q, 2H,  $J = 7.1$  Hz), 1.41 (t, 3H,  $J = 7.1$  Hz), 1.06 (t, 3H,  $J = 7.1$  Hz). **<sup>13</sup>C NMR** ( $CDCl_3$ , 100 MHz):  $\delta$  162.3, 161.0, 152.5, 147.6, 128.8, 126.7, 119.5, 63.0, 62.0, 14.0, 13.6. **HRMS (MALDI-FT ICR)** exact mass  $[M+H]^+$  calculated for  $C_{13}H_{16}NO_4$ : 250.1074, found: 250.1070.

### 3-(phenylimino)pentane-2,4-dione (172w)



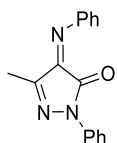
Yellow oil, 47.7 mg, 63% yield. **FTIR** $v_{\max}$ (KBr)/ $cm^{-1}$ :

3464, 1697, 1484, 1358, 771, 697. **<sup>1</sup>H NMR** ( $CDCl_3$ ,

300 MHz):  $\delta$  7.36 (t, 2H,  $J = 7.5$  Hz), 7.22 (t, 1H,  $J =$

7.5 Hz), 6.94 (d, 2H,  $J = 7.5$  Hz), 2.55 (s, 3H), 1.99 (s, 3H). **<sup>13</sup>C NMR** ( $CDCl_3$ , 75 MHz):  $\delta$  203.5, 198.5, 163.9, 146.7, 129.2, 127.0, 120.0, 30.3, 25.1. **HRMS (MALDI-FT ICR)** exact mass  $[M+H]^+$  calculated for  $C_{11}H_{12}NO_2$ : 190.0863, found: 190.0860.

### (Z)-5-methyl-2-phenyl-4-(phenylimino)-2,4-dihydro-3H-pyrazol-3-one (172x)



Red solid, 59.0 mg, 56% yield. **mp** 130.2-131.6 °C.

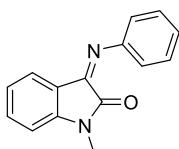
**FTIR** $v_{\max}$ (KBr)/ $cm^{-1}$ : 1735, 1607, 1470, 1101, 780. **<sup>1</sup>H**

**NMR** ( $CDCl_3$ , 300 MHz):  $\delta$  7.95 (d, 2H,  $J = 7.8$  Hz,

minor), 7.89 (d, 2H,  $J = 7.7$  Hz), 7.48-7.33 (m, 8H, Major + minor),

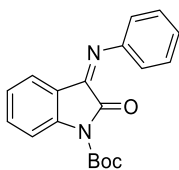
7.21 (t, 1H,  $J = 7.4$  Hz), 6.97 (d, 1H,  $J = 7.3$  Hz, minor), 2.35 (s, 3H), 1.79 (s, 3H, minor).  $^{13}\text{C}$  NMR ( $\text{CDCl}_3$ , 150 MHz):  $\delta$  153.4 (minor), 152.5, 151.1, 150.7, 148.3 (minor), 146.3, 142.0 (minor), 137.6, 137.4 (minor), 129.1 (minor), 128.94 (minor), 128.89, 128.6, 126.9 (minor), 125.7 (minor), 125.5, 121.8, 118.7 (minor), 118.4, 118.3 (minor), 16.4 (minor), 12.3. **HRMS (MALDI-FT ICR)** exact mass  $[\text{M}+\text{H}]^+$  calculated for  $\text{C}_{16}\text{H}_{14}\text{N}_3\text{O}$ : 264.1131, found: 264.1125.

**(Z)-1-methyl-3-(phenylimino)indolin-2-one (172y)**



Orange solid, 85.1 mg, 90% yield. **mp** 98.6-103.4 °C. **FTIR** $v_{\text{max}}$ (KBr)/ $\text{cm}^{-1}$ : 1733, 1604, 1470, 1101, 776.  $^1\text{H}$  NMR ( $\text{CDCl}_3$ , 600 MHz):  $\delta$  7.43 (d, 1H,  $J = 7.6$  Hz) overlapped with 7.42 (d, 1H,  $J = 7.6$  Hz), 7.36 (td, 1H,  $J = 7.6, 1.2$  Hz), 7.24 (tt, 1H,  $J = 7.6, 1.2$  Hz), 7.00 (dd, 2H,  $J = 7.8, 0.9$  Hz), 6.85 (d, 1H,  $J = 7.8$  Hz), 6.75 (td, 1H,  $J = 7.8, 0.9$  Hz), 6.61 (dd, 1H,  $J = 7.8, 0.9$  Hz), 3.31 (s, 3H).  $^{13}\text{C}$  NMR ( $\text{CDCl}_3$ , 150 MHz):  $\delta$  163.3, 154.3, 150.3, 148.0, 134.0, 129.4, 126.1, 125.2, 122.6, 117.8, 115.6, 109.2, 26.3. **HRMS (MALDI-FT ICR)** exact mass  $[\text{M}+\text{H}]^+$  calculated for  $\text{C}_{15}\text{H}_{13}\text{N}_2\text{O}$ : 237.1022, found: 273.1020.

**Tert-butyl (Z)-2-oxo-3-(phenylimino)indoline-1-carboxylate (172z)**



Yellow solid, 103.2 mg, 80% yield. **mp** 136.3-139.6 °C. **FTIR** $v_{\text{max}}$ (KBr)/ $\text{cm}^{-1}$ : 1735, 1602, 1465, 1345, 1293, 1219, 1149, 771.  $^1\text{H}$  NMR ( $\text{CDCl}_3$ , 400 MHz):  $\delta$  7.99 (d, 1H,  $J = 8.3$  Hz), 7.92 (d, 1H,  $J = 7.8$  Hz, minor), 7.80 (d, 1H,  $J = 7.8$  Hz, minor), 7.52 (t, 1H,  $J = 7.8$  Hz, minor), 7.44-7.39 (m, 3H), 7.35 (t, 3H,  $J = 7.8$  Hz, minor), 7.23 (t, 1H,  $J = 7.7$  Hz), 7.16 (t, 1H,  $J = 7.8$  Hz, minor), 6.98

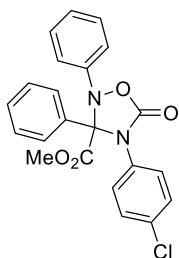


(d, 2H,  $J = 7.8$  Hz, minor), 6.95 (d, 2H,  $J = 7.7$  Hz), 6.86 (t, 1H,  $J = 7.7$  Hz), 6.72 (d, 1H,  $J = 7.7$  Hz), 1.66 (s, 9H), 1.58 (s, 9H, minor).  $^{13}\text{C}$  NMR ( $\text{CDCl}_3$ , 150 MHz):  $\delta$  160.7, 154.6 (minor), 152.4, 150.2, 149.6 (minor), 149.0 (minor), 148.9 (minor), 148.8, 144.4, 143.1 (minor), 134.3, 134.1 (minor), 129.6, 128.7 (minor), 125.7, 125.4, 125.3 (minor), 124.9 (minor), 124.2, 122.9 (minor), 122.0 (minor), 118.7, 117.4, 116.5 (minor), 116.1, 115.6 (minor), 85.1, 84.9 (minor), 28.09, 28.07 (minor). **HRMS (MALDI-FT ICR)** exact mass  $[\text{M}+\text{H}]^+$  calculated for  $\text{C}_{19}\text{H}_{19}\text{N}_2\text{O}_3$ : 323.1390, found: 323.1389.

### General procedure for the synthesis of cycloadducts **225**

Nitrone **215** (0.08 mmol), isocyanate **226** (0.096 mmol) and anhydrous toluene (0.4 mL) were introduced in a vial. The reaction mixture was stirred at room temperature and monitored by TLC (eluent: hexane/ethyl acetate 8/2). After completion, the crude reaction mixture was purified by flash chromatography (eluent: hexane/ethyl acetate 100/0 to 95/5 for product **225a**, hexane/diethyl ether 100/0 to 95/5 for product **225b**) to afford products **225a** and **225b** in 83% and 89% yield, respectively.

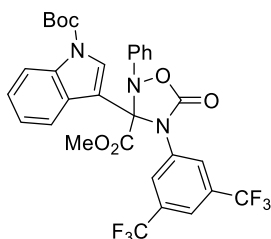
### Methyl 4-(4-chlorophenyl)-5-oxo-2,3-diphenyl-1,2,4-oxadiazolidine-3-carboxylate (**225a**)



White solid, 27.1 mg, 83% yield. **mp** 128.8-131.3 °C. **FTIR** $_{\text{Vmax}}$ (KBr)/ $\text{cm}^{-1}$ : 1782, 1747, 1496, 1452, 1364, 1252, 1151, 1091, 1016, 825, 794, 762, 697.  $^1\text{H}$  NMR ( $\text{CDCl}_3$ , 400 MHz):  $\delta$  7.64 (d, 2H,  $J = 7.2$  Hz), 7.48-7.43 (m, 1H), 7.40-7.36 (m, 2H), 7.26-7.22 (m, 2H), 7.19-7.13 (m,

3H), 7.06 (dd, 2H,  $J = 1.4, 8.6$  Hz), 6.87 (d, 2H,  $J = 8.8$  Hz), 3.46 (s, 3H, minor).  $^{13}\text{C}$  NMR ( $\text{CDCl}_3$ , 100 MHz):  $\delta$  166.2, 153.3, 143.5, 134.0, 132.8, 132.1, 130.5, 129.8, 129.3, 129.1, 128.6, 128.5, 126.4, 119.5, 91.4, 52.9. **HRMS (MALDI-FT ICR)** exact mass  $[\text{M}+\text{H}]^+$  calculated for  $\text{C}_{22}\text{H}_{18}\text{ClN}_2\text{O}_4$ : 409.0950, found: 409.0945.

**Methyl 4-(3,5-bis(trifluoromethyl)phenyl)-3-(1-(tert-butoxycarbonyl)-1H-indol-3-yl)-5-oxo-2-phenyl-1,2,4-oxadiazolidine-3-carboxylate (225b)**



White solid, 46.2 mg, 89% yield. **mp** 60.3-63.4 °C. **FTIR** $_{\text{v}_{\text{max}}}$ (KBr)/ $\text{cm}^{-1}$ : 1787, 1746, 1452, 1393, 1279, 1152, 764, 683.  $^1\text{H}$  NMR ( $\text{CDCl}_3$ , 400 MHz):  $\delta$  8.19 (d, 1H,  $J = 8.2$  Hz), 8.11 (d, 1H,  $J = 8.2$  Hz), 7.99 (s, 1H), 7.62 (s, 1H), 7.44-7.39 (m, 3H), 7.33 (t, 1H,  $J = 7.5$  Hz), 7.28-7.25 (m, 2H), 7.20-7.16 (m, 1H), 7.03 (d, 2H,  $J = 7.7$  Hz), 3.60 (s, 3H), 1.67 (s, 9H).  $^{13}\text{C}$  NMR ( $\text{CDCl}_3$ , 100 MHz):  $\delta$  165.1, 153.0, 148.9, 142.6, 135.6, 135.4, 132.1 (q,  $^2J_{\text{CF}} = 33.7$  Hz), 130.7, 128.9, 127.5, 126.9, 125.8, 125.6, 124.0, 122.5 (q,  $^1J_{\text{CF}} = 271.3$  Hz), 121.6, 120.8 (q,  $^3J_{\text{CF}} = 3.5$  Hz), 119.5, 115.5, 110.7, 88.7, 85.3, 53.2, 28.0. **HRMS (MALDI-FT ICR)** exact mass  $[\text{M}+\text{H}]^+$  calculated for  $\text{C}_{31}\text{H}_{26}\text{F}_6\text{N}_3\text{O}_6$ : 650.1720, found: 650.1718.

**Mechanistic investigations**

**Synthesis of nitrone 215a in the presence of radical inhibitor TEMPO**

In an oven-dried vial, methyl phenylacetate **219a** (0.4 mmol), nitrosobenzene **177a** (1.2 mmol), TEMPO (0.44 mmol), 3Å molecular sieves (~90 mg) and anhydrous dichloromethane (2 mL)

were introduced. BEMP (0.04 mmol) was added to this solution under nitrogen atmosphere and the reaction mixture was stirred at room temperature for 1 hour. After completion, the crude reaction mixture was concentrated under reduced pressure and then purified by flash chromatography (eluent: hexane/ethyl acetate 100/0 to 50/50) to afford product **215a** in 90% yield (*E/Z* 90/10).

### **General procedure for the reaction between diphenylmethanol and nitrosobenzene**

In an oven-dried vial diphenylmethanol **229** (0.2 mmol), nitrosobenzene **177a** (0.4 mmol), 3Å molecular sieves (~45 mg) and anhydrous dichloromethane (1 mL) were introduced. To this solution BEMP (0.2 mmol) was added under nitrogen atmosphere and the reaction mixture was stirred at room temperature for 23 hours. After completion, the crude reaction mixture was purified by flash chromatography (eluent: hexane/ethyl acetate 100/0 to 80/20) to afford benzophenone **230** in 45% yield and azoxybenzene in 55% yield.

### **Monitoring of the reaction of 219a and 177a promoted by BEMP in deuterated dichloromethane by <sup>1</sup>H-NMR spectroscopy**

Methyl phenylacetate **219a** (0.12 mmol), nitrosobenzene **177a** (0.36 mmol), 3Å molecular sieves (~30 mg), BEMP (3.5 μL, 0.012 mmol, 0.1 equiv.) and anhydrous CD<sub>2</sub>Cl<sub>2</sub> (0.6 mL) were loaded into the NMR tube under nitrogen atmosphere. The tube was shaken and the reaction was monitored by <sup>1</sup>H NMR spectroscopy at 600 MHz at room temperature.

**Monitoring of the deuteration reaction of **219a** by  $^1\text{H}$ -NMR spectroscopy**

Anhydrous  $\text{CD}_2\text{Cl}_2$  (0.6 mL), 3Å molecular sieves (~30 mg), methyl phenylacetate **219a** (0.12 mmol) and BEMP (35  $\mu\text{L}$ , 0.12 mmol, 1 equiv.) were loaded into the NMR tube under nitrogen atmosphere. After 30 minutes,  $\text{D}_2\text{O}$  (25  $\mu\text{L}$ ) was added, the tube was shaken and the reaction was monitored by  $^1\text{H}$ -NMR spectroscopy at 600 MHz at room temperature.

**The work contained within this thesis is partially described in the following publications:**

*“Catalytic Enantioselective One-Pot Approach to cis- and trans-2,3-Diaryl Substituted 1,5-Benzothiazepines”*

S. Meninno, I. Quaratesi, C. Volpe, A. Mazzanti, A. Lattanzi, *Org. Biomol. Chem.* **2018**, *16*, 6923.

*“1,5,7-Triazabicyclo[4.4.0]dec-5-ene (TBD) Triggered Diastereoselective [3+2] Cycloaddition of Azomethine Imines and Pyrazoleamides”*

C. Volpe, S. Meninno, A. Capobianco, G. Vigliotta, A. Lattanzi, *Adv. Synth. Catal.* **2019**, *361*, 1018.

*“Diaryl Prolinols in Stereoselective Catalysis and Synthesis: An Update”*

S. Meninno, C. Volpe, A. Lattanzi, *ChemCatChem* **2019**, *11*, 3716.

*“Direct  $\alpha$ -Imination of N-Acyl Pyrazoles with Nitrosoarenes”*

C. Volpe, S. Meninno, G. Mirra, J. Overgaard, A. Capobianco, A. Lattanzi, *Org. Lett.* **2019**, *21*, 5305.

*“Nitron/Imine Selectivity Switch in Base-Catalysed Reaction of Aryl Acetic Acid Esters with Nitrosoarenes: Joint Experimental and Computational Study”*

C. Volpe, S. Meninno, A. Roselli, M. Mancinelli, A. Mazzanti, A. Lattanzi *Adv. Synth. Catal.* **2020**, *362*, 5457.